

A STOCHASTIC, DAILY TIME-STEP MODEL FOR THE
CONJUNCTIVE USE OF SURFACE WATER,
GROUNDWATER, DESALINATION AND WATER
RECLAMATION FOR MUNICIPALITIES.

by

ERIKA GERTRUD BRAUNE

*Thesis presented in partial fulfilment of the requirements for
the degree of Master of Engineering in Hydrological Engineering in
the Faculty of Engineering at Stellenbosch University*



Department of Civil Engineering,
University of Stellenbosch,
Private Bag X1, Matieland 7602, South Africa.

Supervisor: Prof JA du Plessis

March 2020

PLAGIARISM DECLARATION

By submitting this thesis electronically, I declare that the entirety of the work contained therein is my own, original work, that I am the sole author thereof (save to the extent explicitly otherwise stated), that reproduction and publication thereof by Stellenbosch University will not infringe any third party rights and that I have not previously in its entirety or in part submitted it for obtaining any qualification.

Date: March 2020

ABSTRACT

South Africa has a broadly-developed water infrastructure based mainly on surface water, localised groundwater and occasional desalination as resources. However, the most suitable sites for surface water storage have been utilised and with population growth and economic factors driving the increase in demand, as well as changing climate conditions, it is projected by the Department of Water and Sanitation that South Africa's water demand will exceed the available fresh-water by 2025. To mitigate water scarcity, more conjunctive water use solutions need to be investigated.

To implement conjunctive management of scarce water resources at a local authority level, a Microsoft Excel model was developed to assess the combined yields of surface water, groundwater and desalinated and reclaimed water, using a daily time step. The model is stochastically driven by synthetically generated streamflow sequences. Monthly streamflow is disaggregated into daily streamflow and a streamflow-rainfall relationship is established to generate corresponding synthetic rainfall sequences. The conventional dam balancing equation, with daily streamflow, is used in the modelling.

Groundwater is modelled using a similar approach as the Aquifer Firm Yield Model with the saturated volume fluctuation equation as the stochastic link between rainfall, recharge and water levels. This model is paired with the Cooper-Jacob model and data from Groundwater Resource Assessment Phase 2 project. Desalination and water reclamation are modelled as one source which provides water at 100% assurance of supply at different operational capacity levels over fixed three-monthly time steps.

The model evaluates the available yield of the system with water from desalinated sources (including reclaimed) and groundwater used first, according to minimum operational procedures, after which surface water is utilised. A control is built into the model which shuts down the desalination plant if the dam capacity reaches user-defined levels. The model allows for multiple alternative water resources, based on consumer defined input. Additionally, the short-term and long-term assurance of supply is graphically presented which can aid management decisions. An analysis of the historical water supply system is produced while information towards improvement of water management is also provided.

OPSOMMING

Suid-Afrika beskik oor 'n watervoorsieningsinfrastruktuur wat oor 'n breë spektrum ontwikkel is, maar hoofsaaklik gebaseer is op oppervlak waterbronne, plaaslike grondwater en, in sommige gevalle, ontsouting. Die mees geskikte liggings vir die berging van oppervlak waterbronne is reeds in gebruik, terwyl bevolkingsgroei, ekonomiese faktore en veranderende klimaatomstandighede die vraag na water steeds laat styg. Daar word beraam volgens die Departement van Water en Sanitasie dat Suid-Afrika se verskillende water bronne teen 2025 gesamentlik nie meer aan die vraag sal kan voorsien nie. Om water tekorte te bestuur, moet volledige ondersoeke na die gebruik van verskillende bronne ingestel word.

Om meer geïntegreerde oplossings van hierdie skaars bron te implementeer, is 'n model in Microsoft Excel ontwikkel om plaaslike waterverskaffers, byvoorbeeld munisipaliteite, te help om die gekombineerde opbrengs van verskeie waterbronne op 'n daaglikse basis te bepaal. Die model is stogasties (ewekansig) van aard, deurdat dit gebruik maak van tydsreeksse wat sinteties gegenereer is. Tydsreeksse is gebaseer op die agtereenvolgende veranderinge in die vloei van 'n stroom (rivier) oor 'n bepaalde tydperk. Maandelikse vloei word verdeel in daaglikse vloei met behulp van ooreenstemmende sinteties gegenereerde reënval tydsreeksse. Die verhouding tussen die vloei van die stroom en reënval word bepaal om die bogenoemde te bewerkstellig. Die konvensionele dam balanseringsvergelyking, met behulp van die daaglikse tydsreeksse, word in die modelleering gebruik.

Grondwater bronne word gemodelleer deur 'n metode soortgelyk aan die "Aquifer Firm Yield Model" met die "saturated volume fluctuation"-vergelyking as die stogastiese (ewekansige) skakel tussen reënval, hervulling van die waterdraer en veranderinge in watervlakke. Die model maak ook gebruik van die "Cooper-Jacob"-vergelyking en inligting wat ingesamel is tydens die "Groundwater Resource Assessment Phase 2"-projek van die destydse Departement van Waterwese en Bosbou. Ontsoute waterbronne word gemodelleer as 'n bron met 100% sekerheid van lewering gegee teen spesifieke bedryfsvlakke, oor 'n drie-maandelikse tydperk.

Die model gebruik die balanseringsvergelyking om die lewering van die stelsel, waar ontsouting en grondwater eerste benut word, in ooreenstemming met minimum bedryfsvlakke, waarna oppervlak waterbronne benut word. 'n Kontrole is in die model ingebou om die ontsouting af te skakel indien 'n dam 'n gespesifiseerde kapasiteit bereik. Die model maak voorsiening vir 'n reeks alternatiewe waterbronne, gebaseer op die gebruiker se gedefinieerde invoer data. 'n Ontleding van 'n watervoorsieningstelsel word gedoen en die korttermyn en langtermyn versekerde lewering word grafies voorgestel, as hulpmiddels wat aangebied word vir die verbetering van bestuur van waterbronne.

ACKNOWLEDGEMENTS

Prof J. A. du Plessis, for being an invested study leader, instrumentally guiding my research and encouraging my self-development to reach new heights; I hold him in the highest regard and I am grateful for the opportunity to have completed my degree of Master of Engineering under his tutelage.

Dr R. Dennis, who with limitless patience and genuine eagerness explained groundwater concepts of the Aquifer Firm Yield Model and the Cooper-Jacob Model during the course of my research; I am grateful for this time shared and the information imparted.

Mr J. Hoffman, for sharing his Microsoft Excel skills, as well as the willingness to assist with methodologies of concepts, such as daily disaggregation of streamflow; I am thankful.

The Stellenbosch Municipality, for making it possible for me to complete my degree and for allowing me to use municipal data sets in my Thesis. Mr A. Kurtz and Mrs T. Carstens, at the Stellenbosch Municipality; a special word of thanks for assistance in a variety of ways.

GEOSS and GLS, consulting companies that undertook a variety of studies on behalf of the Stellenbosch Municipality, who readily provided valuable information; I am thankful for the inputs provided. Mr J. Conrad, Mr K. Murray and Mr D. Barrow at GEOSS, and Mr F. du Plessis at GLS, thank you for extending a helping hand.

Eberhard Braune and Prof. Y. Xu for their time and willingness to share information on groundwater and groundwater modelling.

Ms A. P. Prinsloo, for sharing her wisdom, conceptualization and linguistic (proofreading and editing) skills; I am grateful for the guidance.

My sincerest thanks and my earnest gratitude to everyone who had contributed to this thesis.

DEDICATION

I dedicate this Master of Engineering degree to the members of my family. My Father, Matt Braune, and my mother, Annegret Braune, who had both shown me, by their own example, that a good work ethic and a good attitude can result in some of the most beautiful things, and my sister, Christa Braune, for showing me that one can have fun in the process of reaching one's goals on the path to success.

I also want to dedicate this degree to everyone who had been a true friend during a challenging, but also enjoyable season, and who had kept me in their prayers. I dedicate this to my faithful Father in Heaven; whose steadfast love and goodness knows no bounds and whose every intention is for our greater good.

CONTENTS

Plagiarism Declaration.....	i
Abstract.....	ii
Opsomming.....	iii
Acknowledgements.....	iv
Dedication.....	v
Contents	vi
List of Tables	x
List of Figures	xi
List of Abbreviations and Acronyms	xiii
1 Introduction.....	1
1.1 Overview and Motivation	1
1.2 Aims and Objectives	2
1.3 Thesis Statement	3
1.4 Chapter Overview	3
2 Literature Review.....	4
2.1 Assessment of Water Resources Overview.....	4
2.1.1 Water Level Management.....	5
2.1.2 Yield of a Water Supply System.....	5
2.1.3 Stochastic Model of South Africa (STOMSA)	12
2.1.4 Daily Disaggregation of Streamflow	16
2.2 Surface Water Reservoir Simulation.....	17
2.2.1 Quaternary catchments.....	18
2.2.2 Surface Reservoir Inflow Sequences	19
2.2.3 Demand	20
2.2.4 Rainfall and Runoff.....	20
2.2.5 Evaporation	22
2.2.6 Surface-Area of Reservoirs	23
2.2.7 Seepage Losses	25

2.2.8	Overflow	25
2.3	Groundwater Yield Modelling	26
2.3.1	Classification of Aquifers	26
2.3.2	Hydrogeological parameters: Transmissivity and Storativity	27
2.3.3	Traditional Borehole Yield Determination	28
2.3.4	Factors Impacting Aquifer Yield	29
2.3.5	Groundwater Resource Assessments: GRA I & GRA II	29
2.3.6	Recharge	30
2.3.7	Aquifer Firm Yield Model	38
2.3.8	Cooper-Jacob Wellfield Model	44
2.4	Desalination and Reuse as augmentation resources	47
2.4.1	Desalination in South Africa	47
2.4.2	Reuse in South Africa	49
2.4.3	Future usage of desalination and water reclamation in South Africa	50
2.5	Optimization of Water Resources	50
2.5.1	South African Hydrological Modelling	51
2.5.2	Conjunctive Use Principles	52
2.6	Summary	53
3	Methodology	55
3.1	Overview	55
3.2	Generating Stochastic Monthly Streamflow	57
3.2.1	STOMSA Input File Preparation	57
3.2.2	STOMSA Output Files Processing	57
3.3	Disaggregation of Stochastic Streamflow	58
3.3.1	Streamflow classification according to Source Station	59
3.3.2	Disaggregation of Monthly Streamflow	62
3.4	Rainfall-Runoff Relationship	63
3.5	Surface Water Simulation	64
3.5.1	Inflow Streams	65

3.5.2	Net Evaporation	67
3.5.3	Demand	69
3.5.4	Seepage and Overflow	70
3.6	Groundwater Simulation	70
3.6.1	Quaternary Catchment Aquifer Water Balance	71
3.6.2	Borehole Interference Indication.....	81
3.7	Desalination and Reclamation	83
3.8	Conjunctive System Simulation.....	84
3.8.1	Operational Rules.....	84
3.8.2	Conjunctive Use System Yield	86
3.8.3	Long-term reliability	87
3.8.4	Short-term management	88
3.9	Summary of Excel Setup.....	89
4	Case Study: Stellenbosch.....	92
4.1	Background	92
4.1.1	Location	92
4.1.2	Overview of Municipal Water Resources	93
4.1.3	Aims and Objectives	95
4.2	Schematic Model of Stellenbosch Water Resources.....	95
4.3	Stochastic Streamflow Generation using STOMSA	96
4.4	Streamflow Disaggregation.....	97
4.4.1	Streamflow Classification	97
4.4.2	Stochastic Streamflow Disaggregation	100
4.5	Rainfall-Runoff Relationship.....	100
4.6	Surface Water.....	101
4.6.1	Idas Valley Dams	101
4.6.2	Inflow Streams into Idas Valley System.....	103
4.6.3	Inflow into Paradyskloof WTW.....	104
4.6.4	Net Evaporation	104

4.7	Demand	105
4.8	Groundwater Simulation	106
4.8.1	Quaternary Catchment Water Balance	107
4.8.2	Borehole Interference	115
4.9	Conjunctive Use System Simulation	117
4.9.1	Groundwater Yield	117
4.9.2	Inter-Basin Transfer from WCWSS	119
4.9.3	Surface Water	120
4.10	Yield Analysis and Discussion	120
4.10.1	Historical Firm Yield	120
4.10.2	Long-term Reliability	128
4.10.3	Short-term Management	139
4.11	Critical Evaluation of the Model	143
5	Conclusion	143
6	Recommendations	146
7	References	147
	Appendix A – User Guide	A-1
	Appendix B – Methodology Appendix	B-1
	Appendix C – Stellenbosch Case Study and Data	C-1

LIST OF TABLES

Table 2-1: Factors influencing firm yield	6
Table 2-2: Desalination plants commissioned as a result of drought periods	48
Table 2-3: Conjunctive interaction between surface water and groundwater	52
Table 2-4: The similarities and differences between Surface Water and Groundwater.....	53
Table 3-1: Monthly flow classes as percentages of MMR.....	60
Table 3-2: Daily streamflow distribution as percentage of total monthly flow	62
Table 3-3: Aquifer System in Equilibrium	74
Table 3-4: Components for baseflow separation at catchment scale	77
Table 3-5: Stressed aquifer system with increased discharge	79
Table 3-6: Pumping rate scenarios for abstraction yield.....	86
Table 3-7: Legend for the Excel workbook data transferral	91
Table 4-1: Hydrological characteristics of quaternary catchments.....	93
Table 4-2: Streamflow class boundaries as percentages of MMR for streamflow of October	98
Table 4-3: Monthly flow classes for G22F as percentage of MMR	99
Table 4-4: Main features of the Idas Valley Dams	102
Table 4-5: Monthly evaporation coefficients.....	104
Table 4-6: Monthly distribution of demand in percentage of annual demand.....	105
Table 4-7: Summary of functional municipal borehole data	107
Table 4-8: Hydrogeological data for quaternary catchments G22F and G22G	107
Table 4-9: Average monthly discharge and water level calculations for catchment G22F	109
Table 4-10: Baseflow separation for catchment G22F	111
Table 4-11: Long-term potential abstraction for October 1920 of historical sequence for G22F.....	113
Table 4-12: Input values of the historical yield analysis for the base scenario.....	121
Table 4-13: Sensitivity analysis results for Scenario 1, 2 and 3	124
Table 4-14: Sensitivity matrix of the historical firm yield for the base scenario.....	126
Table 4-15: Long-term analysis results for scenario 1, 2 and 3	134
Table 4-16: Input data of a drought situation for a short-term management graph	140

LIST OF FIGURES

Figure 2-1: Surface reservoir storage trajectory with critical period	4
Figure 2-2: Surface water reservoir water management levels	5
Figure 2-3: Draft-Yield Curve for historical yield analysis	8
Figure 2-4: Stochastic sequences ranked in descending order to determine the breakpoint Figure 2-5: Firm yield line for long-term stochastic analysis.....	9
Figure 2-6: Probabilistic storage projections for an example reservoir starting at 80% storage.....	11
Figure 2-7: Summary of requirements for historical and stochastic yield analysis	12
Figure 2-8: Primary catchments of South Africa (adapted from Huizenga et al.,2013).	19
Figure 2-9: Spatial distribution of rainfall across Southern Africa (DWA, 2018).....	21
Figure 2-10: The warming trend South Africa had experienced since 1961 (DWA, 2013).	22
Figure 2-11: Capacity-Depth curve for a surface water reservoir.....	25
Figure 2-12: Hydrological cycle with aquifer terminology (redrawn from Ponce, 2007).	27
Figure 2-13: Surface water and groundwater interaction (Dennis et al., 2012)	35
Figure 2-14: Hydrograph separation of surface flow and groundwater flow.....	38
Figure 2-15: Lumped-parameter box model of the AFYM.	40
Figure 2-16: Riparian zone and evapotranspiration extinction depth (Murray et al., 2012).....	42
Figure 2-17: The 3D nature of the cone of depression of a borehole (Murray et al., 2012)	44
Figure 2-18: Classes and connections of water resources models (Seago et al., 2008).	51
Figure 2-19: Proposed model components for conjunctive water resource use for municipal supply .	54
Figure 3-1: Data and components for yield assessment of a conjunctive use system.....	56
Figure 3-2: “ <i>STOMSA File Combiner</i> ” program user interface	58
Figure 3-3: Flow diagram of daily disaggregation of streamflow	58
Figure 3-4: Monthly medium-flow class with 4 daily distributions	61
Figure 3-5: Linear relationship of rainfall and runoff.....	64
Figure 3-6: Single-dam capacity-yield modelling components	64
Figure 3-7: Streamflow gauges in quaternary catchments	66
Figure 3-8: Input data and process to determine net evaporation	67
Figure 3-9: Surface area - capacity curve for a surface water reservoir	69
Figure 3-10: Cross section of a quaternary catchment aquifer system	71
Figure 3-11: Process followed during groundwater yield assessment	72
Figure 3-12: Process followed to determine stochastic recharge.....	73
Figure 3-13: Quaternary catchment aquifer system equilibrium state	76
Figure 3-14: Herold Baseflow Separation hydrographs.....	78
Figure 3-15: Water level fluctuation of natural and stressed aquifer system.....	80
Figure 3-16: Radii of influence of boreholes within a wellfield.....	83

Figure 3-17: Ranked stochastic sequences for 1 target draft	88
Figure 3-18: Reliability of supply and firm yield line for 5 target drafts.....	88
Figure 3-19: Short-term management curve	89
Figure 3-20: Excel workbook data transferral setup	90
Figure 4-1: Stellenbosch with adjoining quaternary catchments (Google Earth)	92
Figure 4-2: Stellenbosch water supply system setup	93
Figure 4-3: Schematic diagram of the simplified Stellenbosch water resource system.....	96
Figure 4-4: Streamflow gauging station G2H037 in quaternary catchment G22F (Google Earth)	98
Figure 4-5: Medium streamflow class for October with 10 daily distributions	99
Figure 4-6: Mean monthly RAIN-RUNOFF ratios.....	101
Figure 4-7: Surface Area-Capacity Curve for combined Idas Valley dams.	102
Figure 4-8: Stellenbosch annual water demand per source from 2006 to 2017 (GLS, 2018).....	105
Figure 4-9: Geological map (3318 Cape Town) of Stellenbosch with boreholes (Google Earth)	106
Figure 4-10: Water level response to recharge for catchment G22F and G22G.....	110
Figure 4-11: Hydrographs with surface water and groundwater contribution for G22F	112
Figure 4-12: Stressed aquifer system with minimum water level for G22F	114
Figure 4-13: Long-term potential abstraction from G22F and G22G.....	114
Figure 4-14: Borehole positions, names and radii of influence	117
Figure 4-15: Combined pumping rate less than average long-term potential abstraction rate.....	118
Figure 4-16: Combined pumping rate larger than average long-term potential abstraction rate	119
Figure 4-17: Daily Idas Valley dams' time-capacity graph with critical period for base scenario....	122
Figure 4-18: Base scenario Draft-Yield curve with firm yield point for historical sequence	123
Figure 4-19: Percentage increases and decreases in the yield at 100% structural capacity	127
Figure 4-20: Percentage increases and decreases in the yield at 100% diversion efficiency.....	128
Figure 4-21: Yields of 101 stochastic sequences for a target draft of 7 638 Mℓ/a	130
Figure 4-22: Cumulative monthly flows for the naturalized historical streamflow sequence	131
Figure 4-23: Base yields for stochastic sequences at different target drafts	132
Figure 4-24: Reliability of supply and firm yield line for scenario 1	133
Figure 4-25: Observed streamflow and naturalized streamflow	136
Figure 4-26: Ratio results of observed flow and naturalized streamflow before patching	137
Figure 4-27: Ratio results of observed flow and naturalized streamflow after patching	138
Figure 4-28: Reliability of supply curve for scenario 1 with patched streamflow.....	139
Figure 4-29: Probabilistic storage projection for Idas Valley dams with starting level at 50%.....	141
Figure 4-30: Probabilistic storage projection for Idas Valley dams with starting level at 40%.....	142

LIST OF ABBREVIATIONS AND ACRONYMS

3D	Three-dimensional
AADD	Annual Average Daily Demand
AFYM	Aquifer Firm Yield Model
CoCT	City of Cape Town
CMB	Chloride mass balance
CRD	Cumulative Rainfall Departure
DWAF	Department of Water Affairs and Forestry (up to 2009)
DWA	Department of Water Affairs (2009-2014)
DWS	Department of Water and Sanitation (2014)
FSC	Full Supply Capacity
ha	Hectare
GEOSS	Geohydrological and Spatial Solutions International (Pty) Ltd
GLS	Geustyn Loubser Streicher Inc (Pty) Ltd
km ²	Square kilometre
m	Meter
m ²	Square meter
m ³	Cubic meter
m ³ /a	Cubic meters per annum
mil	Million
m/mil m ³	Meters per million cubic meters
mbgl	Meters below ground level
mm/a	Millimetres per annum
NWRS	National Water Resource Strategy
SANCOLD	South African National Committee of Large Dams

SAWS	South African Weather Service
SRK	Steffen R Kirsten (Company)
STOMSA	Stochastic Model of South Africa
SVD	Singular Value Decomposition
SVF	Saturated Volume Fluctuation
UTM	Universal Transverse Mercator
UN	United Nations
WCWSS	Western Cape Water Supply System
WMA	Water Management Area
WHO	World Health Organisation
WL	Water Level
WRC	Water Research Commission
WRM2000	Water Resource Simulation Model 2000
WRYM	Water Resources Yield Model
WTW	Water Treatment Work
WWF	World Wildlife Fund

1 INTRODUCTION

1.1 Overview and Motivation

The need for water, especially in arid and semi-arid regions, necessitates integration of conventional and supplementary water resources to meet the growing demand. The United Nations (UN) forecasts that the world population will increase to 9.8 billion by 2050, putting additional pressure on already stressed natural resources, likely to result in increased service delivery failures.

According to the second edition of the *National Water Resource Strategy* (NWRS2), released in 2013 by the Department of Water Affairs (DWA), now referred to as the Department of Water and Sanitation (DWS), South Africa is the 30th driest country in the world and has a country-wide average rainfall of 450 mm/a compared to the average rainfall worldwide of 990 mm/a. Rainfall is influenced by seasonal variation, as well as unpredictable climate events. Furthermore, the country faces challenges related to water scarcity, such as high levels of evaporation, due to its hot climate, and water pollution, due to economic activities. It is understood that South Africa has less water per person than countries widely considered much drier, such as Namibia and Botswana (DWA, 2013b).

The Western Cape Province experienced a severe drought from 2014 onwards, reaching its peak in 2017, triggering a water crisis for the City of Cape Town Municipality (CoCT). Speculation concerning the cause and severity of the water crisis swirled in the public sphere and comprehensive analyses was conducted to establish the facts. Wolski (2018) concluded that this drought was indisputably caused by the El Niño phenomenon (periodic sea surface temperature fluctuations), with some weather stations recording the lowest annual cumulative rainfall since 1933. The following factors only exacerbated the water crisis further: population and water demand growth (tourism included); unreported agricultural use; invasive species depleting water in catchments; poor planning; mismanagement of the water supply system; and lack of foresight in development of new water resources. The crisis prompted emergency interventions to be implemented, such as water restrictions, tariff increases and other demand management schemes.

Surface water resources account for 77% of the country's bulk water supply, provided by rivers, large surface water reservoirs, dams (in some cases inter-basin transfer schemes), and irrigation return flow (11%). According to the South African National Committee on Large Dams (SANCOLD, 2019), the development of new surface water storage sites is not economically viable and surface water is highly climate sensitive. Thus, it would be most beneficial to augment surface water resources with alternative water resources. Current water resources used for augmentation of the water supply in South Africa include (DWA, 2013b): groundwater from boreholes (9%); and desalination of seawater (less than 1%).

The Karoo and Little Karoo regions predominantly use groundwater as its water supply and municipalities in these areas have already had to employ augmentation strategies, as existing resources

have been over-exploited and further dam development is not possible. Runoff has become insufficient in filling existing storage systems on a regular basis. Augmentation strategies included a water reclamation plant, commissioned in 2010, in Beaufort West, turning effluent into potable water, through reverse osmosis combined with other processes (DWA, 2013b).

Following the successful implementation of supplementary strategies, involving less climate sensitive water sources, development to utilize more of these sources, or larger quantities thereof for augmentation or conjunctive use, should be considered for all drought-susceptible regions in the country (DWA, 2013b). Conjunctive use employs the complimentary characteristics of resources to increase the yield and associated reliability of water supply systems (Pulido-Velázquez et al., 2006).

The Water Resource Yield Model (WRYM) is used by cities and other large water supply institutions to manage water resources (Nkwonta et al., 2017); however, local municipalities do not have the required capacity to perform such analysis and the process of outsourcing incurs excessive spending, without facilitating the development of internal capacity. The WRYM using a monthly time step is also more likely to overestimate the available water resources in smaller systems, due to the nature of runoff from smaller catchments.

Both consumer demand and rainfall vary on a daily basis. Therefore, the need to implement strategies based on daily yields, have to be developed for local municipalities, to carefully plan and diligently manage water resources to avoid crisis situations.

1.2 Aims and Objectives

The aim of this research is to address the challenges that changing climate conditions and lack of capacity has on local municipalities in arid regions. Therefore, an accessible, in-expensive and user-friendly water resource management tool, to equip local municipalities in the development of environmentally sustainable buffering strategies, have to be developed.

This can be accomplished by undertaking the following:

- Evaluating and comparing existing water resource management tools (Stochastic Model of South Africa, referred to as STOMSA, WRYM, AFYM and the Cooper-Jacob Model);
- Investigating relationships between various water resources for augmentation and conjunctive use;
- Developing a suitable model in Microsoft Excel (version 2016) to determine safe yields of combined water resource use based on a daily time step; and
- Testing the model on water supply systems to evaluate application potential for all local municipalities throughout the country.

1.3 Thesis Statement

The relationship between the deterministic (seasonal) and random variability of rainfall is deemed to be stochastic in nature. A generic stochastic model to assess the yield, based on a daily time step, during augmentation or conjunctive use of water resources was developed and tested on a water supply system, namely that of Stellenbosch Municipality, to determine its application potential for all local municipalities.

1.4 Chapter Overview

- Chapter 2 Literature Review: Assessment of Water Resources Overview; Surface Water Reservoir Simulation; Groundwater Yield Modelling; and Desalination and Reuse as Augmentation Source.
- Chapter 3 Methodology of Model Development: Data sourcing; Generating Stochastic Sequences (STOMSA); Disaggregation of Stochastic Sequences; Surface Water Simulation; Groundwater Simulation; and Simulation of Desalination and Reuse sources.
- Chapter 4 Case study on Stellenbosch Municipality: Data sourcing; Generating Stochastic Sequences (STOMSA); Disaggregation of Stochastic Sequences; Surface Water and Groundwater simulation; and Yield analysis for different scenarios.
- Chapter 5 Conclusion on the setup and performance of the stochastic, daily time-step model for the conjunctive use of surface water, groundwater and desalination and water reclamation for municipalities. Summary of findings from the Stellenbosch Municipality case study.
- Chapter 6 Recommendations to further enhance the range of applicability of the stochastic, daily time-step, conjunctive use model are suggested for the different components.

2 LITERATURE REVIEW

2.1 Assessment of Water Resources Overview

An effective water resource management strategy ensures that the balance between available water resources in a water supply system, and the demands and losses imposed on that system is maintained (Waldron and Archfield, 2006). A primary consideration in the water resource management strategy is the planning process, which includes assessing the supply capability of the system, and the associated reliability of this supply (Nkwonta et al., 2017). Therefore, a historical yield analysis, as well as stochastic yield analysis is undertaken. A historical yield analysis determines the historical capability of the system to satisfy the expected demand. A stochastic yield analysis determines the long-term reliability of the system to supply the expected demand. For arid to semi-arid regions calculating when critical periods will occur is essential, to avoid crisis scenarios that can lead to a variety of social and economic challenges. A further consideration in water resource management is that of management processes which are used for short-term decision making based on short-term analysis of possible hydrological events and the associated supply capability of the system.

The period, during which a reservoir is emptied, from a full supply capacity, to the minimum operating level, to the point in time where it is starting to fill up again (Figure 2-1), is termed a critical period (Basson et al., 1994). In drought-stricken regions critical periods can last as long as eight years. According to Basson et al. (1994), a longer historical record of streamflow (runoff) or rainfall, is necessary to accurately assess the reliability of a water supply system when a longer critical period is experienced. Basson et al. (1994) developed a methodology to primarily assess surface water resources using a critical period approach; however, this methodology can also be applied to assess a number of resources if time-series data is available.

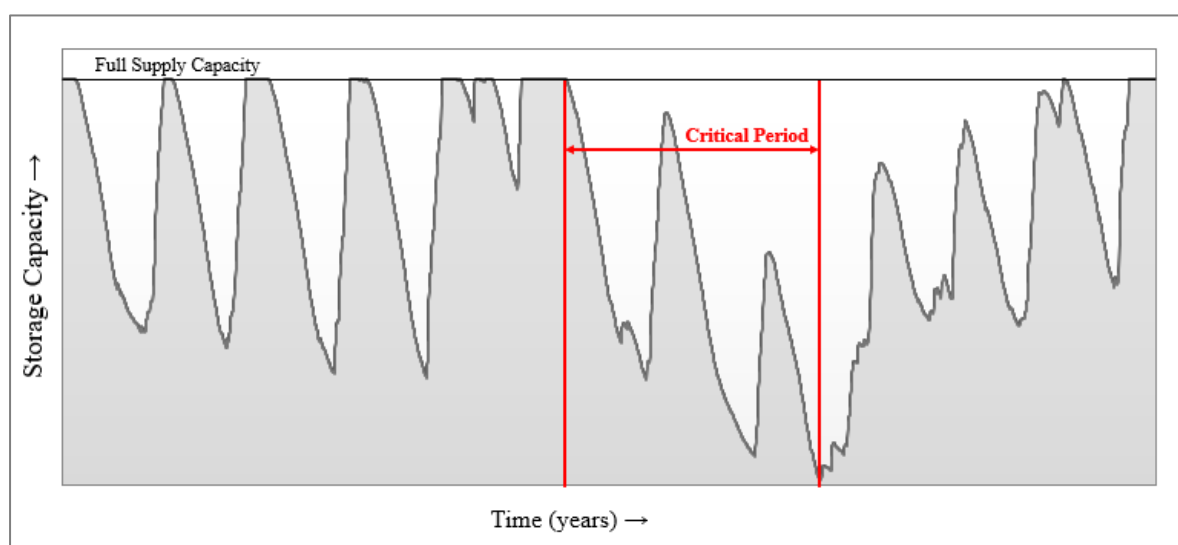


Figure 2-1: Surface reservoir storage trajectory with critical period

2.1.1 Water Level Management

The surface water management levels were employed by Basson et al., (1994) while developing the critical period yield analysis method. The different reservoir surface water management levels are illustrated in Figure 2-2.

The full supply level indicates that the reservoir is at full storage capacity (100%). Water above the full supply level is considered as overflow volume, which flows from the reservoir basin through a spillway or in some cases the non-overspill crest. The active operating storage volume is the amount of water between the full supply level and the minimum operating level. Water under the minimum operating level is defined as reserve storage, consisting of the dead storage volume and environmental requirements (including sediment accumulation). The lowest abstraction point is situated at the minimum operational level.

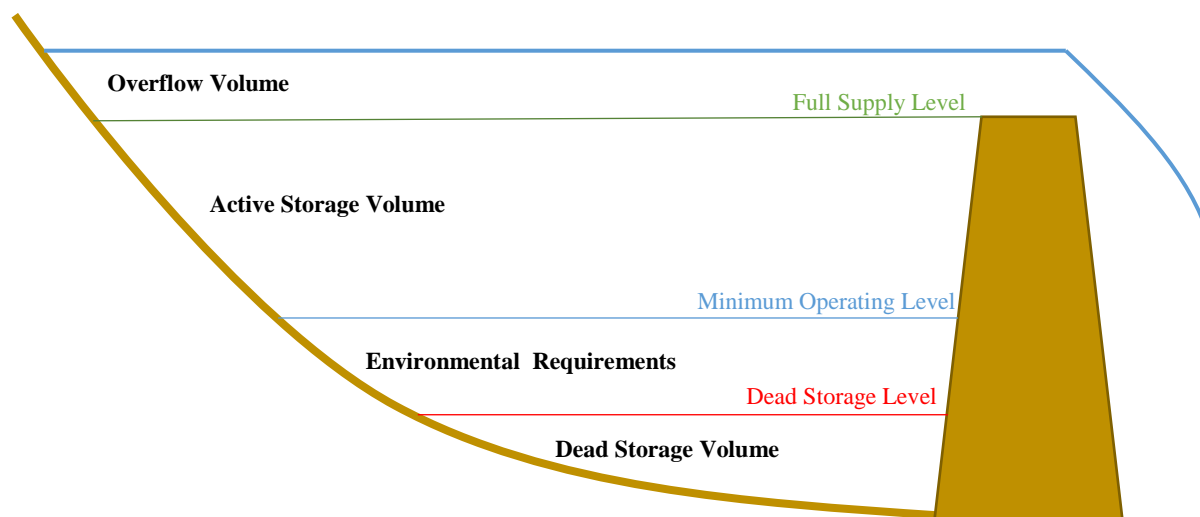


Figure 2-2: Surface water reservoir water management levels

2.1.2 Yield of a Water Supply System

The yield is the amount of water that a water supply system can provide annually. Methodologies to assess the water supply system capacity, also referred to as yield, are used to aid water providers in decision-making processes on policy, operating procedures and strategies for allocation of water amongst users. The main objective of a yield analysis is to determine the yield potential of a system under various physical constraints (reservoir size, initial storage level, inflow hydrology, target draft and operating policy, etc.). Basson et al. (1994) studied international literature on assessing the capabilities of surface water resources, utilized by a supply system, and the associated reliability thereof, after which they developed standardised methods of analyses, still in use today, to determine the yield of a system as applicable in South Africa. There are two methods used to determine time-dependent capacity characteristics of a water supply system, as well as the associated reliability of the supply in question, namely the historical yield and the stochastic yield analysis (Seago & McKenzie, 2008).

Firm yield is the maximum annual draft for a specified full supply capacity (FSC) that can be sustained by an inflow sequence of given length, without incurring a single failure (Du Plessis, 2017). In other words, the firm yield is the maximum expected annual withdrawal (demand) for a specified FSC that can be sustained over a particular period of time, without failing.

The firm yield is dependent on the following factors (Basson et al., 1994):

- FSC of the reservoir system;
- Inflow sequence used (processed streamflow records);
- Length of inflow sequence (duration of streamflow records);
- Target draft (estimated annual withdrawal to supply expected demand); and
- Operational policy (minimum operating level of dam).

The influence of each of the above-mentioned factors on the firm yield is summarized in Table 2-1.

Table 2-1: Factors influencing firm yield

Factor	Influence	Firm Yield Result
Full Supply Capacity (FSC)	decrease in capacity	decrease in yield
Number of streamflow sequences	increase in number of streamflow sequences used	decrease in yield
Inflow sequence length	longer sequence length	decrease in yield
Target draft	if target draft < firm yield if target draft > firm yield	yield = target draft decrease in yield compared to base yield
Operating policy	higher min. operational level	decrease in yield

2.1.2.1 Historical Yield Analysis

A historical yield analysis gives an indication of the supply capability of a water supply system to satisfy the target drafts required over a specific period of time. It is established by evaluating a historical streamflow sequence, which is a record of streamflow measured at a specific source station over a period of time. A historical streamflow sequence is generated using input data recorded at inflow gauges (source stations), situated across the country. Input data is then patched, extended and naturalized through deterministic methods, as applied by the Water Resource Simulation Model 2000 (WRSM2000), available at the Water Research Commission (WRC) online resource centre (Bailey et al., 2019).

Patching of data entails identifying errors and artificially correcting them with deterministic methods. Deterministic methods involve cause-dependant processes. Typically, rainfall data in South Africa dates back to the early 1900s and is reasonably reliable, whereas recording of streamflow data only started in the 1950s and is less consistent, and only available at a limited number of locations (Blersch & Du Plessis, 2017). Rainfall-runoff models make it possible to generate long-term flow sequences for any location, provided there is sufficient recorded rainfall data available. Naturalization is the process whereby natural river streamflow is simulated by removing any manmade influences, such as agricultural activities and storage reservoirs. The established historical streamflow sequence, used for simulations to determine yield provided by the WRC (2012), can be accessed at their online database. It can be used to assess the supply capabilities of any water supply system in South Africa.

To determine the supply capabilities of a water supply system more accurately, the following concepts are investigated: historical firm yield; average yield; secondary yield; and base yield. Du Plessis (2017) defines historical firm yield as the maximum annual draft for a specific full supply capacity (FSC), without incurring a single failure of supply. Average yield is the average amount of water that can be provided in response to a specified monthly draft, calculated with values obtained over a 12-month period. Secondary yield is defined as the yield that could additionally be stored in off-channel or downstream dams and is deemed as the water spilling from the dam. The non-firm zone describes the region between the base yield and the average yield. The non-firm yield indicates the yield ranges in which the target draft can still be satisfied frequently, but not continuously. Base yield is the minimum annual withdrawal for a specific FSC that can be sustained, while attempting to satisfy a particular draft using a particular inflow sequence.

When the target draft is less than the firm yield, the base yield is equal to the target draft, but when the target draft exceeds the firm yield, the base yield decreases due to one or more periods of failure to supply. The number of these failure periods and their intensity increase as the target draft increases (Du Plessis, 2017). The base yield might break away from the target draft before the maximum base yield has been reached. This occurs in instances where the storage to inflow volume ratio of a reservoir is either large for shallow dams or where the storage to inflow volume ratio is very small (baseflow of the river contributes an unusually large part to the yield). To determine the maximum and minimum amounts of water that can be annually withdrawn from a reservoir while remaining operational, the historical firm yield point needs to be established. The historical flow sequence is used to perform a simulation, using different target drafts increased in increments to determine their associated yields. The values of the incrementing target drafts are then plotted against their associated yields on a draft-yield curve, illustrated in Figure 2-3. The historical firm yield point is found where the first variance between target draft and yield occurs.

According to Basson et al. (1994) historical sequences are relatively short, therefore the historical firm yield can only be considered as a representative supply capability. Increased sequence length (years) will increase the number of failures observed. When stochastic sequences are included, they can also (instead of extending) be used to complete the data set and assess the reliability of supply.

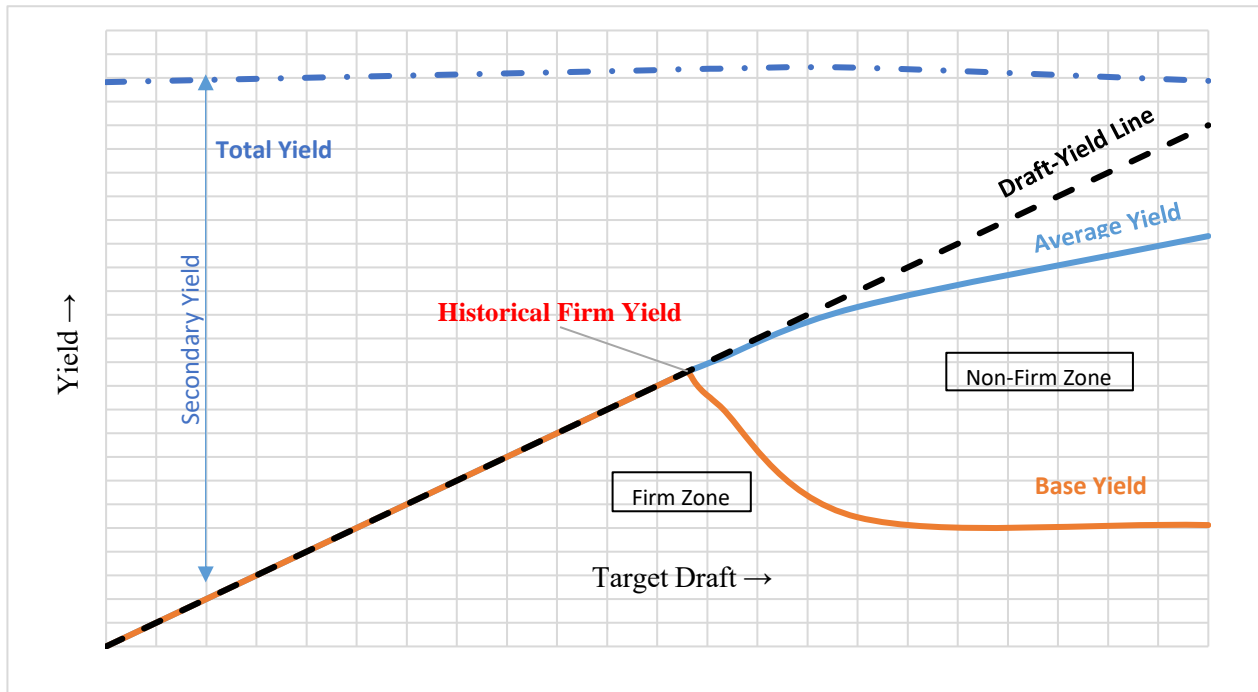


Figure 2-3: Draft-Yield Curve for historical yield analysis

2.1.2.2 Stochastic Yield

A stochastic yield analysis indicates whether the capability of the water supply system can be depended upon and is referred to as the reliability of supply. The reliability of supply is determined through the use of stochastic sequences. Stochastic yield analysis can be divided into two categories, namely the long-term and the short-term yield analysis. Long-term yield analysis is used for future planning (forecasting), while a short-term stochastic yield analysis is used for real-time operation and management decisions.

Stochastic sequences are based on random variations of the historical streamflow sequence, while retaining deterministic historical characteristics (seasonality). To generate stochastic streamflow sequences the Stochastic Model of South Africa (STOMSA) is used (further discussed in section 2.1.3). Stochastic sequences propose a variety of alternative scenarios to the historical streamflow sequence.

Long-term stochastic analysis is used to determine the base yields for different target drafts, using stochastic sequences and starting the simulation at FSC (Basson et al., 1994). The calculated base yields of each sequence are then ranked on a graph in descending order, as illustrated in Figure 2-4. The point on the graph where the first descent appears represents the point before the first failure occurs, which

is defined as the break point. The break points of the different target drafts are plotted on a second graph and then connected to form the firm yield line as illustrated in Figure 2-5. The firm yield line indicates the reliability of supply for different target drafts. Depending on the sequence length, the reliability of supply for a specific number of years can be determined in this way. A long-term analysis is most sensitive to the lowest streamflow sequence. Therefore, to reach reasonable convergence in the firm yield, Basson et al. (1994) suggests that at least 40 streamflow sequences of the total available length are used in the analysis.

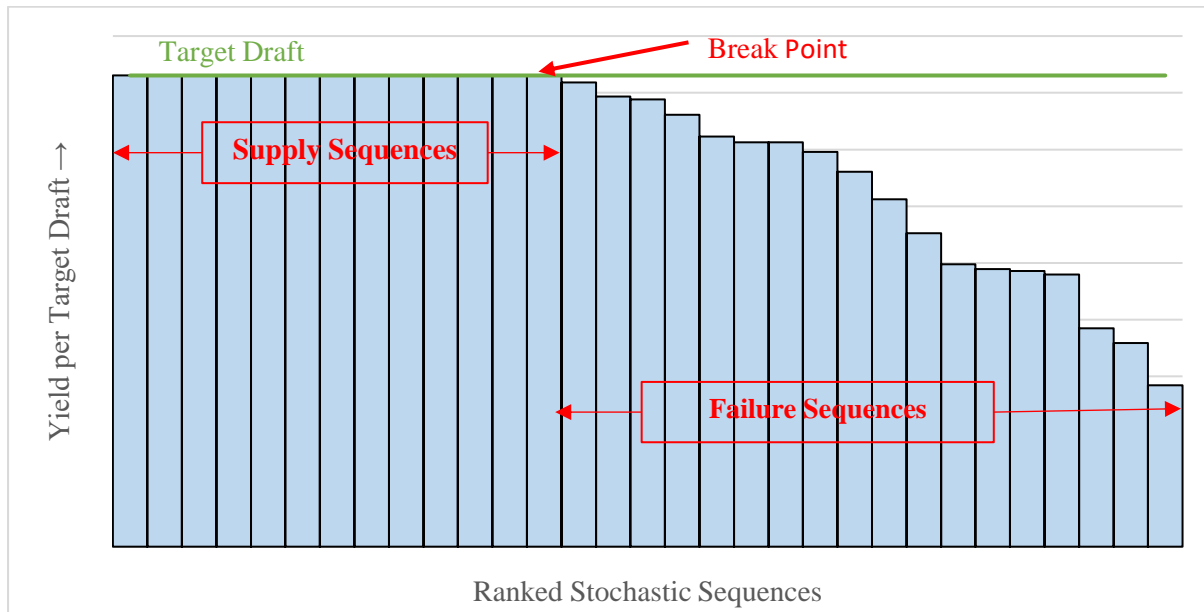


Figure 2-4: Stochastic sequences ranked in descending order to determine the breakpoint

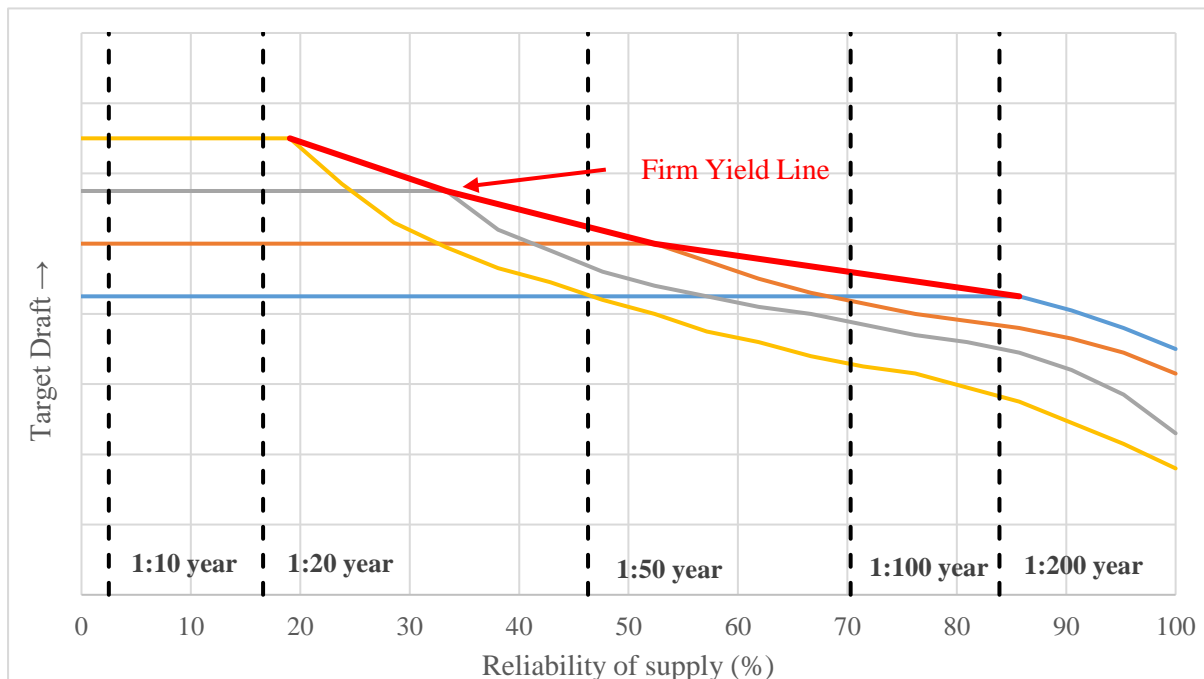


Figure 2-5: Firm yield line for long-term stochastic analysis

The number of sequences indicating a failure of supply, divided by the total number of stochastic sequences used in the simulation, is known as long-term risk of failure. While the reliability of supply is the converse of risk of failure, and is calculated with Equation 2-1 adapted from Basson et al. (1994).

$$\text{Reliability of Supply (\%)} = 1 - \frac{\text{Number of Failure Sequences}}{\text{Total Number of Sequences}} \quad (2-1)$$

The recurrence interval of failures is calculated with Equation 2-2. The recurrence intervals indicate the number of years during which a failure is most likely to occur. For example, a recurrence interval of 1:50 indicates that one failure event (at a specific target draft) would most likely occur in the span of 50 years. The record length, indicated as a number of years together with the reliability of supply, is required to calculate the recurrence interval.

$$\text{Recurrence Interval of Failure} = \frac{1}{\left[1 - (\text{Reliability of Supply})^{\frac{1}{\text{record length}}}\right]} \quad (2-2)$$

Short-term stochastic analysis uses the same stochastic sequences to determine reliability of supply, with different starting supply capacities (rather than different target drafts) as input data at the beginning of the simulation. Also, more sequences (5 x more than the number used in the long-term analysis) of shorter length are used in these simulations (Basson et al., 1994). The length of these stochastic sequences, span over a period of approximately 5 years corresponding to decision making periods for large water resource systems (such as the Vaal river). For smaller water resource systems management periods can be as short as 1 to 2 years (single dam scenarios). The stochastic short-term analysis is incorporated in the operational and management analysis, to enhance and verify yield capabilities of the system during decision-making periods (Basson et al., 1994).

According to Basson et al. (1994), the operational and management analysis includes simulation and optimization techniques in which different decisions can be evaluated for their impact on the yield of the system. Water allocation decisions are primarily undertaken on a seasonal or annual basis. Between the decision dates, the behaviour of the system is monitored to detect any change in expected system performance. To aid the evaluation of the system performance, operational guidelines are developed, through which the system manager can gauge whether the water drawdown in the system is more or less severe than expected. For instance, when a lack of water availability is detected (by simulating storage behaviour), a decision can be made to introduce water restrictions or to augment the water supply with alternative short-term water resources. Probabilistic management curves are developed to simulate the system behaviour into the future (Basson et al., 1994). These probabilistic management curves are generated by obtaining different plausible storage trajectories of the reservoir for different stochastic sequences of shorter length (as used in a short-term stochastic analysis). The simulation process would simulate the expected performance in meeting a specific target draft over the decision-period time horizon starting at the observed storage level.

From the many storage projections obtained from the short-term stochastic analysis, box plots of the storage levels for each simulation period can be derived. These box plots of the storage level form the probabilistic storage projections that the system manager can use as an operational guideline. Over the decision period, the system manager can plot the actual system storage on the probabilistic storage projections (Basson et al., 1994). The actual system storage behaviour can be compared to the expected system behaviour, this will help to evaluate whether the system is drawn down more than expected or whether the system is recovering from a draw down position faster than expected. By monitoring the system in this manner, it can be decided whether to impose or lift a restriction or curtailment policy. Figure 2-6 illustrated the probabilistic storage trajectory of an example surface water reservoir in a summer rainfall region, with a box plot for exceedance probabilities associated with each storage trajectory (Basson et al., 1994).

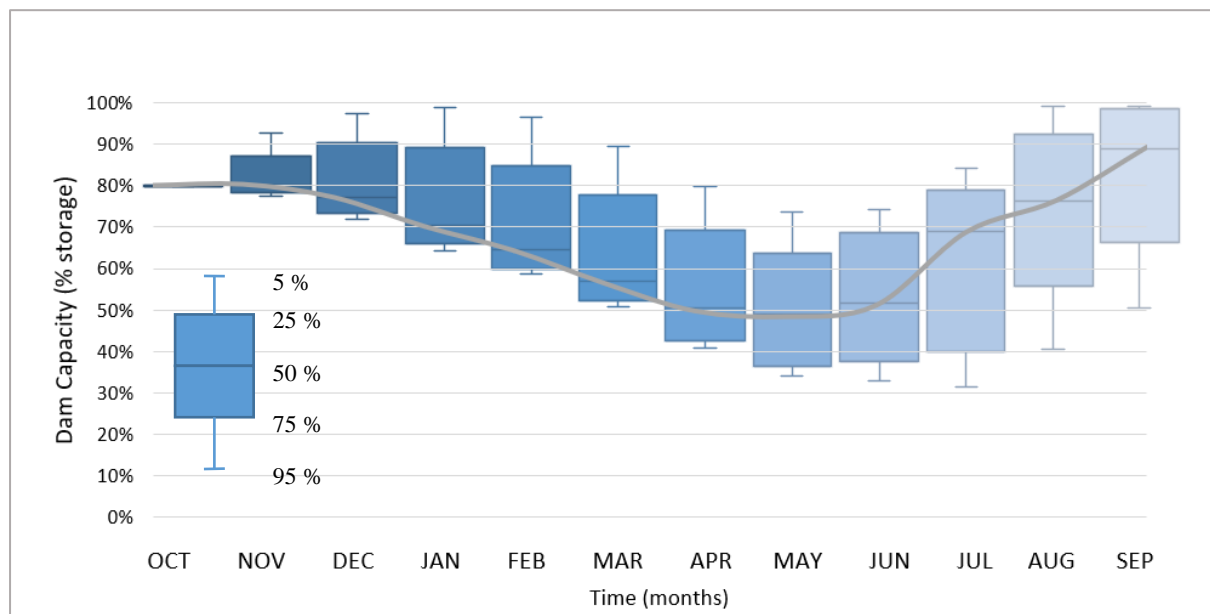


Figure 2-6: Probabilistic storage projections for an example reservoir starting at 80% storage

2.1.2.3 Summary of Yield Analyses

Historical analysis is undertaken to calculate the historical firm yield, average yield, secondary yield and base yield, of a historical sequence. The historical analysis is used to establish the historical firm yield point indicating the capability of the water supply system to satisfy the expected demand. A historical streamflow sequence is used to simulate the behaviour of the system. The simulation is dependent on FSC and different target drafts as input data at the start of the simulation.

Stochastic analysis is undertaken to calculate the long-term and short-term reliability of the system's capability to supply. Stochastic sequences are used to simulate the behaviour of the system. The long-term reliability simulation requires a FSC at the start of the simulation, different target drafts as input data, and a sequence length of approximately 64 years and 41 sequences (Basson et al., 1994). The short-term reliability simulation requires only one target draft, but different supply capacities as input

data at the start of the simulations, a sequence length of approximately 5 years and 5 times the number of sequences used in the long-term simulation (205 sequences). Figure 2-7 indicates the differences between historical and stochastic yield analysis.

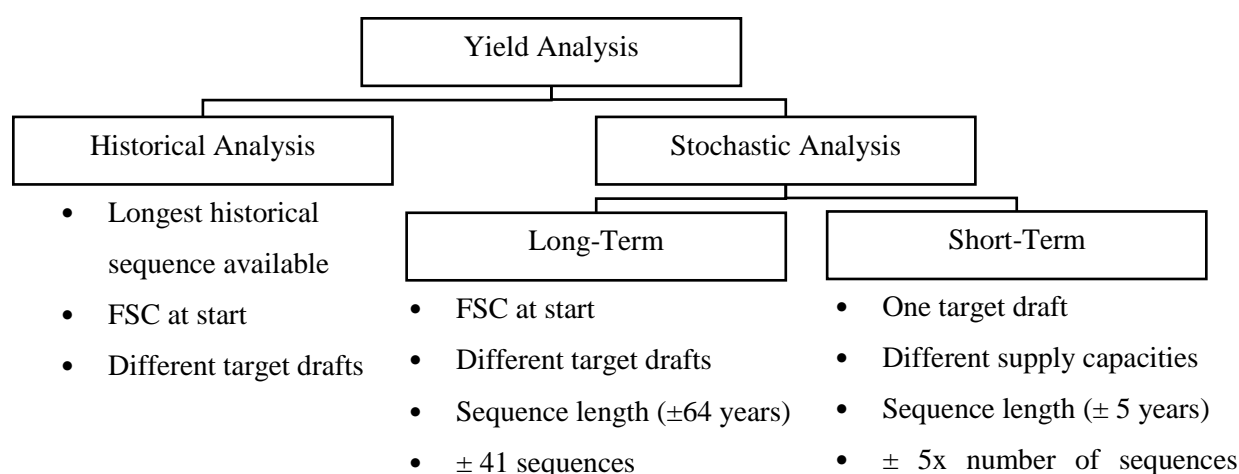


Figure 2-7: Summary of requirements for historical and stochastic yield analysis

2.1.3 Stochastic Model of South Africa (STOMSA)

According to Maass and Du Plessis (2017), there are a number of stochastic models that exist in the field of hydrology. They differ from each other in that they use different mathematical approaches. According to Haan (1997), as cited in Maass and Du Plessis (2017), stochastic models which solely use historical sequence statistics to generate stochastic sequences provide unrealistic results as no natural occurring hydrological event would repeat itself. Purely random stochastic models are considered to be the most simple models, as simulated events are independent of each other and only the probability distribution of the event is known (Xu, 2002). The purely random distribution does not accurately describe the existing hydrological deterministic relationships. Autoregressive stochastic models have a random element but also take similar statistics between consecutively simulated events into consideration (Maass, 2017). According to Maas and Du Plessis (2017) a stochastic model that uses historical statistics to generate random values, while applying cross-correlation, provides the most realistic and varied stochastic flow sequences for computations.

The Stochastic Model of South Africa (STOMSA) meets all the criteria for generating stochastic streamflow sequences as mentioned above. According to Maas and Du Plessis (2017), STOMSA is a monthly, multi-site, stochastic model that serves as a generic streamflow generator which is technically sound and versatile in nature. STOMSA is both used as a stand-alone and built-in model to generate stochastic streamflow sequences. These streamflow sequences are used as input data for the WRYM when analyses are undertaken. The WRYM produces annual time step sequences which are then disaggregated into monthly time steps.

The first step when generating stochastic streamflow is to capture the many statistical properties inherent to the natural historical streamflow sequence of the water resource being assessed. The

appropriate statistical distribution models and parameters must be identified to achieve this. These historical statistical parameters are contained in a PARAM.DAT data file and include marginal distribution, serial correlation and cross-correlation. Annual stochastic sequences are generated after which they are disaggregated into monthly flows.

2.1.3.1 Marginal Distribution

According to Van Rooyen and McKenzie (2004), the marginal distribution of a historical streamflow sequence represents the relationship between all the annual flows when ranked in ascending order. Annual streamflow values (volume) are plotted against the probability of exceedance (percentage) in a graph to indicate the marginal distribution. The marginal distribution can also be produced on a transformed graph, by plotting the probability of exceedance in terms of standard deviations from the mean against the annual flows. The objective is to find a marginal distribution that can be used to transform the annual historical streamflow to a volume that resembles normal distribution most accurately. For this purpose, four curves will be depicted on both the marginal distribution graph and the transformed graph, representing the results of an alternative marginal distribution model. The following parameter distributions are used respectively (Van Rooyen and McKenzie, 2004):

- 3-parameter Log-normal (LN3);
- 2-parameter Log-normal (LN2);
- 4-parameter Bounded (SB4); and
- 3-parameter Bounded (SB3).

The Log-normal distribution:

$$y = \gamma + \delta \ln(x - \xi)$$

The Bounded distribution:

$$y = \gamma + \delta \ln(x - \xi) / (\lambda + x - \xi)$$

Where:

x = an annual streamflow variant

y = the transformed variant

γ (Gamma), δ (Delta) = distribution parameters

ξ (Xi) and λ (Lambda) = distribution parameters and where $\xi < x < \lambda$

The selection of distribution is based on various statistical criteria, which are described by the *Hill Algorithm* that is based on the *Johnson Transform Suite* (Hill, Hill and Holder, 1976).

More information on the statistical criteria and algorithm can be found in *Stochastic Modelling of Streamflow* (DWAF, 1986).

2.1.3.2 Serial Correlation

After normalizing the annual historical streamflow for a particular sequence, it is analysed based on an Auto Regressive Moving Average (ARMA) model. According to Van Rooyen and McKenzie (2004), ARMA (ϕ , θ) is a linear stochastic difference equation to determine the time-series model for the parameter set, which most accurately represents the serial correlation exhibited by the data. The serial correlation characteristics of a particular sequence are depicted on a correlogram. The most appropriate of nine ARMA models may be selected, based on a set of standard selection criteria applied in STOMSA. These models are: ARMA(0,0); ARMA(0,1); ARMA(1,0); ARMA(1,1); ARMA(0,2); ARMA(1,2); ARMA(2,0); ARMA(2,2); and ARMA(2,2).

The ARMA (ϕ , θ) time series model is defined as follows:

$$x_t - \phi_1 x_{t-1} - \phi_2 x_{t-2} = a_t - \theta_1 a_{t-1} - \theta_2 a_{t-2};$$

Where:

$x_1, x_2 \dots x_n$	=	stationary sequence centered (zero mean) normal variates
a_t	=	sequence of independent random variables with a normal distribution having zero mean and constant variance
ϕ_1 and ϕ_2 (Phi 1 and 2)	=	autoregressive model parameters
ξ (Xi) and λ (Lambda)	=	distribution parameters and where $\xi < x < \lambda$
θ_1 and θ_2 (Theta 1 and 2)	=	moving average model parameters

Once STOMSA has selected the appropriate time-series model, it is applied to the normalized historical streamflow sequence to eliminate its serial correlation characteristics. The result is a corresponding set of normalised residual annual historical streamflows (Van Rooyen and McKenzie, 2004).

2.1.3.3 Cross-Correlation

When stochastic streamflow data is generated for two or more water sources within the same catchment simultaneously, the inherent relationship between the flows of these water sources must be maintained. The generated sequences must produce correlating characteristics for the sub catchments, as the interdependence of the flows need to be preserved, particularly for the yield analysis of systems with inter-basin transfers. A technique called *Singular Value Decomposition* (SVD) is applied to the normalised residual annual historical streamflow data, to determine cross-correlations that occur between flows from multiple catchments. The result is a set of matrices, used to re-generate the cross-correlation dependencies among all the runoff sequences that are considered for a water resource system. The matrix parameters along with the marginal distribution results and serial correlation analyses are written to a stochastic parameter file (PARAM.DAT file). The file, together with complex computational routines, is used to generate stochastic streamflow sequences (Van Rooyen and McKenzie, 2004).PARAM.DAT File

The PARAM.DAT file is created by a program called CRSMK6. The file includes data on the calculated marginal distribution of the annual flows, as well as the parameters applied in the process of normalizing residual annual historic streamflow. CRSMK6 computes the inter-dependence between the annual flow residuals from the various flow stations, using the fitted ARMA (ϕ , θ) model, parameters (ϕ , $\theta = 0, 1$ or 2), and white noise residuals. The calculation is done under the assumption of normality of the residuals so that the cross-covariance matrix is the measure of the extent of the inter-dependence of the residuals. The cross-covariance matrix is then decomposed into its square root, using SVD. Thus, the PARAM.DAT file contains all the information relevant to generating accurate cross-correlated annual flow sequences, with the correct serial dependence structure (DWA, 2010). Stochastic annual streamflow sequences are generated by incorporating the PARAM.DAT files along with computational routines.

2.1.3.4 Monthly disaggregation

According to Van Rooyen and McKenzie (2004), disaggregation of annual streamflow values into monthly streamflow values is an acceptable practice as it does not require the development of a complex stochastic flow generator, and it was found that this method results in realistic monthly flow values. The disaggregation process involves the identification of a strategic gauge within a catchment, from which historical monthly distribution records are obtained and then applied to disaggregate generated annual flow values. Each year that forms part of the generated annual flow sequence is matched with a hydrological year in the historical sequence of the gauge, using the least square fit-analysis. The least square fit-analysis is performed by comparing the historical and generated streamflow sequences so that a single year with the least amount of difference, between historical and generated annual flow values, can be identified. The monthly distribution values of the gauge and the identified historic year is then used to distribute the generated annual flow value into monthly flow values.

In the case of various flow gauges situated in different catchments, the identified historical year and associated monthly distribution is used to disaggregate the annual generated flows in each catchment (Van Rooyen and McKenzie, 2004).

According to Waldron and Archfield (2006) drinking-water supply systems should be analysed on a daily basis, as withdrawals from a drinking-water system occur on a daily basis. It is also necessary to analyse the daily supply capacity during drought conditions. Thus, stochastic streamflow generated with monthly time steps, would have to be disaggregated further into daily flow values for a water supply system analysis to be performed daily.

2.1.4 Daily Disaggregation of Streamflow

Generating daily data for streamflow is particularly difficult as linear responses to channel characteristics and non-linear responses to groundwater flow interactions are not easily expressed through auto-correlation. Therefore, to model daily streamflow data, monthly values would have to be disaggregated into daily time steps (Xu, 2002).

Acharya and Ryu (2014) developed a simple linear and deterministic technique to disaggregate monthly stream flow volumes into daily values, which was tested in an arid to semi-arid region in the United States of America. The effectiveness of the method was demonstrated through its application at both regulated and unregulated waterways located in the states of Idaho and Wyoming.

A target station (point of investigation) and a source station (inflow gauge with daily historical flow data) are identified within a specific catchment. Streamflow at the target station is recorded on a monthly basis, while streamflow at the source station is recorded on a daily basis. Streamflow records of inflow gauges in a catchment are customarily supplied in monthly time steps to eliminate excess information, which complicates processing for a variety of purposes. It is accepted that the monthly flow values at the source station are the sum of all daily flows. To determine daily flow volumes at the target station, the monthly counterparts at the source station are selected for disaggregation, based on minimum error criteria. Minimum error criteria involve using flow data recorded within a 3-month window, to establish seasonal patterns and to closely investigate variability of streamflow among embedded months. Proportional adjustments are often required to be able to estimate daily flow more accurately during the disaggregation process (Kumar et al. 2000). Using a root mean square error method, the month (within the 3-month window) reflecting flow data at the source station most accurately is selected, and the corresponding daily distribution is calculated to disaggregate the target station's monthly time steps into daily time steps. This approach is capable of generating extreme values that were previously not detected in historical records. The model is transparent, user friendly, less energy-intensive and time-consuming. It bridges the gap among interdisciplinary water research activities, especially concerning impacts of hydrologic events, possibly driven by extreme weather variability and changing climate conditions (Acharya and Ryu, 2014).

Acharya and Ryu (2014) recommended that the historical streamflow is checked for errors and patched appropriately before commencing with disaggregation. The simple model is widely applicable, as it was written in Excel and can be used to disaggregate any streamflow in a catchment given a relevant source station.

Hoffman (2019) proposed a daily disaggregation method that is similar to that of Acharya and Ryu (2014), but the observation window is wider to do a more detailed investigation into flow scenarios. The historical streamflow sequences for a number of years are obtained and the streamflow data is grouped according to the respective months of the year. For example, if the observation window is 10

years, there will be 10 historical sequences for each month. The accumulated flow data for each month is then investigated to identify typical distributions and streamflow fluctuations. The process results in different ranges of typical distributions for the month, which are simplified by way of categorization into 3 classes, namely high flow, medium flow and low flow scenarios. The three types of flow classes for each month have associated daily distributions as percentage of the monthly flow.

The flow classes and daily distributions are then used to disaggregate monthly inflow sequences to daily inflow sequences. The assumption is that the bigger the observation window is, the more accurate the assessment of the yield will be.

Having considered components and processes followed in stochastic streamflow generation, as well as streamflow disaggregation, the surface water reservoir simulation modelling components have to be established on daily time steps.

2.2 Surface Water Reservoir Simulation

Although perennial rivers in South Africa exhibit recurring streamflow, due to rainfall-runoff and other contributing factors, there is a sizeable amount of variability between high and low flows throughout the year. Seasonal rivers in the country also indicate large variability between high and low flow periods. Low flow or no-flow periods do not support sustainable water use. Therefore, surface water reservoirs have been constructed at suitable locations throughout the country, to capture and store water during all flow ranges. This is to be distributed to end-users over an extended period of time, satisfying the demand at a pre-determined risk. To determine the ability of the reservoirs to satisfy these demands, the yield of a reservoir (water supply system) is assessed through modelling. The modelled data informs water providers of the current status of the system as well as possible future scenarios, which results in more effective water resource management strategies, including potentially averting crisis scenarios.

The iterative process used to determine system yield entails simulation of the natural behaviour of the water supply system. To simulate the storage behaviour of a single dam, relationships between inflow characteristics, reservoir capacity, downstream demand, net evaporation and spillage have to be established (Waldron and Archfield, 2006). The single components can be evaluated separately and then added together for each time step. The dam balancing equation is used to simulate the storage behaviour of a dam and is based on the principle of water mass balance. Performing a mass balance requires that inflows, dam characteristics and outflows are considered as components, for calculating yield on a daily basis.

Equation 2-3 (adapted from Waldron and Archfield, 2006) shows the dam balancing equation with daily time steps:

$$S(t + 1) = S(t) + Q(t) - D(t) - E(t) - L(t) - O(t) \quad (2-3)$$

Where:

$S(t+1)$ = Storage capacity at the end of the day (Mℓ)

$Q(t)$ = Storage capacity at the beginning of the time step (Mℓ)

$S(t)$ = Inflow volume per time step (Mℓ/day)

$D(t)$ = Demand per time step (Mℓ/day)

$E(t)$ = Evaporation losses per time step (Mℓ/day)

$L(t)$ = Losses due to seepage and environmental releases per time step (Mℓ/day)

$O(t)$ = Overflow/ spillage losses (Mℓ/day)

The firm yield estimator model of the Massachusetts Department of Environmental Protection, developed by Waldron and Archfield (2006), utilized the mass balance principle to determine the maximum average daily withdrawal rate from a surface water reservoir.

Inflow sequences and losses, in terms of modelling considerations, as well as how to assess them on a daily basis (measured in daily time steps) are discussed 2.2.1 to 2.2.6.

2.2.1 Quaternary catchments

A catchment is an area from which any rainfall will drain into multiple, or only parts of, watercourses, through surface flow to one or more common points (DWA, 2013b). The South African landscape is currently divided into 1946 quaternary catchments. A quaternary catchment is defined by Dennis et al. (2012) as a fourth order catchment in a hierarchal classification system, in which a primary catchment is the major unit. Quaternary catchments constitute the most fundamental, but adequately detailed, level of operational catchment for general planning purposes (Midgley et al., 1994). A quaternary catchment is delineated through careful consideration of topographic boundaries, such as mountain ranges and the unique climate and rainfall characteristics in each catchment. Input data derived from quaternary catchments include the following: Mean Annual Precipitation (MAP), Mean Annual Runoff (MAR), rainfall zone, evaporation zone and surface area (Vegter & Pitman, 2003). Regional surface and groundwater studies, such as the Groundwater Resources Assessment Phase II (GRA II) and the WR2012, make use of quaternary catchment boundaries to group information in a readily available format. Delineation of primary catchments in South Africa (DWA, 2000) is illustrated in Figure 2-8. The objective of developing and refining quaternary catchments is to be able to perform spatially comparative simulations to assess the following: streamflow, baseflow, total runoff, impacts of land use and change on hydrological responses, as well as the impact of changing climate conditions on hydrological responses of crop yields, sediment yield, irrigation water demand (Schulze et al., 2007).

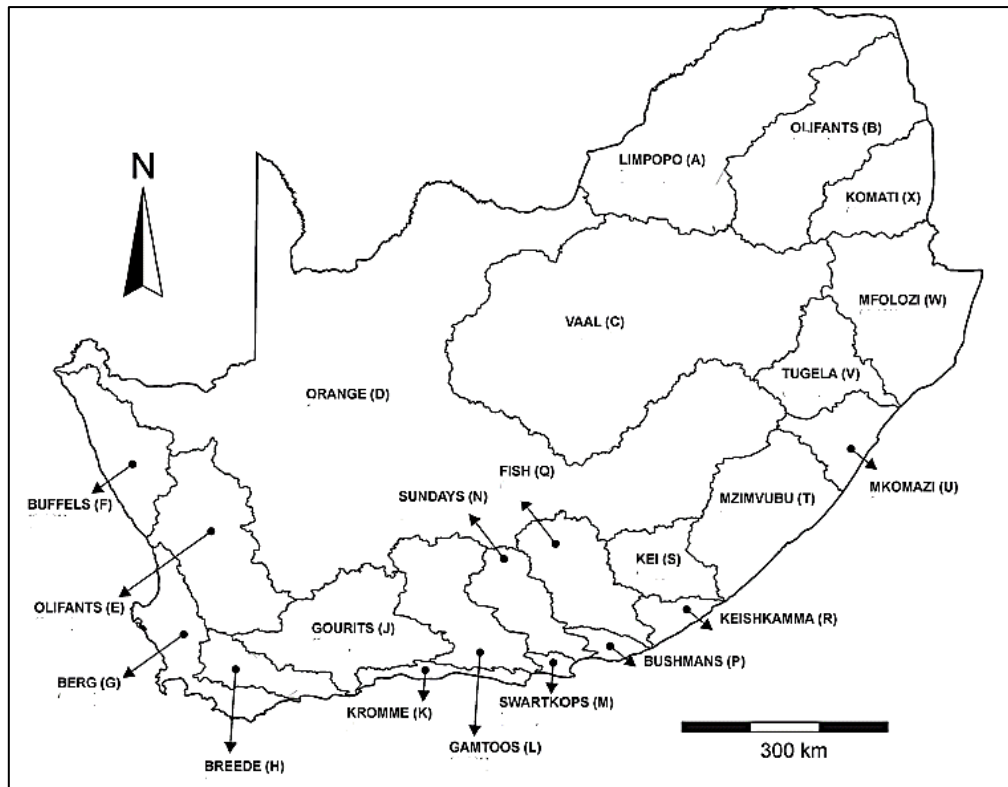


Figure 2-8: Primary catchments of South Africa (adapted from Huizenga et al., 2013).

2.2.2 Surface Reservoir Inflow Sequences

Informed water resource planning and decision-making is based on updated and reliable streamflow information, as the accuracy thereof is crucial for the development and calibration of surface water models (simulations). The Directorate of Hydrological Services at the DWS is tasked with gathering hydrological data (streamflow information) by managing a streamflow gauging network, to develop a historic record of the streamflow conditions pertaining to the rivers in South Africa (DWAF, 2007). Streamflow information is recorded and monitored at streamflow gauging stations, which are selected sites on rivers, equipped and operated to provide the basic data, from which systematic records of water levels (stages) and discharges may be derived (Wessels and Rooseboom, 2009).

Gauging weirs, equipped with automatic water level recorders, are built inside rivers to establish streamflow records (Du Plessis, 2017). The main gauging station (weir) types used in South Africa are the crump weir, sharp-crested weir or sluicing flume. During the early years of streamflow observations only a few gauging stations were equipped with automatic flow recorders and data was manually recorded on a daily or weekly basis. Although the earliest automatic flow recordings (stages) date back to the 1920s, automatic streamflow recordings generally started in the 1960s, producing instantaneous continuous streamflow records. The stage records are then converted into flow rates through the use of rating tables, which resulted in a continuous record of flow rates, customarily indicated in cubic meters per second (m^3/sec) (Du Plessis, 2017). Daily streamflow records can be obtained through the DWS website.

There are two main ways in which streamflow is stored in surface water reservoirs in South Africa, namely in-channel storage and off-channel storage (Basson, 2005). In-channel storage dams refer to the reservoirs receiving unrestricted volumes of water directly from sources flowing into it, like rivers and rainfall. There are no limitations to the streamflow entering the reservoir in terms of manmade structures. Daily distribution of streamflow is mainly dependent on seasonal variation. Off-channel storage dams receive inflow through abstraction (pump stations) and diversion infrastructure (weirs). According to Basson (2005) diversion structures are customarily used to divert water from an existing natural watercourse into a water supply conveyance system. Daily abstraction rates are limited by infrastructural capacity and diversion efficiency of the diversion structure. Diversion efficiency refers to the level of effectiveness in diverting the streamflow. Depending on the volume of the streamflow in the river and the catchment characteristics, flooding events can cause steep hydrographs (high flow rate over short period of time). The steeper the daily hydrograph, the lower the effectivity of the flow, as only a percentage of the total daily flow can be diverted into the pipeline

Flow measurements in South African rivers are often hampered by the high variability of water discharges, as well as heavy sediment and debris loads in water supply systems.

2.2.3 Demand

Population growth and economic factors as well as social development, is giving rise to growing demands for water, as water plays a central role in all sectors of society. Demand is defined as the total volume of all annual water required by end-users, which have to be satisfied by water providers, through withdrawal from the reservoir (Du Plessis, 2017). South-Africa's end-users are categorised by the NWRS (DWA, 2013b) as follows: agriculture (66%); urban (18%); rural (4%); mining (5%); power generation (2%); afforestation; (3%) and transfer out (1%).

Demand varies according to seasons. Monthly demand is typically expressed as a percentage of the annual demand. Daily demand is on average considered to be constant and is described as an Average Annual Daily Demand (AADD), although demand is higher in the dry season than in the wet season (DWA, 2013b).

2.2.4 Rainfall and Runoff

SAWS rainfall records indicate that rainfall had decreased from 2012 onwards, resulting in dry to very dry conditions countrywide (DWA, 2013). Poor spatial distribution of rainfall, as indicated in Figure 2-9, as well as variability due to seasonality, impacts the natural availability of water resources across the country negatively. Rainfall ranges from 100 mm/a to over 1 500 mm/a in some parts of the country, while the national average is estimated to be 450 mm/a. Linking this low rainfall rate to the

high level of aridity results in a mean annual runoff (MAR) of less than 10%, which is a very low percentage when compared to countries with a similar amount of average rainfall (DWA, 2013b).

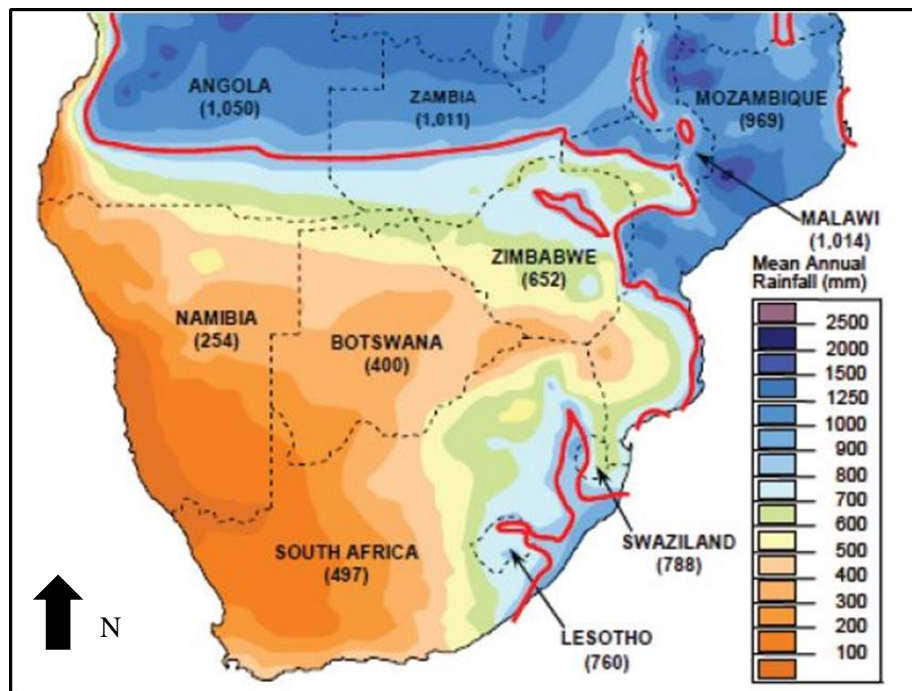


Figure 2-9: Spatial distribution of rainfall across Southern Africa (DWA, 2018).

Runoff is a result of precipitation (e.g. rainfall), after infiltration has taken place, that moves along the surface of the earth and subsequently drains to low lying areas where it accumulates to flow into or form rivers and streams (DWA, 2013b). Rainfall is initially intercepted by vegetation, after which rain infiltrates the soil/ground surface until the soil reaches a saturated stage. At this stage, the rainfall rate (intensity) exceeds the rate of infiltration and runoff is the result (Critchley & Siegert, 1991).

According to Critchley and Siegert (1991), the amount of runoff resulting from rainfall is influenced by the following factors; rainfall intensity (distribution and duration), soil moisture conditions (infiltration), soil type, catchment slope and vegetation cover. Rainfall intensity refers to the rainfall depth over the period of the rainfall event. More runoff is generated from a rainfall event with higher intensity, as time for infiltration is shorter. Initial soil moisture conditions during the rainfall event have an impact on the infiltration rate and therefore also runoff contributions. For example; during (and directly after) a rainfall season the soil can be saturated and more water contributes to runoff than to infiltration. Furthermore, different soil types - gravels and sands - allow for faster infiltration, therefore decreased runoff, while others -clay and hard rock- increase runoff. A steeper slope causes greater runoff than a gentler slope, as it allows less time for infiltration. An increase in vegetation cover increases infiltration and therefore decreases runoff (Critchley & Siegert, 1991).

The abovementioned factors are site specific and therefore, vary between different catchments. Even though within a particular catchment there is also a variety of vegetation and soil types as well as different surface slopes, each catchment has unique rainfall runoff responses. For each catchment a

runoff coefficient can be determined by dividing runoff by rainfall for a specific rainfall event. Critchley & Siegert (1991), suggest that seasonality can also be incorporated in the runoff coefficient, therefore, if a yearly runoff coefficient is determined, the total yearly runoff is divided by the total yearly rainfall. Monthly rainfall-runoff modelling at catchment level has also been undergone and shows good correlation since the monthly runoff coefficient takes into consideration a variety of rainfall intensities specific to a certain month, evaporation and interception which can also differ from month and soil saturation (Chang & Chen, 2018).

Increased runoff does not necessarily result in higher water supply levels, as some water may infiltrate into the ground, or evaporate in areas with high evaporation rates, or discharge into the sea. Increased rainfall intensity due to changing climate conditions (e.g. warming trends & El Niño/ La Niña phenomena) could worsen soil erosion, especially on the river banks, as water puts pressure on unstable banks. It also has the potential to damage areas with shallow water tables. All of the above-mentioned affects water quality negatively and impacts on the health of aquatic ecosystems. Thus, augmentation and conjunctive use of various water resources will become essential, should climate conditions continue on the current trajectory.

2.2.5 Evaporation

Evaporation is the physical process during which water (liquid state) turns into atmospheric water vapour (gaseous state), due to an increase in temperature or pressure. In South Africa, evaporation losses from reservoirs are significant and it impacts the yields of water supply reservoirs negatively, which affects the feasibility of building new reservoirs irrespective of the size. The Annual National State of Water Report (DWA, 2013) indicates that South Africa has been experiencing a warming trend since 1961, upon examining temperatures recorded at 27 SAWS climate stations across the country as highlighted in Figure 2-10.

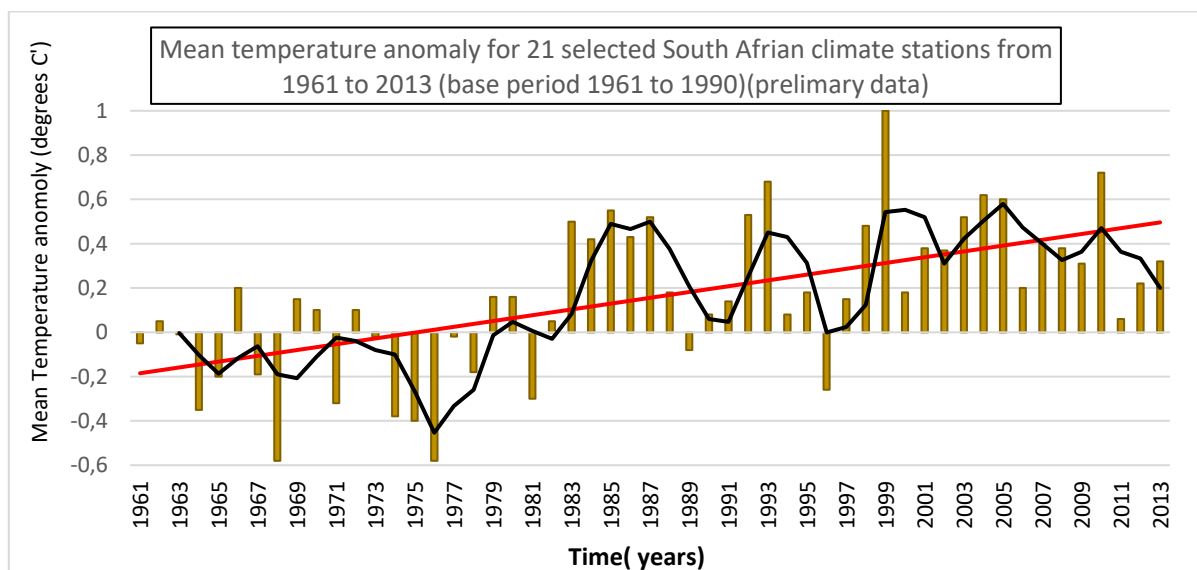


Figure 2-10: The warming trend South Africa had experienced since 1961 (DWA, 2013).

This ongoing trend exacerbates evaporation rates. According to Watkins (1993), evaporation occurs in vegetated areas (wetlands), as well as open water areas (rivers and reservoirs) and open water evaporation levels are further dependent on weather conditions (wind, temperature, cloud cover) and surface area. The average annual rainfall in South Africa is 460 mm, while the mean annual evaporation (MAE) rate is 1400 mm (Van Dijk and Van Vuuren, 2008). Just like rainfall, evaporation is also influenced by environmental and geographical factors, with the highest rate recorded in the Northern Cape Province (3000mm) and the lowest rate recorded in the mountainous regions of the KwaZulu-Natal Province (less than 1400mm) (Van Dijk and Van Vuuren, 2008). Thus, improved and stringent water management strategies towards conserving water, need to be implemented and maintained throughout the country, to secure yields.

Evaporation volumes are established by studying events occurring on the surface area of the reservoir. Pan evaporation is a measurement that combines the effects of several climate elements: temperature, humidity, rainfall, drought dispersion, solar radiation and wind. Symons pan (S-pan) and A-pan factors are used to convert MAE into open water evaporation and land evaporation respectively. Thus, S-pan factors are used when determining evaporation rates for reservoirs in South Africa. The evaporation map of South Africa is used to obtain input data when conducting reservoir simulations, and can be accessed at the website of the Department of Water and Sanitation (DWS, 2019). The evaporation potential is indicated as MAE rates for different geographical areas, denoted in S-pan values. Monthly MAE values of an evaporation zone within a quaternary catchment are then converted to open water evaporation using open water coefficients, which are given as monthly percentages applied to the S-pan monthly evaporation. According to Fourie et al. (Groundwater Dictionary 2nd Edition) a quaternary catchment is the basic hydrological unit used to plan integrated water resource management in South Africa. Net evaporation on surface water is calculated by subtracting rainfall from open water (S-pan) evaporation. If no monthly rainfall record is available, a drought rainfall record is used for calculations. Drought rainfall is the average of the five lowest annual rainfall values on historic record for the specific catchment.

To calculate daily net evaporation, both daily evaporation and daily rainfall are required as input parameters, as well as the surface area of the reservoir over which net evaporation takes place.

2.2.6 Surface-Area of Reservoirs

To support decision-making processes regarding reservoir planning and water management, information about reservoir volumes and surface areas have to be obtained. According to Rodrigues and Liebe (2013), depth-capacity and area-capacity curves are the most important outcomes when assessing the ability of surface water reservoirs. Capacity in this case refers to the reservoir volume. The curves provide information used for reservoir routing (flood routing), determination of surface area for calculating evaporation, obtaining operational levels of dams, classification of reservoirs, as well as

determination of sedimentation rates (Rodrigues and Liebe, 2013). Different methods are used to determine and plot the depth-capacity and area-capacity relationships.

According to Napoles and Berber (2017), a recommended volume computational method is the contours method. The contours method is applicable in cases where volume information is needed within a short time-frame and where a lack of information occurs. It also provides more accurate results when compared to other methods (Napoles and Berber, 2017). Contour methods make use of topographical maps or topographical surveys where the area of each contour can be determined. The volume between contours is then calculated by averaging out the areas between two consecutive contours and multiplying it by the contour interval as described by Equation 2-4. In cases where small dams are constructed a completion survey is undertaken, during which 3D models are created, by surveying the dam basin at 1m contour intervals or by using digital terrain modelling instruments (drones or satellites).

$$Volume = CI \left(\frac{A_1 + A_2}{2} \right) \quad (2-4)$$

Where:

CI = Contour interval (m)

A₁ and A₂ = Area (m²)

Mathematical equations which describe the relationship between depth and volume are represented by linear, logarithmic and power functions. Grin (2014) established that the power function describes the depth-capacity relationship for a number of dam basins which were analysed. An analysis by Rodrigues and Liebe (2013) also made use of the power function to describe depth-capacity, as well as area-capacity relationships. The depth-capacity relationship using a power function can be described by Equation 2-5. The derivative of which is used to describe the area-capacity relationship. Coefficient (b) is related to hillside concavity in which the basin is situated.

$$Volume = a (Depth^b) \quad (2-5)$$

Where:

a = Constant

b = Exponential coefficient

Depth = Depth (m)

Although each depth-capacity curve and area-capacity curve is site specific, as different reservoir basins have different topologies, Rodrigues and Liebe (2013) suggest that planners can use the power function with confidence when simulating volumes and surface areas. Therefore, the power function and linear

function will be the focus in this research. An example of a dam capacity versus depth curve is illustrated in Figure 2-11.

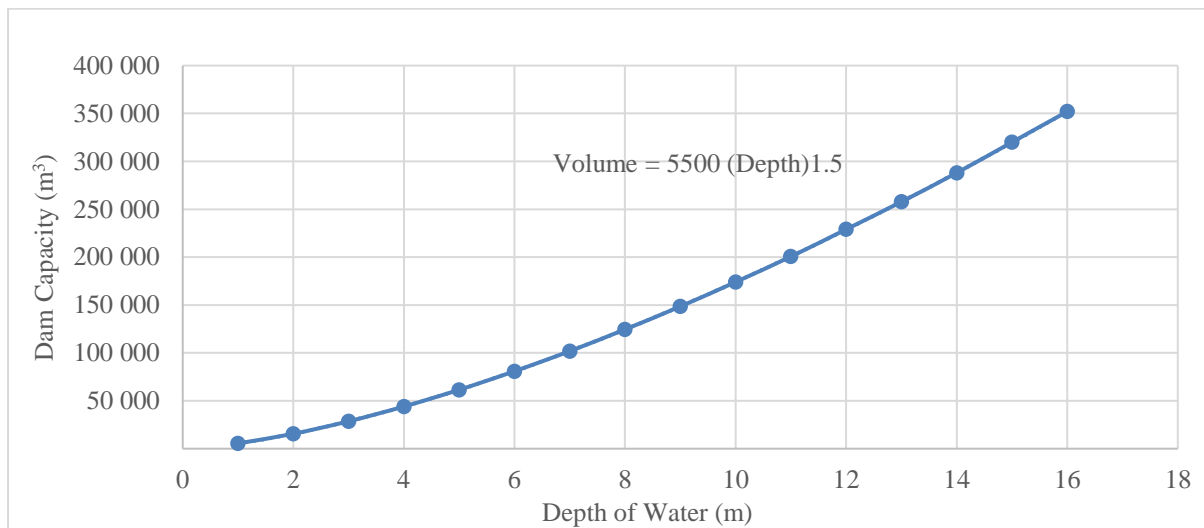


Figure 2-11: Capacity-Depth curve for a surface water reservoir

2.2.7 Seepage Losses

Seepage losses are defined as water flowing through the dam basin into the underlying soil formations. Seepage is expected to occur for reservoirs built on unconsolidated materials, gravels, or permeable rock. For reservoir basin design, the foundation material is carefully inspected (geological survey) and an appropriate lining is proposed to reduce seepage. The linings that are customarily used include: clay linings, and geomembranes, such as High-Density Polyethylene (HDPE) and Polyvinyl Chloride (PVC), which reduce the permeability (Hagen, 2019). In some cases where there are deep foundational cracks or where granites occur, grouting is applied. In other cases, when it is not feasible to line the dam, the dam wall is designed with drains (toe drain, blanket drains etc.) to monitor seepage.

Most small dams have linings to minimize seepage losses through the foundation. For small dams, the seepage losses are small in comparison to the water changes due to evaporation (Hagen, 2019). However, the amount of seepage should be determined for each dam on a case to case bases. Seepage is not modelled in this research, as it is assumed that the seepage losses are negligible compared to evaporation losses.

2.2.8 Overflow

Spillage is defined as water overflowing the dam, either through a spillway, or over the top of the crest. Overflow, also referred to as spillage, occurs when the water in the reservoir reaches a higher level than full supply capacity. Surface water reservoirs are built not only to store water for supplying large populations of cities and towns, but also to regulate large volumes of water in the event of flooding. Therefore, dams are designed with spillways, so that in the event of the dam being at full supply capacity, water can spill from the dam without overtopping the dam crest, potentially resulting in

damage or failure (Hagen, 2019). In some cases, water spilling from the dam can be stored in downstream storage dams.

2.3 Groundwater Yield Modelling

Groundwater is an indispensable resource in many rural regions of South Africa, for domestic use, irrigation of arable agricultural land, and sustaining livestock and game. Mining and other industries also rely on groundwater for some of their processes. The most recent estimate of sustainable potential yield of groundwater resources for South Africa at high assurance is 7 500 million m³/a, while current groundwater use is estimated at 2 000 million m³/a. Allowing for an underestimation on groundwater use, roughly 3 500 million m³/a could be available for further development (DWA, 2013). The DWS has been developing *Reconciliation Strategies* to assess water balance against future needs, including key components such as increased value and utilisation of groundwater.

Groundwater forms part of the hydrological cycle, which is climate driven. The hydrological cycle gives an indication to the stochastic nature of groundwater. Some of the rainfall becomes surface runoff, while some return back to the atmosphere through evaporation and transpiration, and the remainder seeps into the ground (Tarbuck et al., 2014). According to Heath (2004), groundwater is water that is stored in the cavities and crevices of rock and sand below the earth's surface, referred to as aquifers. Groundwater concepts predominantly used in literature are outlined in section 2.3.1 to 2.3.5.

2.3.1 Classification of Aquifers

An aquifer is a saturated, permeable geological formation, from which water can be abstracted through either wells (boreholes) or springs (Ponce, 2007). There are two main types of aquifers, namely unconfined and confined as depicted in Figure 2-12. Unconfined aquifers have no impermeable layer, thus there is no restriction of the seepage from the surface above it, into that aquifer. The upper boundary of an unconfined aquifer is marked by the water table (Ponce, 2007). Unconfined aquifers can be classed into primary and secondary aquifers. Primary aquifers consist of porous sands and gravel and are distinctive of alluvial deposits. Secondary aquifers consist of fractured rocks, formed by igneous intrusions (Murray et al., 2012). Confined aquifers have an impermeable layer as an upper boundary and their recharge area is often far away from an abstraction point. Recharge is an addition of water to an aquifer. Boreholes drilled into confined aquifers are often controlled by hydrostatic pressure which push up the water level. Therefore, the water levels of the confined aquifer boreholes are well above the upper boundary of the aquifer (confining boundary) (Heath 2004).

In South Africa, 80% of the aquifer systems are unconfined, shallow, weathered and/or fractured-rock aquifers, most of which are low yielding, found along coastal regions (Pavelic et al, 2012). The remainder of the aquifer systems in South Africa are dolomitic and quartzitic in nature; however, this research will focus on the shallow, unconfined and fractured aquifers as mentioned above.

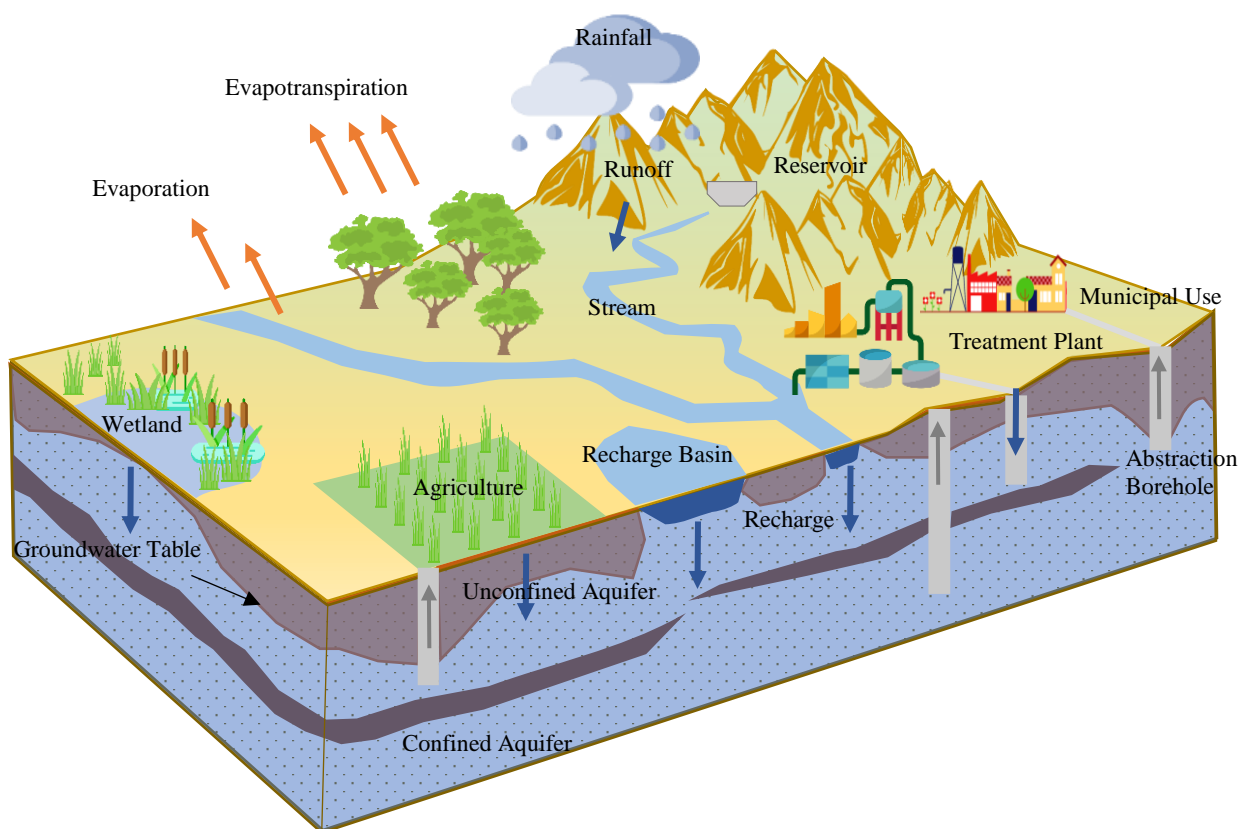


Figure 2-12: Hydrological cycle with aquifer terminology (redrawn from Ponce, 2007).

2.3.2 Hydrogeological parameters: Transmissivity and Storativity

The two main hydrogeological parameters impacting the yields of aquifers and boreholes are transmissivity and storativity. Transmissivity is the rate at which water flows through a unit aquifer width under a unit hydraulic gradient and is expressed in m^2/day (AQTESOLV, 2017). Soil mediums with larger or more pore spaces have a higher transmissivity, as the flow is easier, resulting in a higher potential yield.

Storativity, also referred to as specific yield, in unconfined aquifers, is the amount of water that can be released from a unit aquifer volume under a unit hydraulic gradient (Murray et al, 2012). Storativity is given by a storage coefficient, which is the amount of water recoverable over a unit aquifer volume. The storage coefficient for surface water is one, while the storage coefficient for groundwater is less than one, because not all water can be recovered from the rock pores (Heath, 2004).

The configuration of the water table varies seasonally and from year to year, because the addition of water to the groundwater system is closely related to the quantity, distribution and timing of precipitation (Tarbuck et al, 2014). Even though groundwater resources are less climate-susceptible than surface water resources, they are still rainfall driven, which is climate-dependent. The stochastic nature of groundwater and its related recharge are discussed in section 2.3.3 to 2.3.5.

2.3.3 Traditional Borehole Yield Determination

By estimating how much groundwater is available for abstraction without depleting the aquifer and thereby lowering the water level to below critical levels, it is possible to ensure a long, safe supply for future use (Nel, 2017). The method used to arrive at a sustainable pumping regime is the pumping test (AQTESOLV, 2018). The sustainable yield, determined through borehole pumping tests, is considered as the volume that can be abstracted, pumped at a specific rate, without causing the aquifer water level to drop below a specified maximum drawdown level, while disregarding recharge over a long period of time (customarily 2 years).

The sustainable yield of an aquifer system will depend on the size, behaviour and utilization of the system. A large system, such as aquifer systems in quaternary catchment regions or municipal wellfields, require that abstraction is less than recharge, for the system to be sustainable (AQTESOLV, 2018). Small-scale sustainability requires that the water level of the borehole remain above the maximum allowable drawdown.

Hydrogeologists traditionally use borehole pumping tests to determine both the sustainable yield, as well as the hydrogeological characteristics of a particular borehole and the aquifer system it is located within. The type of pumping test and the extent thereof is chosen based on the planned utilization of the borehole (Van Tonder et al, 2002). The tests follow a general procedure of pumping water at a constant rate (or increasing the pumping rate with specific steps) for a test borehole, and then monitoring the water level in various observation boreholes. The drawdown and recovery behaviours of the water table are monitored and recorded (AQTESOLV, 2018). The response of the water level to the pumping action is used to estimate the hydrogeological parameters of the borehole and give an indication of the boundary conditions of the aquifer system, categorised using Flow Characterisation Methods (FC Methods). The FC methods make use of the Theis Groundwater analysis, discussed in section 2.3.8. Parameters such as pumping rate, transmissivity, storativity (ability to store) sustainable yield and maximum allowable drawdown are established by pumping tests. However, since these tests only focus on a single time-invariant scenario, the sustainable yield of a borehole is not always assured in drought conditions or when boreholes are subjected to over-utilization (Murray et al., 2012). According to Gelhar (1993) groundwater not only varies with space, but also with time. Therefore, available abstraction estimates at a single point in time is not deemed dynamic enough to determine sustainability over long periods of time. Murray et al. (2012) considers time-invariant yield estimations, using average inputs and outputs (mean annual recharge and evapotranspiration etc.) to be unreliable, especially in arid regions where rainfall patterns largely determine groundwater yield.

2.3.4 Factors Impacting Aquifer Yield

Groundwater is not only dependent on hydrogeological parameters, but also on the inflow into the system and the outflows out of the system, which maintains mass balance. According to Sophocleous (1998) as quoted by Murray et al (2012) groundwater safe yield is defined as the attainment and maintenance between abstraction and recharge. Therefore, estimation of groundwater abstraction ability, surface water interactions with groundwater and vice versa also have to be considered, referred to as recharge and discharge (Lerner, 2003). Recharge is defined as the addition of water to groundwater resources through precipitation, while discharge is water originating from a groundwater source that enters streamflow (baseflow).

According to Tarbuck et al. (2014), groundwater levels experience seasonal variation based on the quantity, distribution and time-variation of rainfall (precipitation). Gelhar (1993) further states that water level response of aquifer systems follows natural recharge events, dependent on precipitation. The challenge with groundwater quantification and modelling is the extreme variability of material properties over small distances and time-periods (Gelhar, 1993).

Gelhar suggests that the following factors are considered when modelling groundwater, especially when limited data is available):

- Geological parameters (transmissivity and storativity);
- Stochastic nature of groundwater (natural recharge with rainfall runoff); and
- Physical laws of underground flow (water balance).

The integrated nature of groundwater and surface water requires a greater number of variables to be modelled, thus lumped-parameter water-balance models were developed (Gelhar, 1994). A lumped-parameter model refers to input data and output data that incorporate spatial and temporal variation of hydrological, geological and hydrogeological data across the model area. This type of water-balance model is particularly applicable to aquifers where time variation is of primary concern and overarching policy dictating management decisions relating to the behaviour of the aquifer, over an extended period of time, are important (Murray et al., 2012). Furthermore, this model is applicable even with a limited amount of data.

2.3.5 Groundwater Resource Assessments: GRA I & GRA II

The significance of accessing groundwater resources in South Africa was recognized in the early 1990s. A map series of groundwater potentials was published in 1995, becoming the first ever groundwater availability assessment on a national scale, intended for better planning and management. Groundwater Resources Assessment Phase 1 (GRA I) was triggered and the process was coordinated by the Department of Water Affairs and Forestry (DWAF, 2009). By 2003 a set of 21 hydrogeological maps, covering the entire country was made available. The national maps and the GRA I process did not,

however, produce estimates of the total volume of groundwater that can be abstracted for annual utilization in South Africa, and disregarded utilization factors such as recharge and water quality.

The GRA Phase 2 (GRA II) began in 2003, concentrating on unresolved matters such as the quantification of groundwater available for use, the production of a “planning potential” map, the quantification of recharge, the interaction between groundwater and surface water, the classification of aquifers, and the quantification of existing groundwater utilization throughout the country. Both GRA I and GRA II rely heavily on historical data held by the DWS in its databases, much of which was gathered over three decades of government sponsored drilling programmes. Relatively little data generated by private companies, is made available (DWA, 2009).

2.3.6 Recharge

Natural recharge is the replenishment of an aquifer through the addition of water to the saturated zone, either by vertical (downward) percolation/ infiltration of precipitation, or surface water, and/ or the horizontal (lateral) movement of groundwater from adjacent aquifers to the recharge area (Dennis et al., 2012). The recharge process is vital for groundwater to be regarded as a renewable fresh water resource, utilized for provision to end-users in arid and semi-arid regions (Xu and Beekman, 2018). In South Africa, the need for reliable recharge estimations originated from an aspiration to manage its limited groundwater resources in a more sustainable manner (Xu and Beekman, 2018). Accuracy of recharge estimates is critical for the health and protection of existing freshwater ecosystems, as groundwater is playing an increasingly significant role in arid to semi-arid regions. In certain areas groundwater abstraction is occurring at an alarming rate, impacting surface water flows, groundwater and its associated ecosystems negatively (Conrad et al., 2004). Protecting existing freshwater ecosystems while keeping the water resource in a functioning condition and maintaining its quality is critical to groundwater recharge areas, and can be achieved by managing riparian and wetland buffers (DWA, 2013).

Natural and artificial recharge are two of the ways in which wetland buffers can be maintained. Artificial recharge can occur in one of the following ways (Beekman and Xu, 2018): induced recharge from nearby surface-water bodies resulting from groundwater abstraction; borehole injection; and/ or man-made infiltration ponds or dams. Artificial recharge has the potential to ensure water security together with resource sustainability. This can also be extrapolated from the NWRS2 (DWA, 2013), which considers artificial recharge as a storage arrangement for surface water to eliminate evaporation. Artificial recharge schemes have been successfully implemented in Namibia (Windhoek and Omdel), as well as in South Africa, such as the Atlantis Aquifer Recharge Scheme and Polokwane Wastewater Recharge Scheme, however; the remainder of the potential artificial recharge schemes in South Africa are still in experimental (Langebaan and Calvinia) or feasibility study phases (Plettenberg Bay and

Prince Albert) (DWA, 2014) . Therefore, artificial recharge schemes are not considered in this research, as the natural groundwater yield is investigated.

This research focuses on natural recharge by way of downward flow of water (runoff from rainfall) through the unsaturated zone, accumulating in the saturated zone, which is the most prominent type of recharge in arid and semi-arid regions. Recharge can be expressed as a percentage of annual rainfall. According to Breedenkamp and Xu (2003) rainfall related recharge is dependent on the variability, intensity and spatial distribution of rainfall. Chemical and physical water balance approaches are used to determine recharge figures. Recharge estimation is applicable to the saturated and unsaturated zone. Saturated soil has high moisture content, while unsaturated soil is considered to have a low moisture content. Methods used to determine recharge as a result of rainfall, are the Chloride Mass Balance (CMB), Cumulative Rainfall Departure (CRD) and the Saturated Volume Fluctuation (SVF). These recharge methods were rated the most appropriate for arid and semi-arid regions by Beekman and Xu (2018).

2.3.6.1 Chloride Mass Balance

The Chloride Mass Balance (CMB) approach is a chemical tracer approach, to determine recharge of groundwater, based on the assumption of conservation of chemical mass balance. This method determines the recharge coefficient based on the variance between chloride concentrations in rainfall, and the chloride concentrations at the deepest point in the soil profile, or discharge at a spring. The CMB method utilizes Equation 2-6 (Xu & Maclear, 2003) to determine recharge as a percentage of the mean annual rainfall.

$$R_e = \frac{Cl_{rf}}{Cl_{gw}} (R_f) \quad (2-6)$$

Where:

- R_e = Recharge (mm)
- Cl_{rf} = Rainfall Chloride concentration (mg/litre)
- Cl_{gw} = Chloride concentration of groundwater flow (mg/litre)
- R_f = Mean annual rainfall over recharge area (mm)

The CMB method was used during case studies in South Africa and Botswana, from which it became evident that Chloride concentrations of rainfall in coastal regions are significantly higher than those of rainfall from inland areas, thus the CMB method should be used with caution in coastal regions. However, the CMB method is useful in areas where no fluctuations in the water level are observed in the saturated zone. Furthermore, according to Xu and Beekman (2018) the CMB method can be used as a first approximation of the average recharge in a region in both unsaturated and saturated zones.

The GRA II average annual recharge factor grid was derived using the CMB coupled with a GIS-based model that took into account factors likely to affect rainfall recharge, e.g. lithology, soil type, topography etc. (DWAF, 2005a). These results were cross-checked against results obtained from field measurements and detailed catchment studies. Alternatively, physical approaches make use of water mass balance taking rainfall, abstraction and water level fluctuations into consideration. These include the Cumulative Rainfall Departure and the Saturated Volume Fluctuation methods.

2.3.6.2 Cumulative Rainfall Departure

The Cumulative Rainfall Departure (CRD) method is a physical approach, based on the assumptions of mass balance, estimating recharge through observation of rainfall events and the corresponding water level fluctuation. According to Beekman and Xu (2003) water level fluctuations are a result of not only rainfall events, but lateral flow as well.

Using the CRD method, the relationship between rainfall and water level fluctuations can be described by observing and then physically modelling lag time. Lag time is defined as the time rainfall takes to percolate through the unsaturated zone to reach the water table of the saturated zone (Sun et al, 2013). In surface water hydrology, lag time is indicated on a hydrograph as the amount of time it took for the water to reach a certain point of measurement, along the longest flow path in the catchment. Similarly, groundwater recharge also displays a lag time trend, which can be indicated on a graph similar to the hydrograph. Groundwater lag time can be short (within hours or days), intermediate (within months or a year) or long (over a number of years). Lag time is based on the intensity and length of preceding rainfall events, the thickness of the unsaturated zone, as well as hydrogeological characteristics of the aquifer (Sun et al, 2013). Short to intermediate recharge lag times are generally observed for unconfined, shallow aquifers, as well as fractured aquifers. The CRD method utilizes Equation 2-7 and Equation 2-8 (Xu & Maclear, 2003) to determine recharge.

$$R_e = r(CRD) = S_y [\Delta h_i + (Q_p + Q_{out})/(A S_y)] \quad (2-7)$$

$$\text{With } CRD_i = \sum_{i=1}^N P_i - \left(2 - \frac{1}{P_{av} i} \sum_{i=1}^N P_i\right) i P_t \quad (2-8)$$

Where:

CRD	=	Cumulative Rainfall Departure over a certain period of months
i	=	Total length of rainfall sequences
r	=	fraction of CRD which contributes to recharge
S_y	=	Specific Yield
Δh_i	=	Change in water level during specific month (m)
Q_p	=	Groundwater abstraction (m ³ /month)

$$\begin{aligned}
 Q_{out} &= \text{Natural outflow (m}^3\text{/month)} \\
 P_i &= \text{Rainfall for a month (m/month)} \\
 P_t &= \text{Threshold value representing aquifer boundaries (0 for closed aquifers and} \\
 &\quad P_{av} \text{ representing aquifer systems with a spring)}
 \end{aligned}$$

After examining Equation 2-7 and Equation 2-8, it is evident that this method requires a rainfall breakthrough (rainfall resulting in water level changes) for observing water level fluctuations. Natural outflow, as well as abstraction rate, has to be known to determine the recharge of the aquifer. When using Equation 2-6 the ratio between the fraction of cumulative rainfall contributing to recharge (r) and specific yield (S_y) can be estimated through an optimisation process, which minimises the difference between calculated and observed water level fluctuations over a specific period of time (time interval). Although Excel models have been developed for the use of this method (Xu & Beekman, 2003), the optimisation process is not deemed the most user-friendly for individuals who are not specialists in the field of hydrology, as expertise are required.

This method can be applied on both the saturated and unsaturated zones, as well as on small-scale boreholes and large-scale aquifer systems. However, as the depth in aquifer water level increases, CRD recharge estimation becomes more ambiguous (Beekman & Xu, 2018). A more recent method based on the CRD method, is the Rainfall Infiltration Breakthrough (RIB) method. Both the CRD and the RIB methods investigate the relationship between mean rainfall from a preceding time and water level fluctuations as a result thereof (Sun et al, 2013). However, the applicability of the RIB method is limited to unconfined aquifers in which water level fluctuations can be observed. According to Beekman and Xu (2018) monthly rainfall records, water levels and borehole abstractions are required, as well as hydrogeological characteristics of the recharge area. Fractured rock aquifers are particularly sensitive to rainfall recharge and the CRD and RIB methods can be applied with greater confidence in such cases (Beekman and Xu, 2018). The accuracy of recharge estimation increases with the distribution of boreholes over a wider extent of the recharge area of the aquifer, and with increased frequency of monitoring (Xu & Beekman, 2003).

Water level monitoring in unsaturated soils can be uncertain, resulting in discrepancies when doing calculations (Xu & Beekman, 2003). Additionally, local municipalities might not have information readily available and have to incur expenses in the process of obtaining information, such as outsourcing of assessments. Therefore, another physical method that is less data intensive and easily applied to the saturated zone is required.

2.3.6.3 Saturated Volume Fluctuation

The Saturated Volume Fluctuation (SVF) method is a physical method that determines recharge, linking specific information from the atmosphere, and unsaturated and saturated zones. This method examines the water balance over a specific period of time based on averaged groundwater levels obtained from

monitoring boreholes. According to Xu and Beekman (2003), methods that correlate rainfall, abstraction and water-level fluctuations have great potential for forecasting recharge. The SVF method incorporates both hydrogeological parameters as well as time-varied parameters in a mass balance equation, relating inflow and outflow volumes to water volume changes, as outlined in Equation 2-9 adapted from Bredekenkamp et al. (1995):

$$\Delta h = \frac{\Delta V}{A \times S_y \times \Delta t} = \frac{\text{In} - \text{Out} + R_e - Q_{abst}}{A \times S_y} \quad (2-9)$$

Where:

Δh	=	Change in Water level (mbgl)
ΔV	=	Change in saturated aquifer volume (m ³)
Δt	=	Time increment at which SVF is calculated (monthly)
S_y	=	Specific yield (%)
A	=	Aquifer Recharge Area (m ²)
R_e	=	Recharge volume per time step (m ³)
In	=	Inflow per time step (m ³)
Out	=	Outflow volume per time step (m ³)
Q_{abst}	=	Abstraction per time step (m ³)

The water level is measured in meters below ground level (mbgl) and the number will decrease, with an increase in recharge. Should a negative value be obtained when measuring the water level, it would be indicative of a wetland. If the values of the water level, baseflow and abstraction rate in a specific aquifer area are known, both recharge and specific yield can be determined with Equation 2-9. The aquifer recharge area is not easily delineated, as some aquifers are recharged from high lying areas far away from the point of abstractions, while others are recharged directly by rainfall over a specific area which is dictated by geological formations.

The SVF method is similar to the CRD, in that it considers rainfall recharge, water level responses as a result of rainfall, and it is applicable to boreholes (small-scale), as well as aquifer systems (large-scale). However, it does not make use of the concept of lag time between rainfall (preceding) and water level fluctuation. Thus, the SVF method requires less monitoring data than the CRD method to calculate recharge. Therefore, it can be considered a cost-effective recharge estimation method. Furthermore, the SVF considers recharge only for saturated zones, thereby estimating the actual recharge and not the potential recharge by incorporating the unsaturated zone.

According to Van Tonder and Bean (2003), the SVF method is most applicable to unconfined aquifer systems, as the water level that corresponds with the aquifer under investigation is known, which is often not the case in layered, deep or confined aquifer systems. The main concern regarding the SVF

method is that uniform recharge occurs over the modelled area, which is considered to be an oversimplification of reality. The SVF method also considers baseflow components (lateral recharge) and is often applied as a water level representative measure for the aquifer as a whole.

According to Van Tonder and Kirchner (1990), the primary advantage of the SVF method lies in how it is conventionally used; baseflows are known and abstraction is known, thus, storativity and recharge can be determined from water level fluctuations. The SVF method is incorporated into the Aquifer Firm Yield Model (AFYM), as it is a model which considers both recharge and baseflow, and it was developed for South African aquifer systems. Recharge and baseflow are stochastic components to consider when determining long-term sustainability of groundwater abstraction.

Streamflow is a result of runoff that enters the stream channel (river) through a number of different ways, namely channel precipitation, surface runoff, interflow and groundwater discharge (Vegter & Pitman, 2003). Surface runoff is equal to precipitation minus evaporation, interception, infiltration and surface water retention. Interflow occurs through the unsaturated zone where water infiltrates the ground at high lying areas and intercepts the streamflow in low lying areas. Groundwater discharge is water which enters the stream channel from the saturated zone (aquifer) (Figure 2-13). Baseflow, as defined by Dennis et al. (2012), is a sustained low flow in a river during dry conditions, which is a contribution to the stream channel as a result of groundwater discharge and/or interflow.

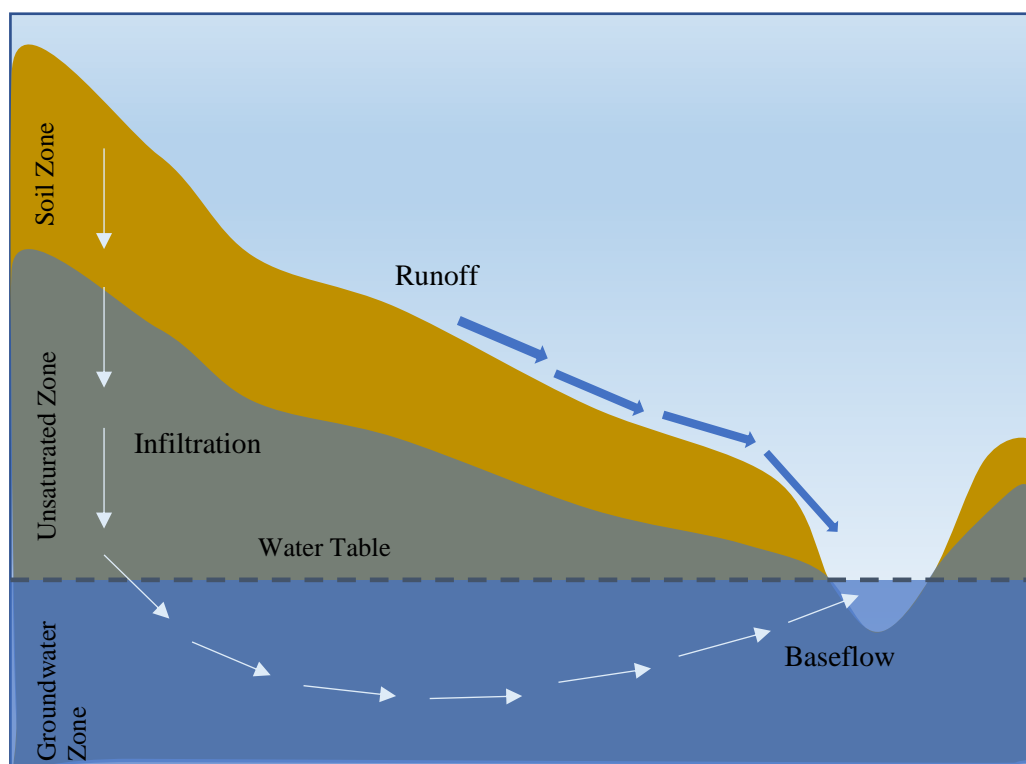


Figure 2-13: Surface water and groundwater interaction (Dennis et al., 2012)

There are a number of models used to separate and describe the different components of streamflow on a quaternary catchment scale, namely numerical models, analytical models and graphical models. The type of model used to determine the contribution's volume to streamflow, is chosen based on the following criteria: scale of the project; data availability; budget availability; river classification; and underlying geology. The three model types are applicable to alluvial aquifers, in which there is a direct contact zone between surface water and groundwater components. Graphical models make use of hydrograph curves on which streamflow values, recorded over a period of time, are plotted. Baseflow is separated from streamflow by removing the direct runoff from the hydrograph. Surface water runoff and in-channel precipitation, result in an almost immediate streamflow response (direct runoff) with high peak values over short periods of time, while baseflow indicates a delayed runoff response. The baseflow volume, however, may still contain some interflow component (Dennis et al, 2012).

According to Pitman and Vegter (2003), for the country as a whole base flow accounts for just over 20% of the total runoff of approximately $51 \times 10^9 \text{ m}^3$ per annum. The total base flow is less than 2% of the rainfall and this percentage is almost insignificant in the primary catchments F, J, L, N, P, and Q. The highest percentages are to be found in the (mostly) well-watered regions of the western and southern Cape (G, H, & K) and the eastern escarpment (T, U, V, W, & X).

From year to year the base flow is far less variable than the quick flow component of runoff. In extreme dry years the base flow is about one-quarter to one half of the mean and in very wet years the base flow is about two to three times the mean. Addition of the quick flow component renders a total runoff that is far more variable, with dry year flows in the range of zero to one third and wet years in the range of three to twenty times the mean. In the case of both base flow and total flow the lower variability is associated with the higher rainfall areas, and vice versa (Vegter and Pitman, 2003).

2.3.6.4 Herold Baseflow Separation method

To assess the availability of groundwater for usage, without impacting the surface water negatively, the groundwater component contributing to baseflow has to be separated from the surface streamflow (river). The Herold (1980) method is used in South Africa (Dennis et al, 2012) to split monthly flows into surface water components and groundwater components, using a graphical hydrograph. The main assumptions made by Herold are: the total flow in the river is equal to surface water contribution and groundwater contribution; and flow in the river below a certain value (known as GGMAX) is groundwater flow. Each month GGMAX is adjusted, depending on the surface runoff during the previous month (Dennis et al, 2012). The calculation for each monthly time step is described below, as adapted from Vegter & Pitman (2003) and Murray et al. (2012):

Equation 2-10 reflects the assumption that total streamflow consists of groundwater contribution and surface water contribution:

$$Q_i = QG_i + QS_i \quad (2-10)$$

Where:

$$\begin{aligned} Q_i &= \text{Total flow in the river (Volume)} \\ QG_i &= \text{Groundwater contribution (Volume)} \\ QS_i &= \text{Surface water contribution (Volume)} \end{aligned}$$

Equation 2-11 suggests that the surface water component can be differentiated as the total flow minus a specified maximum value which is adjusted on a monthly basis (**GGMAX**). Flow below the **GGMAX** volume is assumed to be groundwater flow. Therefore, if there is less water flowing in a river than the minimum baseflow (**QGMAX**), the flow is assumed to be mainly groundwater and not surface water. The first estimate for **QGMAX** is the average flow of the river.

$$QS_i = Q_i - \mathbf{GGMAX}_i \text{ (for } Q_i > \mathbf{QGMAX}\text{)} \quad (2-11)$$

$$\text{Or } QS_i = 0 \text{ (for } Q_i \leq \mathbf{QGMAX}\text{)}$$

$$\text{Hence } QG_i = Q_i - QS_i$$

The value of **GGMAX** is adjusted each month (Equation 2-12) as groundwater discharge is dependent on gradient between groundwater level in surrounding areas and the water level of the stream. When the groundwater level increases, there is an increase in gradient as well, resulting in an increase in groundwater discharge. Therefore, a **DECAY** and **GROWTH** factor should be incorporated to include seasonal fluctuations. The **DECAY** factor accounts for a decline in groundwater contribution to baseflow, while the **GROWTH** factor accounts for an increase in groundwater contribution to baseflow. An additional constraint to determine **GGMAX**, is that **GGMAX** may not fall below the minimum baseflow volume of **QGMAX**.

$$\mathbf{GGMAX}_i = \mathbf{DECAY} \cdot \mathbf{GGMAX}_{i-1} + (\mathbf{GROWTH} \cdot QS_{i-1})/100 \quad (2-12)$$

Where:

$$\begin{aligned} i &= \text{Current month} \\ i - 1 &= \text{Previous month} \\ \mathbf{DECAY} &= \text{Groundwater decay factor (0 < DECAY < 1)} \\ \mathbf{GROWTH} &= \text{Groundwater growth factor (0 < GROWTH < 10)} \end{aligned}$$

The hydrograph separation method is illustrated in Figure 2-14. The total streamflow (Q_i) of a quaternary catchment consists of a surface water contribution (QS_i) and a groundwater contribution (QG_i).

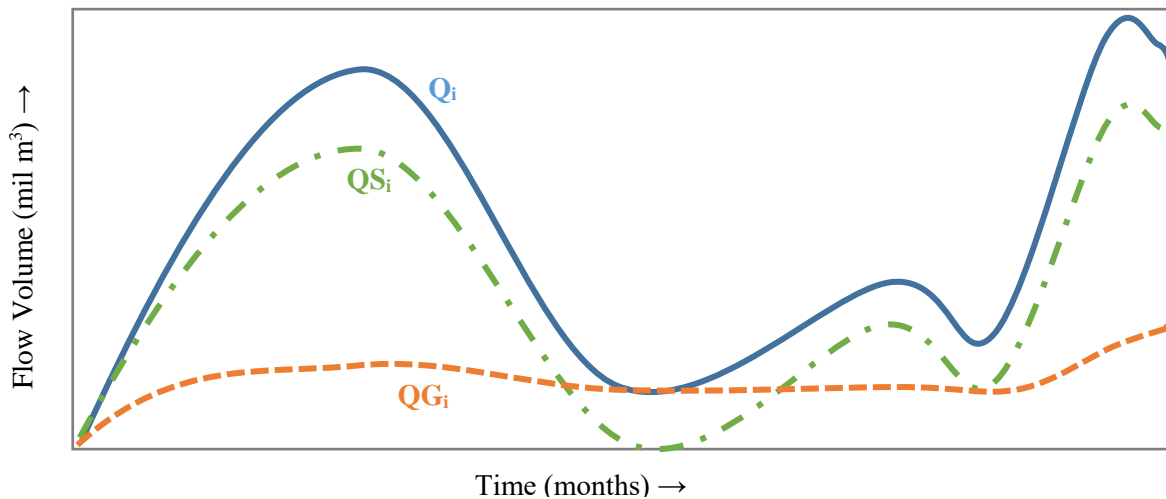


Figure 2-14: Hydrograph separation of surface flow and groundwater flow

2.3.7 Aquifer Firm Yield Model

The Aquifer Firm Yield Model (AFYM) was developed as part of a WRC project to provide hydrologists and engineers with tools to identify, assess and quantify groundwater, suitable for municipal supplies presented in an accessible manner (Murray et al., 2012). The model was developed to incorporate both static data sets as well as time variant data sets, while exploration and assessments of groundwater volumes (aquifers) for potential use in the Karoo basin, were conducted. Another aim of the AFYM was to develop generic methodologies to assess groundwater yields, similar to those used in surface water yield assessments.

The AFYM is a single-celled, lumped-parameter box model as described by Gelhar (1994), incorporating hydrogeological and stochastic parameters, as well as physical groundwater laws. Single-celled or box-model refer to the conceptual model of aquifer systems in the sense that it is represented as a single element which is connected through adjacent elements through inflow and outflow parameters. Aquifer volumes cannot be established without rigorous numerical modelling; therefore, to conceptually model groundwater storage, a water level management system is adopted to represent storage volume and available yield within an aquifer. The critical management water level defines the volume of water held in an aquifer as storage, which is similar to surface water resources, with the exception that the exact volume of a surface water reservoir can be more readily established. Abstraction can only be sustainable if it does not exceed annual recharge, thereby preventing impacts to the water table that might cause violation of water rights or damage to the environment (Murray et al., 2012)

The AFYM maintains that a water balance is to be sustained for both surface water and groundwater resources within a quaternary catchment. The implication is that the boundaries of the catchment area

are accepted as natural groundwater divides and that groundwater eventually drains from the system at some point. Due to its over-simplification of reality, the AFYM is intended for early planning stages in areas where alternative water schemes are considered and where there is a shortage of spatial and temporal information.

A six-step procedure to determine the sustainable yield of an aquifer, based on a single-cell lumped-parameter model, is outlined by Mandel and Shiftan (1981), as quoted by Murray et al. (2012) as follows:

1. Determine the average annual recharge of the aquifer.
2. Identify the most stringent constraint, namely the first undesirable effect that will occur when the groundwater level is lowered.
3. Establish the quantitative relationship between water level elevation and the occurrence of this undesirable effect.
4. Delineate an average minimum water level for the entire aquifer system.
5. Calculate the natural outflow that will occur at the start of a would-be steady-state flow regime in accordance with the prescribed minimum water levels.
6. The sustainable yield of the groundwater resource is the difference between (1) and (5).

2.3.7.1 Water Balance: Lumped-parameter Box Model

By applying the quaternary catchment boundaries, when separating groundwater flow from surface water flow, the natural system (water balance) can be represented by a single-celled lumped-parameter box model. Critical management water level is used as the volume of water stored in the aquifer. Drawn down below this level cannot occur to provide estimates of aquifer firm and assured yields (Murray et al., 2012), as illustrated in Figure 2-15. Thus, the aquifer's reserve storage is the volume of water below the minimum or environmental water level limit, which takes into account environmental, legal and physical constraints (Murray et al., 2012). According to Murray et al. (2012), the operation of the model requires that Effective Recharge (Q_{re}) is based on the demand of the evapotranspiration, baseflow and pumping. Effective Recharge (Q_{re}) can be less than the Recharge (%MAP) and the difference between them is the volume of Potential Recharge (Q_r). Effective Recharge (Q_{re}) can never have a higher value (larger volume) than the Recharge (%MAP), as Effective Recharge (Q_{re}) is acquired from the Recharge (%MAP). Thus, each time step of the model has a different Potential Recharge (Q_r) value associated with it. External demands do not have an influence on the water level in the box, provided that the Potential Recharge (Q_r) exceeds the external demand. Equation 2-13 and Equation 2-14 describes the water balance of the lumped-parameter box model:

$$Q_{re} = Q_e + Q_b + Q_p \quad (2-13)$$

$$Q_{re} = Recharge - Q_r \quad (2-14)$$

Where:

Q_r	=	Potential recharge (m^3)
Q_{re}	=	Effective recharge (m^3)
Q_e	=	Evapotranspiration (m^3)
Q_b	=	Baseflow (m^3)
Q_p	=	Pumping (m^3)

Under natural conditions the effective recharge should equal the discharge from the system, including evapotranspiration and contribution to baseflow. For the system to remain in equilibrium when pumping is induced without affecting evapotranspiration and baseflow, a dynamic equilibrium is created whereby water is sourced from the potential recharge. The dynamic equilibrium is achieved through sourcing water not only from the effective recharge, but from the potential recharge (%MAP).

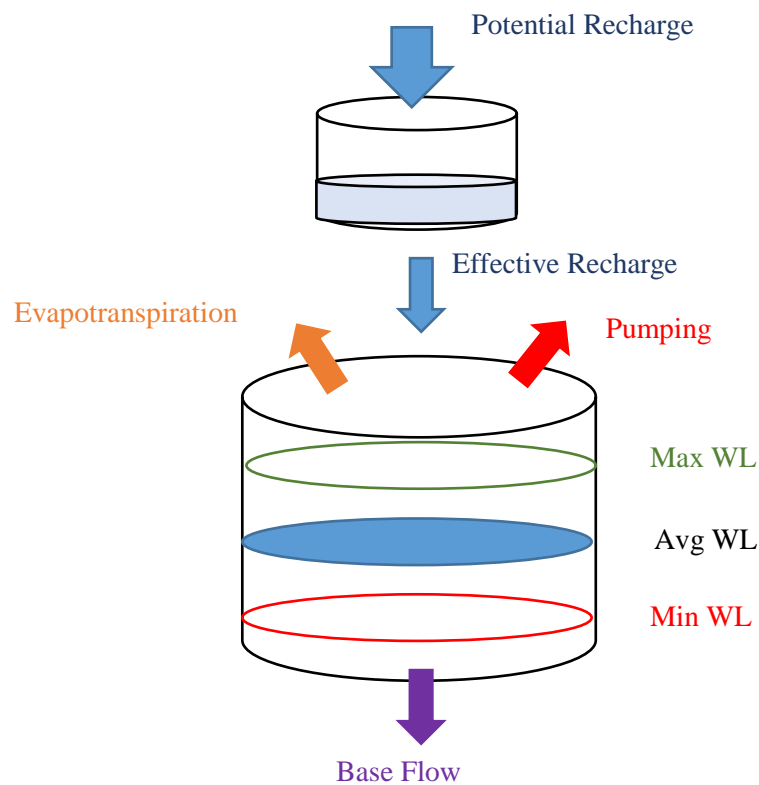


Figure 2-15: Lumped-parameter box model of the AFYM.

When pumping is greater than the recharge available, water from the baseflow will be sourced. Once water from baseflow is depleted the system will aim towards a new equilibrium where water will be sourced from rivers. The AFYM does not allow for this to happen.

Estimates for Q_r , Q_e and Q_b are obtained from the WR2005 and GRAII data sets, available at the WRC and DWS online databases respectively. The pumping rate Q_p is controlled in the model to determine the potential maximum pumping rate without causing a failure within the system. A failure occurs when the water level of the aquifer is lower than the specified maximum allowable water level drawdown (the level below which the aquifer cannot yield water). In the AFYM a maximum allowable water level

drawdown of 5 meters below the average water level fluctuation is specified as failure criterion. This was done to compare the results of the AFYM with the Average Groundwater Exploitation Potential values obtained as part of the GRAII study. The average groundwater exploitation potential values were determined by also using a 5m maximum allowable drawdown as failure criterion.

2.3.7.2 Evapotranspiration

Evapotranspiration is defined as water released back into the atmosphere through transpiration of plants and evaporation from soil. Aquifer storage is only impacted by evapotranspiration when the aquifer is underlying a riparian zone. A riparian zone describes the vegetated area surrounding a stream or surface water environment (Dennis et al., 2012). According to Murray et al. (2012), the riparian zone covers between 0.1% and 10% of the surface area of quaternary catchments. In South Africa, the riparian zone only exceeds 5% of the surface area of catchments located in the Eastern Cape and KwaZulu-Natal Provinces.

In the AFYM, evapotranspiration is modelled by means of a linear relationship between rate of evapotranspiration and water level depth. When water level depth increases, the evapotranspiration rate will decrease. At a specific depth, evaporation is considered to stop entirely; this water level depth is known as the evapotranspiration extinction depth (Figure 2-16). In South Africa the extinction depth is dependent on the type of vegetation and their associated root depth, but it is universally accepted in the hydrogeological community that evapotranspiration ceases between the depth of 4 mbgl and 5 mbgl (Murray et al., 2012). A similar approach was adopted in a multi-step planning model by Onta et al. (1991), where the extinction depth was assumed to be at 3.5 mbgl.

In the evapotranspiration rate approach, the user is required to enter an extinction depth and the area of the riparian zone should be known (Murray et al, 2012). It can be concluded from the study by Onta et al. (1991) that an array of data (aquifer area, aquifer depth, recharge potential, water table and root depth) is required to produce the most accurate results. Although recharge percentages, and average water table depths are available in the GRAII data set, rigorous surveys would be required to establish root extinction depth and aquifer area as well as the evapotranspiration rate of different plants. Municipalities are often not internally equipped for the extent of these surveys.

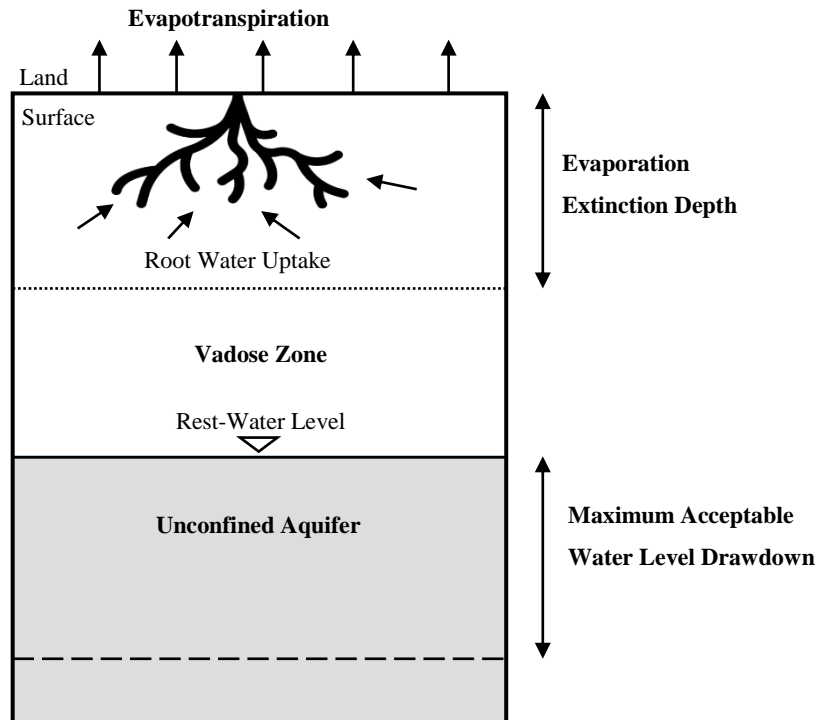


Figure 2-16: Riparian zone and evapotranspiration extinction depth (Murray et al., 2012).

Evapotranspiration mostly takes place in the Vadose Zone (unsaturated zone), however when looking at the water level fluctuation related to changes in aquifer storage volume, the saturated zone is considered. Furthermore, due to riparian zones making up a small percentage of surface area as well as the average water levels of aquifers being lower than 5 mbgl, (SRK, 2005), the effect of evapotranspiration is deemed negligible. Thus, the impact of evapotranspiration is not considered any further in this research.

2.3.7.3 Baseflow component

The surface-groundwater interaction is a component of the AFYM. Existing baseflow estimates from previous quaternary catchment studies done by Pitman (1994), Schulze (1997), Hughes (2007) and Van Tonder (2004) are included in the AFYM. Within the AFYM the user is given the choice to choose an average baseflow value for the quaternary catchment based on the methods available. Thereafter, the Herold Baseflow Separation method is applied, with monthly flow data obtained from WR2005.

An assumption made by the AFYM is that when baseflow is depleted, no seepage or recharge occurs from the streamflow back into the aquifer system.

2.3.7.4 Water level fluctuation

The AFYM assesses water level fluctuation on a monthly basis. The SVF method was adopted for the purpose of transforming time series rainfall values into time series water level information, by considering various inflow and outflow values. Equation 2-16 (Murray et al, 2012) is an adaptation from the SVF recharge method in that it is used to translate volumes into water level changes. Equation 2-15 shows the adaption of the SVF (Murray et al, 2012).

$$h_{t+1} = h_t - \frac{R_i}{Sy} + \frac{E_i A_r}{Sy * A_t} + \frac{(Q_b + Q_r + Q_p)}{Sy * A_t} \quad (2-15)$$

Where:

h_{t+1}	=	Water level at the end of the time step (mbgl/month)
h_t	=	Water level at the beginning of the time-step (mbgl/month)
Sy	=	Specific Yield (%)
R_i	=	GRA II recharge percentage of MAP (m/month)
E_i	=	Evapotranspiration (m/month)
A_r	=	Area of Riparian zone (m ²)
A_t	=	Area of Aquifer (m ²)
Q_b	=	Baseflow rate in month (m ³ /month)
Q_r	=	Potential recharge in month (m ³ /month)
Q_p	=	Pumping abstraction rate per month (m ³ /month)

It is evident from Equation 2-16, that the water level drawdown will increase as water is depleted from aquifer storage. This can either be due to evapotranspiration losses or high abstraction rates. Water levels will increase when the opposite scenario occurs (Murray et al., 2011).

The Aquifer area parameter is regarded as the recharge area; however, as this is difficult to establish, the entire quaternary catchment area is used, together with the assumption that rainfall is uniform over the catchment.

Soil moisture content plays a significant role on the potential recharge that can occur, especially in expansive clays. If the soil or sediment has not received rain over a very long period of time, the soil first soaks up what is in deficit before it is 'permeable' enough to allow water to pass through.

While water level fluctuations can be mistaken for a one-dimensional phenomenon the AFYM illustrates that the entire aquifer displays an average water level response to the recharge in 3-dimensional (3D) space (Murray et al., 2011). Each borehole will also reflect a 3D water level response over a smaller area than the aquifer system. Therefore, it is important to evaluate water level drawdown at single boreholes and the effects thereof on boreholes within the same wellfield. The Cooper-Jacob Wellfield Model can be used for this evaluation.

2.3.8 Cooper-Jacob Wellfield Model

When developing wellfields – two or more boreholes in close proximity of each other, abstracting water within the same aquifer system - the 3D nature of groundwater flow requires consideration. The water table at a borehole subjected to pumping, forms a cone of depression as illustrated in Figure 2-17. The cone of depression is formed when water moves from the surrounding pores in the aquifer, into the borehole, causing the water level to drop radially around the borehole, from the original rest water level (Heath, 2004). The distance between the original rest water level and the cone of depression at any given time is called the drawdown (s). The radius of influence describes the position of the drawdown as the horizontal distance from the borehole (r) to the cone of depression. The end of the cone of depression is signified by a drawdown of zero.

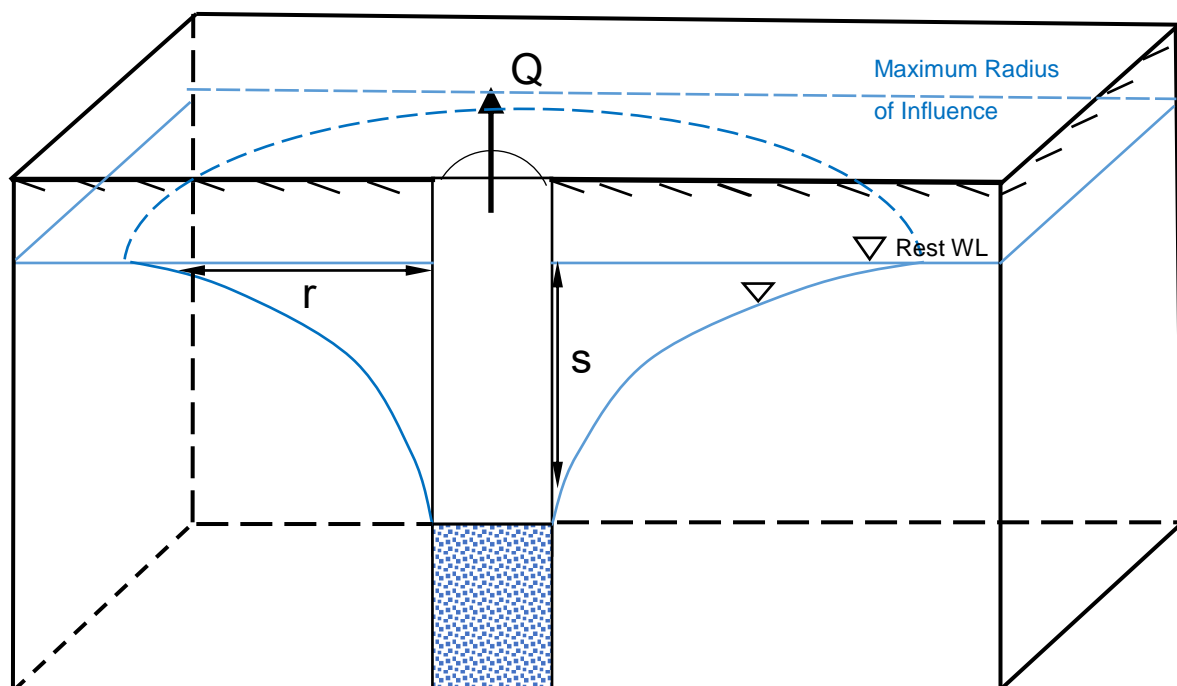


Figure 2-17: The 3D nature of the cone of depression of a borehole (Murray et al., 2012)

In 1935 the radial flow equation was developed by Theis (Murray et al., 2012). Theis, as cited in Heath (2004), developed the radial flow equation based on the following assumptions:

- Transmissivity is constant throughout the aquifer, or at least up to the end of the cone of depression;
- Water pumped from the borehole is withdrawn from aquifer storage; and
- The water discharged from the system penetrates the entire aquifer system, and water storage in the borehole itself is considered negligible to the water abstracted from the aquifer.

An approximation equation (Cooper-Jacob equation) was derived from the Theis radial flow equation and its associated assumptions. The Cooper-Jacob equation maintains that if both the transmissivity and storativity of the aquifer is known, the drawdown behaviour can be described. If there are various

boreholes in a wellfield located in the same aquifer system, subjected to pumping their respective drawdown behaviours can interfere with one another resulting in a water level drop below the maximum allowable water level, causing borehole failure. Furthermore, overlapping failures can result in an overall drop in aquifer water level, impacting the sensitive ecosystems found in groundwater.

According to Murray et al (2012), the Cooper-Jacob model was developed to aid in the design of boreholes in wellfields for minimizing interference, achieved by testing different pumping rates and borehole placement scenarios. The drawdown at a borehole is most sensitive to the borehole pumping rate and aquifer transmissivity.

The Cooper-Jacob equation (Equation 2-16) as cited by Murray et al. (2012) is as follows:

$$s = \frac{2.3Q}{4\pi T} \log\left(\frac{2.25Tt}{r^2 S}\right) \quad (2-16)$$

Where:

s	=	Drawdown (m)
Q	=	Pumping rate (m ³ /day)
T	=	Transmissivity (m ² /day)
t	=	Pumping duration from commencement (days)
r	=	Radius of borehole or radius of influence if drawdown is known (m)
S	=	Storativity ($0 < S < 1$)

Furthermore, the radius of influence for a single borehole can be calculated by using Equation 2-17 and setting drawdown to zero (end of cone of depression), as previously explained. Therefore, the radius of influence is expressed by Equation 2-17 as retrieved from HydroSOLVE (2019).

$$r = 1.5 \times \sqrt{\frac{T \times t}{S}} \quad (2-17)$$

Where:

r	=	radius of influence (drawdown = 0) (m)
T	=	Transmissivity (m ² /day)
t	=	time from commencement of pumping (days)
S	=	Storativity ($0 < S < 1$)

The Cooper-Jacob Equation is both applicable to unconfined and confined aquifers, although their respective drawdown behaviours are different. In unconfined aquifers the cone of depression follows

the same 3D pattern as illustrated in Figure 2-17, which expands slowly as the borehole is subjected to pumping. If an aquifer's transmissivity is high, groundwater is able to move through the aquifer rapidly during pumping resulting in a gentle drawdown slope. The radius of influence is high because a medium that allows a high rate of groundwater flow can affect a larger area during a given time period. Conversely, an aquifer with a low transmissivity will produce a steep drawdown curve during pumping and limited areal extent of drawdown (Heath, 2004). Additionally, storativity plays a part in drawdown regarding the nature of the aquifer. Unconfined aquifers have larger storativity values (known as specific yield) than confined aquifers (known as specific storage).

Ability to store groundwater in unconfined aquifers is equal to specific yield of the aquifer (Heath, 2004). In a confined aquifer, the water table inside the borehole will be controlled by hydrostatic pressure upon pumping. When accessed water underneath a confining layer enters the borehole under pressure, the cone of depression expands rapidly, resulting in a smaller radius of influence (Heath, 2004). For the stochastic analysis of groundwater, when using the SVF method, the usage of the Cooper-Jacob equation will be restricted to unconfined aquifers and boreholes.

One criticism of the Cooper-Jacob equation is that it does not take any recharge into consideration, which means that the water level of the borehole or aquifer would just drop infinitely, which is not a true reflection of reality. There are also a number of boundary conditions that exist for boreholes in aquifer systems, such as rivers and impermeable rock structures. For more information on boundary conditions and the expected drawdown behaviour of each scenario, Heath (2004) can be consulted. For the purpose of investigating whether potential failure of boreholes occur due to borehole interference, the aquifer system is restricted to the assumptions made by Theis and Cooper-Jacob.

2.3.8.1 Coordinate System

If there are a number of boreholes within one wellfield, the boreholes might influence each other, by causing a drawdown on each other. A drawdown on a specific borehole will be imposed if the boreholes within the area have a larger radius of influence than the distance between the specific borehole and each other borehole in the area. To determine if the radius of influence of one borehole overlaps another borehole, the distance between the boreholes will have to be determined (Xu & Beekman, 2003).

However, distance can only be calculated for cartesian coordinates. Therefore, to determine the distance between boreholes, spherical coordinates (latitude and longitude) have to be converted to the x, y coordinate system. The Universal Transverse Mercator (UTM) system is based on an ellipsoidal model of the Earth and is used to convert spherical coordinates into grid coordinates. In the UTM coordinate system a grid is used to specify locations on the surface of the Earth. Instead of a single map projection, the UTM makes use of a series of sixty zones, each being a six-degree band of longitude, and uses a secant transverse Mercator projection in each zone. A UTM coordinate comprises a zone number, a

hemisphere (N-S), an easting and a northing. Eastings are referenced from the central meridian of each zone and northings from the equator, both in meters.

2.4 Desalination and Reuse as augmentation resources

Desalination and reuse technology, involving membrane processes, was first developed in the arid and semi-arid regions of California (USA) and Lanzarote (Spain), where water was already considered a scarce commodity in the 1960s and water security is still of concern today (Buenaventura, 2019). Other arid countries such as Israel and Australia are now leading the way in water conservation by adopting desalination technology on a large scale (Rayne of the Valley, 2015). Australia spent \$11 billion over the course of their drought (12-year period from 1997 to 2009) on desalination plants and today the city of Perth (Western Australia), still uses desalination to provide nearly half of the city's water.

Membranes made of cellulose acetate are capable of blocking salts, while allowing water to pass through at a reasonable rate of flow under high pressure. This process is referred to as reverse osmosis. Desalination is defined as the process of reducing the levels of multi-valent and mono-valent ions in saline water to make it acceptable for potable use (Du Plessis et al., 2008). Desalination through reverse osmosis can be applied to the following water sources, making it potable for reuse: seawater; brackish or polluted groundwater; and effluent for reuse (water reclamation). Desalinated water resources are climate-resilient and have the potential to provide water without interruption 100% of the time; however, large capital costs are involved in the construction, operation and maintenance of desalination and reclamation plants. Expensive membranes have to be replaced every 6 years and the application of constant pressure for the reverse osmosis process is energy-intensive (Blersch and Du Plessis, 2017). A brief overview of the capability and feasibility of desalination and water reclamation plants, as possible options for augmentation to the existing water supply systems on a larger scale in South Africa are discussed from section 2.4.1 to 2.4.3. The brine of such desalination plants are considered hazardous waste. There are various methods employed for the disposal of brine, for example, mixing treated effluent with the brine and releasing it into the ocean. However, this research will focus on the water resource of desalination to meet the demand.

2.4.1 Desalination in South Africa

Surface water and groundwater are widely recognized as conventional water resources when compared to desalination and reuse. Coastal towns in arid regions of South Africa, with limited access to surface water and/or groundwater have readily made use of seawater desalination, as it can supply an unlimited quantity of high-quality, fully assured (potable) fresh water at a predictable price (DWS, 2018). This attribute effectively converts water from an economic constraint to an uncapped economic commodity.

In South Africa, most seawater desalination plants were developed as drought-response interventions. In other words, short-term augmentation options to address supply shortages, as its introduction into

the water supply system, is immediate. Desalination projects implemented in the southern and western regions of the Western Cape Province were undertaken under emergency conditions during drought periods with considerable time pressure, which differentiate them from other desalination projects. Table 2-2 gives more detail about the locations, costs and commencement dates of these desalination plants (Blersch and Du Plessis, 2017; DWS, 2018; Patel, 2018).

Table 2-2: Desalination plants commissioned as a result of drought periods

Town/ City	Capacity	Output	Capital Cost	Date in commission
Sedgefield	1.5 Mℓ/day	1.5 Mℓ/day	R 16 million	December 2009
Plettenberg Bay	2 Mℓ/day	2 Mℓ/day	R 32 million	December 2010
Mosselbay	15 Mℓ/day	Plant is on standby, as dams are full. (according to DWS)	R 210 million	September 2011
Saldanha Bay (Transnet)	3.6 Mℓ/day	2.4 Mℓ/day	R500 million (estimation by dti)	August 2012
Lambert's Bay	1.7 Mℓ/day	1.7 Mℓ/day	R 60 million	Still to be decided

In response to the *Day Zero* crisis scenario, four of the seven planned augmentation projects bringing new water sources online for CoCT, are desalination plants, located at the V&A Waterfront, Cape Town harbour, Monwabisi and Strandfontein (False Bay coast). Another desalination plant was constructed at Koeberg for Eskom's usage.

Desalination has also been used as augmentation resource for mining and other industries, such as PetroSA (Mossel Bay) and Transnet (Saldanha Bay).

Four main operational scenarios with regard to implementation and integration of desalination plants into existing water supply systems were identified (Blersch & Du Plessis, 2017; Mallory et al, 2013):

- Augmentation of surface water and groundwater resources in crisis situations;
- Conjunctive use of resources as an integrated system, with desalination plants operating at full capacity on a permanent basis, providing a constant base supply;
- Desalination used as augmentation resource during periods of high demand (summer months, including peak tourism season); and
- Desalination either operational or on standby, depending on dam levels.

Mallory et al. (2013) suggested that desalination plants be continually operational due to its drought resilient characteristics, the flexibility of the placement (location), immediate integration into the water distribution network, as well as its ability to respond to population and economic factors.

An evaluation of the cost-effectiveness of seawater desalination, as part of the effort to augment CoCT water supply, was carried out by Blersch and Du Plessis (2017). A desalination plant was simulated as a constant inflow channel, using both the Water Resource Yield Model (WRYM) and Water Resource Planning Model (WRPM). The study concluded that the most cost-effective way to incorporate a desalination plant into the existing water supply system, was to use it on a continuously operational level as a base supply. The reason for continuous use is that expensive membrane technology deteriorates when the desalination plant is not in use. It was also found that electricity constitutes approximately 50% of the total operational and maintenance costs of desalination plants.

2.4.2 Reuse in South Africa

The reuse of water through water reclamation has positive environmental benefits, as it protects aquatic ecosystems (wetlands and coastlines) from impacts related to over-abstraction, degradation, and wastewater (effluent) discharge.

Aurecon (2011) studied water reclamation and its potential in the Olifants River Catchment on behalf of the DWS. The study defines the related terms as follows:

- **Recycle:** When water is used in a process and then reused in the same process with or without any purification / treatment or improvement of the water quality.
- **Reuse:** When water is used and the return flow is then used again for another purpose. This may include purification (treatment) to some acceptable level for the secondary use, but the water is not treated to potable standard.
- **Reclaim:** Water that was previously used for potable or any other purpose, treated up to potable quality standards so that it can again be used for potable purposes.

Even though the agricultural sector uses the largest percentage of total water supplies in South Africa, only a fraction of these enterprises utilize their own wastewater (treated) directly for irrigation (Aurecon, 2011). The reuse of water is however widely implemented by water intensive industries, such as mining and manufacturing, through process water recycling and cascading water uses (Aurecon, 2011). The extent of reuse and the specific details as to how water is reused is industry and process specific. Numerous examples of small water reuse schemes in South Africa exist, but these are generally implemented on an ad hoc basis or as an emergency measure during severe drought, rather than incorporated as an integral part of the water system (Gorelick and Serjak, 2018).

The focus of this research is on developing a tool for determining yields when the water supply system of a municipality is optimized for domestic use, by combining different water resources (inflow

streams). Thus, water reclamation processes occurring independent of municipalities (water providers) for industrial and agricultural use will not be further included in this research.

At the Goreangab Water Reclamation Plant in Windhoek, Namibia, wastewater and semi-purified sewage is treated to a potable standard, providing the city with a sustainable supply of approximately 21 Mℓ/day (a third of the city's total potable water supply) (Gorelick and Seriak, 2018).

Windhoek increased its reliance on reused water from 16% to 29% during its 2015/16 drought. This water reclamation plant is world-renowned, as it has the ability to facilitate the economic and social growth of this arid region.

Similarly, the Municipality of Beaufort West, the largest town in the arid Karoo region of South Africa, had commissioned a water reclamation plant, providing potable water for domestic use. The reclamation plant first came online in January 2011 and delivers 1.8 Mℓ/day of potable drinking water. Beaufort West blends approximately 20% (has the potential to be increased to 25%) reused water into its water supply from local dams (Marais and Von Durkheim, 2011). The project was groundbreaking, in that it unlocked a significant water source, which was historically either overlooked or under-utilized. The treatment plant uses a nine-step process that includes pre-treatment, rapid sand filtration, membrane ultra-filtration, reverse osmosis, and advanced oxidation.

This multi-barrier treatment approach adds complexity and cost compared to traditional treatment processes. Treating wastewater for potable water reuse using reverse osmosis necessitates only one-third the energy requirement of sea water desalination and costs approximately 30 percent less (Gorelick and Serjak, 2018). However, treatment costs are offset by the fact that the source water is essentially free compared to other bulk water sourced from dams or groundwater. Furthermore, the water produced from reused water is often of a higher quality than other potable water sources.

2.4.3 Future usage of desalination and water reclamation in South Africa

After successful implementation of desalination and water reclamation plants locally, the DWS decided to investigate the possibility of bringing more of these sources online for future use. In South Africa, as of October 2018, 30 desalination plants have been built, for both surface and groundwater treatment, and are in various states of operation, with a combined installed capacity of 208 Mℓ/day (DWS, 2018). Another four plants were under construction, and a further 19 were in various stages of planning. Cape Town was, in the early half of 2018, exploring the viability of a desalination plant in the 150-450Mℓ/day range, to supplement water supply to a demand in the region of 950 Mℓ/day.

2.5 Optimization of Water Resources

Water resource optimization is undertaken by applying models to real life scenarios, such that different situations can be simulated before they occur. Simulating future events provides the water resource manager with valuable information used for planning, managing and optimizing water resources. South

African models which are currently in use within the water resources management sector are discussed. Furthermore, conjunctive use models which have been developed by international authors are summarized with regard to key application tools to South African optimization and modelling of conjunctive water resources.

2.5.1 South African Hydrological Modelling

The hydrological planning models of South Africa consist of three primary tools, namely deterministic, stochastic and system related models. A deterministic tool relating rainfall to runoff is the Water Resources Simulation Model (WRSM2000). In this model, rainfall and runoff data is used to determine the volume of water that moves through an inter-related water system. It also provides the basis at which streamflow extension and natural streamflow generation takes place, through calibration processes and subtracting manmade influences respectively (Seago et al., 2008). Deterministic outputs of the WRSM2000 are used as inputs for stochastic models. The second group of modelling tools encompass stochastic modelling, whereby probabilistic and deterministic parameters of historical sequences are used to generate stochastic sequences, which represent climatic variations. The third group of modelling tools consist of system modelling, which makes use of stochastic sequences (Seago et al., 2008). These modelling tools include the WRYM, the WRPM and the Water Quality and Sulphates Model (WQS). Figure 2-18 illustrates the technical classification groups for water resource models, as well as the available South African water resource models' inter-relationships.

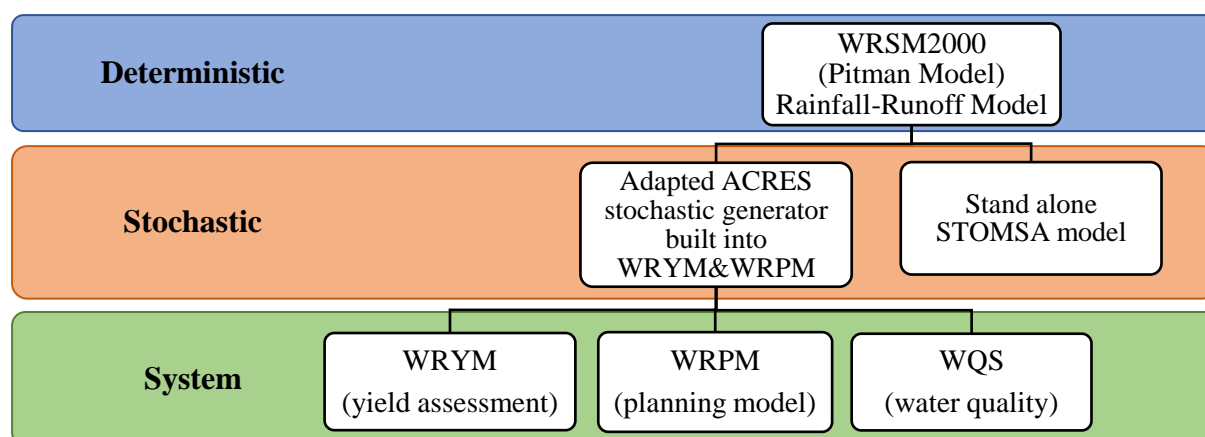


Figure 2-18: Classes and connections of water resources models (Seago et al., 2008).

Both groundwater professionals and water resource planners are stressing the importance of not only developing groundwater or surface water solutions, but seeking conjunctive use solutions to ensure water security in an environmentally sustainable manner, especially in arid regions where droughts are forecasted to occur more frequently in future, due to changing climate conditions. The National Water Resource Strategy (DWS, 2013), states the following in terms of conjunctive use solutions, "Conjunctive use of surface and groundwater consists of harmoniously combining the use of both

sources of water in order to minimize the undesirable physical, environmental and economic effects of each separate solution and to optimize the efficient use of the total water resource.”

2.5.2 Conjunctive Use Principles

Three international articles on the conjunctive interaction between surface water and groundwater were reviewed. The main principles taken from the three articles are summarized in Table 2-3. Both the Conjunctive Use Model (Mahjoub et al., 2011) and the Multi-step Planning Model (Onta, Gupta, and Harboe, 1991) were utilized for the optimization of surface- and ground-water use for irrigation within a basin area with seasonal time-steps. All models took the aquifer parameters into account when developing dynamic water balance models, even though the models were different in each case, as different sets of assumptions and limitation criterion existed. Interconnections between system components were expressed using different mathematical models in each case. Models for separate system components in a South African context are discussed in the sections to follow.

Table 2-3: Conjunctive interaction between surface water and groundwater

Models developed by:	Region and time-steps	Main Approach
Conjunctive Use Model (Mahjoub, et al., 2011)	River Basin Scale (Maraghe Plain, Iran) Seasonal	Constrains on aquifer storage were based on maximum water level drawdown of 3m. Soil humidity was taken into account. Ratios of 75% surface water and 25% groundwater was deemed to be most viable on yearly basis. Simple reservoir mass balance.
Multi-step Planning Model (Onta, et al., 1991)	River Basin Scale (Bagmati River Basin, India) Seasonal	Stochastic model considering sub-components in water balance equations. Simulating the lumped characteristics of the aquifer system for each time-step. Considering three flow categories and an unconfined aquifer system.
Economic Optimisation (Pulido-Velázquez, et al., 2006)	River Basin Scale (Andra River Basin, Spain) Monthly	Multi-reservoir system with interlinked flow equations between system components. Eigenvalue equations provide basis for mass balance in the system while taking physical boundaries and physical characteristics into account.

2.6 Summary

Literature findings for modelling the conjunctive use of surface water and groundwater are presented in Table 2-4. Surface water and groundwater have a number of overlapping principles and some key differences, as presented by both Xu and Beekman (2003, 2018) and Murray et al. (2012).

Table 2-4: The similarities and differences between Surface Water and Groundwater

Surface Water	Groundwater
Similarities	
Rainfall results in storage increase	Rainfall results in recharge of aquifers
Streamflow response to rain as seen in hydrograph curve	Baseflow response to recharge represented by a smoothed hydrograph curve
Overflow into downstream rivers or storage	Overflow into river streams as baseflow
Minimum Operational Level where failure occurs	Minimum Aquifer storage level where failure occurs (In case of AFYM 5m below lowest average)
Can be assessed on a quaternary catchment scale	Can be assessed on a quaternary catchment scale
Differences	
Specific volume that can be determined through basin analysis	Specific volumes of aquifers are not easily established because of water in rock pores
Infinitely permeable with storativity of 1	Permeability dependent on geology, storativity is less than 1

The inter-relationship between surface water and groundwater can be established by examining rainfall (recharge) and baseflow. Xu and Beekman (2018) suggest that a number of recharge estimation methods should be applied in a study to cross-check values and “extinguish” some limitations. Furthermore, Gelhar (1994) suggested that groundwater models should incorporate geological parameters, the stochastic nature of groundwater and rely on physical laws of underground flow. Therefore, the AFYM lumped-parameter box model is deemed applicable, as it uses both CMB values from GRA II and the SVF method to evaluate aquifer storage at critical management levels. Furthermore, borehole yields are affected by multiple boreholes pumping from the same aquifer system, thus it is deemed necessary to take the interference between the boreholes into account with the Cooper-Jacob equation.

According to Xu and Beekman (2003, 2018) and Murray et al. (2012), further development is required in the sphere of managing groundwater in a multi-disciplinary context. Furthermore, more conjunctive use related solutions should be developed that incorporate all available resources and expand on the use of the desalination and reuse where applicable.

After reviewing different models and their components, as well as examining their differences and similarities, the conclusion is that components used for modelling conjunctive use of a variety of water resources should satisfy the criteria that will suit a local municipality: simple management tool; daily time step measurement of yield; easily accessible and user-friendly nature; and combine all the water resources available for domestic use.

Each component of the conjunctive use model is integrated into a single daily time-step model. The conjunctive system is evaluated on a daily basis to simulate water availability. In order to perform a system balance, inflows from the different components are balanced against the demand. Demand is given in monthly percentages of the draft which are distributed evenly over the days of each month. Therefore, as illustrated by Figure 2-19, surface water enters a storage dam, while desalination and/or water reclamation, and groundwater enter into the supply system directly (without being stored).

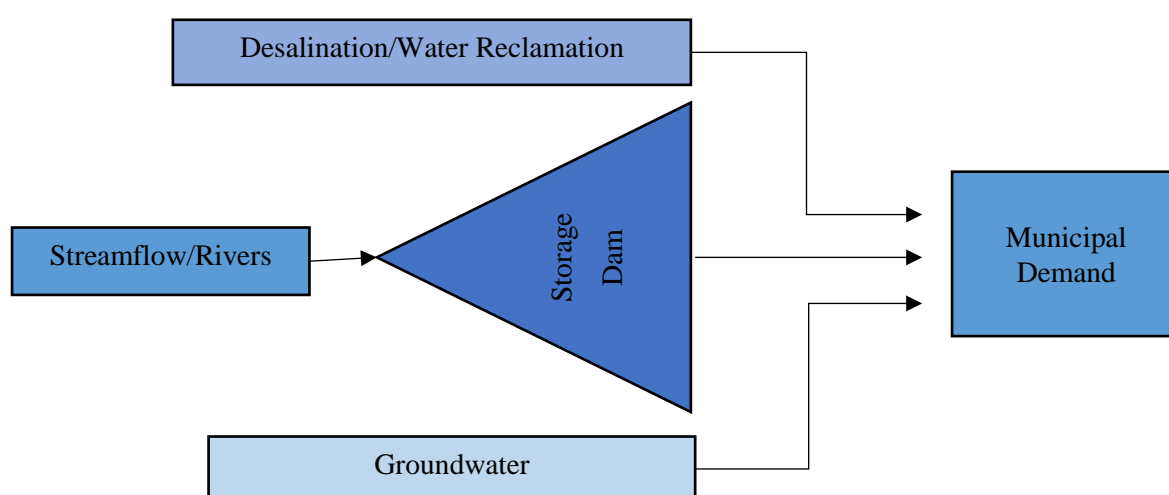


Figure 2-19: Proposed model components for conjunctive water resource use for municipal supply

Augmentation of water resources utilizes water resources in succession, as one water resource fails to supply the demand, another is utilized until it fails, and then the next water resource is used until it too fails. However, in the context of this research, conjunctive use is considered a more sustainable utilization of resources. Conjunctive use refers to utilizing water resources simultaneously, by incorporating the links between different component. Different water resources, with different characteristics, are utilized as a single unit to supply the demand. The components should ideally be scaled in such a way that a part of the demand can safely be supplied by the base supply of desalination or water reclamation (climate independent characteristics), another part by groundwater resources, and another by surface water resources (climate dependent characteristics). Depending on the availability of the resources within the municipal area, one resource might provide for a larger part of the demand than another resource. The aim of conjunctive use is to utilize each water resource sustainably, while meeting increasing demands.

3 METHODOLOGY

The literature, reviewed in Chapter 2, indicates that it will become necessary to use water resources in a conjunctive manner to ensure sustainability of available water supplies. It also provides a basis of the modelling principles from existing models and simulations of the separate water resources, some of which are already used by practitioners in the field of hydrology. Furthermore, it also indicates that the possibility to develop a tool for assessing the yield of a conjunctive use system, can be undertaken by incorporating the array of existing models and simulations. The components of such a comprehensive conjunctive use model can be identified and readily available data can be obtained and processed, after which it can be modelled with a user-friendly and inexpensive tool, rendering it ideal for usage at local municipalities.

3.1 Overview

To determine the yield of a conjunctive use model, a conjunctive use system balance is performed, using data obtained for resources such as surface water, groundwater, desalination and water reclamation. Surface water and groundwater are linked through rainfall, and stochastic analysis is performed using stochastic sequences generated by STOMSA. Desalination and water reclamation are modelled in a similar way, and both are considered to make use of reverse osmosis membrane technology without being climate dependent.

The conjunctive use model (system balance) is developed in Microsoft Excel 2016. Excel worksheets are used as computational interfaces, while Visual Basic Macros are used for formulas making use of recurring processes. Although the storage capacity of Microsoft Excel is limited to a certain extent, it is ideal for local municipalities, as it is accessible in terms of practical implementation and user-friendly in terms of conceptualization.

The WR2012 quaternary hydrological data sets, hydrogeological parameters from GRA II, information specific to municipal reservoirs and demand all serve as input data to the conjunctive use model. Figure 3-1 outlines the steps followed for assessing the yield of a conjunctive use system, starting from the point of obtaining data, then processing the data for use as input to the components of the model, and finally performing a system balance simulation.

The conjunctive use model involves the application of stochastic links between surface water and groundwater as indicated in Figure 3-1. WR2012 data (generated by WRS2000), is fed into STOMSA (external model excluded from Excel sheets) to generate monthly stochastic sequences. Monthly streamflow sequences are then disaggregated into daily sequences, using historical streamflow categories and their associated daily distributions. The daily sequences are then used to model inflow to the surface water reservoir. Rainfall-Runoff relationships are established and applied to generate daily rainfall data, to determine net evaporation. Stochastic rainfall is also used to model the

groundwater component, together with catchment data from the GRA II. By applying the SVF equation and the principles of the AFYM to aquifer parameters of the catchment, potential available abstraction can be assessed in monthly time steps. Desalination and water reclamation are combined and used as a single component, as both sources follow identical operational rules, namely that the minimum operational periods are 3-monthly blocks dictated by the demand.

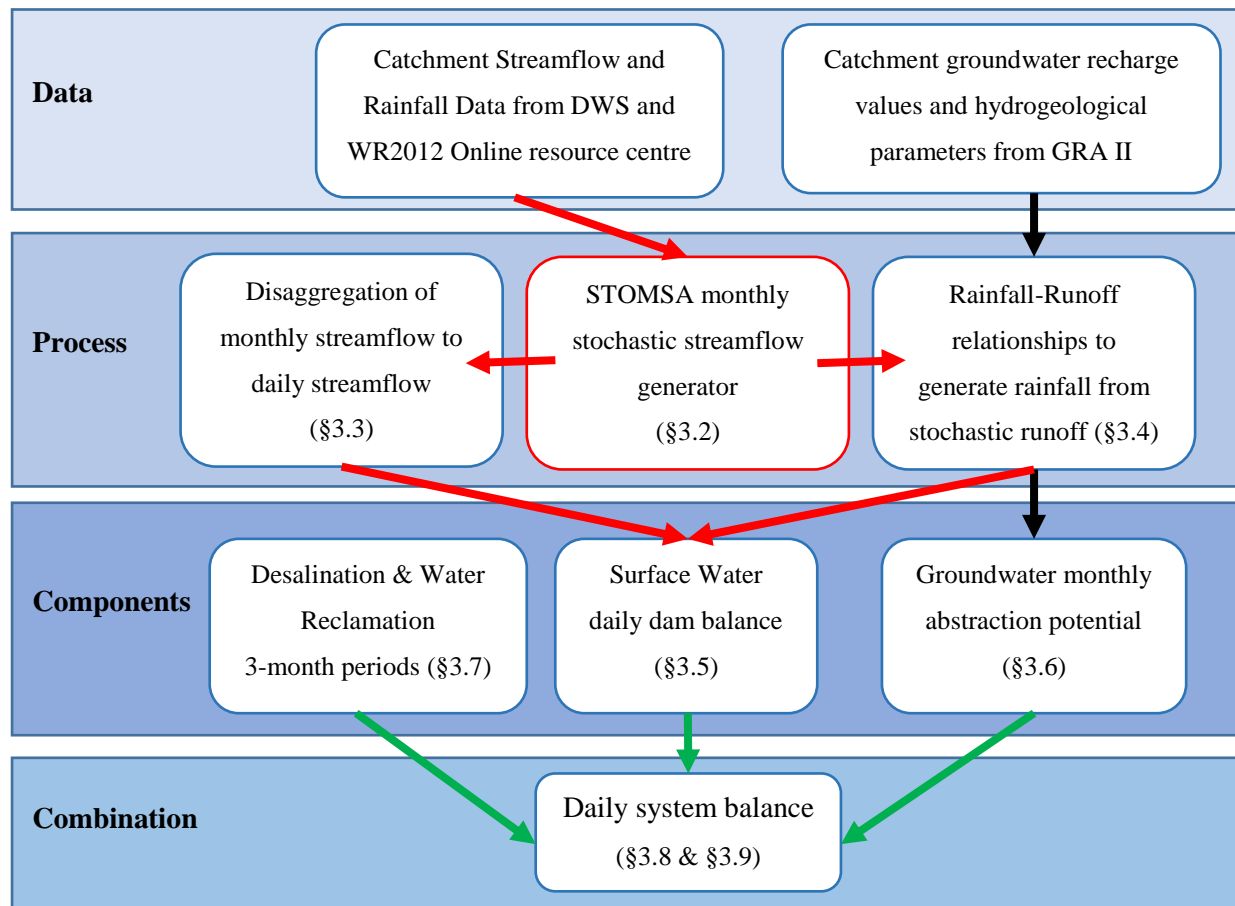


Figure 3-1: Data and components for yield assessment of a conjunctive use system.

The three components as mentioned above are integrated when performing the daily system balance analysis, which is used to determine the yield and the reliability of supply of the conjunctive use system.

The components as indicated in Figure 3-1 are arranged into 4 separate Microsoft Excel workbooks as follows:

1. Streamflow Classes - daily streamflow is categorised into monthly flow classes with associated daily streamflow distributions, calculated with the established historical RAIN-RUNOFF ratio.
2. Streamflow Disaggregation - monthly stochastic streamflow sequences (generated by STOMSA) are disaggregated into daily stochastic streamflow sequences.
3. Groundwater Simulation - potential groundwater abstraction for the aquifer system is determined with recharge as a percentage of rainfall.

4. System Balance Simulation - yield calculation sheet of conjunctive use of groundwater, desalination and water reclamation, and surface water.

Concepts, equations and assumptions are discussed from section 3.2 to section 3.8 and follow the order in which the excel sheets (computational interfaces) are used. However; a more detailed set of instructions for the steps followed as mentioned in Figure 3-1, as well as instructions for navigation of the program, are contained and discussed within the User Guide, included in Appendix A.

3.2 Generating Stochastic Monthly Streamflow

STOMSA is used to generate stochastic streamflow sequences in monthly time steps. Naturalized streamflow data, retrieved from WR2012, serves as the historical streamflow sequence of a quaternary catchment for input into STOMSA. The historical streamflow sequence of a quaternary catchment is used for groundwater simulations, while only a portion of a catchment's streamflow contributes as inflow to a surface water reservoir (discussed in section 3.5.1). Naturalized streamflow data is available in monthly time steps per quaternary catchment. The suitable quaternary catchment is selected based on the location for which yield analysis is to be conducted.

3.2.1 STOMSA Input File Preparation

The input file required by STOMSA is a space delimited text file format with an “.INC” extension. The historical streamflow data file is a text file with an “.ans” extension, which can be opened with Microsoft Excel in the form of a spreadsheet. The historical streamflow data is split into columns using a fixed delimited width. The width of all the columns are adjusted to 8 inches (61 pixels) and then saved as a “.prn” space-delimited file. The name (file extension) of the “.prn” file is then changed to “.INC”, and the historical streamflow sequence is ready to be inserted into the STOMSA model.

STOMSA has a default setting, which can be used to apply the marginal distribution and serial correlation to the historical monthly streamflow data to generate stochastic sequences. No cross correlation is applied as only one catchment is considered (Section 2.1.3).

3.2.2 STOMSA Output Files Processing

STOMSA creates 101 stochastic sequences with a separate text file (csv file) for each sequence, containing monthly streamflow values. To disaggregate the stochastic streamflow sequences the 101 csv files are first combined into one super file to serve as input into Microsoft Excel 2016. A program to combine the 101 csv files into 1 Excel worksheet was developed using the Microsoft Office Visual Studio 2017 application. The program created with the Visual Studio 2017 application, is called “*STOMSA File Combiner*” and can be run on computers with Windows as its operating system, as is customarily the case in South Africa. The user interface is illustrated in Figure 3-2. Upon selecting the start button, a new file called “*combine*” is created which contains the “*STOMSA_superfile*”. The program adds each string of text in each csv file horizontally to the previous csv file, thus, a horizontal

stochastic record of sequences, is created. The super file can be opened by the user in Microsoft Excel 2016 once the process of combining the stochastic sequences are completed.

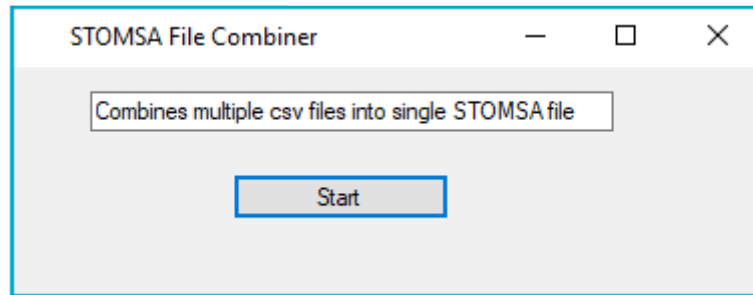


Figure 3-2: “STOMSA File Combiner” program user interface

3.3 Disaggregation of Stochastic Streamflow

Daily streamflow data for a source station, located within the catchment of interest, is obtained at the DWS website under the *Dams, Flows and Floods* section. Instead of using a 3-month window of data to assess the variance in daily flow distributions to provide for seasonality as suggested by Acharya and Ryu (2014), a classification system as suggested by Hoffman (2019), was adopted. The historical daily streamflow recorded over a number of years, is categorized into three streamflow classes (high, medium and low flow scenarios within the same month). This can be applied to disaggregate historical and stochastic streamflow for any target station within the same catchment. Thus, the need for a root mean error computation is eliminated.

The overarching methodology to disaggregate monthly streamflow data into daily streamflow data is outlined in Figure 3-3. Methodologies applied during each step of the disaggregation process are discussed in sections 3.2.1 and 3.2.2.

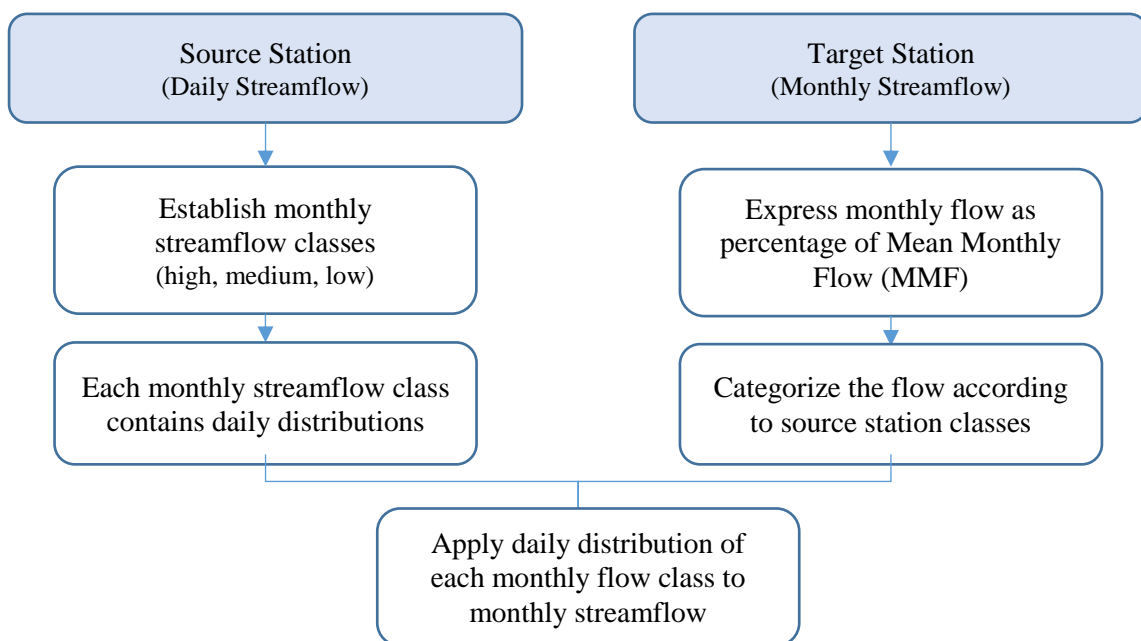


Figure 3-3: Flow diagram of daily disaggregation of streamflow

3.3.1 Streamflow classification according to Source Station

Daily historical streamflow data is retrieved from the DWS website by selecting the “*Dam, Flows and Floods*” link, and searching for the source station in the “*verified streamflow*” section. A source station (streamflow gauge) is selected based on its proximity to the site of abstraction, the length of the historical streamflow record available, and the continuity of the historical record (no information gaps). To maintain accuracy of results and preserve the computational abilities of the Microsoft Excel application, the daily streamflow distribution data used for simulations should consist of a historical record of at least 20 years, but should be limited to 60 years, as excess information slows down computation time.

Data recorded at flow gauges, obtained from the DWS website, is expressed as an average flow in cubic meters per second (m^3/s). It is converted to an average daily volume (m^3/day) by multiplying the given figure with the number of seconds occurring within one day ($\text{m}^3/\text{s} \times 60 \times 60 \times 24 = \text{m}^3/\text{day}$). It should be noted that data for 20 consecutive years (7000 lines) can be retrieved from the DWS website at a time, due to information recall capacity limitations of the website. Thus, upon the second and third attempts of data retrieval, different start dates would have to be selected to retrieve the remainder of the available record. The above-mentioned streamflow data is labelled with quality codes, indicating whether the data is accurate, continuous or sufficiently edited, or whether its unreliable, due to discrepancies, such as malfunctioning of the gauges resulting in information gaps. For a full description of all quality codes refer to Appendix B.1. Should a quality code indicate that the data is unreliable for some reason, such daily streamflow data will be disqualified and the whole month will be eliminated from usage during the streamflow classification process, as the associated monthly total will be inaccurate or misleading.

The eligible (reliable) daily flow volumes are then categorized into 3 different classes to provide for seasonality or variability of rainfall, due to climate systems (El Niño/ La Niña) or changing climate conditions, when considering disaggregation. Some years might have been dry years and others might have been wet or close to average rainfall years. Thus, it is deemed necessary to categorize daily streamflow distributions of each month in the historical record, into 3 different streamflow classes, representing 3 main scenarios, namely monthly high, medium and low flow scenarios. Streamflow classes are established through the following steps:

1. All the daily streamflow volumes, belonging to a specific month, are totalled and then grouped according to its associated month. For example, if a historical record of 20 years is in use, there will be 20 sets of monthly flow volumes for each month. The 20 sets of monthly flow volumes are then ranked in descending order.

2. The ranked monthly flow volumes are then categorized according to 3 classes, namely high, medium and low flow, in such a way as to have approximately the same number of volumes in each flow class. For example, if there are 10 monthly streamflow volumes available for a specific month, over the historical record, the 3 highest monthly streamflow volumes are used to establish the bounds of the highest streamflow class and the 3 lowest streamflow volumes are used to establish the lowest streamflow upper bound. Thus, the remaining streamflow volumes will fall into the medium flow class.
3. Mean Monthly Runoff (MMR) is the average monthly streamflow volume for a specific month over the span of the historical record. For example, if the historical record is 25 years long, effectively there will be 25 different volumes associated with a specific month, i.e. November. The 25 monthly volumes (sum of daily volumes) associated with November are totalled and then divided by the number of years in the historical record (25 in this case) to determine the MMR of November.
4. Daily flow distributions for each month are expressed in percentages, by dividing daily average streamflow (mil m³/day) by the corresponding month's total streamflow (mil m³/month) (Equation 3-1).

$$\text{Daily Distribution} = \frac{\text{Daily Average Streamflow}}{\text{Total Monthly Streamflow}} \quad (3-1)$$

An example of the monthly streamflow classes, which are established as a result of applying the abovementioned steps, are presented in Table 3-1.

Table 3-1: Monthly flow classes as percentages of MMR

Monthly Flow classes (%MMR)			
Month	High	Medium	Low
OCT	> 130%	130% - 70%	< 70%
NOV	> 101%	101% - 13%	< 13%
DEC	> 137%	137% - 17%	< 17%
JAN	> 106%	106% - 14%	< 14%
FEB	> 107%	107% - 75%	< 75%
MAR	> 64%	64% - 20%	< 20%
APR	> 162%	162% - 32%	< 32%
MAY	> 123%	123% - 91%	< 91%
JUN	> 126%	126% - 51%	< 51%
JUL	> 121%	121% - 66%	< 66%
AUG	> 115%	115% - 87%	< 87%
SEP	> 114%	114% - 56%	< 56%

The next step, before disaggregation can be undertaken, entails that user selects the most appropriate distribution for each monthly flow class, or a random distribution value within the available range established for every month. The selected daily distribution represents the daily distributions within the flow class, therefore it should reflect the main trend of daily distributions in that flow class. This is done so that the daily variation with regard to height and occurrence of daily flow peaks can be taken into account. For example, the medium flow class illustrated in Figure 3-4, consists of 4 established daily distributions. Two dominant trends can be identified, namely distributions with one peak and distributions with 2 peaks. The trend that occurs more than once in a monthly streamflow class, can be selected to represent the distribution of that streamflow class. If there are two distribution trends occurring more than once (in terms of peak number), as is the case in Figure 3-4, the peak height that is repeated, in conjunction with the number of peaks, is chosen as the dominant trend.

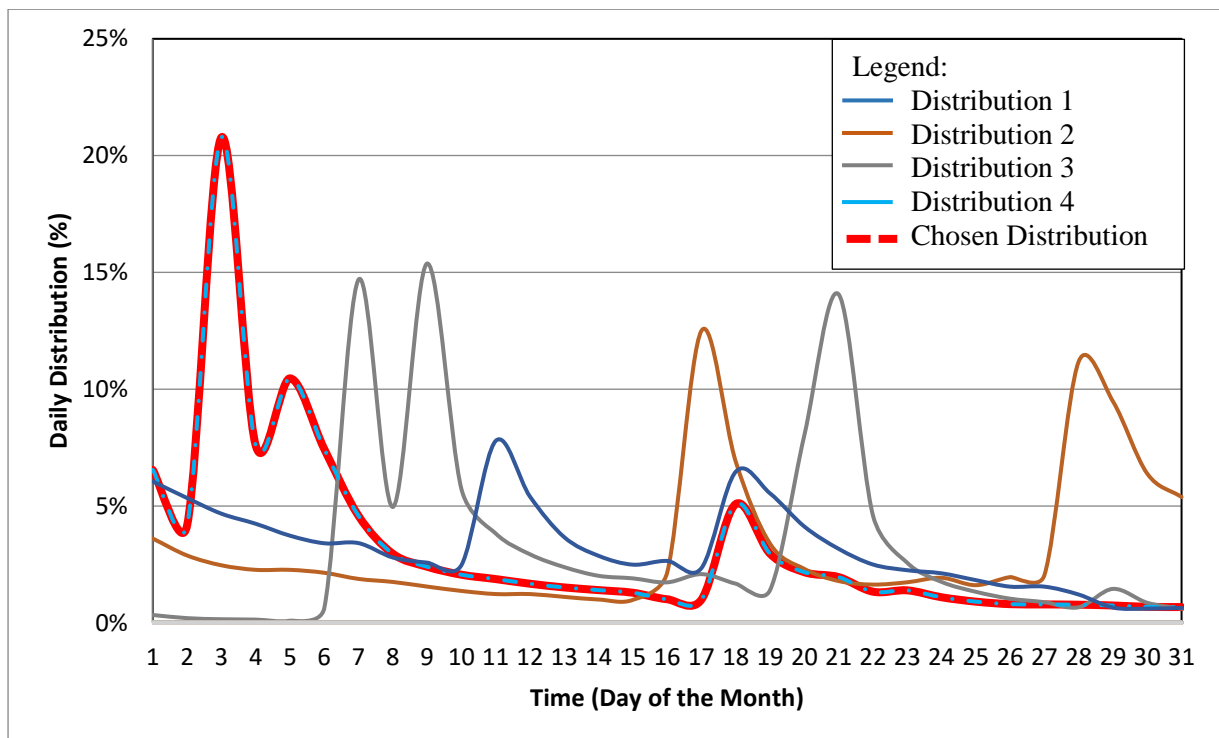


Figure 3-4: Monthly medium-flow class with 4 daily distributions

After the representative daily distribution for each of the 3 flow classes are chosen for each month, the daily distribution table is updated with the relevant percentages. For example, daily distributions for the first 7 days of a month are summarized in the Daily Distribution Table (Table 3-2). Each month has three streamflow classes, corresponding to the percentage limits set in Table 3-2 for the months of October, November and December, and the selected daily streamflow distribution as percentage of the corresponding monthly total.

Table 3-2: Daily streamflow distribution as percentage of total monthly flow

Month	Class % of MMR	Class	1	2	3	4	5	6	7
OCT	>130%	high	7.44%	17.64%	8.74%	6.60%	5.43%	4.72%	4.22%
	130%-70%	medium	6.54%	4.17%	20.78%	7.59%	10.46%	7.44%	4.57%
	<70%	low	3.63%	4.26%	3.55%	3.68%	4.54%	3.67%	2.82%
NOV	>101%	high	0.04%	0.04%	0.04%	0.05%	0.04%	0.04%	0.04%
	101%-13%	medium	0.14%	0.19%	0.14%	10.05%	69.53%	10.00%	0.88%
	<13%	low	0.63%	0.53%	0.74%	0.74%	0.32%	0.53%	0.63%
DEC	>137%	high	0.40%	0.21%	0.08%	0.21%	0.13%	0.13%	0.13%
	137%-17%	medium	17.62%	11.73%	7.99%	6.91%	3.12%	1.19%	1.13%
	<17%	low	3.30%	3.30%	3.30%	2.97%	2.64%	2.64%	2.31%

3.3.2 Disaggregation of Monthly Streamflow

Historical monthly streamflow values recorded at the target station, and stochastic streamflow sequences generated by STOMSA, are disaggregated into daily streamflow sequences, by applying the monthly streamflow values (expressed as percentages of MMR), according to the streamflow class selected by the user, as described in section 3.2.1.

Monthly streamflow values are expressed as percentages of MMR to make them comparable with the historical classification table (refer to Table 3-1). Once the most suitable monthly streamflow class is identified, the corresponding daily distribution (percentage of total monthly flow) is used to disaggregate the monthly flow values into daily flow values by applying Equation 3-2. Daily streamflow corresponding to a time stamp (year, month, day) is the result of the monthly streamflow corresponding to the same time stamp (year, month) and the associated daily distribution corresponding to the classification of the streamflow for a particular month and day. To generate the stochastic monthly streamflow sequences the separate STOMSA stochastic sequence generator program is used.

$$Daily\ Flow_{y,m,d} = Monthly\ Flow_{y,m} \times Daily\ Distribution_{m,c,d} \quad (3-2)$$

Where:

y, m, d = year, month, day

y, m = year, month

m, c, d = month, flow class (High, Medium, Low), day

$Daily\ Flow_{y,m,d}$ = Daily flow in a certain year, month and day (mil m³)

$Monthly\ Flow_{y,m}$ = Monthly flow for a specific year (mil m³)

$Daily\ Distribution_{c,m,d}$ = Daily Distribution associated with flow classification of specific month

3.4 Rainfall-Runoff Relationship

Literature indicates that the main stochastic link between surface water and groundwater is rainfall. Rainfall is used in both surface water modelling, to determine net evaporation, and groundwater modelling, to determine recharge of aquifers. STOMSA generates stochastic streamflow sequences and not rainfall sequences; thus, a rainfall-runoff relationship has to be established to generate stochastic rainfall data from the stochastic streamflow sequences. The stochastic streamflow sequences generated with STOMSA can be used to this end.

The rainfall-runoff relationship, used to convert streamflow to rainfall, is established between the historical monthly rainfall and the historical monthly streamflow for the catchment of interest. Both the rainfall and the runoff data for a particular catchment can be retrieved from the Water Resources of South Africa (2012 Study) WR2012 data base. The resource centre is accessed through registration on the <http://waterresourceswr2012.co.za/> website. On the “Resource Centre” page, data is grouped into different folders and within each folder according to WMA. The “Quaternary data spreadsheets” folder contains quaternary data spreadsheets with information including: MAP, MAR, MAE rainfall zone and evaporation zone. The naturalized streamflow sequences per catchment are obtained from the “Naturalized flow datafiles” folder, while catchment rainfall in percentage of MAP corresponding to a certain rainfall zone is obtained from the “Catchment based rainfall datafiles” folder. The data retrieval process is thoroughly discussed in the user guide (Appendix A).

It is assumed that monthly rainfall-runoff relationships incorporate factors impacting the runoff generated from rainfall such as soil moisture (infiltration), rainfall intensity, catchment slope and vegetation as suggested by literature (section 2.2.3). The historical monthly average RAIN-RUNOFF ratio is expressed as Mean Monthly Precipitation (MMP) - mm converted to m - for a selected month, over MMR for the same month, determined with Equation 3-3:

$$\text{RAIN_RUNOFF } ratio(i) = \frac{MMP_i/1000}{MMR_i} \quad (3-3)$$

Where:

ratio (i) = Historical RAIN-RUNOFF ratio for each month (m/mil m³)

MMP_i = Mean Monthly Precipitation for each month (mm)

MMR_i = Mean Monthly Runoff for each month (mil m³)

In Figure 3-5 monthly rainfall volumes for the month of October were plotted against the naturalized monthly streamflow sequences for the same month (90-year record length), for the catchment of interest. A trend line was fitted to the plotted data points, to establish a relationship between the two variables. The trend line in Figure 3-5 indicates that a linear relationship exists between rainfall and runoff. Although not many points lie exactly on the linear trend line, roughly the same number of points

lie above and below this trend line. Stochastic rainfall sequences are generated by applying the RAIN-RUNOFF ratio determined by Equation 3-3, to the stochastic streamflow sequences generated by STOMSA. The stochastic monthly rainfall values serve as input to the groundwater simulation, while in surface water simulation, the RAIN-RUNOFF ratio is applied to daily streamflow values.

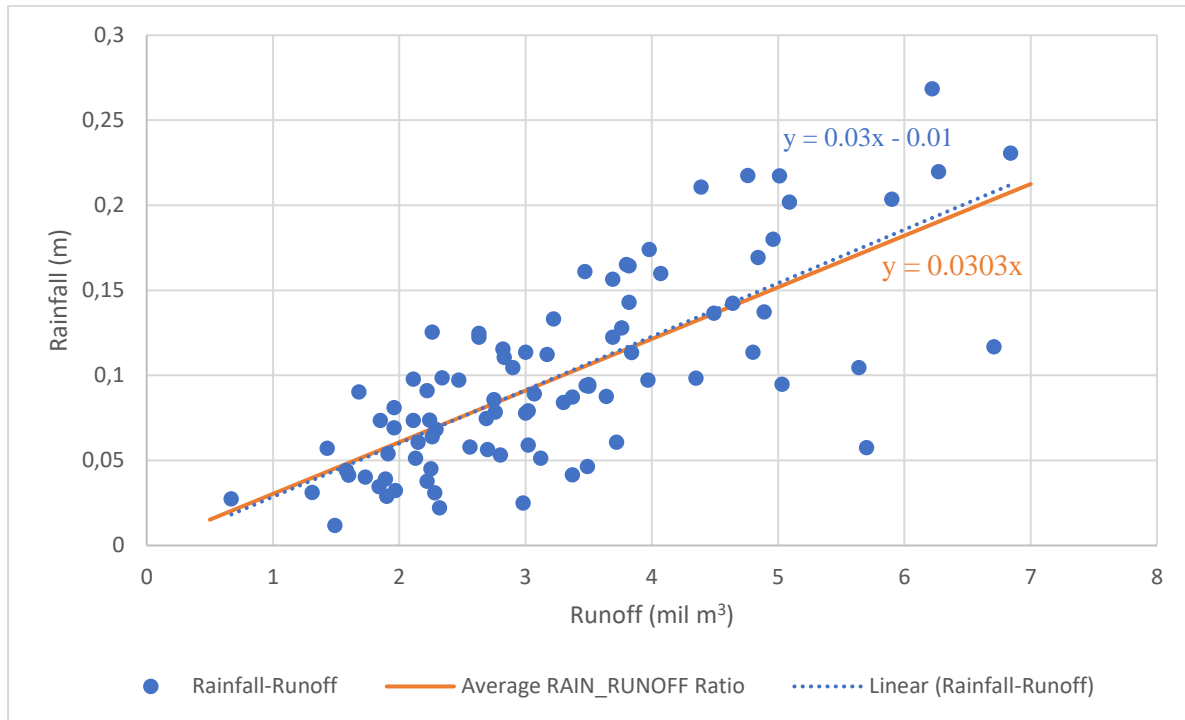


Figure 3-5: Linear relationship of rainfall and runoff

3.5 Surface Water Simulation

Surface water modelling is done through simulation of the reservoir storage, to determine the yield of a water supply system. Figure 3-6 indicates the general layout of a single dam scenario with inflow and outflow volumes. Should there be 2 or 3 dams used for water storage by a municipality, their volumes and surface areas are combined to utilize as input data for performing simulations.

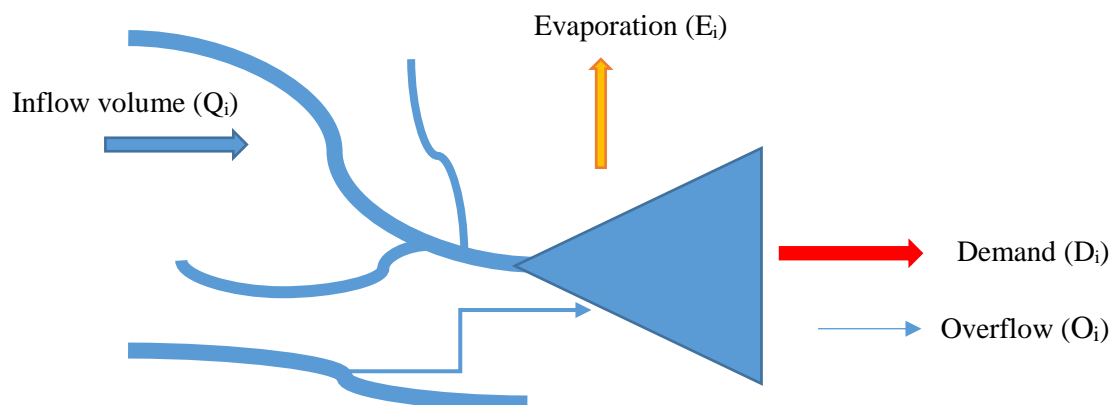


Figure 3-6: Single-dam capacity-yield modelling components

The general time step equation (Equation 2-3 in section 2.2) is used to perform a daily time-step surface water simulation. Environmental releases or seepage losses have not been taken into consideration in this research; thus, the surface water simulation equation is applied in daily time steps, as presented in Equation 3-4:

$$S_{i+1} = S_i + Q_i - D_i - E_i - O_i \quad (3-4)$$

Where:

- S_{i+1} = Storage capacity at the end of the day (Mℓ)
- S_i = Storage capacity at the beginning of the day (Mℓ)
- Q_i = Inflow volume per day (Mℓ/day)
- D_i = Demand per day (Mℓ/day)
- E_i = Evaporation losses per day (Mℓ/day)
- O_i = Overflow volume per day (Mℓ/day)

Inflow volume is the combined volume of a number of different inflow streams contributing to the reservoir. Demand is the volume distributed to the area that the municipality provides water for on a daily basis. Evaporation and overflow volumes are not utilized when supplying for the demand, as these volumes leave the reservoir before distribution to the supply area. Each component of the surface water modelling for this research, as well as the associated concepts and assumptions, as deduced from the literature review, are presented in section 2.2.

3.5.1 Inflow Streams

The daily historical and disaggregated daily stochastic streamflow sequences (discussed in section 3.2 and section 3.3) are respectively used to represent inflow streams to the surface water reservoir when performing simulations to model surface water components, towards determining the yield. Additionally, both in-channel and off-channel storage scenarios are considered when inflow sequences are used as input data for surface water modelling.

To model in-channel storage, the streamflow values of a gauging station in close proximity to the inflow stream should be known, or the MAR of the stream entering the surface reservoir can be calculated by using the catchment area of the dam as well as the rainfall of the respective catchment it is situated in. Modelling off-channel storage scenarios require that the abstraction capacity and the diversion efficiency be known, as both can limit the amount of water that can be abstracted from a stream. Pipeline capacities can be infrastructural limiting capacities, lower abstraction volumes than potentially available, and are expressed in litres per second (ℓ/s). For an off-channel storage scenario, the MAR recorded at a flow gauge closest to the point of abstraction should be known.

In Figure 3-7 the quaternary catchments, A and B, have a number of streams and streamflow gauges, respectively. In this scenario the dam is situated in catchment A, therefore, the daily streamflow record over a period 60 years (maximum) from catchment A is required to establish the streamflow class (high, medium and low flow scenarios), to obtain reliable streamflow values, which will later be applied during disaggregation. Naturalized streamflow sequences of catchment A can be used to generate stochastic streamflow sequences with STOMSA. The dam receives water from Stream 2 and Stream 3, however; Stream 3 is situated in catchment B and has a different size and different catchment characteristic; therefore, Stream 3 will have a different MAR that the MAR of Stream 2. It is assumed, however, that the adjacent catchments do have the same hydrological response and fall within the same rainfall zone. Furthermore, the catchments should be similar in their terrain, (both either mountainous, or flat, etc.).

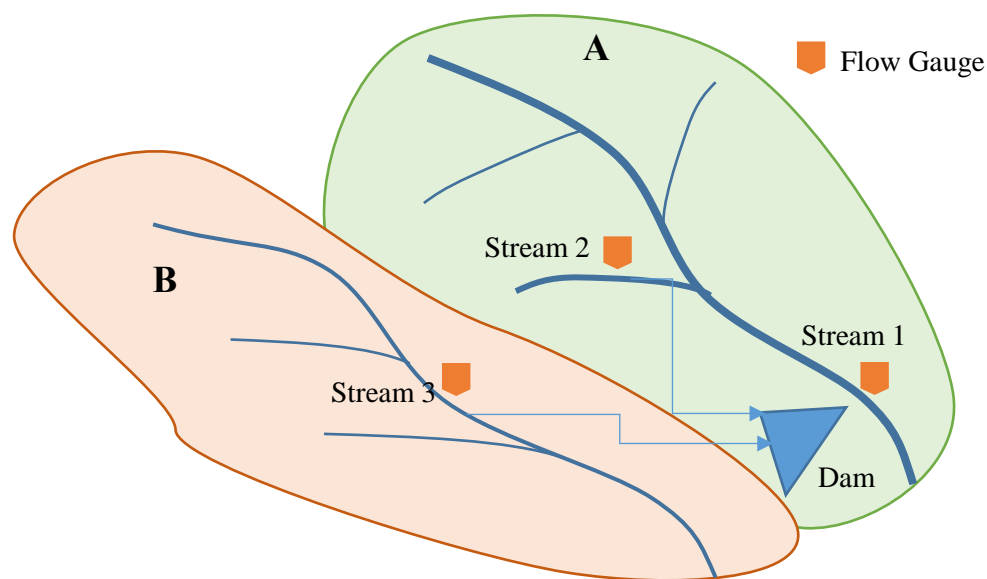


Figure 3-7: Streamflow gauges in quaternary catchments

To relate the MAR of Stream 2 and Stream 3, so that the stochastic relationship between the two catchments (A and B) is maintained, a historical MAR ratio is applied. The historical catchment MAR ratio is used to establish the abovementioned relationship, expressed in Equation 3-5, where the historical MAR of catchment B, referred to as the neighbouring catchment ($MAR_{Neighbour}$), is divided by the historical MAR of catchment A, referred to as the catchment of origin (MAR_{Origin}). The historical MAR values for different catchments are available on the WR2012 data base. Catchment MAR ratios should only be calculated for catchments with similar topography and hydrological responses to maintain continuity between different catchments.

$$\text{Catchment MAR ratio} = \frac{MAR_{Neighbour}}{MAR_{Origin}} \quad (3-5)$$

If the dam were to receive water from both Stream 1 and Stream 2, it is assumed that the historical ratio between the catchment MAR (MAR_{Origin}) and the MAR of the required stream (MAR_{Stream}), can be used as a constant relationship to relate the streamflow sequence of the stream to the stochastic

naturalized catchment streamflow sequence. For relating a stream to the catchment streamflow of the catchment of origin (MAR_{Origin}) for different stochastic sequences, the relationship is established by applying Equation 3-6.

$$Stream\ MAR\ ratio = \frac{MAR_{Stream}}{MAR_{Origin}} \quad (3-6)$$

Inflow sequences can also be influenced by downstream abstraction requirements, such as agricultural activities (irrigation). The scenario of inflow stream volume being reduced by downstream abstraction requirements is modelled by first considering downstream requirements of the inflow stream and then using the remainder of the inflow stream volume for abstraction towards supplying the municipal demand.

3.5.2 Net Evaporation

Net evaporation is evaporation minus rainfall over the dam surface area. Figure 3-8 is used to outline the data required and the process used to model daily evaporation of a surface water reservoir.

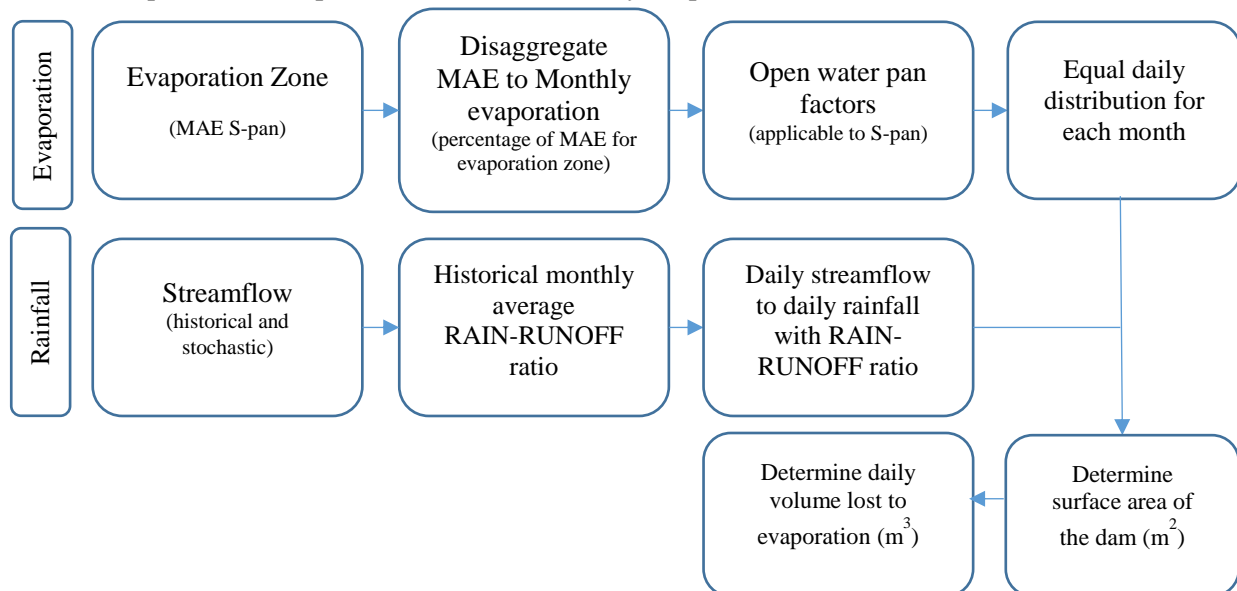


Figure 3-8: Input data and process to determine net evaporation

3.5.2.1 Evaporation

The evaporation zone as well as the S-pan MAE is retrieved from the WR2012 quaternary catchment summary sheet which are grouped according to their respective primary catchments. Monthly evaporation percentages of the MAE, as well as open water pan coefficients are available on the DWS website. The MAE is disaggregated into monthly evaporation by applying the evaporation percentages and the open pan factors. Thereafter, monthly evaporation is further disaggregated into daily evaporation by assuming that evaporation occurs at a constant rate throughout each day within the specified month.

3.5.2.2 Rainfall

The stochastic streamflow sequences, generated by STOMSA, are used to determine the corresponding stochastic rainfall data. The previously discussed monthly RAIN-RUNOFF ratio (refer to section 3.4) is applied to the daily streamflow volumes (disaggregated STOMSA sequences as previously discussed in section 3.3) to generate daily rainfall values (Equation 3-7).

$$Rainfall_i = Streamflow_i \times RAIN_RUNOFF_i \quad (3-7)$$

Where:

i	=	day
$Rainfall$	=	Rainfall per day (m/day)
$Streamflow_i$	=	Streamflow volume (mil m ³ /day)
$RAIN_RUNOFF_i$	=	RAIN -RUNOFF ratio (m/mil m ³)

It is assumed that rainfall is uniform over the catchment area and therefore the volume of the rainfall contribution to the dam is calculated by first converting it from millimetres to meters and then multiplying it by the surface area of the dam.

3.5.2.3 Surface Area of the reservoir

The relationship between depth and capacity of a dam is mostly provided in dam design as well as dam safety reports, which should be available from the owner of the dam. Following the literature on dam capacity and its related calculations in section 2.2.5, it is assumed that either a power relationship or a linear relationship between depth and capacity can be used to represent the depth-capacity curve for a large variety of dams. The derivative of the depth-capacity relationship is used to define the surface area – capacity relationship. Therefore, for the purpose of calculating the surface area at a certain capacity, the power function (Equation 2-5) has to be derived, as suggested in section 2.2.5. Thus, the derivative volume in terms of depth is equal to the surface area (SA). The derivation from first principles is attached in Appendix B.2. Deriving the volume (capacity) in terms of depth is calculated by applying Equation 3-8.

$$SA = a \times b \times \left(\frac{Volume}{a} \right)^{\left(\frac{1}{b} \right) \times (b-1)} \quad (3-8)$$

If a linear relationship exists between capacity and depth, the constant (b) takes on the value of 1. Provision is made for the user to enter the constants from the dam characteristics curve into the Microsoft Excel Sheet for doing this computation. With every time step the volume of water (capacity value) in the dam changes and so does the surface area, which is needed for calculating evaporation.

For example, the graph used in section 2.2.5, where the capacity-depth curve was presented as the power function (Equation 3-9), the surface area-capacity curve can be derived as Equation 3-10.

$$Volume = 5500 \times (Depth)^{1.5} \quad (3-9)$$

$$SA = 5500 \times 1.5 \times \left(\frac{Volume}{5500} \right)^{\left(\frac{1}{1.5} \right) \times (1.5-1)} \quad (3-10)$$

Which when simplified can be expressed as follows (Equation 3-11):

$$SA = 467.4 \times (Volume)^{\left(\frac{1}{3} \right)} \quad (3-11)$$

The surface area-capacity graph is illustrated in Figure 3-9 with Equation 3-9 used to establish the relationship between surface area and capacity (volume).

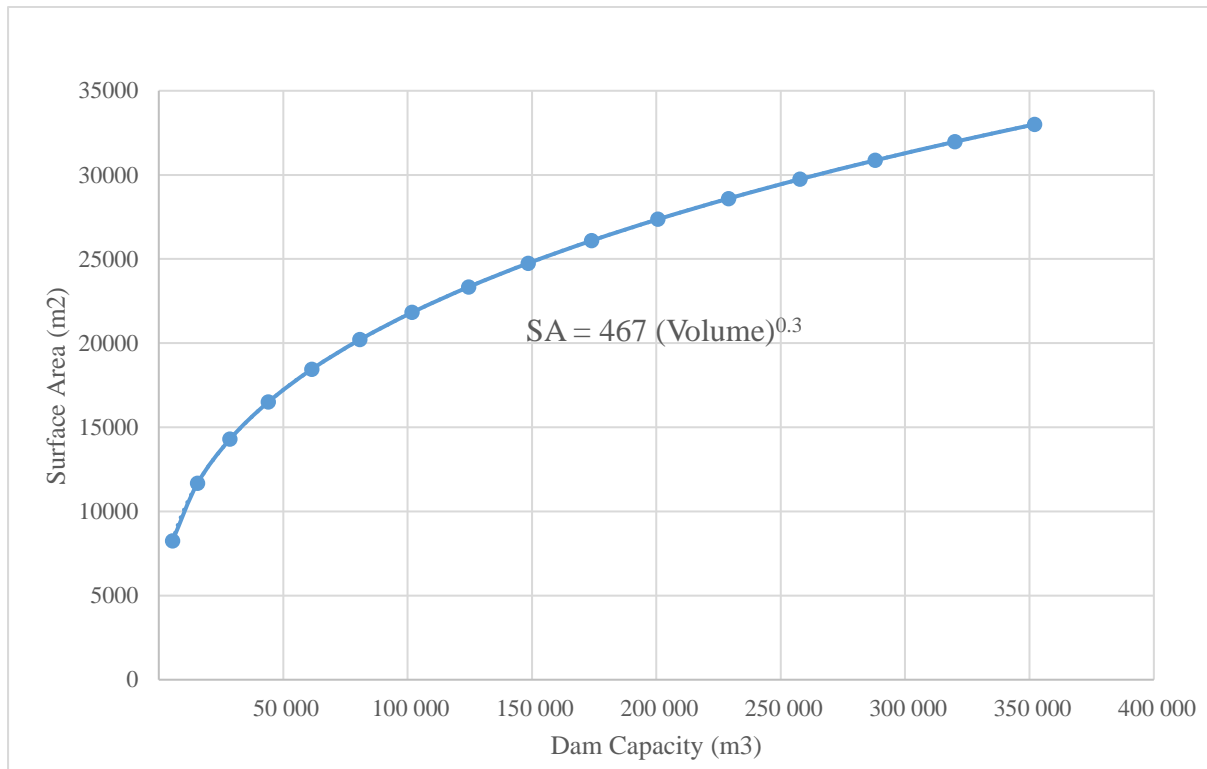


Figure 3-9: Surface area - capacity curve for a surface water reservoir

3.5.3 Demand

For the purpose of developing an analysis tool for local municipalities, demand is limited to those end-users receiving their water supply directly from the municipality. Thus, the analysis tool will focus on the demand of domestic end-users (urban and rural), as water for other sectors, such as the agricultural sector (irrigation), is usually abstracted independently from the watercourse.

The annual target draft is distributed over a 12-month period, according to a user specified monthly distributions. Monthly demand distributions should be available at the local municipality itself, who is the user of the analysis tool. Daily demand is considered to be occurring at a constant rate; thus, the monthly demand is evenly distributed over the amount of days in a month.

3.5.4 Seepage and Overflow

Seepage is assumed to be negligible (refer to Section 2.2.4 for the motivation thereof). Overflow is the volume of water that is spilled from the dam. If the demand is satisfied and the reservoir is spilling, it is considered as water lost to the system, as no provision for storage of overflow is made downstream.

3.6 Groundwater Simulation

A relationship between groundwater and surface water is established through rainfall, as rainfall causes runoff, also referred to as streamflow to surface water, while simultaneously recharging aquifers in the catchment of interest, contributing to groundwater. Due to this stochastic rainfall link between surface water and groundwater, it is proposed that groundwater be modelled in a similar fashion to surface water. This is accomplished by adopting the principles of the AFYM, which suggests that an aquifer at quaternary catchment scale is modelled as a single-celled, lumped parameter box model. The water balance of the aquifer consists of recharge - a percentage of rainfall - (modelled as inflow) as well as baseflow and abstraction (modelled as outflows). Evapotranspiration is not taken into consideration when performing the water balance, as evapotranspiration mainly occurs in the riparian zones which make up a small percentage of area of quaternary catchments (section 2.3.8). The SVF method is then applied to relate water levels to volume changes caused by the respective inflows and outflows.

Recharge is specified for each quaternary catchment as percentage of rainfall, this percentage of rainfall is obtained from the GRA II database on the DWS website. While the AFYM only made use of the historical sequence to determine the long-term abstraction and associated aquifer yield, stochastic sequences are additionally incorporated to determine the long-term abstraction rate for each stochastic sequence. The historical and stochastic sequences obtained or generated during the surface water modelling, are also applied during groundwater modelling. The AFYM is restricted to fractured and unconsolidated, alluvial aquifers; since these types of aquifers show relatively fast runoff responses and volume changes can be modelled with changes in water levels. Therefore, this model is also restricted to fractured and unconsolidated, alluvial aquifers.

Should a municipality have information on its boreholes, such as specific yield (storativity), transmissivity, pumping rates and maximum allowable drawdown, borehole interference can be determined. The extent borehole interference can be determined by applying the Cooper-Jacob model, to calculate the drawdown and radius of interference that boreholes have on one another when pumped, to prevent potential over-abstraction at a local-scale (discussed in section 3.5.5).

A conceptual diagram of a cross section of an example quaternary catchment is illustrated in Figure 3-10. It depicts the portion of the rainfall which becomes runoff, also referred to as streamflow, flowing along the earth's surface into streams and rivers as well as the portion of rainfall percolating through the earth's surface, resulting in recharge of aquifers. Some of the recharge syphons through the

underground structures horizontally and contribute to baseflow, which sustains natural equilibrium of the integrated surface-groundwater system. However, if pumping is induced, a dynamic equilibrium is created whereby water for potential abstraction is sourced from the baseflow and the aquifer becomes a stressed system. The pumping rates of the boreholes indicate how much water is pumped from the aquifer system. In reality, due to high regional variation in hydrogeological characteristics, single boreholes have different drawdown levels at which failure occurs, therefore the interference of different boreholes should be investigated at local scale.

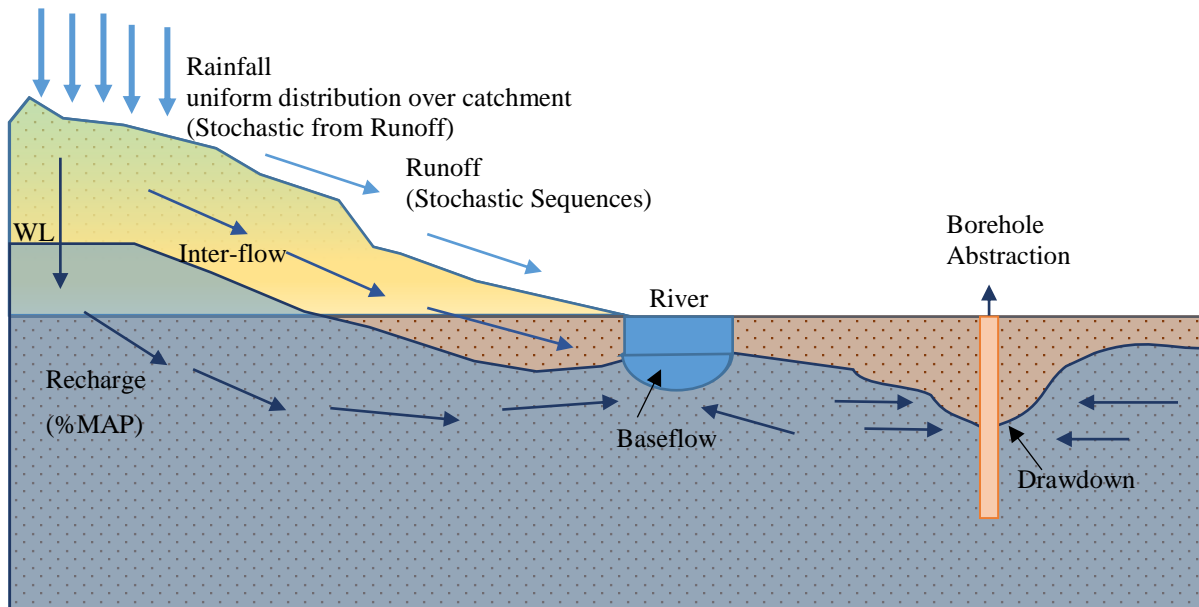


Figure 3-10: Cross section of a quaternary catchment aquifer system

3.6.1 Quaternary Catchment Aquifer Water Balance

Long-term potential groundwater abstraction can be determined on a quaternary catchment bases as suggested by Murray et al. (2012). Long-term potential average abstraction takes the stochastic nature of groundwater into consideration over a long time period. While actual abstraction refers to the amount of water that is being abstracted from a wellfield as typically determined through borehole-yield tests as a snap-shot in time.

The principles of the AFYM to model groundwater and the steps to determine the long-term potential monthly abstraction from an aquifer at quaternary catchment scale are outlined in Figure 3-11. The stochastic monthly recharge was previously calculated using stochastic rainfall of the GRAII (%MAP), obtained through the DWS website, and inflows into the system was determined. The monthly time step, reflecting the monthly time step of the WR2012 data, was also applied in the AFYM, however, after the monthly long-term abstraction is determined, it is distributed equally over the number of days in a month to be compatible with the surface water daily time step. To determine the long-term potential available abstraction, in other words, abstraction that does not damage the natural eco-system associated with the aquifer, the natural equilibrium of an aquifer system is modelled, after which a stressed aquifer

system is simulated by introducing abstraction to the system. The aim is to quantify the amount of water available for abstraction from the potential recharge (%MAP) and baseflow on a quaternary catchment wide basis.

The abovementioned is undertaken to obtain a holistic view of the outflow of the system and for the user to consider whether limitations should be placed on them. The natural equilibrium is established by balancing the average inflow with the average outflow (discussed in section 3.5.2). Thereafter, baseflow separation is performed to refine monthly discharge volumes, using the Herold Baseflow Separation Method (discussed in section 3.5.3). The maximum sustainable abstraction volume is

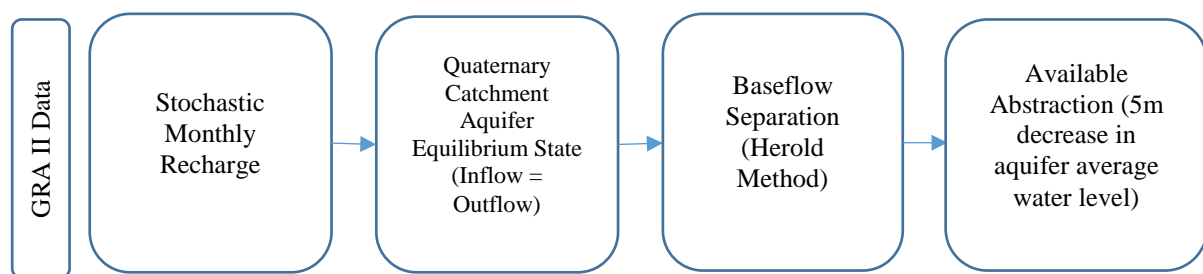


Figure 3-11: Process followed during groundwater yield assessment

determined by decreasing the minimum average water level, as established during natural equilibrium, by 5 m, thereby simulating a stressed aquifer system (discussed in section 3.5.4). The 5 m decrease in average water level is applied, as it is assumed by the AFYM that ecological disruption will start to occur at that level. The volume of water available for monthly abstraction for each stochastic sequence (subjected to a number of pre-conditions) becomes the input data for the groundwater component to the conjunctive use system model.

The modelling procedure is outlined as follows:

1. Retrieve annual recharge percentages (%MAP) for the quaternary catchment of interest, from the GRAII database, obtained through the DWS website, to determine recharge as percentages of monthly rainfall.
2. Use the RAIN-RUNOFF Ratio as previously determined for surface water components, to determine monthly rainfall from monthly stochastic streamflow (generated using STOMSA).
3. The SVF method is used to simulate time-series water levels corresponding to recharge volumes to time series water level fluctuations, representing changing aquifer storage levels over the sequence length (historical or stochastic sequence). The average water level fluctuation at the equilibrium state of the aquifer system is determined for the quaternary catchment of interest, by balancing recharge with discharge (baseflow).
4. Discharge volumes are refined by applying the Herold Baseflow Separation Method.
5. Decrease the average minimum water level of the aquifer system by 5 m and calculate the increased discharge (representing baseflow and abstraction). The difference between the natural equilibrium

recharge determined in step 1 and the discharge (baseflow and abstraction) determined at the 5 m below average water level in step 3, becomes the sustainable available abstraction.

3.6.1.1 Data Retrieval Process

Data on the recharge percentage (%MAP), specific yield (storativity), average water level (mbgl) and characteristics of the quaternary catchment of interest, are retrieved from the GRAII database, which is obtained through the DWS website, by selecting the *Groundwater* section and applying for the data (www.dwa.gov.za/Groundwater/GRAII.aspx) via (georequests@dws.gov.za). The naturalized stochastic monthly streamflow sequences required for the groundwater simulations are the exact same sequences previously generated with STOMSA for the surface water simulations. These sequences are used due to the stochastic link between surface water and groundwater established through rainfall.

3.6.1.2 Stochastic Monthly Recharge

The input data and conversions used to determine monthly recharge volumes are outlined in Figure 3-12. Stochastic monthly streamflow sequences - historical naturalized streamflow sequence retrieved from the WR2012 database used as input to STOMSA (section 3.3) - are converted to stochastic monthly rainfall by applying the RAIN-RUNOFF ratio calculated with Equation 3-3 (section 3.4.2). Stochastic monthly recharge is determined by using the GRAII recharge percentage of MAP and then multiplying it by the stochastic monthly rainfall as well as the quaternary catchment area (size) to determine a stochastic monthly recharge volume.

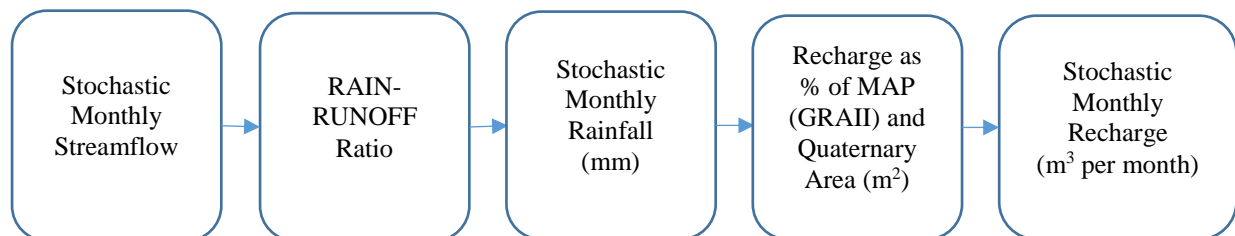


Figure 3-12: Process followed to determine stochastic recharge

Thus, stochastic monthly recharge volumes are determined by applying Equation 3-12.

$$Recharge_i = Streamflow_i \times RAIN_RUNOFF_i \times \%MAP \times Area \quad (3-12)$$

Where:

i	=	Month
$Recharge_i$	=	Monthly recharge volume (m ³ /month)
$Streamflow_i$	=	Monthly streamflow volume (m ³ /month)
$RAIN_RUNOFF_i$	=	Monthly RAIN -RUNOFF ratio (m/mil m ³)
$\%MAP$	=	Monthly percentage of rainfall contributing to recharge (GRAII)
$Area$	=	Quaternary catchment area (m ²)

The stochastic monthly recharge as determined with Equation 3-12 forms the inflow component to the aquifer water balance simulations.

3.6.1.3 Aquifer in Equilibrium

When an aquifer is in equilibrium state, the inflow to the aquifer system is equal to the outflow from the system, in other words the average recharge is equal to the average discharge and the expected long-term average water level fluctuation is equal to zero. Thus, the system maintains its balance between inflows and outflows. Recharge is determined as a monthly volume with Equation 3-12, and an average monthly discharge volume - remaining constant for every monthly time step (until refined with Herold Baseflow Separation Method) – can be calculated by applying Equation 3-13, using the average monthly recharge volume as input data. Additionally, the constant monthly discharge is adjusted by applying an adjustment factor to the average recharge volume (Equation 3-13), in order to maintain a long-term water level fluctuation of zero between recharges and discharges.

$$Avg Q_b = adjF \times \sum Recharge_i / \sum i \quad (3-13)$$

Where:

$$\begin{aligned} Avg Q_b &= \text{Average Discharge volume constant for every month (m}^3\text{/month)} \\ adjF &= \text{Adjustment factor} \\ \sum i &= \text{Month} \\ \sum Recharge_i &= \text{Sum of monthly recharge volumes over sequence length (m}^3\text{)} \end{aligned}$$

The first estimate for the average monthly discharge (constant) is the average recharge with an adjustment factor of 1. When water levels are generated for each month (step 3), the long-term water level fluctuation is evaluated and if it is not equal to zero, the adjustment factor is changed so that the discharge causes no net change in water level over the sequence length.

Table 3-3 is an example of input data with representative values for each month, which are used for calculating recharge and discharge when applying Equation 3-13.

Table 3-3: Aquifer System in Equilibrium

Quaternary Catchment Equilibrium				
Time	Start Water Level	Monthly Recharge	Average Discharge	End Water Level
months	mbgl	(m ³ /month)	(m ³ /month)	mbgl
OCT	7.8 (1)	976 941 (2)	1 514 146 (5)	7.92 (4)
NOV	7.92 (6)	686 273	1 514 146	8.11
DEC	8.11	525 492	1 514 146	8.33
JAN	8.33	625 777	1 514 146	8.54
FEB	8.54	1 627 950	1 514 146	8.51
...
<i>i</i>	<i>h_i</i>	<i>Recharge_i</i>	<i>Avg Q_b</i>	<i>h_{i+1}</i>
$\sum i$		$\bar{x} = \sum Recharge_i / \sum i \quad (3)$		

Each number corresponds to an action or step taken during the process:

1. Retrieve the average water level for the quaternary catchment of interest from the GRAII database. The average water level for the quaternary catchment represents the average groundwater depth of the aquifer system located within the quaternary catchment of interest and is used as the start water level of the simulation. For every month after the starting month the new starting water level is calculated by applying Equation 3-14
2. Calculate the monthly recharge volume with Equation 3-12. The recharge volume has a different value for each month, as the amount of rainfall varies each month.
3. Determine the average monthly discharge ($Avg Q_b$), for each year in the full record length, using Equation 3-13.
4. Determine the water level at the end of the month, using the SVF equation, adapted to include only the recharge and discharge over the quaternary catchment area. The entire quaternary catchment area is modelled as the recharge area. At this stage recharge ($Recharge_i$) is different for every month, while the discharge is a constant ($Avg Q_b$). The SVF equation (Equation 2-15) is adapted to incorporate only recharge and discharge by assuming pumping (natural equilibrium) and evapotranspiration to be equal to zero respectively. The adapted SVF equation is given by Equation 3-14 and is used to determine the monthly water level fluctuation (mbgl).

$$h_{i+1} = h_i - \frac{Recharge_i}{Sy \times Area} + \frac{Avg Q_b}{Sy \times Area} \quad (3-14)$$

5. The average long-term water level fluctuation (the average difference in water level change over number of months in a sequence) should be equal to zero to preserve the integrity of the natural equilibrium of the aquifer. To achieve this, the adjustment factor ($adjF$) is changed by using the “Goal Seek” function in Excel; setting the long-term average water level fluctuation to zero while changing the adjustment factor ($adjF$).
6. The water level at the end of the previous month becomes the starting level of the month.

In Figure 3-13 the water level fluctuation in meters below ground level is displayed as well as the water level response to rainfall events on a monthly basis. Although different aquifer systems have different lag times associated with them, for the unconfined alluvial aquifer system it is assumed that within a month recharge from rainfall has reached the water table as suggested in section 2.3.5. Also illustrated in Figure 3-13 is the linear trendline indicating the zero slope between the water levels over the period of 90 years. The slope over a long-term period, for the case of 90 years (from 1st October 1920 to 31st September 2010) as available per WR2012 monthly time step sequences, is equal to zero.

The water level in the equilibrium state can fluctuate above ground level as it represents the entire system and in some parts of the system there might be a greater contribution to baseflow.

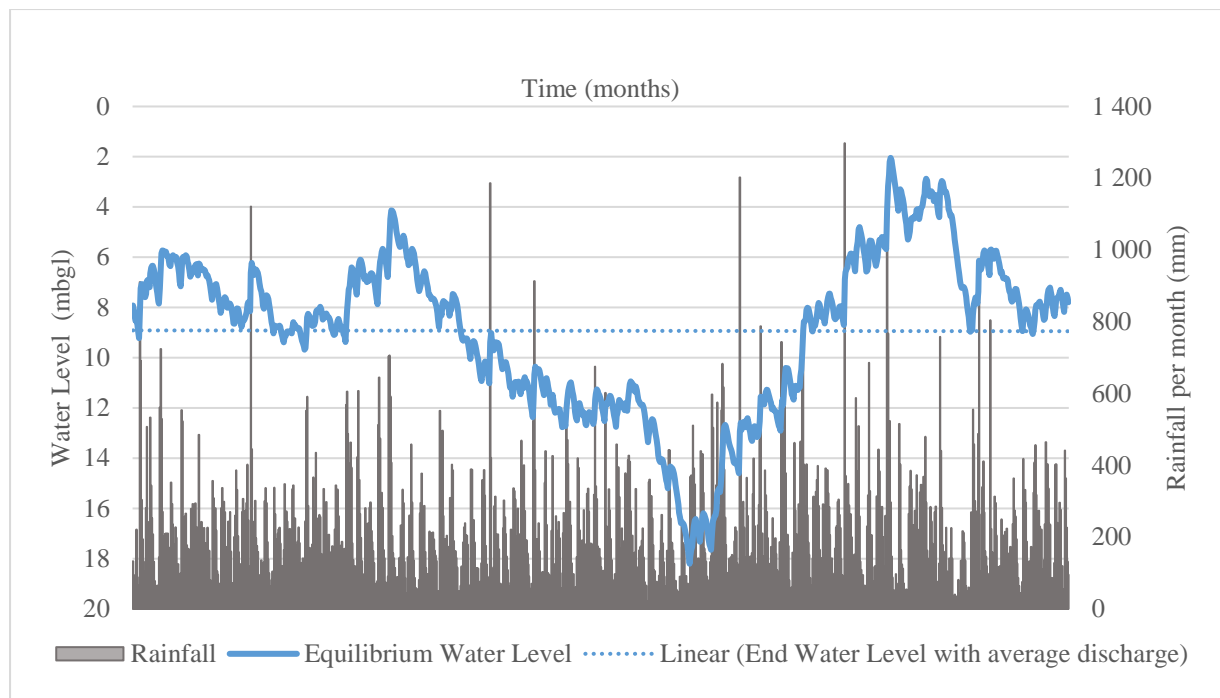


Figure 3-13: Quaternary catchment aquifer system equilibrium state

Following on the quaternary catchment aquifer system equilibrium is the knowledge that the groundwater contribution to the baseflow in rivers is not a constant value but also varies from month to month. Therefore, baseflow separation has to be performed so that the groundwater contribution to the low flow of the river can be better estimated for monthly time steps.

3.6.1.4 Baseflow Separation

To quantify interactions between surface water and groundwater on a catchment wide scale, the monthly groundwater contribution to baseflow is determined. The naturalized streamflow sequences represent the total streamflow of a river or stream, of which there is a surface water component (runoff) and a groundwater component. The Herold Baseflow Separation Method is used to separate the monthly groundwater contribution from the streamflow (monthly discharge). The groundwater contribution can be higher in certain months than others as a result of fluctuations in recharge and storage.

The monthly time-series of the streamflow volumes, as generated with STOMSA (stochastic streamflow sequences) are used as total monthly flow values (Q_i), which consists of the combined surface water and groundwater contributions, as indicated in Equation 2-10:

$$Q_i = QG_i + QS_i$$

Where:

- Q_i = Total Flow (m^3/month)
- QG_i = Groundwater Contribution to the total flow (m^3/month)
- QS_i = Surface water contribution to the total flow (m^3/month)

The average monthly streamflow over the complete record length (90 years), is used as the first estimation of **QGMAX**, which is the minimum volume of baseflow.

The surface water contribution is determined by subtracting the minimum groundwater contribution (**GGMAX**) from the total flow, through the application of Equation 2-11:

$$QS_i = 0 \text{ (for } Q_i \leq \text{QGMAX)}$$

$$\text{Or } QS_i = Q_i - \text{GGMAX}_i \text{ (for } Q_i > \text{QGMAX)}$$

If the total amount of streamflow in the river is less than the minimum baseflow volume (**QGMAX**), the surface water contribution is fixed at zero. If the total amount of streamflow is greater than **QGMAX**, the surface water contribution is calculated using the second part of Equation 2-11 with **GGMAX**.

GGMAX is determined using Equation 2-12, where the DECAY and GROWTH factors are represented by the average values of the suggested range:

$$\text{GGMAX}_i = \text{DECAY} \cdot \text{GGMAX}_{i-1} + (\text{GROWTH} \cdot QS_{i-1})/100$$

Suggested ranges for DECAY and GROWTH are ($0 < \text{DECAY} < 1$) and ($0 < \text{GROWTH} < 10$) respectively. Thus, the DECAY factor is set to 0.5 and GROWTH factor is set to 5 respectively. A further constraint is that **GGMAX** may not fall below **QGMAX**.

Table 3-4 represents the components, with example values, required to perform the baseflow separation on a catchment scale.

Table 3-4: Components for baseflow separation at catchment scale

Baseflow Separation (Herold Method)						
Time	Total Flow	Surface water contribution	DECAY	GROWTH	GGMAX	Groundwater contribution
months	m ³ /month	m ³ /month	ratio	ratio	m ³ /month	m ³ /month
OCT	2 260 000 (1)	16 158 (3)	0.5	5	2 243 842 (4)	2 243 842 (5)
NOV	1 250 000	0	0.5	5	2 243 842	1 250 000
DEC	540 000	0	0.5	5	2 243 842	540 000
JAN	500 000	0	0.5	5	2 243 842	500 000
FEB	410 000	0	0.5	5	2 243 842	410 000
...
i	Q_i	QS_i	Decay	Growth	GGMAX_i	QG_i
$\text{QGMAX} = \Sigma Q_i / \Sigma i \text{ (2)}$				$\text{Avg } QG_i = \Sigma QG_i / \Sigma i \text{ (6)}$		

The process followed during the baseflow separation on a catchment scale, is explained using a numbering system (in bold) as indicated in Table 3-4. Each number in Table 3-4 corresponds to an action or step taken during the process:

The groundwater contribution is determined by using Equation 2-11. At this point the total flow and the surface water flow is known (step 1 and step 3) and the rest is groundwater contribution to baseflow (step 5). **QGMAX** is calibrated as suggested in section 2.3.6.1 by setting the average groundwater contribution ($\text{Avg } Q_{Gi}$) (step 2), determined after the baseflow separation, to the average discharge (step 6) as determined in section 3.5.1.3.

The result of the Herold Baseflow Separation is a hydrograph, illustrated in Figure 3-14, where the total streamflow is separated into surface water and groundwater contributions, over the first 35 months of the example sequence (data in Table 3-4). The orange line, representing the surface water contribution, indicates a noticeable increase and decrease according to the amount of rainfall over this period. The red line, representing the groundwater contribution, indicates a lesser response. It is evident from Figure 3-14 that the groundwater contribution to streamflow does change on a monthly basis and therefore it is deemed necessary to refine the average discharge from the system by applying the Herold Baseflow Separation Method.

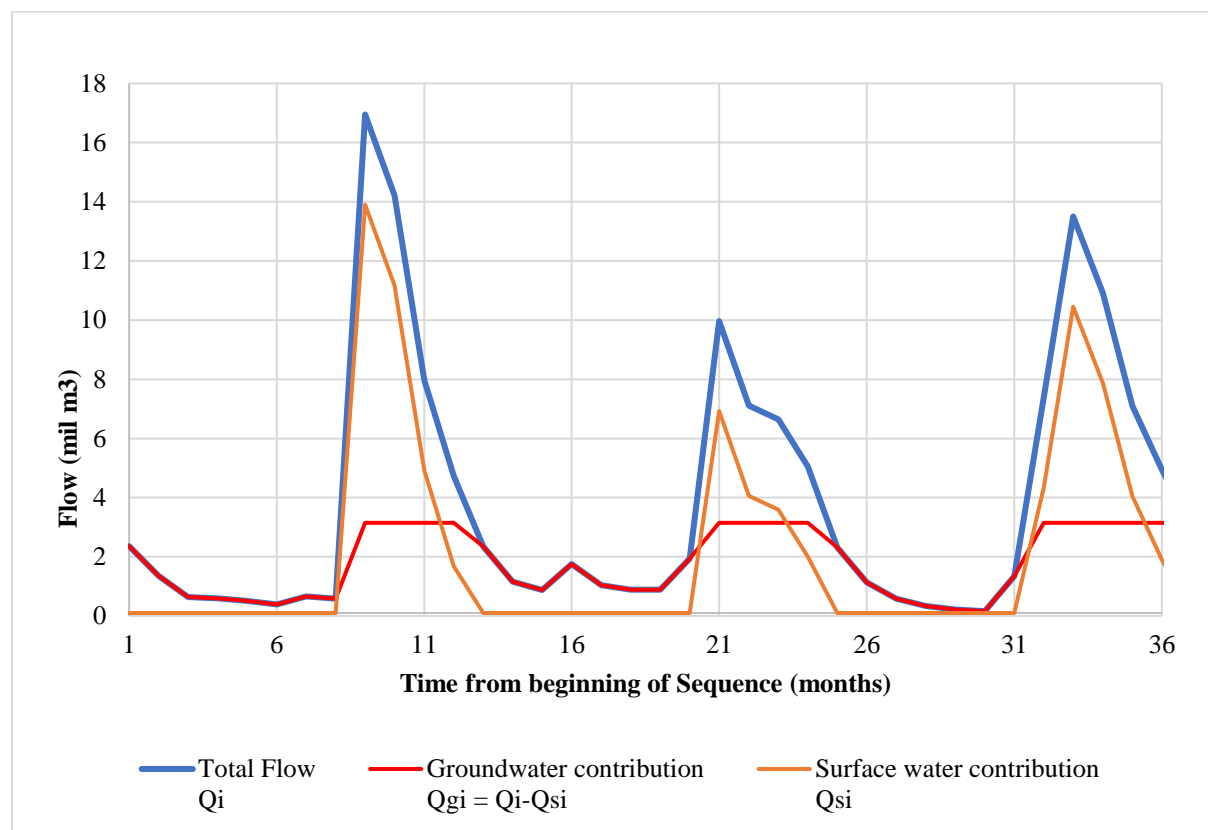


Figure 3-14: Herold Baseflow Separation hydrographs

3.6.1.5 Minimum Average Aquifer Water Level

A refined natural equilibrium is established, based on the results of the Herold Baseflow Separation method, when the discharge is no longer a constant average, but fluctuating from month to month. When pumping is introduced to the refined natural equilibrium the aquifer becomes a stressed aquifer and decreases in the average water level will occur. The minimum average aquifer water level is decreased by 5 m to establish a new value for discharge (baseflow plus abstraction), as this is the level where ecological degradation starts to occur, resembling a stressed aquifer system. The difference between the discharge at the stressed aquifer state, and the discharge after determining the groundwater contribution to baseflow, becomes the sustainable abstraction volume. To determine the discharge for a stressed aquifer system, Equation 3-15 is applied:

$$Qab_i = (QG_i \times adjF) - QG_i \quad (3-15)$$

Where:

- Qab_i = Long-term sustainable abstraction (m³/month)
- $adjF$ = Adjustment factor increasing abstraction such that the minimum simulated water level is decreased by 5 m
- QG_i = Groundwater Contribution to the total flow (m³/month)

Table 3-6 is an example of data required for an aquifer system in a stressed state, to calculate the discharge and sustainable abstraction volume. The 90 years of data (1050 months) are used in the simulation and the water level for the start of the simulation, is obtained from the GRA II data base.

Table 3-5: Stressed aquifer system with increased discharge

Aquifer system with abstraction						
Time	Start Water Level	Monthly Recharge	Groundwater Contribution	Increased Discharge (baseflow plus abstraction)	End water Level (5)	Monthly Abstraction volume available
months	mbgl	m ³ /month	m ³ /month	m ³ /month	mbgl	m ³ /month
OCT	7.8 (1)	976 941 (2)	2 243 842 (3)	2 329 969	8.11 (4)	86 127
NOV	8.11	686 273	1 250 000	1 297 979	8.25	47 979
DEC	8.25	525 492	540 000	560 727	8.25	20 727
JAN	8.25	625 777	500 000	519 192	8.23	19 192
FEB	8.23	1 627 950	410 000	425 737	7.96	15 737
...
i	h_i	$Recharge_i$	QG_i	$QG_i \times adjF$ (6)	h_{i+1}	$Qab_i = QG_i \times adjF - QG_i$ (7)

1. The process followed during the baseflow separation on a catchment scale, is explained using a numbering system (in bold) as indicated in Table 3-5. Each number corresponds to an action or step taken during the process: Obtain the start water level from the GRA II average water level (mbgl).

2. Determine monthly recharge ($Recharge_i$) as percentage of rainfall (%MAP) from GRA II (section 3.6.1.2).
3. Determine the groundwater contribution to baseflow (QG_i), as determined with the Herold Baseflow Separation method (section 3.6.1.4).
4. Calculate the water level for the end of the month with Equation 3-14. The monthly fluctuating discharge being the groundwater contribution to baseflow (QG_i), therefore the equation is adapted to the following formula:
$$h_{i+1} = h_i - \frac{Recharge_i}{Sy \times Area} + \frac{QG_i}{Sy \times Area}$$
5. Identify the average minimum water level (maximum drawdown) of the aquifer system with monthly recharge and refined monthly groundwater contribution to baseflow (QG_i), within the sequence.
6. Apply an adjustment factor (adjF) to the discharge, thus, increasing the minimum average water level (mbgl) simulated in natural state, by 5 meters.
7. The difference between the groundwater contribution to baseflow (QG_i), and the increased discharge ($QG_i \times adjF$) is the abstraction volume available per month (Qab_i). The stressed aquifer water level fluctuation can therefore be expressed as follows (Equation 3-16):

$$h_{i+1} = h_i - \frac{Recharge_i}{Sy \times Area} + \frac{QG_i + Qab_i}{Sy \times Area} \quad (3-16)$$

The water level fluctuation as a result of natural recharge, groundwater contribution to baseflow and discharge as a result of abstraction (pumping) is illustrated in Figure 3-15. The water level fluctuation of the natural as well as the stressed aquifer system is illustrated in Figure 3-15.

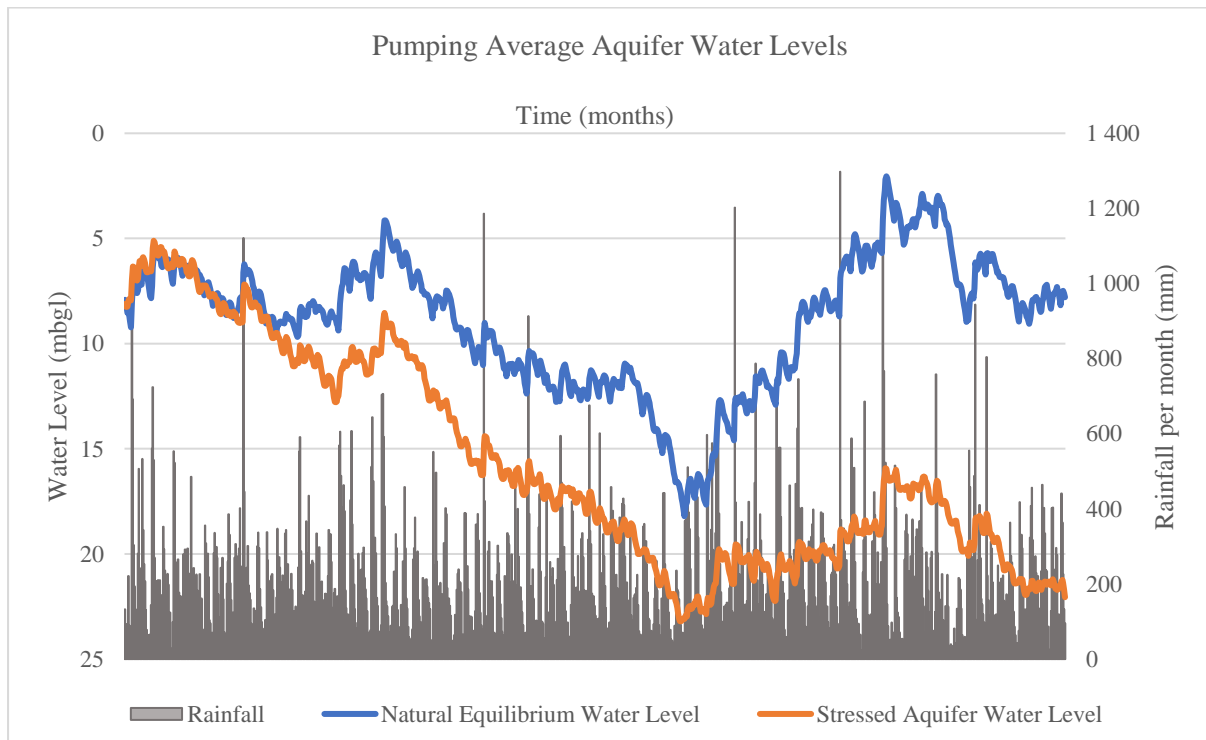


Figure 3-15: Water level fluctuation of natural and stressed aquifer system

To calculate the monthly abstraction volume for each of the stochastic sequences, the calculations followed in section 3.5.1.2 to section 3.5.1.5 are repeated for each stochastic sequence using a Microsoft Excel Visual Basic button. After repeating the calculations for each sequence, long-term potential monthly abstraction volumes (Qab_i) are summarized in a table for each stochastic sequence.

The volume of water available for abstraction is determined for the entire catchment, thus it should be scaled to the area which delineates the aquifer, from which is pumped. This area is delineated through geological structures determined by lithology and should be modelled as the unconfined alluvial aquifer system within a municipal area. The area can be larger than the municipal area in question. The first order (default) approximation of this area is the area of that surrounds the boreholes in question by following the outline of the alluvial aquifer system using regional geology maps from the geological map series from the Council for Geoscience. If only one borehole is available, the radius of influence can be used as the first approximation for the study area. The radius of influence is discussed in section 3.6.2.

3.6.2 Borehole Interference Indication

The Cooper-Jacob equation is used to determine the extent of interference that boreholes have on one another when located in the same wellfield. This is measured by obtaining borehole yield tests from the municipality and determining the amount of drawdown that boreholes impose on one another, as a result of abstraction activities within the wellfield. The radius of influence is the distance from the borehole centre to the point where the drawdown is zero and is most sensitive to transmissivity, pumping duration and storativity, while the drawdown of a borehole is most sensitive to the transmissivity and pumping rate. The Cooper-Jacob equation serves as an indication as to where the radius of influence of each borehole overlaps with the radius of influence of another borehole within the same wellfield.

Although aquifers rarely conform to assumptions, the assumptions made by Theis and Cooper-Jacob (section 2.3.9) are assumed to hold true and are as follows: the aquifer has a uniform thickness, transmissivity and storativity until at least the end of the cone of depression. The well is fully penetrating, has laminar flow, infinite areal extent and while testing is undertaken the boreholes are without recharge. In other words, the geology surrounding the borehole is uniform without impermeable boundaries. To calculate the impact of drawdown that boreholes have on one another, the distance between boreholes has to be known, as well as the drawdown of each borehole on a particular borehole. To plot the borehole coordinate points on a cartesian plane so that the distance can be determined, the spherical coordinates have to be transformed to cartesian coordinates.

3.6.2.1 Coordinate Transformation

The spherical coordinates of the borehole are transformed to a cartesian coordinate system (section 2.3.9.1). Open source (free of charge) UTM conversion software, created by Dutch (2018), is available online at: <https://stevedutch.net/UsefulData/UTMFormulas.htm> to this end. This was incorporated within the Excel workbook used to perform the groundwater simulation, to perform the coordinate conversion for the Cooper-Jacob Equation automatically.

3.6.2.2 Cumulative Drawdown

The radius of influence for each borehole in the wellfield is determined with Equation 2-17:

$$r = 1.5 \times \sqrt{\frac{T \times t}{S}}$$

For example, if there are two boreholes ‘A’ and ‘B’, and if the radius of influence of borehole ‘A’ is larger than the distance between it and ‘B’, there will be borehole interference. The drawdown of borehole ‘B’ will be its own drawdown plus the drawdown from borehole ‘A’ at the distance between the two boreholes.

If there are more than 2 boreholes in a wellfield, the process of determining the drawdown at each borehole, as a result of its own pumping, as well as the pumping of another borehole in the wellfield, becomes an iterative process. A Microsoft Excel Visual Basic button is used to perform the iterative process, which determines the cumulative drawdown at the borehole, where interference was imposed by other boreholes in the same wellfield.

If there are multiple boreholes having an influence on the drawdown of a specific borehole within the same wellfield, the radii of influence of the boreholes can be plotted as bubbles, to illustrate the borehole interference in Excel. However, it does not necessarily accurately depict the extent of this interference to scale, as the bubbles are plotted relative (to the size) to each other. Nonetheless, an example of the approximated radii of influence, of various boreholes in the same wellfield, is illustrated in Figure 3-16, giving an indication of possible overlap, resulting in borehole interference. The cartesian coordinates (northing and easting) and of the radii of influence, as calculated for each borehole with Equation 2-16, is indicated by the size of the bubble. After calculating the cumulative drawdown at each borehole (as result of its own drawdown, as well as the drawdown due to borehole interference), it is compared to its own drawdown, and if the cumulative drawdown is larger than that of the borehole itself, a “YES” is displayed next to the specific borehole, otherwise a “NO” is displayed. The abstraction rates at the boreholes indicated with a “YES”, will have to be decreased so that minimal overlap occurs. This will ensure that water abstraction between the different boreholes is sustainable, and that any one borehole in the wellfield should not fail due to another borehole.

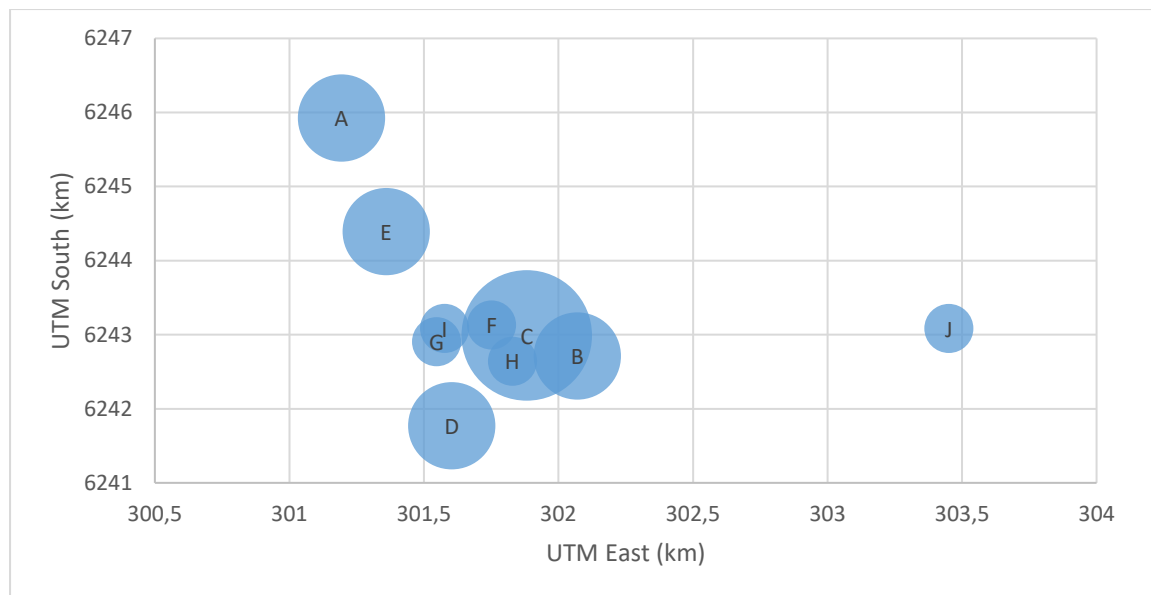


Figure 3-16: Radii of influence of boreholes within a wellfield

3.7 Desalination and Reclamation

Desalination and water reclamation plants make use of reverse osmosis membrane technologies, to remove salts and other harmful compounds from water, which renders it potable. Desalination or water reclamation is predefined by the user when undertaking the modelling, according to the number of reverse osmosis units available. The total plant capacity can be divided equally between the numbers of units in the plant. It is assumed that each reverse osmosis unit is equal in capacity. For example, if a desalination or water reclamation plant has 4 units, then the available capacities to be utilized are 25%, 50%, 75% and 100% respectively. In other words, when all 4 reverse osmosis units are utilized, the full plant capacity is utilized (100%), however, if 3 reverse osmosis units are utilized then only 75% of the plant capacity can be utilized. Modelling of reverse osmosis units in this research, are done according to the most cost-effective utilization of the plant, thus, prerequisites for the modelling process are as follows:

1. The entire plant capacity (100%) is utilized in every month, throughout the year. The desalination or water reclamation plant is a total capacity, constant base supply.
2. The entire plant capacity is utilized for at least 3 consecutive months. In other words, a specific plant capacity should be utilized for a 3-month period, and for the next 3-month period another plant capacity can be chosen. For example, in tourism towns the demand often spikes over a certain period, in that period the desalination plant should be used at 100% capacity and for at least 3-months, thereafter it can be switched either to a lower capacity or off, depending on the demand.

This scenario utilizes desalination and/or water reclamation as an augmentation resource.

In this research, dam levels are not considered as triggers for switching desalination and water reclamation plants on or off. In other words, the operation of the plant could be triggered by a low surface water storage level (a level less than 40% for instance), and decreased if the surface water

storage rises above a certain level (above 70% for instance). Desalination and water reclamation had previously been utilized as emergency resources, or as augmentation in the event of dam levels dropping below a critically low level, but the model is not programmed according to this scenario.

3.8 Conjunctive System Simulation

The conjunctive use system consists of the combination of the water resources available to the municipality to satisfy the demand. To assess the yield of a conjunctive use system, with components such as groundwater, desalination and water reclamation, as well as surface water, certain operational rules are used as guidelines to determine the order in which the water resources are utilized. The yield for the conjunctive use pertaining to a specific stochastic sequence (stochastic streamflow sequence to which groundwater is related) is determined, after which a number of yield curves for the record length (90 years) can be plotted to determine the long-term reliability of supply of the conjunctive use system. Furthermore, the probabilistic management curves can be drawn up for short-term periods as required between decision-making periods by the municipality.

3.8.1 Operational Rules

The yield analysis for the conjunctive use system is different than that of a system that uses augmentation (section 2.5). A significant difference is that during augmentation water management, the demand would first be supplied by the most prominent water resource. Other water resources would only be utilized in case of an emergency (water shortage). The conjunctive use system requires that the demand be satisfied by the simultaneous use of water resources available to the municipality. Thus, the conjunctive use system is set up in a way that utilizes less climate dependent water resources as a base supply (such as desalination), after which groundwater abstraction, and surface water resources are added to the supply. The aim of the conjunctive use system is to become less dependent on only one type of water resource, by managing all resources available to the municipality in such a way as to have a more reliable or sustainable supply, to provide for a certain target draft.

3.8.1.1 Desalination and Water Reclamation

In the conjunctive use system simulation (Excel workbook), provision is made for 2 reverse osmosis plants, one of which can be a desalination plant, while the other can be a water reclamation plant. Daily volumes are used for simulations, according to the capacities specified by the user for each month. A minimum operational period of 3 months is a prerequisite for every plant during high demand periods to render its usage cost-effective. It is assumed that this daily volume of water is always available, as it is not as climate dependent.

3.8.1.2 Groundwater

When utilizing groundwater in the conjunctive use system, the main assumption is that the demand can be satisfied by the determined long-term potential abstraction volume. In practice, however, a borehole

within an aquifer system might still yield more water than the potential abstraction volume estimated to be available for a specific month. Thus, the operational rules when determining the yield of groundwater sources for a conjunctive use system are as follows:

- The actual combined abstraction rate (ℓ/s) of all the boreholes within the aquifer system is considered when performing yield analysis;
- If the actual combined borehole abstraction rate is lower than, or equal to, the calculated long-term average potential abstraction, for a particular stochastic sequence, the long-term potential abstraction for that specific month will be equal to the actual borehole abstraction rate.
- If the actual combined abstraction rate of all the boreholes within the aquifer system is larger than the calculated long-term average potential abstraction for a particular stochastic sequence, the calculated long-term potential abstraction is less than the actual borehole abstraction rate per month, and there will be a failure. In other words, no water will be available for the yield. This is assumed because only a constant speed pump is considered for abstraction, if a variable speed pump were considered, the long-term potential abstraction for each month could be utilized by making use of a different pumping speed every month.

The abovementioned scenarios can be described, using three examples with representative values, as summarised in Table 3-7.

For example, in the month of October, 2 boreholes were utilized to abstract water from an aquifer system with a combined actual pumping rate of $4 \ell/s$ ($346 \text{ m}^3/\text{day}$). For scenario 1, the stochastic groundwater analysis resulted in a long-term potential average abstraction volume of $16\,500 \text{ m}^3/\text{month}$ ($540 \text{ m}^3/\text{day}$) for a stochastic sequence. However, the monthly abstraction potential is estimated at $9\,100 \text{ m}^3$ ($300 \text{ m}^3/\text{day}$). Therefore, the pumping rate of the boreholes fall within the estimated long-term potential average abstraction; thus, the combined actual pumping rate of $346 \text{ m}^3/\text{day}$ will be available for the yield.

For scenario 2, the combined actual pumping rate of $346 \text{ m}^3/\text{day}$, is more than the long-term average potential of $330 \text{ m}^3/\text{day}$, associated with a different stochastic sequence. However, the potential abstraction available for October is $410 \text{ m}^3/\text{day}$. Therefore, even though the combined actual abstraction is more than the long-term potential average abstraction, it can be satisfied in the month of October because it does not affect the behaviour of the aquifer over the long-term.

However, in scenario 3, less long-term potential abstraction is available and thus a failure to supply the combined actual pumping rate will occur. There is $300 \text{ m}^3/\text{day}$ available for the yield in October, but the borehole will experience a failure and contribute $0 \text{ m}^3/\text{day}$ to the yield, as municipalities, more often than not, make use of constant speed pumps and not variable speed pumps to be able to alter abstraction rates.

Even though a borehole failure occurs in scenario no. 3 the entire conjunctive use system can be managed in a way to supply for the demand, as a borehole failure might not incur an entire system failure, except in a scenario where it is the base supply. Ultimately, if groundwater cannot supply for the demand, and desalination cannot supply for the demand, then the system will fail when the surface water fails to supply the demand.

Table 3-6: Pumping rate scenarios for abstraction yield

Scenario	Actual Borehole Abstraction (m ³ /day)	Long-term average potential abstraction for sequence (m ³ /day)	Potential abstraction for October (m ³ /day)	Sustainable Monthly Abstraction (Yes/No)
1	346	540	300	No
2	346	330	410	No
3	346	330	300	Yes

It is important to note that even if the long-term sustainable abstraction for a certain month is more than what is abstracted, the excess will not be stored for the following month but it will contribute to natural equilibrium. This is a conservative approach.

Ideally, any surface water that is in excess within a certain month, should be pumped back into the aquifer system through artificial recharge, this scenario is however not explored, as discussed in section 2.3.6.

3.8.1.3 Surface Water

Desalinated water and groundwater quantities available for supplying the demand are the first resources to be used to this end, after which surface water resources are added. Thus, the end surface water reservoir capacity as calculated with Equation 3-4 incorporates the portion of the demand that still has to be satisfied after the groundwater and desalinated water had been utilized. Failure specific to surface water occurs when the dam capacity falls below the minimum operating level.

3.8.2 Conjunctive Use System Yield

The failure of the conjunctive system is when the combined water resources are not able to supply the demand on any given day. Even if there is a failure within the groundwater supply, but the conjunctive system can still provide for the demand, the day will not have a failure.

The yield of a system can be analysed for a single sequence (stochastic streamflow sequence to which groundwater is related). The firm yield point of a sequence is determined to access the capability of the system to provide for the demand without a failure occurring. To determine the firm yield point of a

particular sequence, the target draft is sequentially increased in increments of a particular step (starting with an increment of 10 Mℓ) and the system is evaluated for failures. If a failure occurs between two increments, the previous (first) non-failure target draft value is used as a second starting point, and the increment size is halved, and the process of evaluating the target draft continues, until the firm yield point reached. This is also referred to as an iterative process. To perform this analysis (iterative process), a program was written in the Visual Basic application to perform the computations. The default starting capacity of the dam is fixed at the FSC as suggested by Basson et al. (1995).

After the firm yield of the sequence is determined, the draft-yield curve can be drawn up (e.g. Figure 2-3). To plot the curve, a total of 15 target drafts (target drafts in higher and lower percentages surrounding the historical firm yield) are used. The base yield and the average yield for each target draft are evaluated, to ascertain the system supply capability behaviour for increasing target drafts. The firm yield can be determined for every stochastic sequence available (101 stochastic sequences).

3.8.3 Long-term reliability

The historical streamflow data recorded over a number of years (record length) is used when performing simulations to establish the reliability of supply. The record length suggested by Basson et al. (1995) is 64 years, but if data is available for a larger number of years this data of the longer record length should be used. Therefore, the entire 90-year record length available on the WR2012 data base is used during simulations towards determining long-term reliability of supply. The starting capacity for the surface water reservoir is user defined for each stochastic sequence during the simulations.

To plot the long-term reliability graph, the total number of stochastic sequences available (101 sequences), are evaluated for 7 different target drafts. The target drafts represent an equitable range around the historical firm yield value. The historical yield gives an indication of the historical supply capability of system. However, when determining the firm yield of the other sequences, the historical firm yield can be associated with a specific reliability of supply. The 101 sequences are evaluated for their firm yield and are plotted on a graph in descending order (Figure 3-17), to generate a firm yield line for a specific target draft. A break point occurs at the point where the first failure to supply the yield occurs when the yield of the sequence is less than the target draft. The yield lines are generated for the 7 different target drafts, and a reliability of supply percentage is associated with each yield value (Figure 3-18). The firm yield line can be generated by connecting all the breaking points from the different target drafts evaluated (Figure 3-18). The long-term reliability graph is discussed in greater detail in the case study for the Stellenbosch municipality and its associated catchments.

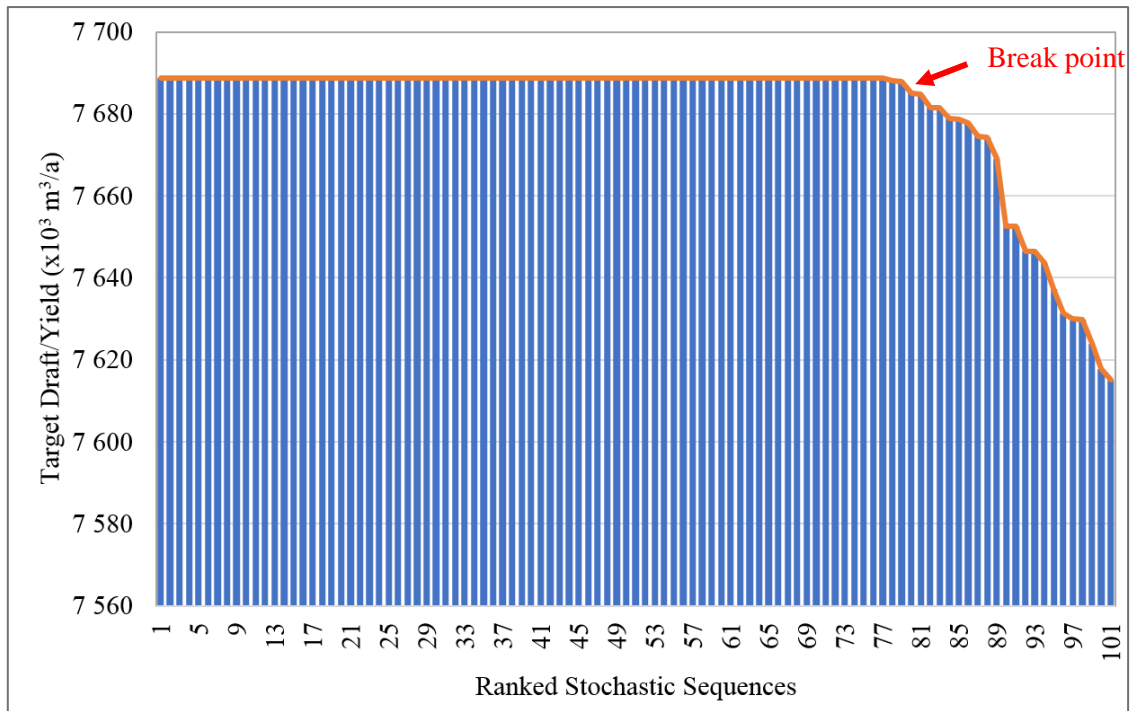


Figure 3-17: Ranked stochastic sequences for 1 target draft

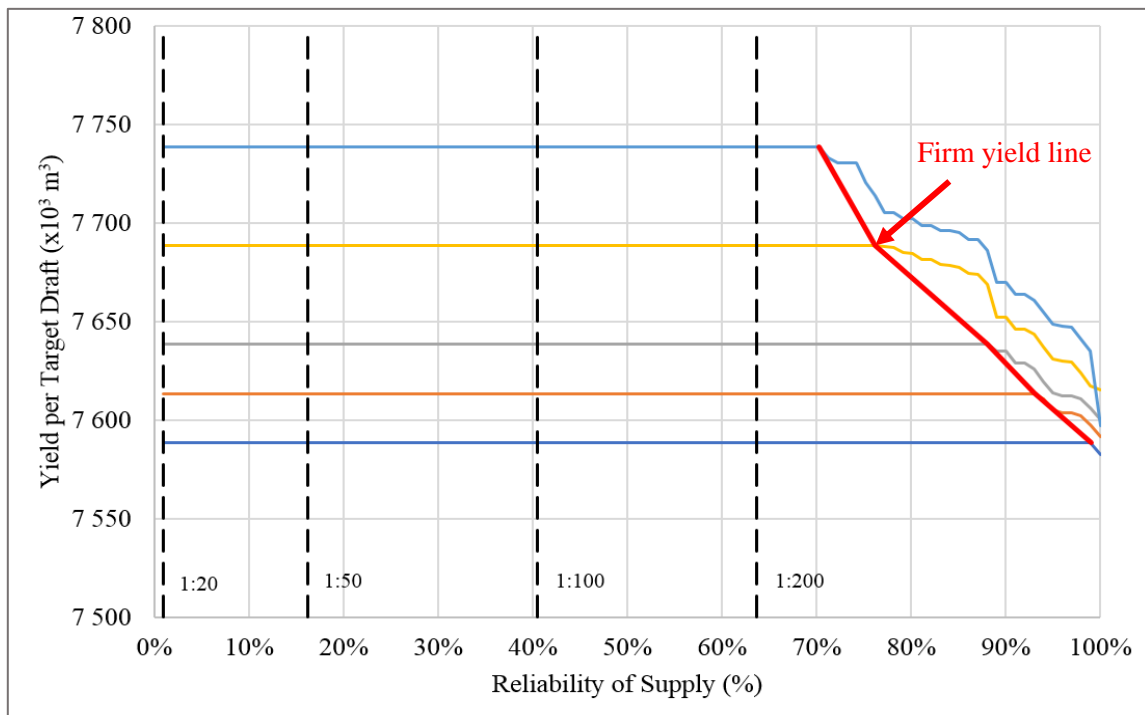


Figure 3-18: Reliability of supply and firm yield line for 5 target drafts

3.8.4 Short-term management

For short-term management, as suggested by Basson et al. (1995) all stochastic sequences are analysed and a planning scope of between 1 to 3 years can be chosen by the user. If groundwater is only used in short-term crisis management situations, which occur between planning timelines (between 1 and 3

years) then it is assumed that the boreholes will not fail even if the abstraction rate is higher than the long-term potential abstraction. Different surface reservoir starting capacities are evaluated and a probabilistic storage curves generated to show the storage trajectory of the reservoir giving the starting situation. By using box plots, a storage trajectory is plotted for the exceedance probabilities of 5%, 25%, 50% (median), 75% and 95% (Figure 3-19). An exceedance probability of 5% indicates that the storage trajectories for only 5 sequences show a trajectory equal to or better than the storage trajectory indicated by the 5% exceedance probability line. The starting situation should reflect the storage percentage, demand, conjunctive use water resources utilized for the commencement date of the analysis. If interbasin transfer systems form part of the supply system, then the inter-basin allocation provided at the commencement of the decision period should also be indicated. The short-term management graph is discussed in greater detail in the case study for the Stellenbosch municipality.

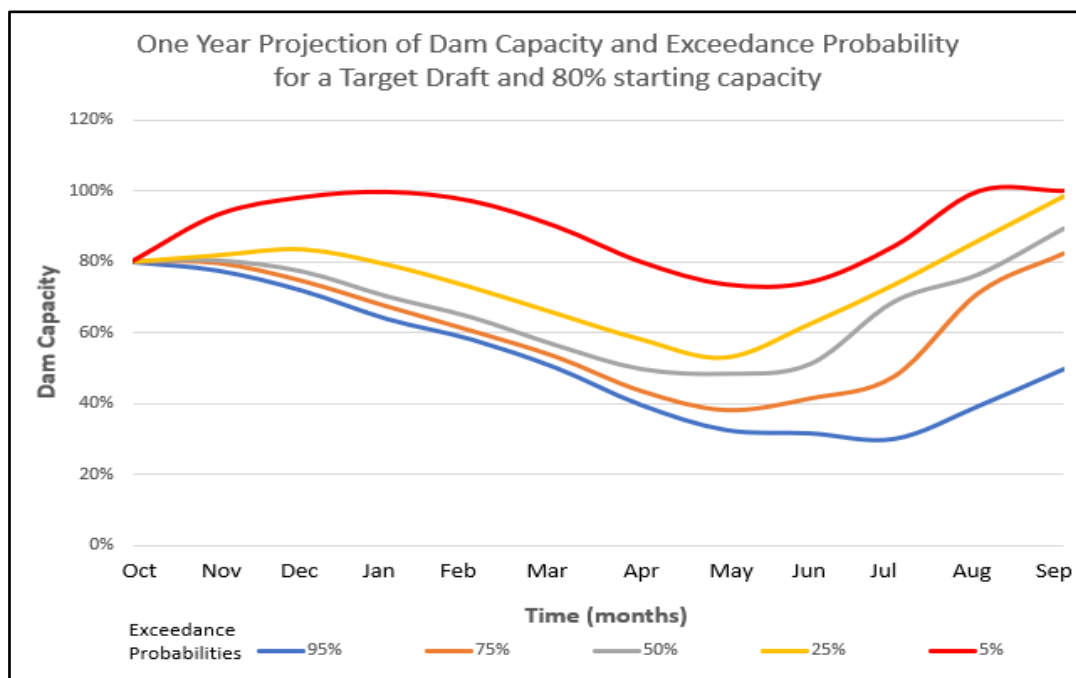


Figure 3-19: Short-term management curve

3.9 Summary of Excel Setup

There are 4 different Microsoft Excel workbooks; 3 for streamflow disaggregation and groundwater simulation and the fourth for the conjunctive use system water balance. The setup and interlinkages between the 4 different workbooks are outlined in Figure 3-20. External input data refers to data obtained from online sources, such as data bases of water research institutions (WR2012) or water management authorities (DWS), while other data necessary for simulations are calculated by the computational interface (Excel worksheets) for the user to apply as input data at a later stage, or as the yield analysis progresses. The arrows represent the data transferal between different Excel workbooks. A short description for each number is summarized in Table 3-7.

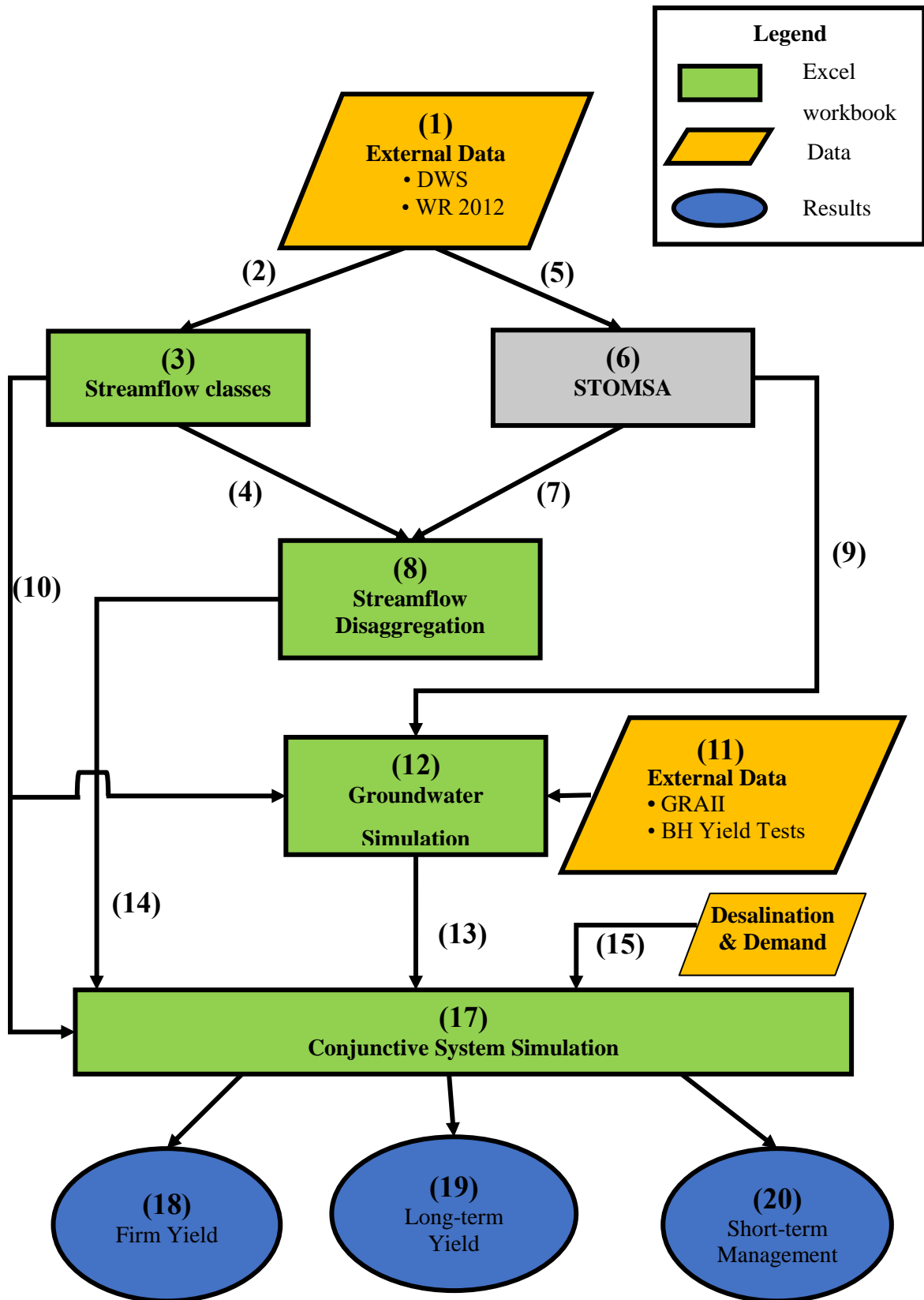


Figure 3-20: Excel workbook data transferral setup

Table 3-7: Legend for the Excel workbook data transferral

Number	Legend	Description
1	Data	Hydrological data retrieval from online data bases External Data from DWS (daily flows) Water Resources 2012 (naturalized monthly runoff for quaternary catchment) Water Resources 2012 (monthly rainfall for quaternary catchment)
2	Input	Daily flows into streamflow classes Excel workbook (DWS) Water Resources 2012 (naturalized monthly runoff for quaternary catchment) Water Resources 2012 (monthly rainfall for quaternary catchment)
3	Workbook/ Process	Streamflow classes Excel Workbook: categorize daily streamflow (section 3.3.1) determine RAIN-RUNOFF ratio (section 3.4)
4	Output/Input	Streamflow classes: monthly streamflow classes and daily distributions
5	Input	WR 2012 naturalized monthly streamflow into STOMSA
6	External Process	Use STOMSA to generate 101 stochastic sequences
7	Output/Input	101 Stochastic sequences (monthly time step) and Historical sequence
8	Workbook/ Process	Monthly streamflow is categorized and disaggregated into daily streamflow for each stochastic sequence (section 3.3.2)
9	Output/Input	101 Stochastic sequences (monthly time step) and Historical sequence
10	Output/Input	RAIN-RUNOFF ratios
11	Data	Quaternary catchment selection, GRA II automatic data retrieval Data on specific boreholes from Borehole Yield Tests
12	Workbook/ Process	Groundwater Simulation: Aquifer system balance to obtain potential monthly abstraction (section 3.6.1) Interference Test (section 3.6.2)
13	Output/Input	Potential monthly abstraction for each stochastic sequence distributed evenly over the number of days in a month
14	Output/Input	Daily stochastic streamflow sequences
15	Data	Reverse Osmosis plant capacity and monthly distribution WR2012 pan evaporation factors Demand monthly distribution Dam characteristics Inflow characteristics and limitations
16	Output/Input	RAIN-RUNOFF ratios
17	Workbook/ Process	System Balance: Operational Rules (section 3.8.1) Daily system simulation
18	Output	Historical Firm Yield and Firm Yield for each stochastic sequence Draft-Yield Curve methodology (section 3.8.2)
19	Output	Long-term reliability curve (section 3.8.3)
20	Output	Short-term management curve (section 3.8.4)

4 CASE STUDY: STELLENBOSCH

The methodology developed for the modelling of the conjunctive use system, which combines all the water resources available to a municipality to satisfy the demand, is applied to the current water resources available, and the use thereof, to the Stellenbosch Municipality, illustrated as a case study. The analysis of the conjunctive use of water resources includes: data retrieval, data processing and modelling, after which the results are used to make recommendations towards optimizing the water resource management of the Stellenbosch Municipality.

4.1 Background

Stellenbosch Municipality is a category B municipality (local municipality) demarcated within the Cape Winelands District Municipality, situated in the Western Cape Province of South Africa. Stellenbosch Local Municipality's governance area does not only include the town and farms of Stellenbosch, but also an array of smaller towns close by, namely Franschhoek, Klapmuts and Pniel (GLS Consulting, 2018). The main economic sectors of Stellenbosch Municipality are agriculture, especially the cultivation of flowers, fruits and wine, due to winter rainfall, as well as tourism in the summer months, and tertiary education (Stellenbosch University) all year round. Each town forms part of a separate water supply system and the urban user demand can be obtained for each supply system (GLS Consulting, 2018). For the purpose of this case study, only the town of Stellenbosch, and its urban (domestic) water users will be considered.

4.1.1 Location

The town of Stellenbosch (including Jamestown and De Zalze) is encircled by three quaternary catchments, namely G22F, G22G and G22H, as indicated in Figure 4-1. The quaternary catchments are part of the Berg Water Management Area, and fall within the Hottentots-Holland mountain range.

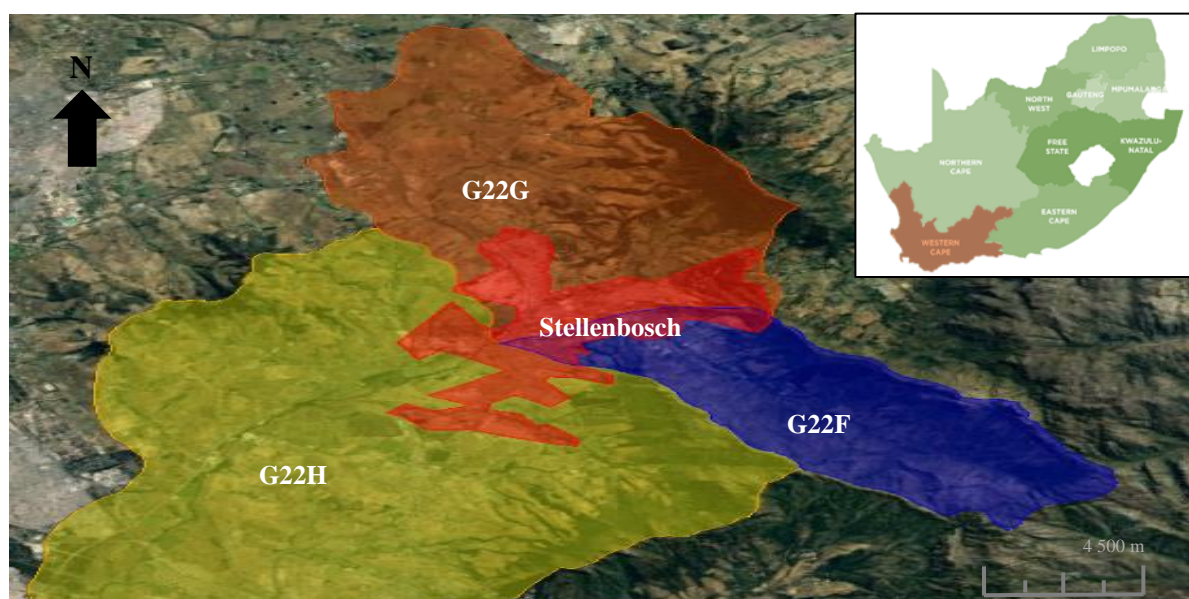


Figure 4-1: Stellenbosch with adjoining quaternary catchments (Google Earth)

The hydrological characteristics for each quaternary catchment, as retrieved from the WR2012 database (Berg WMA/Quaternary data spreadsheets) are summarized in Table 4-1.

Table 4-1: Hydrological characteristics of quaternary catchments

Quaternary Catchment	Area (km ²)	MAP (mm)	Naturalized Net MAR (mil m ³)	MAE (mm)	Rainfall Zone	Evaporation Zone
G22F	66	1465	36.58	1450	G2C	23C
G22G	106	754	14.92	1455	G2C	23C
G22H	227	669	25.1	1415	G2C	23C

4.1.2 Overview of Municipal Water Resources

Urban water users of Stellenbosch are supplied with purified water from the Idas Valley Water Treatment Works (WTW) and the Paradyskloof WTW. The raw water supplied to the respective WTW is sourced from the Eerste River and the Western Cape Water Supply System (WCWSS) through the Theewaterskloof tunnel system (GLS Consulting, 2018). Furthermore, Stellenbosch Municipality has access to a number of boreholes, some of which were developed as augmentation water resources, as part of the drought intervention scheme for the period between 2014 and 2017 (GEOSS, 2018).

A simplified layout of the bulk water supply system of Stellenbosch is illustrated in Figure 4-2, adapted from the Drought Intervention Planning Report (GLS Consulting, 2018). Supply

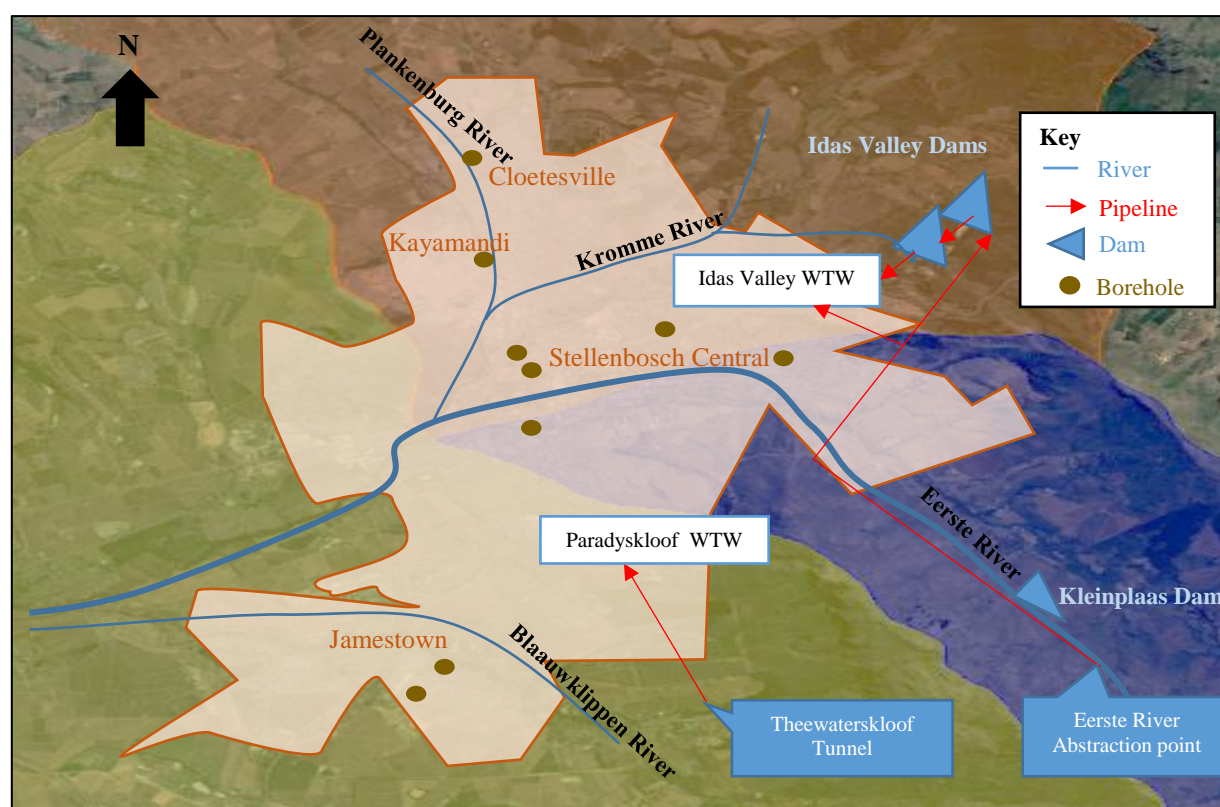


Figure 4-2: Stellenbosch water supply system setup

areas within Stellenbosch, borehole locations, as well as surface water reservoirs are depicted in Figure 4-2. The existing water resources of the Stellenbosch supply system are briefly outlined in sections 4.1.2.1 to 4.1.2.3.

4.1.2.1 Idas Valley WTW and Idas Valley Dams

The Idas Valley WTW is supplied with raw water for purification directly with a pipeline from the Eerste River in the Jonkershoek Valley, during winter months when rainfall is prevalent. The license issued by the DWS to the Stellenbosch Municipality allows for the abstraction of 7 224 Mℓ/a from this system (GLS Consulting, 2018). The Idas Valley WTW has a supply capacity of 26 Mℓ/day. Surplus water from the Eerste River is transferred to the Idas Valley dams during winter months. A shortage from the Eerste River occurs in the dryer summer months and the raw water supply to the WTW is supplemented from the Idas Valley storage dams. The pipeline capacity to transfer water from the Eerste River directly into the Idas Valley WTW is 300 ℓ/s, while the pipeline capacity to transfer water from the Eerste River to the Idas Valley dams is 170 ℓ/s (GLS Consulting, 2018).

4.1.2.2 Paradyskloof WTW

The Paradyskloof WTW receives raw water for purification from the Western Cape Water Supply System (WCWSS) through the Theewaterskloof tunnel, with a water allocation of 3 000 Mℓ/a (GLS Consulting, 2018). The WCWSS is supplied with water through the Riviersonderend Government Water Scheme, which is a large-scale inter-basin transfer scheme that manages water between different dams (Theewaterskloof, Voëlvlei, Wemmershoek, Bergrivier, Upper and Lower Steenbras) in the Western Cape through tunnels and releases, according to demand and storage requirements of different water users. The Paradyskloof WTW supply capacity is 20 Mℓ/day. During the drought, urban users of Stellenbosch were encouraged to decrease their demand by 45%, as water allocation from the WCWSS to the municipality was limited, due to low rainfall and extreme heat conditions, which decreased the water levels of the Theewaterskloof dam to lower than normal operating levels (GLS Consulting, 2018).

4.1.2.3 Groundwater

According to the 1:250 000 geological map (3318 Cape Town), the geology of the Stellenbosch Municipality ranges between different types of rock and sediments, namely basement rocks of the Malmesbury Supergroup (Shale and Sandstone), the Cape Granite Suite and Table Mountain Group, and Quaternary sediments overlying many areas (Olianti et al., 2018). Stellenbosch is situated in a valley surrounding the Eerste River, which is mainly underlain by unconsolidated sediments from the Table Mountain Group sandstones, as well as faults and fractures (GEOSS, 2018).

Stellenbosch Municipality is dependent on surface water for its municipal supply; however, during the dry period that occurred between 2014 and 2017, Stellenbosch Municipality sought to augment the bulk water supply system with groundwater to increase its water security. While Stellenbosch Municipality already has access to a number of existing boreholes, most of which have been used for irrigation

purposes, new boreholes are in the process of being commissioned and could potentially add water directly into the distribution network (GLS, 2018). Information pertaining to the boreholes in Stellenbosch and their use are provided in section 4.5.

4.1.3 Aims and Objectives

The Stellenbosch water supply system for urban use is modelled by applying the most suitable methods (including adaptation of certain methods), and their associated assumptions, as selected during the course of this research. The yields of different water resources available to the Stellenbosch Municipality are assessed and a conjunctive use system water balance is performed to determine the amount of water available to the municipality on a daily basis. This is done to assist the municipality in short-term decision-making processes, especially during times of drought. The long-term reliability of the conjunctive use system is evaluated by generating the long-term reliability curves. This is done to assist the municipality with long-term water management planning in terms of water security.

4.2 Schematic Model of Stellenbosch Water Resources

A model is a simplification of reality based on certain principles, with a number of associated assumptions. The Stellenbosch water supply system (Figure 4-2), as adapted from GLS Consulting (2018) and GEOSS (2018), is simplified to a schematic model (Figure 4-3) as follows:

Stream1 – The streamflow abstracted from the Eerste River in the Jonkershoek Valley transferred to the Idas Valley WTW is limited by the capacity of the pipelines (470 ℓ/s). It is located in quaternary catchment G22F.

Stream 2 – The surface water inflow stream to the Idas Valley dams (modelled as a single dam) is calculated from the runoff generated in the catchment area contributing to the upper dam (Idas Valley Dam 1). It is a tributary to the Kromme River and is located in quaternary catchment G22G.

To simplify the inter-relationship of water transfers between the Idas Valley WTW and the Idas Valley dams, the system is modelled in such a way that all the water enters the Idas Valley dams directly. Therefore, the Idas Valley dams (modelled as one dam) capacity is increased by a volume pertaining to the maximum abstraction capacity from the Eerste River (Jonkershoek Valley) into the Idas Valley WTW (300 ℓ/s) so that the daily water available for treatment can be stored. If the dam capacity is not increased the daily inflow used by the Idas Valley WTW would spill, thereby not forming part of the yield.

Inter-basin transfer – The inflow to the Paradyskloof WTW from the Theewaterskloof tunnel (Riviersonderend scheme of the WCWSS) is modelled as a constant inflow stream of 3 000 $M\ell/a$. The Paradyskloof WTW capacity does not limit the inflow.

Groundwater - The pumping rates (capacities) of boreholes in use are totalled and modelled as a single inflow stream. For the long-term analysis the combined pumping rates will be evaluated against the long-term potential average abstraction. For the short-term management analysis, it is assumed that the groundwater yields will be available regardless of the long-term analysis.

Evaporation – Evaporation over the combined surface area of the two Idas Valley dams is modelled as a loss.

Overflow - Water overflowing the Idas Valley dam enters the Kromme River and is not available for the yield.

Municipal Demand – The daily municipal demand (obtained from GLS, 2018), is given as a percentage of total annual demand for urban water users.

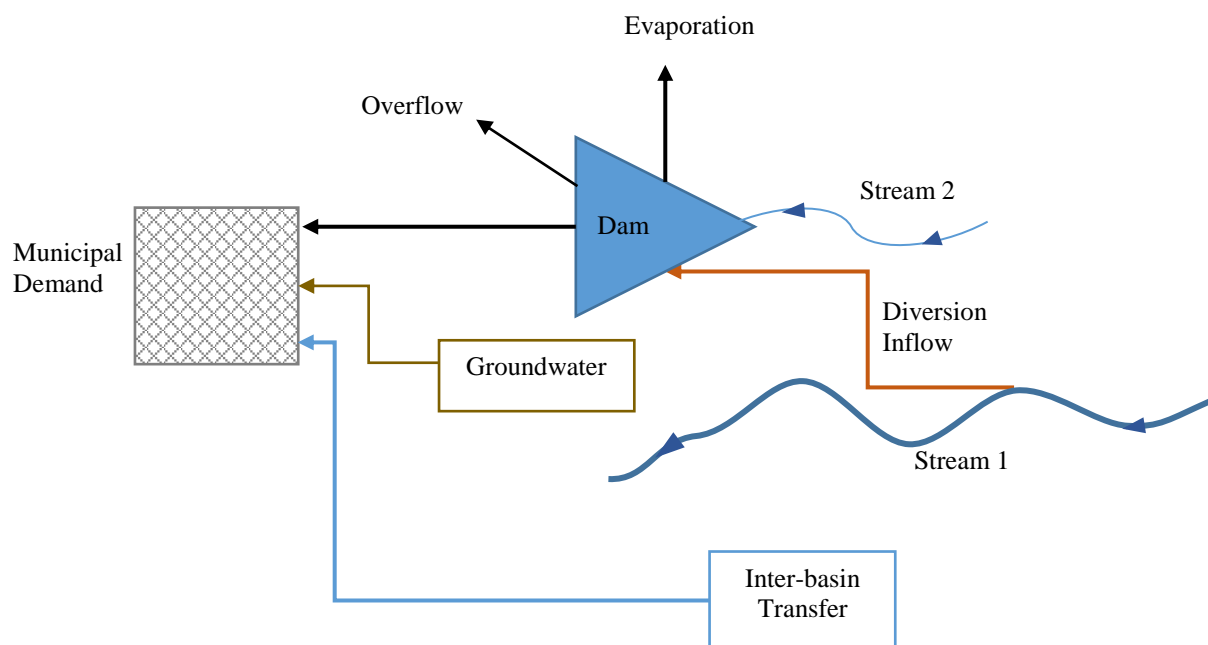


Figure 4-3: Schematic diagram of the simplified Stellenbosch water resource system

4.3 Stochastic Streamflow Generation using STOMSA

The naturalized streamflow sequence for catchment G22F is retrieved from the WR2012 online database. The entire record length (90 years) of the historical streamflow sequence for catchment G22F is attached as Appendix C.1.

The abovementioned data is then prepared for input into STOMSA to generate stochastic streamflow sequences, by saving it to a space delimited text file. There after it is saved with an “.INC” extension, as required for STOMSA computations (discussed in section 3.2.1). The “.INC” file for catchment G22F is named “*ExcelG22F.INC*”. A flow diagram of the data preparation process for input into STOMSA is attached as Appendix C.1.2. A flow chart is attached as Appendix C.1.3 illustrates the steps followed while using the STOMSA application. An example of a stochastic sequence

(“*ExcelG22F.003*”) as a text file resulting from STOMSA, is attached as Appendix C.1.4. The STOMSA output files are then combined with the “*STOMSA File Combiner*” program developed with the Visual Studio application, as discussed in section 3.2.2.

4.4 Streamflow Disaggregation

The largest inflow stream supplying water to the Idas Valley WTW and storage dams is the abstraction pipeline network from the Eerste River (300 ℓ/s and 170 ℓ/s) (GLS Consulting, 2018). The daily streamflow data for the Eerste River (retrieved from the DWS website) is recorded at a streamflow gauge situated in close proximity to the streamflow diversion structure (weir) in quaternary catchment G22F. The daily streamflow is used to create the 3 streamflow classes (low-, medium-, and high-flow) with associated daily streamflow distributions. The stochastic sequences generated from the naturalized streamflow of catchment G22F (naturalized streamflow from WR2012) are disaggregated to daily streamflow, by using the 3 streamflow classes and associated daily distributions. The processes used for streamflow classification and the stochastic streamflow disaggregation following it are discussed in sections 4.4.1 to 4.4.2. The raw data as well as the processing thereof are attached in Appendix C.2.

4.4.1 Streamflow Classification

A number of streamflow gauges are located in catchment G22F, as illustrated in Figure 4-3, however; only the streamflow data of gauging station G2H037 is required, as it is closest in proximity to the point of abstraction (discussed in section 3.2). The daily streamflow data obtained for G2H037 was recorded between the years of 1989 and 2019. This 30-year record length contained information gaps (missing data) indicated by the quality code, namely 170 (see Appendix B1 for quality codes). The information gaps occurred randomly throughout the record, with the largest consecutive gaps between 5 June 1990 and 17 July 1990 (sequence numbers 19900605 to 19900717). A section of the raw daily streamflow data, with sequence numbers, is provided in Appendix C.2.1. The months during which the gaps occurred were discarded from the sequence used to perform streamflow classification to preserve accuracy. The streamflow record must start on the same day as the hydrological year, namely the 1st of October 1989.

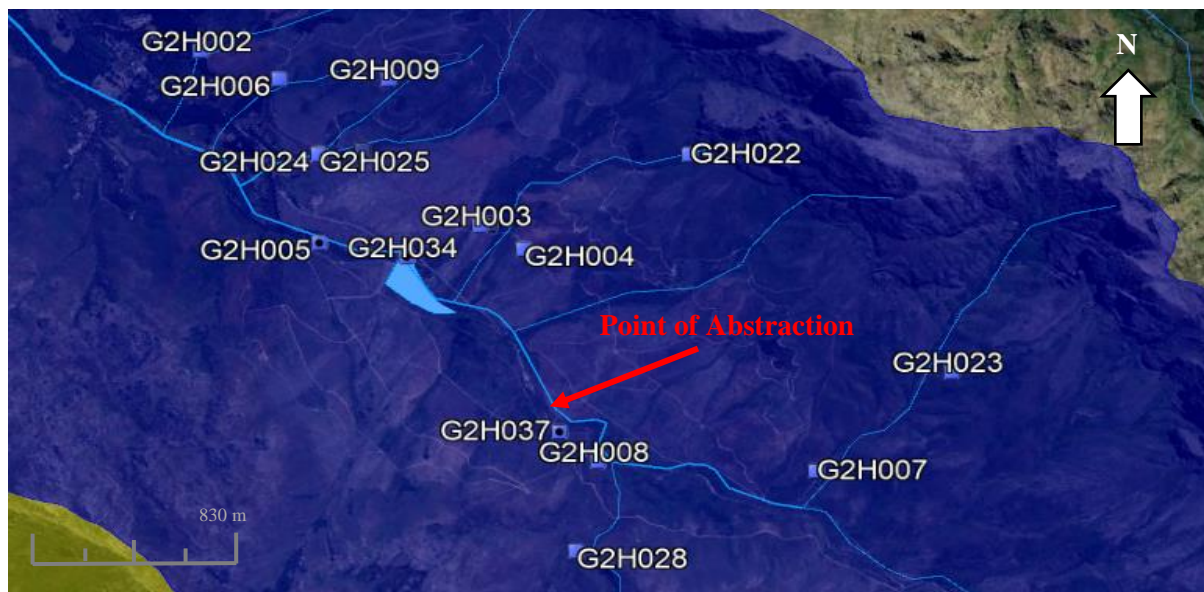


Figure 4-4: Streamflow gauging station G2H037 in quaternary catchment G22F (Google Earth)

The daily streamflow values obtained for G2H037, are converted to monthly streamflow values (from m^3/s to $\text{mil m}^3/\text{m}$) and then grouped according to the month in which they were recorded, irrespective of the year, in order to start the streamflow classification process (discussed in section 3.3.1).

The streamflow classification process, with values pertaining to gauging station G2H037, is outlined in a flow diagram, attached as Appendix C.2.2.

The high and medium flow classes for October are attached in Appendix C.2.3. According to the streamflow record of G2H037 (provided in Appendix C.1.2), the highest amount of streamflow was recorded in October 1996. As the hydrological year starts in October, streamflow distributions for October were used in the flow diagram. The ranges of the streamflow classes are expressed in percentages of the MMR. The MMR for the October streamflow group amounts to 1.625 mil m^3 per month. The boundaries for the 3 different streamflow classes for the month of October (30-year record length) are summarized in Table 4-2. The boundaries for the streamflow classes of every monthly group in the record length are summarized in Table 4-3.

Table 4-2: Streamflow class boundaries as percentages of MMR for streamflow of October

OCTOBER	Upper Boundary	Lower Boundary
High Range:	None	119%
Medium Range:	119%	39%
Low Range:	39%	None

Table 4-3: Monthly flow classes for G22F as percentage of MMR

Monthly streamflow classes (%of MMR)			
Month	High	Medium	Low
OCT	> 119 %	119 % - 39 %	< 39 %
NOV	> 107 %	107 % - 17 %	< 17 %
DEC	> 76 %	76 % - 20 %	< 20 %
JAN	> 79 %	79 % - 23 %	< 23 %
FEB	> 72 %	72 % - 46 %	< 46 %
MAR	> 43 %	43 % - 29 %	< 29 %
APR	> 76 %	76 % - 36 %	< 36 %
MAY	> 125 %	125 % - 57 %	< 57 %
JUN	> 114 %	114 % - 73 %	< 73 %
JUL	> 106 %	106 % - 84 %	< 84 %
AUG	> 117 %	117 % - 85 %	< 85 %
SEP	> 121 %	121 % - 52 %	< 52 %

The daily distributions, calculated as percentages of total monthly streamflow (Appendix C.2.4), are plotted on three different graphs, one for each streamflow class, to enable the user to select a specific daily distribution to apply during the disaggregation process. The graph of the medium flow class for October is illustrated in Figure 4-5, which indicates that there are larger distribution peaks between day 6 and day 12 of October and then again from day 18 to 23 of October. The dashed red line on the medium flow class graph is selected as the distribution representing this two-peak trend in October. The daily distributions for each streamflow class, associated with each month of the year, are summarized in Appendix C.2.5.

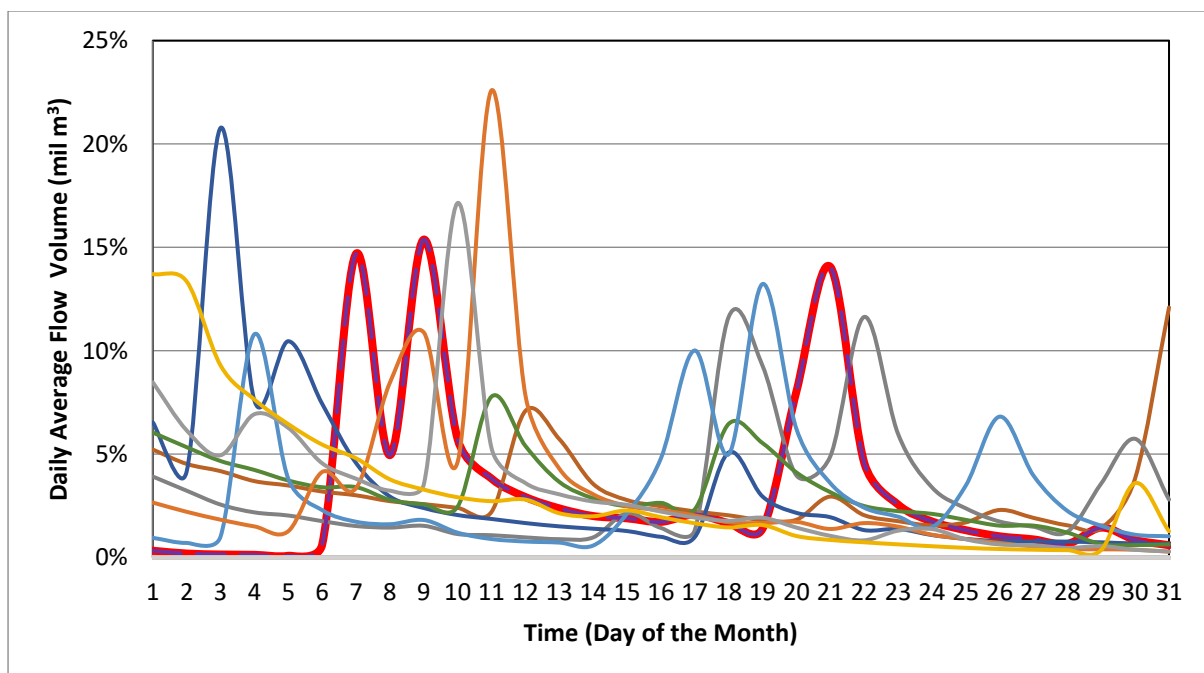


Figure 4-5: Medium streamflow class for October with 10 daily distributions

4.4.2 Stochastic Streamflow Disaggregation

The stochastic sequences generated from the naturalized streamflow (WR2012) of catchment G22F using STOMSA, are expressed as monthly streamflow sequences. The stochastic monthly streamflow sequences are disaggregated into daily streamflow sequences by applying the applicable most compatible daily distribution, selected from the applicable streamflow classes, as established in section 4.4.1. The record length for the monthly streamflow sequences is 90 years (1080 months), as per the WR2012 online database.

The monthly streamflow volume for October 1920 (stochastic sequence no. 3) is expressed as a percentage of MMR, in this case 61.6%. This percentage is compared to the class boundary percentages listed in Table 4-3, to determine the streamflow class under which stochastic sequence no. 3 falls. After performing the comparison, it can be concluded that stochastic sequence no. 3 falls under the medium streamflow class (band: 117% - 45%). The selected daily distributions associated with the medium streamflow class, are then multiplied by the monthly flow volume, to generate daily streamflow sequences for October 1920. The respective values are inserted into Equation 3-2 to calculate the daily streamflow.

$$Daily\ Flow_{1920,Oct,1} = Monthly\ Flow_{1920,Oct} \times Daily\ Distribution_{Oct,Medium,1}$$

$$\begin{aligned} Daily\ Flow_{1920,Oct,1} &= 1.95 \times 0.33\% \\ &= 0.006\ \text{mil m}^3/\text{day} \end{aligned}$$

To explain the streamflow disaggregation process, the stochastic sequence for October 1920, “*ExcelG22F.003*” generated through STOMSA, is used to construct a flow diagram. The flow diagram is attached as Appendix C.2.6.

4.5 Rainfall-Runoff Relationship

The data file for the rainfall zone G2C was downloaded from the WR2012 online data base under the “*Catchment based rainfall datafiles*” folder. This rainfall zone was selected as it includes quaternary catchment G22F and G22G. The catchment-based rainfall data files are expressed in percentages of MAP. The monthly percentages of MAP recorded for rainfall zone G2C are multiplied with the MAP of quaternary catchment G22F to generate a historical rainfall sequence in mm/month (Appendix C.3.1). The RAIN-RUNOFF ratios for every month are determined by applying Equation 3-3. The MMP (99.1 mm) and the streamflow (3.24 mil m³) for October are substituted into Equation 3-3 as follows:

$$RAIN_RUNOFF\ ratio(i) = \frac{MMPi/1000}{MMRi}$$

$$RAIN_RUNOFF\ ratio(i) = \frac{99.1/1000}{3.24} = 0.031$$

The monthly RAIN-RUNOFF ratios are plotted on a graph in Figure 4-6, indicating higher ratios in the months that Stellenbosch experiences hotter and drier weather, in other words summer months (January, February and March). This suggests that more interception by vegetation and evaporation, as well as infiltration into the soil (low moisture index), takes place during these months. The monthly RAIN-RUNOFF ratios are used to generate stochastic rainfall sequences from the stochastic streamflow sequences, as generated through STOMSA. The stochastic rainfall sequences are used in the groundwater simulation (recharge as %MAP) and surface water simulation (net evaporation). MMP and MMR values, as well as the corresponding monthly RAIN-RUNOFF ratios are summarized in Appendix C.3.2.

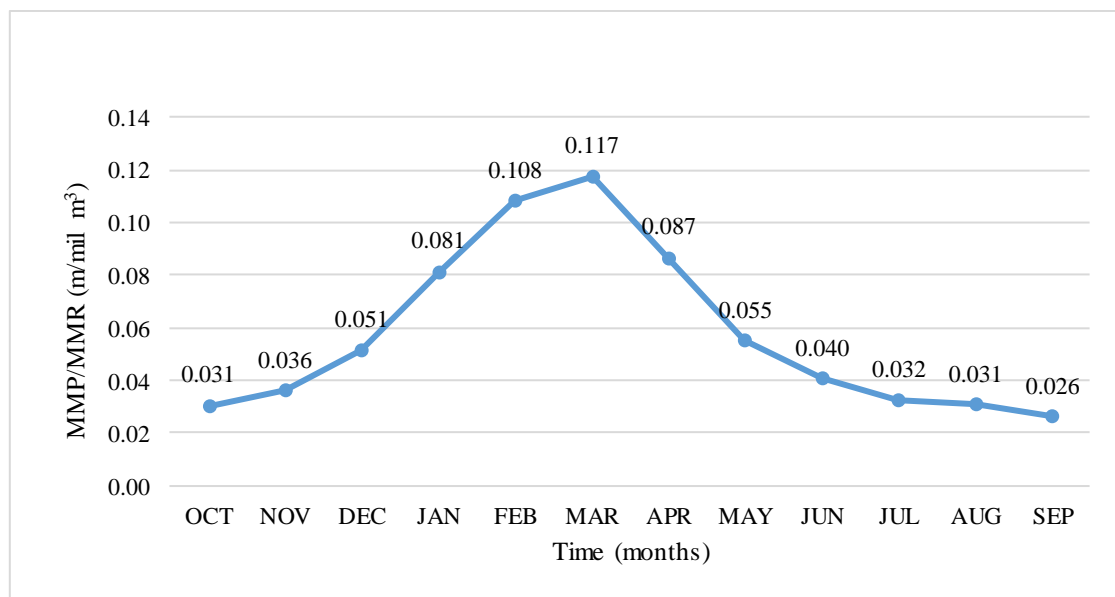


Figure 4-6: Mean monthly RAIN-RUNOFF ratios

4.6 Surface Water

The water balance for the surface water resources from Idas Valley, contributing to the Stellenbosch water supply system, is illustrated in Figure 4-3. The components for the water balance consist of 2 inflow streams, which include the water supply from the Idas Valley WTW and the Idas Valley storage dams (two dams modelled as one dam), as well as overflow, spillage and demand. Each component is discussed briefly.

4.6.1 Idas Valley Dams

The main features of the two Idas Valley dams are summarized in Table 4-4 (Aurecon, 2012). To model the two dams as a single dam, as well as account for the daily capacity of the water treated at the Idas Valley WTW, with a capacity of $300 \text{ l/s} = 25\,920 \text{ m}^3/\text{day}$, the capacities of these water sources are combined. The combined capacity amounts to a total of $2\,380 \times 10^3 \text{ m}^3$ (2 380 Mℓ). The combined surface area of the two dams, when modelled as one, at Full Supply Capacity (FSC), is 16.7 ha ($167\,000 \text{ m}^2$). The size of the catchment area contributing to runoff into the dams is 4.25 km^2 .

Table 4-4: Main features of the Idas Valley Dams

	Idas Valley Dam No 1	Idas Valley Dam No 2
Type of dam	Concrete gravity/arch dam	Earthfilled embankment
Owner	Stellenbosch Municipality	Stellenbosch Municipality
Classification	Category III (Medium Size, High Hazard Potential)	Category III (Large Size, High Hazard Potential)
Capacity	543 Mℓ	1 811 Mℓ
Surface Area at FSL	4.7 ha	12 ha
River into dam	Tributary from Krom River	-
Catchment Area	1.9 km ²	2.35 km ²

The combined surface area-capacity curve for the Idas Valley dams is depicted in Figure 4-7 (Aurecon, 2012). The curve was constructed by fitting a “Power function” trend line between two points (Surface Area 1471 m², Capacity 1 Mℓ) and (Surface Area 167 000 m², Capacity 2 380 Mℓ). The relationship is used to calculate the surface area of the dam for every daily time-step, so that net evaporation over the dam can be calculated (section 4.6.4).

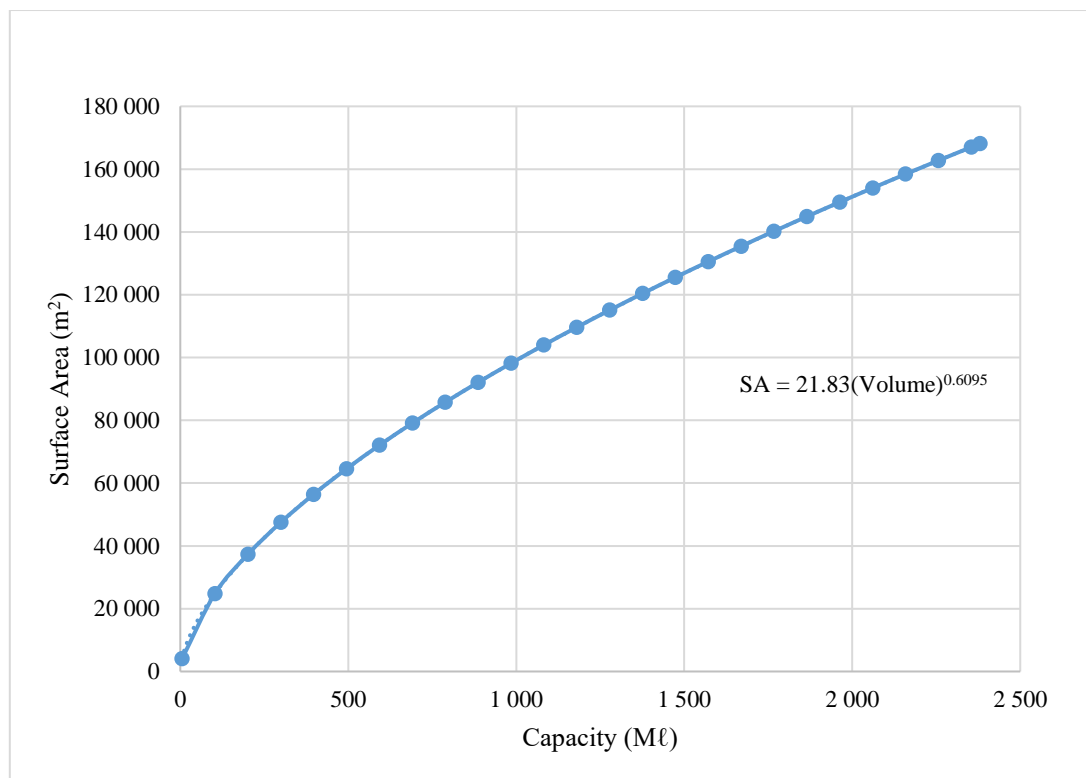


Figure 4-7: Surface Area-Capacity Curve for combined Idas Valley dams.

4.6.2 Inflow Streams into Idas Valley System

Stream 1 is the diversion inflow from the Eerste River to the Idas Valley WTW and dams, effectively the abstraction which is limited by the diversion (and pipe) capacity, as well as the diversion efficiency. The capacity of the diversion structure and the pipeline network has a combined capacity of 470 ℓ/s (170 ℓ/s + 300 ℓ/s) (GLS, 2018), and the diversion efficiency is unknown (in this case 100% efficiency is assumed). There is no downstream abstraction for consideration before abstraction can take place. The MAR of Stream 1 is the average of all monthly flows on record for flow gauge G2H037, multiplied by 12 (12 months in a year). The ratio between the MAR of Stream 1 (22.3 mil m³) and the MAR of quaternary catchment G22F (36.58 mil m³) is as follows (substituted into Equation 3-6):

$$\begin{aligned} \text{Stream 1 MAR ratio} &= \frac{\text{MAR}_{\text{Stream}}}{\text{MAR}_{\text{Origin}}} \\ &= \frac{22.3}{36.58} = 0.610 \end{aligned}$$

The ratio is used to convert stochastic daily flow volumes pertaining to the entire G22F catchment to Eerste River's stochastic daily flow at the point of abstraction. Stream 1 is situated in the mountain catchment which contributes to the entire streamflow of catchment G22F.

Stream 2 is the inflow stream into the Idas Valley dams from the catchment area contributing to inflow (runoff). There is no gauging station located upstream of the dams to record streamflow data, thus, the data to calculate the MAR of the dams cannot be retrieved online. The inflow stream to the Idas Valley dams (tributary to Kromme River), can only be estimated as the runoff occurring over the contributing catchment. Runoff is a result of rainfall over an area, minus interception and evaporation (rainfall-runoff relationship). The dams are situated in catchment G22G, where the MAP is 754 mm and the area contributing runoff to the dams is 4.25 km², while the average rainfall-runoff relationship is 0.18 (754mm/14.92 mil m³). The average relationship does not take into account the density of the forest vegetation which covers the contributing catchment. Therefore, to present a more realistic estimate for the rainfall-runoff relationship to compensate for potential evapotranspiration and interception of the dense forrest, the average rainfall-runoff relationship is halved to 0.09. Thus, the streamflow contributing to the dams is calculated as 0.29 mil m³ per year (Aurecon, 2012).

To relate Stream 2 to the stochastic streamflow available for catchment G22F, the ratio between Stream 2 and quaternary catchment G22F (catchment of origin) is established by using Equation 3-6:

$$\begin{aligned} \text{Stream 2 MAR ratio} &= \frac{\text{MAR}_{\text{Stream}}}{\text{MAR}_{\text{Origin}}} \\ &= \frac{0.29}{36.58} = 0.008 \end{aligned}$$

Stream 2 is situated in a mountainous area similar to the G22F catchment, therefore the ratio can be used to simulate daily inflow of Stream 2 directly into the Idas Valley dams.

4.6.3 Inflow into Paradyskloof WTW

The inflow from the inter-basin transfer scheme of the WCWSS, to Paradyskloof WTW through the Theewaterkloof tunnel, is distributed evenly per day. The allocation capacity of 3 000 Mℓ/a (converted to 3 mil m³/a) averages at 8.2 x 10³ m³ per day (GLS, 2018). The inflow volume, in this case, is not stored in a dam, but directly connected to the Stellenbosch Municipality water supply system through the Paradyskloof WTW to satisfy municipal (urban) demand.

4.6.4 Net Evaporation

Net evaporation from the Idas Valley dams is calculated by determining the evaporation rate over the surface area of the dams, and then subtracting the amount of rainfall over that same surface area, for every daily time step. As the Idas Valley dams are situated in quaternary catchment G22G, the evaporation zone is 23C and the MAE recorded in that zone is 1455 mm (Table 4-1). The monthly distribution of evaporation (% of MAE), also referred to as S-pan factors, for evaporation zone 23C, as well as the open water pan coefficients obtained from WR2012 online database, are summarized in Table 4-5. The combined coefficient is calculated by multiplying the two factors (S-pan factor x open water pan coefficient). The combined coefficient is then multiplied by the monthly percentages of MAE to arrive at the monthly evaporation rates (mm/month). It is assumed that evaporation is distributed evenly over the number of days in the month. Thus, the daily evaporation rate (mm/day) is the monthly evaporation rate divided by the number of days within the specific month. For October, the daily evaporation rate is 3.3 mm/day (102 mm/31 days).

Table 4-5: Monthly evaporation coefficients

	Oct	Nov	Dec	Jan	Feb	Mar	Apr	May	Jun	Jul	Aug	Sep
S-pan factor (%MAE)	8.76	12.2	14.4	14.7	12.4	10.9	6.76	3.9	3	3.52	3.9	5.73
Open water pan coefficient	0.81	0.82	0.83	0.84	0.88	0.88	0.88	0.87	0.85	0.83	0.81	0.81
Combined coefficient	0.07	0.10	0.12	0.12	0.11	0.10	0.06	0.03	0.03	0.03	0.03	0.05
Monthly Evaporation (mm/month)	102	148	179	183	161	141	88	50	38	43	47	68

The daily rainfall for catchment G22G is calculated by multiplying the daily streamflow volumes of the origin catchment (disaggregated stochastic sequences) with the RAIN-RUNOFF ratio (refer to section 4.5). The values pertaining to 1st October 1920 are substituted into Equation 3-7.

$$Rainfall_i = Streamflow_i \times RAIN_RUNOFF_i$$

$$\begin{aligned}
 Rainfall_i &= 0.006 \times 0.027 \\
 &= 0.00016 \text{ m/day}
 \end{aligned}$$

The net volume, lost to evaporation, is determined by multiplying the difference between evaporation and rainfall with the surface area (m^2) of the dam on a specific day. Refer to Appendix C.4.1 for the flow diagram outlining the process of determining net evaporation that occurs from the Idas Valley dams, with values corresponding to 1st October 1920 (stochastic sequence no. 3) starting with a full supply capacity.

4.7 Demand

The average monthly distributions of the annual demand in terms of the urban (domestic) users for the Stellenbosch Municipality are summarized in Table 4-6 (GLS, 2018).

Table 4-6: Monthly distribution of demand in percentage of annual demand

Monthly demand distribution												
Month	Oct	Nov	Dec	Jan	Feb	Mar	Apr	May	Jun	Jul	Aug	Sep
Percentage of Demand (%)	8.56	9.11	9.02	9.54	9.05	9.5	8.54	7.77	6.8	7.25	7.38	7.47

The annual demand averages at 8 000 Mℓ/a (AADD of 22 Mℓ/day). The drought demand can be reduced to 5 500 Mℓ/a (GLS, 2018). The historical annual water demand readings as well as the source contribution to meet the demand, as retrieved from GLS (2018) are presented in Figure 4-8. The resource allocation of 10 244 Mℓ/a (3 000 Mℓ/a from WCWSS and 7 224 Mℓ/a from Eerste River) is stipulated to be available as indicated in Figure 4-9.

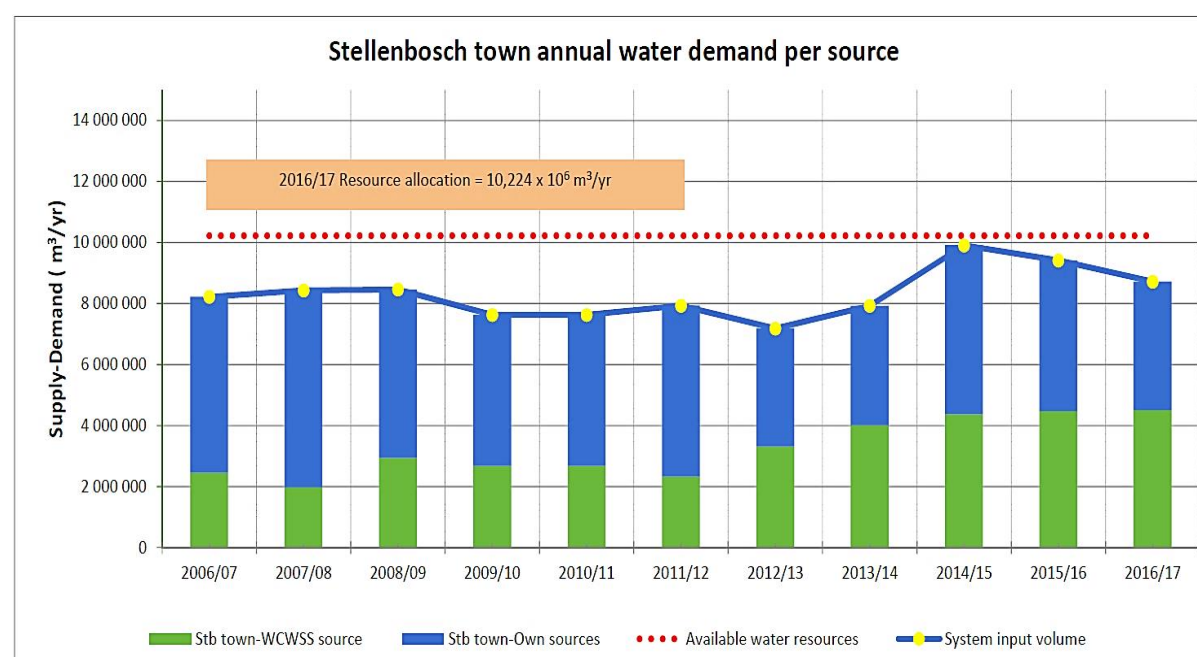


Figure 4-8: Stellenbosch annual water demand per source from 2006 to 2017 (GLS, 2018)

4.8 Groundwater Simulation

As part of the drought intervention plan for the Stellenbosch Municipality, a bulk water supply analysis and groundwater resource study was executed. The groundwater resource assessment included identifying existing boreholes that the municipality has access to, assessing the yields of those boreholes, as well as identifying new sites, in close proximity of the water distribution network, for potential borehole drilling towards abstraction. The central Stellenbosch study area is underlain by river terrace gravel and boulders (associated with alluvial deposits), as well as fractured underlying basement rocks of the Malmesbury Supergroup. The regional aquifer underlying the central area of Stellenbosch is categorized by the DWS (2009) as partly fractured, with yields ranging between 2.0 ℓ/s and 5 ℓ/s , but also partly intergranular and fractured, with yields ranging between 0.1 and 0.5 ℓ/s in some places. Figure 4-9 is the 3318 Cape Town geology map (scale: 1:250 000) adapted from the Council for Geoscience's geological map series, which indicates the geological structures of Stellenbosch, as well as the identified boreholes.

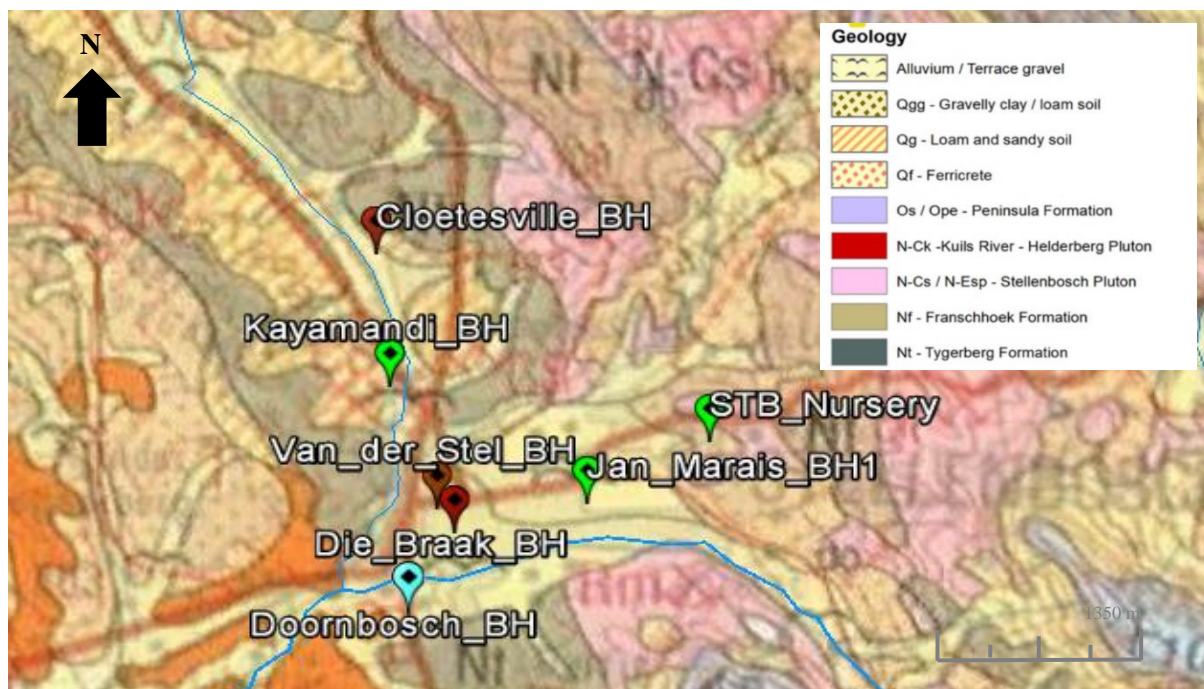


Figure 4-9: Geological map (3318 Cape Town) of Stellenbosch with boreholes (Google Earth)

The Stellenbosch municipality has access to 9 boreholes, namely Cloetesville, Kayamandi, Van der Stel, Die Braak, Municipal Nursery, Jan Marais, Doornbosch, Jamestown 1 and Jamestown 2 (GLS, 2018). Only 3 were identified as potential municipal supply augmentation boreholes. These include Cloetesville, Van der Stel and Die Braak, which are situated close to the water distribution network, where treatment with mobile water treatment units are achievable. The Jamestown 1, Jamestown 2 and Doornbosch boreholes are currently not in use, while the Kayamandi, Municipal Nursery and Jan Marais boreholes provide water for irrigation. Information pertaining to the different

existing boreholes, their yields, pumping rates, pumping durations, maximum water levels as well as rest water levels are summarized in Table 4-7 (GEOSS, 2018).

Table 4-7: Summary of functional municipal borehole data

Name	Pumping rate (ℓ/s)	Pumping duration per day (hours)	Diameter (mm)	Allowable drawdown (mbgl)	Rest Water Level (mbgl)	Storativity	Transmissivity (m^2/day)
Cloetesville	8.5	12	200	70	2.6	0.003	12.1
Die Braak	8.5	12	160	50	4.9	0.002	24.2
Van der Stel BH	12.0	16	180	70	4	0.003	20
Kayamandi	10.0	12	160	100	6.23	0.004	15
Jan Marais	1.0	12	168	25	3.2	0.001	2.3
Municipal Nursery	2.0	12	180	50	3	0.005	2.1

4.8.1 Quaternary Catchment Water Balance

The unconfined, alluvial and fractured aquifer system (bedrock) underlying Stellenbosch, is recharged by rainfall from two quaternary catchments; namely G22F and G22G. To determine the long-term sustainable abstraction rates for boreholes within the study area of Stellenbosch, a simulation of both catchments will have to be performed.

4.8.1.1 Data Retrieval

The hydrogeological characteristics of the two catchments contributing to the recharge of the aquifer underlying Stellenbosch, as retrieved from the GRA II database are summarized in Table 4-8.

Table 4-8: Hydrogeological data for quaternary catchments G22F and G22G

Quaternary catchment	%MAP (GRA II)	Avg WL (mbgl)	Specific Yield (S_y)	Adjusted Specific Yield (S_y)
G22F	11.21%	7.8	0.001	0.022
G22G	9.11%	7.9	0.0003	0.007

The specific yield is adjusted in such a way as to maintain the water level fluctuation within certain defined boundaries (minimum water level is the upper boundary and maximum allowable water level is the lower boundary). The rest water levels, as indicated in Table 4-7 becomes the minimum water

level (mbgl), while the shallowest drawdown is effectively the maximum allowable water level. The adjusted specific yield (Sy) gives a better indication of the geohydrology of the study area, as the specific yield value in the GRA II database only describes the average specific yield of an entire quaternary catchment, but not the specific part of the aquifer where the abstraction occurs. Quaternary catchments G22F and G22G consists of hard, less porous rock (mountains of igneous intrusions), hence the specific yield will be lower, while the municipal boreholes are situated in the more porous part of the catchment (alluvial valley and fractured base), thus, the specific yield ought to be higher, as suggested by Dennis (2019). Therefore, adjusting the specific yield to the water level depths obtained from municipal borehole yield tests, which results in a better representation of the water level fluctuation, the specific yield associated with the specific aquifer can be established. Simulations for both catchments are performed, with the water level fluctuating between 2.6 mbgl and 25 mbgl.

4.8.1.2 Stochastic Monthly Recharge

The first step in the process of determining stochastic monthly recharge of the aquifer underlying Stellenbosch is to convert the stochastic monthly streamflow sequences, previously generated by STOMSA, to stochastic monthly rainfall sequences, by applying the monthly RAIN-RUNOFF ratio. Thereafter the RAIN-RUNOFF ratio is applied to the recharge value (%MAP) obtained from the GRA II database. Quaternary catchment G22F was the catchment of origin upon generating stochastic streamflow sequences were through STOMSA. This RAIN-RUNOFF relationship had been determined during the process of streamflow disaggregation (section 4.4). To preserve the relationship between quaternary catchment G22F and G22G, a historical catchment MAP ratio (similar to the MAR ratio determined with Equation 3-5) is determined, to relate the stochastic rainfall of quaternary catchment G22G to the stochastic rainfall of quaternary catchment G22F. The historical catchment MAP ratio is determined with Equation 4-1 (based on adaptation of Equation 3-5):

$$\begin{aligned} \text{Catchment MAP ratio} &= \frac{\text{MAP}_{\text{Neighbour}}}{\text{MAP}_{\text{Origin}}} \\ &= \frac{\text{MAP}_{\text{G22G}}}{\text{MAP}_{\text{G22F}}} = \frac{754 \text{ mm}}{1465 \text{ mm}} = 0.51 \end{aligned} \quad (4-1)$$

The stochastic monthly recharge volume for quaternary catchment G22F can now be calculated by applying Equation 3-12, as the MAP ratio is established. The recharge volume for October 1920 is calculated by applying the RAIN_RUNOFF ratio to the historical streamflow of October 1920 and applying it to the quaternary catchment area of 66 km² (Table 4-1).

$$\text{Recharge}_{\text{Oct}} = \text{Streamflow}_{\text{Oct}} \times \text{RAIN_RUNOFF}_{\text{Oct}} \times \% \text{MAP} \times \text{Area}$$

$$\begin{aligned} \text{Recharge}_{\text{Oct}} &= 2.26 \text{ mil m}^3 \times 0.031 \frac{\text{m}}{\text{mil m}^3} \times 11.21\% \times 66\,000\,000 \text{ m}^2 \\ &= 510\,716 \text{ m}^3 \end{aligned}$$

Calculations are performed by using the values stored within the Excel sheets (up to 16 decimals). The monthly stochastic recharge for quaternary catchment G22G for October 1920 can be calculated by applying Equation 3-12 to the values pertaining to catchment G22G and multiplying the result by the ratio established in Equation 4-1. The recharge volume is determined as 272 881 m³. The recharge for every stochastic sequence of every month is calculated as demonstrated above. The recharge volume is the inflow component to the aquifer water balance.

4.8.1.3 Aquifer in Equilibrium

Each catchment is modelled as a single-celled, lumped parameter box model. To simulate the equilibrium state, the inflow to the aquifer (recharge) is equal to the outflow from the system (discharge). The recharge was calculated in the previous step as 510 716 m³ for October 1920. The average monthly discharge volume is calculated by applying Equation 3-13, while the water level per month is calculated by applying Equation 3-14. Values corresponding to the historical sequence are substituted into the respective equations for each quaternary catchment (Table 4-9). The total number of months within the historical sequence are 1080 (90 years times 12). The long-term average water level fluctuation is zero, therefore the adjustment factor is equal to 1. The historical sequence for the first 24 months of each quaternary catchment (October 1920 to September 1922), are presented in Appendix C.5.1 and C.5.2 respectively.

Table 4-9: Average monthly discharge and water level calculations for catchment G22F

Catchment	Evaluate Equation	Equation number
G22F	$Avg Q_b = adjF \times \sum Recharge_i / \sum i$	
Monthly	$Avg Q_b = 1 \times 975\,730\,320 / 1080$	(3-13)
Discharge	$= 903\,455 \text{ m}^3/\text{month}$	
G22F	$h_{i+1} = h_i - \frac{Recharge_i}{Sy \times Area} + \frac{Avg Q_b}{Sy \times Area}$	(3-14)
Water level	$h_{i+1} = 7.8 - \frac{510\,716}{0.022 \times 66\,000\,000} + \frac{903\,455}{0.022 \times 66\,000\,000}$ $= 8.07 \text{ mbgl}$	

The average monthly discharge and water level for catchment G22G is was also calculated in this way. The average monthly discharge for G22G amount to 482 801 m³/month and the water level is at 8.17 mbgl. The water level fluctuation for catchment G22F and G22G is illustrated in Figure 4-10 together with the respective monthly rainfall amounts. The rainfall for catchment G22F is on average double that of G22G and it would be expected that the water level fluctuation for catchment G22G should be

lower than that of G22F. However, due to the average water level of the aquifers starting in the same region (between 8.02 mbgl and 8.17 mbgl) and the specific yields almost being the same volume, together with the constant monthly rainfall relationship between the two catchments, the water levels fluctuate almost identically. Even as pumping occurs in the aquifer, it is expected that the water level fluctuation between the two catchments should not differ greatly.

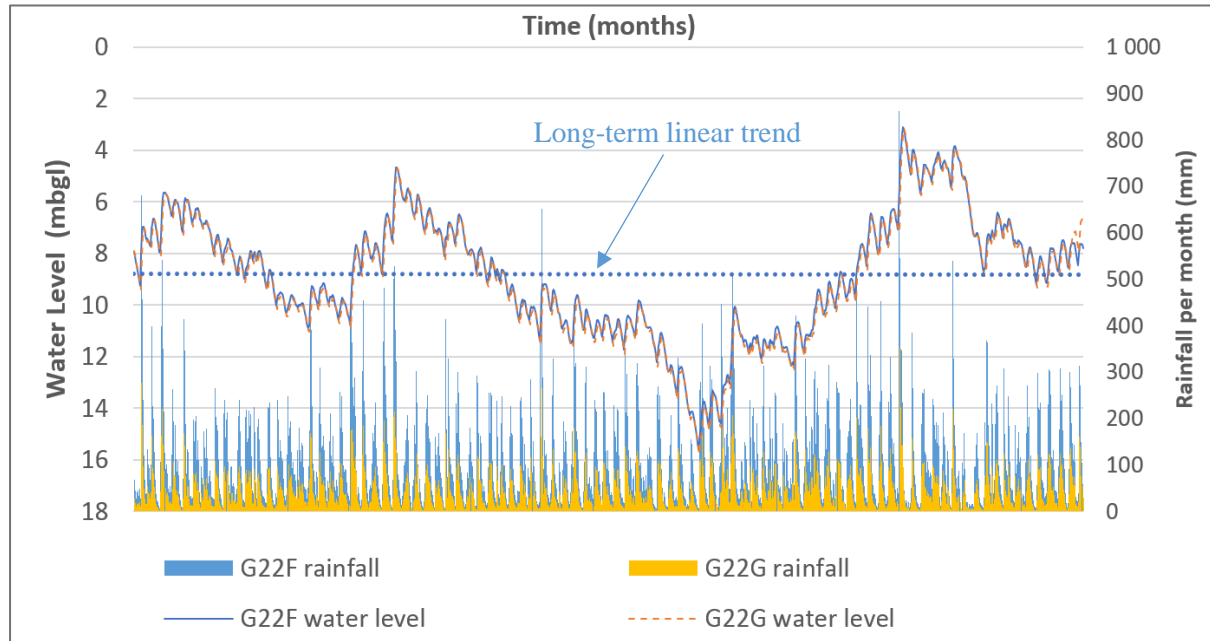


Figure 4-10: Water level response to recharge for catchment G22F and G22G

The groundwater contribution to baseflow is not a constant value, thus the Herold Baseflow Separation method is used to determine monthly contribution of groundwater to baseflow.

4.8.1.4 Baseflow Separation

To separate the groundwater contribution to total streamflow, from the surface water contribution to total streamflow, the Herold Baseflow Separation method is applied (section 3.6.1.4). Naturalized catchment streamflow is used as total streamflow. The catchment of origin is G22F, for which stochastic streamflow sequences were generated. The historical catchment MAR relationship (Equation 3-5) between G22F and G22G is used to maintain continuity between the stochastic streamflow of the 2 catchments.

$$\begin{aligned} \text{Catchment MAR ratio} &= \frac{\text{MAR}_{\text{Neighbour}}}{\text{MAR}_{\text{Origin}}} \\ &= \frac{\text{MAR}_{\text{G22G}}}{\text{MAR}_{\text{G22F}}} = \frac{14.92 \text{ mil m}^3}{36.58 \text{ mil m}^3} = 0.41 \end{aligned}$$

Baseflow separation is performed for each catchment. The first 24 months (October 1920 to September 1922) of the historical sequence for catchment G22F and G22G are attached in Appendix C.5.3 and C.5.4 respectively. A summary of the baseflow separation for catchment G22F is presented in

Table 4-10. Values from October 1920 of the historical sequence are used to evaluate the equations (section 3.6.1.4). The minimum flow volume (baseflow of a river) is defined with the parameter QGMAX, the first estimation of which is the average monthly streamflow. The groundwater contribution to streamflow is calculated with the first estimation of QGMAX (Table 4-10), after which the average monthly groundwater contribution (over the 90-year period) is set to equal the average discharge ($Avg Q_b$) determined in previous section by adjusting QGMAX. There after the process in Table 4-10 is followed again for the estimation of the values of the following month, and so the process continues until the baseflow separation for each month in the historical sequence is completed. The same procedure is followed for catchment G22G, however, the total streamflow (Q_i) is determined by multiplying the streamflow of catchment G22F with the catchment MAR ratio first. The monthly groundwater contribution to streamflow now becomes the refined discharge from the aquifer.

Table 4-10: Baseflow separation for catchment G22F

	Evaluate Equation	Equation Number
Total flow	$Q_i = QG_i + QS_i$ $Q_{Oct} = 2\,260\,000 \text{ m}^3/\text{month}$	(2-9)
Average monthly streamflow	The first estimation of the minimum baseflow (QGMAX) is the average monthly streamflow which is $3\,048\,481 \text{ m}^3/\text{month}$.	
Surface water contribution	<p>For the first month, GGMAX is equal to QGMAX, therefore the surface water contribution is calculated as follows:</p> $QS_i = 0$ (for $Q_i \leq \text{QGMAX}$) Initially $QS_i = 0$ (because $2\,260\,000 \leq 3\,048\,481$) But for other months $QS_i = Q_i - \text{GGMAX}_i$ (for $Q_i > \text{QGMAX}$)	(2-10)
GGMAX	<p>After having determined QS_i, the minimum groundwater contribution to baseflow is calculated for each month by setting DECAY to 0.5 and GROWTH to 5 respectively (section 3.6.1.4).</p> $\text{GGMAX}_i = \text{DECAY} \cdot \text{GGMAX}_{i-1} + (\text{GROWTH} \cdot QS_{i-1})/100$ $\text{GGMAX}_i = 0.5 \cdot 3\,048\,481 + (5 \cdot 0)/100$ $= 3\,048\,481 \text{ m}^3/\text{month}$	(2-11)
Groundwater contribution	The surface water contribution is known; therefore, the groundwater contribution is simply $QG_i = Q_i - QS_i$. For first estimation with $QS_i = 0$, the groundwater contribution is $2\,260\,000 \text{ m}^3/\text{month}$.	(2-10)

Adjustment of QGMAX	The average groundwater contribution to streamflow ($\sum QG_i / \sum i$) should be equal to the average monthly discharge ($Avg Q_b$) determined in previous section (section 4.8.1.3). To achieve this, the QGMAX factor is adjusted to 1 156 437 m ³ /month. And then the monthly calculations are performed again.	
---------------------	---	--

The hydrographs representing the total flow (surface water contribution and groundwater contribution) for catchment G22F (blue) and G22G (orange) is presented in Figure 4-10. The hydrographs of the two catchments follow the same trend; however, the flow volumes per month are of different magnitude because of the historical MAR ratio between them.

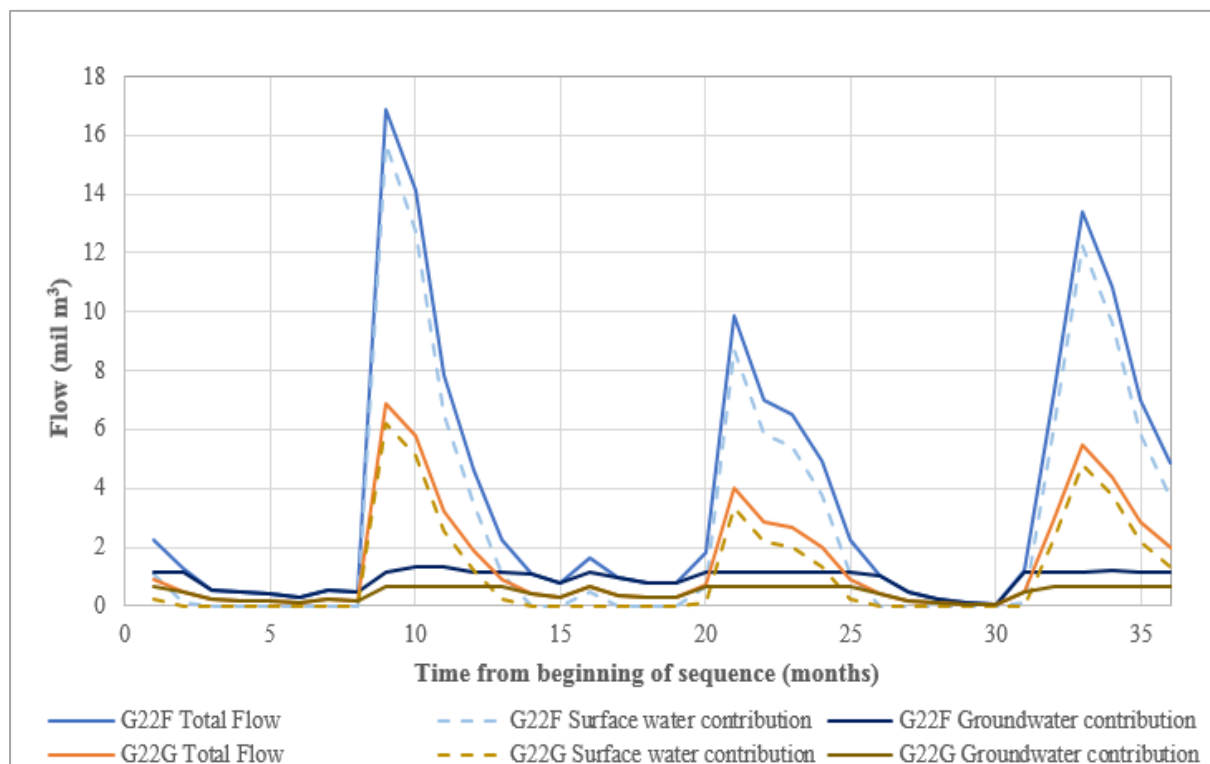


Figure 4-11: Hydrographs with surface water and groundwater contribution for G22F

4.8.1.5 Minimum Average Aquifer Water Level

The refined natural equilibrium consists of the monthly recharge values (inflow) and the monthly baseflow values (discharge). The long-term potential abstraction for each month is calculated by simulating a stressed aquifer through introducing pumping to the system and allowing for a new minimum average water level (5m from lowest natural water level). The stressed aquifer is simulated by increasing the groundwater contribution to baseflow by a factor such that the water level of the refined natural equilibrium is decreased by 5 m (where it is assumed that ecological degradation starts). The difference between the stressed system discharge and the refined natural system discharge is the long-term potential abstraction. Each quaternary catchment aquifer system is modelled separately. The first 24 months forming part of the calculation of the long-term abstraction of the historical sequence

(October 1920 to September 1922) for catchment G22F and G22G are attached in Appendix C.5.5 and C.5.6 respectively. The main equations and respective substitutions are presented in Table 4-11 for October 1920 of the historical sequence for catchment G22F. The maximum allowable is set to 25 mbgl (lowest simulated water level) plus the 5 m decrease in water level, therefore to 30 mbgl. The refined natural equilibrium is simulated by applying Equation 3-15 and the stressed aquifer system (lowest allowed water level of 30mbgl over the 1080-month period) is simulated by applying Equation 3-16. Thereafter the monthly abstraction volume is calculated by applying Equation 3-14.

Table 4-11: Long-term potential abstraction for October 1920 of historical sequence for G22F

Catchment	Evaluate Equation	Equation
	The refined natural equilibrium with monthly recharge and monthly discharge.	
G22F		
Natural Equilibrium	$h_{i+1} = h_i - \frac{Recharge_i}{Sy \times Area} + \frac{QG_i}{Sy \times Area}$ $h_{i+1} = 7.8 - \frac{510\,716}{0.02 \times 66\,000\,000} + \frac{1\,156\,437}{0.02 \times 66\,000\,000}$ $= 8.26 \text{ mbgl}$	(3-16)
	Increased discharge for 5-meter decrease in average minimum water level.	
G22F		
Minimum Water level	$h_{i+1} = h_i - \frac{Recharge_i}{Sy \times Area} + \frac{Avg Q_b}{Sy \times Area}$ $h_{i+1} = 7.8 - \frac{510\,716}{0.02 \times 66\,000\,000} + \frac{1\,182\,101}{0.02 \times 66\,000\,000}$ $= 8.26 \text{ mbgl}$	(3-14)
	Long-term sustainable abstraction.	
G22F	$Qab_i = (QG_i \times adjF) - QG_i$	(3-15)
Abstraction	$= (1\,156\,437 \times 1.02) - 1\,156\,437$ $= 25\,664 \text{ m}^3/\text{month}$	

The process followed in Table 4-11 is applied to every month for every sequence (101 and historical). The monthly abstraction volumes are stored in a separate spreadsheet which becomes part of the input to the final conjunctive use model. Figure 4-11 presents the aquifer water level fluctuations for the aquifer in natural equilibrium and the stressed aquifer system.

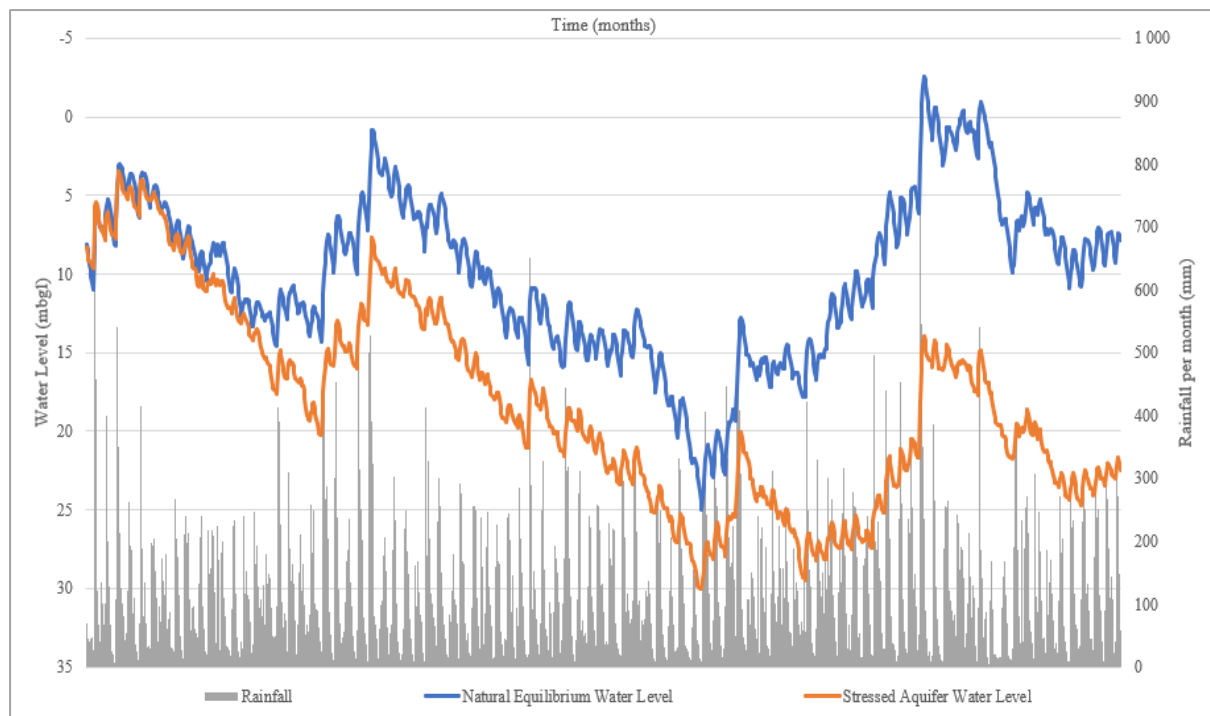


Figure 4-12: Stressed aquifer system with minimum water level for G22F

The long-term potential monthly abstraction for the first 24 months is presented in Figure 4-13. There is not a constant relationship between the potential abstraction from catchment G22F and G22G, even though for some months it seems like there is a constant relationship.

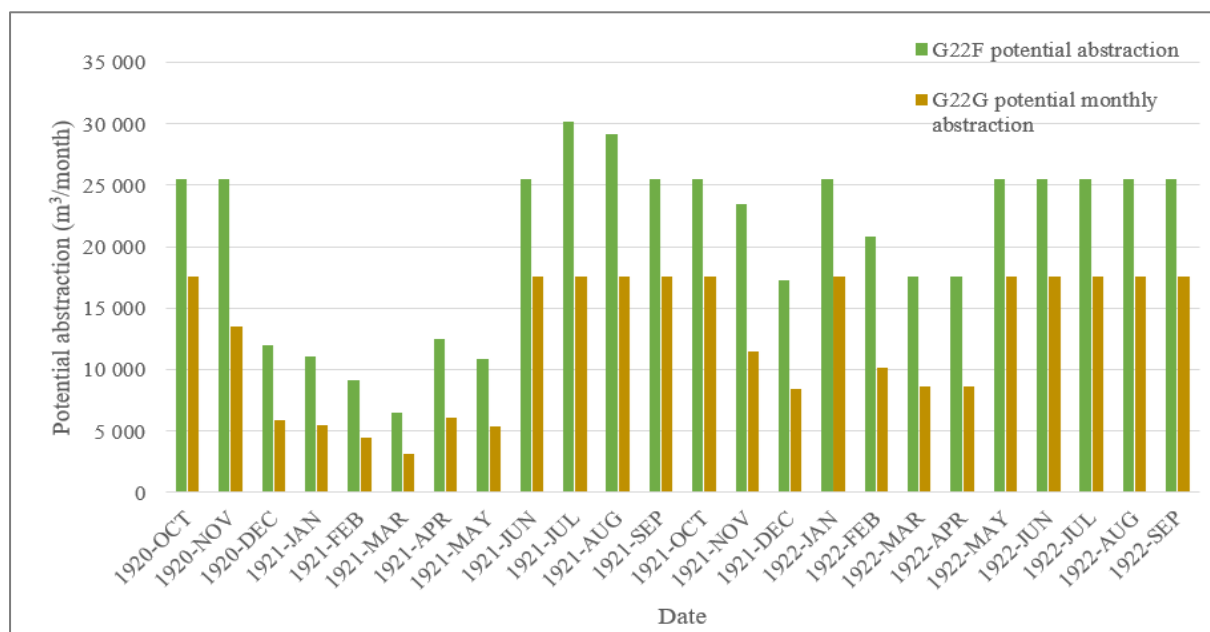


Figure 4-13: Long-term potential abstraction from G22F and G22G

The total long-term potential abstraction from the study area is the sum of each catchment's contribution towards the study area. Using Google Earth, the contributing area of G22F is estimated at 15 km² and the contributing area of G22G is estimated to 20 km². Therefore, the long-term potential abstraction

available from the study area is determined as follows with Equation 4-2. The long-term potential abstraction for the study area for October 1920 of the historical sequence is given as follows:

$$Qab_i \text{ of Study Area} = Qab_i \text{ of G22F} \times \frac{G22F_{study\ area}}{G22F_{total\ area}} + Qab_i \text{ of G22G} \times \frac{G22G_{study\ area}}{G22G_{total\ area}} \quad (4-2)$$

$$\begin{aligned} Qab_i \text{ of Study Area} &= 25\ 664 \times \frac{15}{66} + 16\ 254 \times \frac{20}{106} \\ &= 8\ 887 \text{ m}^3/\text{month} \end{aligned}$$

4.8.2 Borehole Interference

The boreholes accessed by Stellenbosch Municipality, extend a depth within the fractured bedrock; however, the top layer is alluvial deposits and therefore the Cooper-Jacob equation can be applied to monitor abstraction rates to prevent over abstraction. It is assumed that the alluvial (coarse grained rock layer) portrays laminar flow and infinite areal extent while pumping. To calculate the extent of interference between the boreholes, the radius of influence of each borehole has to be determined, as well as the distance between the boreholes. The abstraction rates obtained from the borehole yield tests completed for the existing boreholes within the Stellenbosch are (Table 4-7), are used to calculate the radius of influence and the drawdown of each borehole. The 6 operational boreholes that the municipality has access to were used in this analysis.

The radius of influence of the Van der Stel borehole is calculated by substituting the variables with corresponding values from Table 4-7 into Equation 2-17.

$$r = 1.5 \times \sqrt{\frac{T \times t}{S}}$$

$$r = 1.5 \times \sqrt{\frac{20 \times (365 \times \frac{16}{24})}{0.007}} = 1\ 250 \text{ m}$$

The drawdown at the Van der Stel borehole is calculated by substituting variables with corresponding values (from Table 4-7) into Equation 2-16. The assumption is that the pumping rate, storativity and transmissivity, as well as borehole radius provided by the municipality (GEOSS, 2018) are correct and can be evaluated over a one-year period (with no recharge taking place).

$$s = \frac{2.3Q}{4\pi T} \log\left(\frac{2.25Tt}{r^2 S}\right)$$

$$s = \frac{2.3(12 \times 86.4)}{4\pi(20)} \log\left(\frac{2.25(20)(365 \times \frac{16}{24})}{0.18^2(0.007)}\right) = 72.9 \text{ mbgl}$$

Important to note is that the Van der Stel borehole has an allowable drawdown of 70 mbgl (where the pump is positioned). At the current rates the borehole will fail within a year of commencing pumping (without recharge), as the calculated drawdown exceeds the allowable drawdown. The drawdown value

is sensitive to the specific yield. If a larger specific yield was to be used, the drawdown would decrease considerably. The drawdown at Die Braak borehole is calculated in the same way and results in a 46.3 mbgl drawdown.

The cumulative drawdown and distance between the boreholes are calculated so that the extent of the influence of the boreholes on one another can be assessed. If the distance between two boreholes is less than the radius of influence, there will be interference. The distance between Van der Stel and Die Braak boreholes is 335 m, while the radius of influence of the Van der Stel borehole is 1 250 m, therefore there will be interference between the two boreholes. The cumulative drawdown at a borehole, is its own drawdown, added to the drawdown occurring at the distance between the two boreholes in question. The drawdown caused at Die Braak borehole, due to the influence of the Van der Stel borehole, is calculated by applying Equation 2-16 as follows:

$$s = \frac{2.3Q}{4\pi T} \log \left(\frac{2.25Tt}{r^2 S} \right)$$

$$s = \frac{2.3(12 \times 86.4)}{4\pi(20)} \log \left(\frac{2.25(20)(365 \times \frac{16}{24})}{335^2(0.007)} \right) = 10.9 \text{ m}$$

Thus, the cumulative drawdown at Die Braak borehole is the sum of its own drawdown (46.3 mbgl) plus the drawdown caused by the Van der Stel Borehole (10.9 m), resulting in a cumulative drawdown of 57.2 mbgl. The allowable drawdown at Die Braak borehole is 50 mbgl (Table 4-7), depth where the oumo is positioned. Therefore, the borehole will fail as result of the abstraction from the Van der Stel borehole.

The boreholes that fail due to interference are: Die Braak, Van der Stel, and Kayamandi. The Stellenbosch municipality should adjust the pumping rates of the boreholes which will fail to supply water as result of the interference caused by the other boreholes in the wellfield. The user can run the analysis again with reduced pumping rates and/or pumping durations so that no interference between the respective boreholes takes place, so that they can be sustainably utilized.

The borehole positions, names and radii of influence are depicted in Figure 4-12. The larger radii of influence are the ones associated with smaller specific yield values, while the smaller radii of influence are associated with larger specific yield values.

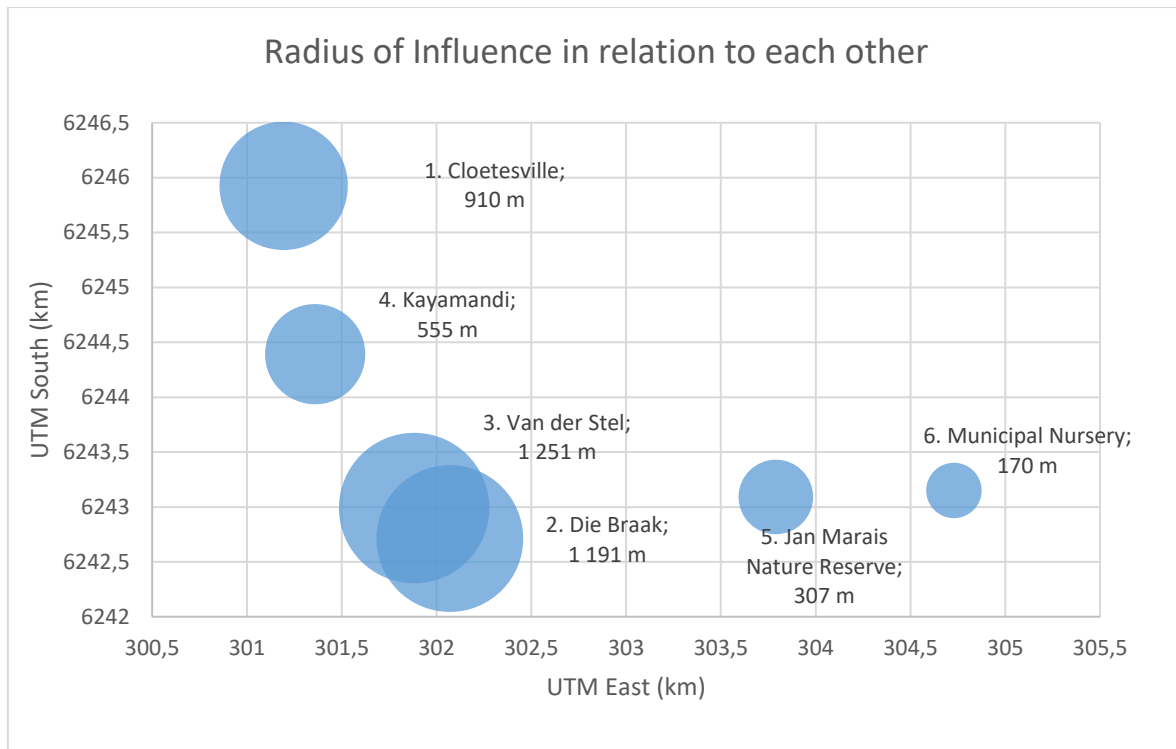


Figure 4-14: Borehole positions, names and radii of influence

4.9 Conjunctive Use System Simulation

The conjunctive use supply system for Stellenbosch consists of: surface water from the Eerste River (Idas Valley WTW), inter-basin transfer from the WCWSS (Paradyskloof WTW), as well as groundwater from the alluvial and fractured rock aquifer underlying the central Stellenbosch region. There are no desalination or water reclamation plants contributing to the water supply system. To assess the yield of the conjunctive use system, operational rules pertaining to each component are devised. The operational rules are established for a conjunctive use system and not an augmentation system. The operational rules applicable in this case, require that the demand be primarily satisfied by the inter-basin transfer of the WCWSS and the groundwater resources, before the surface water from the Eerste River and Idas Valley Dams is utilized. The operational rules pertaining to the way in which each resource is utilized, in the long-term and short-term yield analysis, are discussed in the following sections.

4.9.1 Groundwater Yield

The operational rules applied to the long-term analysis require that only the long-term potential groundwater abstraction volume is made available for the yield. The long-term potential abstraction volume was determined by the quaternary catchment aquifer water balance, as discussed in section 4.8.1. For the short-term analysis, the actual abstraction volume used by the Stellenbosch municipality, as determined during borehole yield tests is available for the yield.

4.9.1.1 Long-Term Operational Rules

The long-term potential average groundwater abstraction rate, pertaining to the historical streamflow sequence of the Stellenbosch area, was determined at 222 m³/day (81 Mℓ/a). The abstraction rate for December 1920, which is the third month in the historical streamflow sequence, was determined at 123 m³/day. Furthermore, it is assumed that the pumps installed at the municipal boreholes, pump water out of the aquifer at a constant rate and cannot be set at variable rates. In practice a borehole within the aquifer system underlying the central area of Stellenbosch, might still subsequently yield water, even if the actual abstraction is larger than the potential abstraction rate for a specific month, for example, the potential abstraction rate for October 1920 is 222 m³/day (81 Mℓ/a), while the actual abstraction rate was 260 m³/day. Therefore, the following operational rules apply to determine the yield of groundwater sources during a long-term analysis:

- If the desired combined pumping rate of the boreholes, is less (i.e. 200 m³/day) than the long-term potential average of 222 m³/day, the required abstraction rate, for each month, towards satisfying the demand, will be attained, even if the groundwater available in a specific month is less than the calculated average. The abovementioned scenario is illustrated in Figure 4-15.
- If the desired combined pumping rate of the boreholes is more (i.e. 260 m³/day) than the long-term potential average (222 m³/day), the required abstraction rate, for each month, towards satisfying the demand, will only be attained in the months when more groundwater is potentially available as a result of recharge. In months during which the combined desired pumping rate is more than the calculated long-term potential average abstraction, no water will be available for the yield (failure will occur). This scenario is illustrated in Figure 4-16.

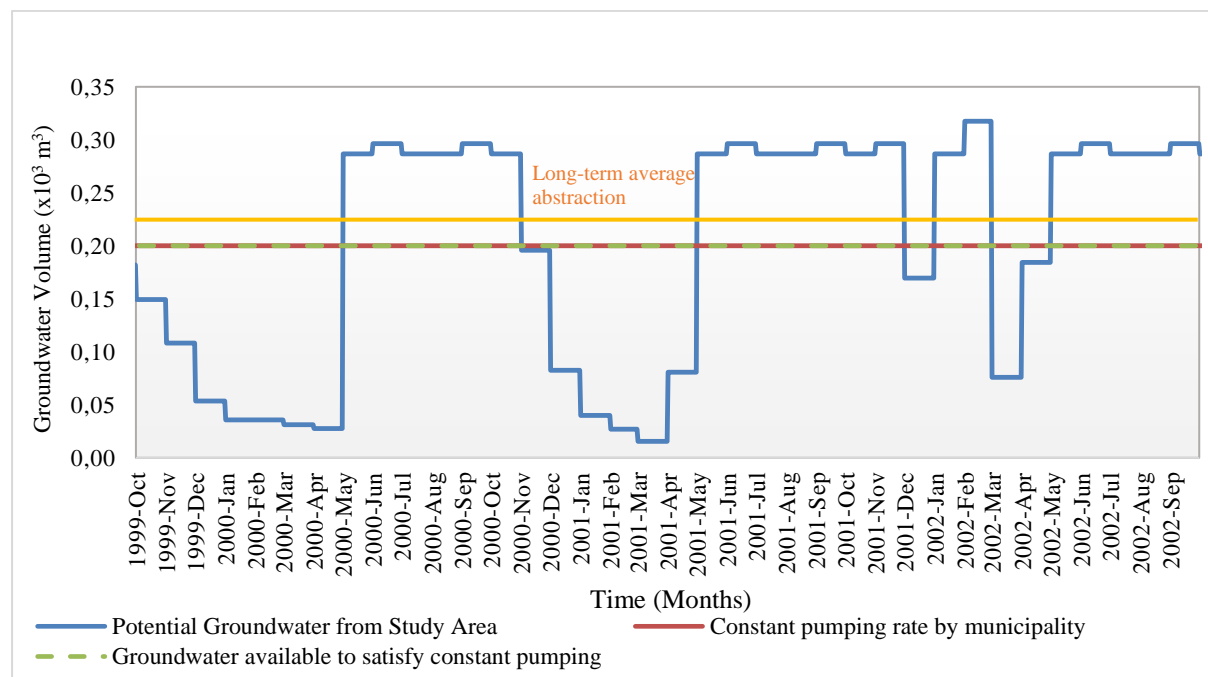


Figure 4-15: Combined pumping rate less than average long-term potential abstraction rate

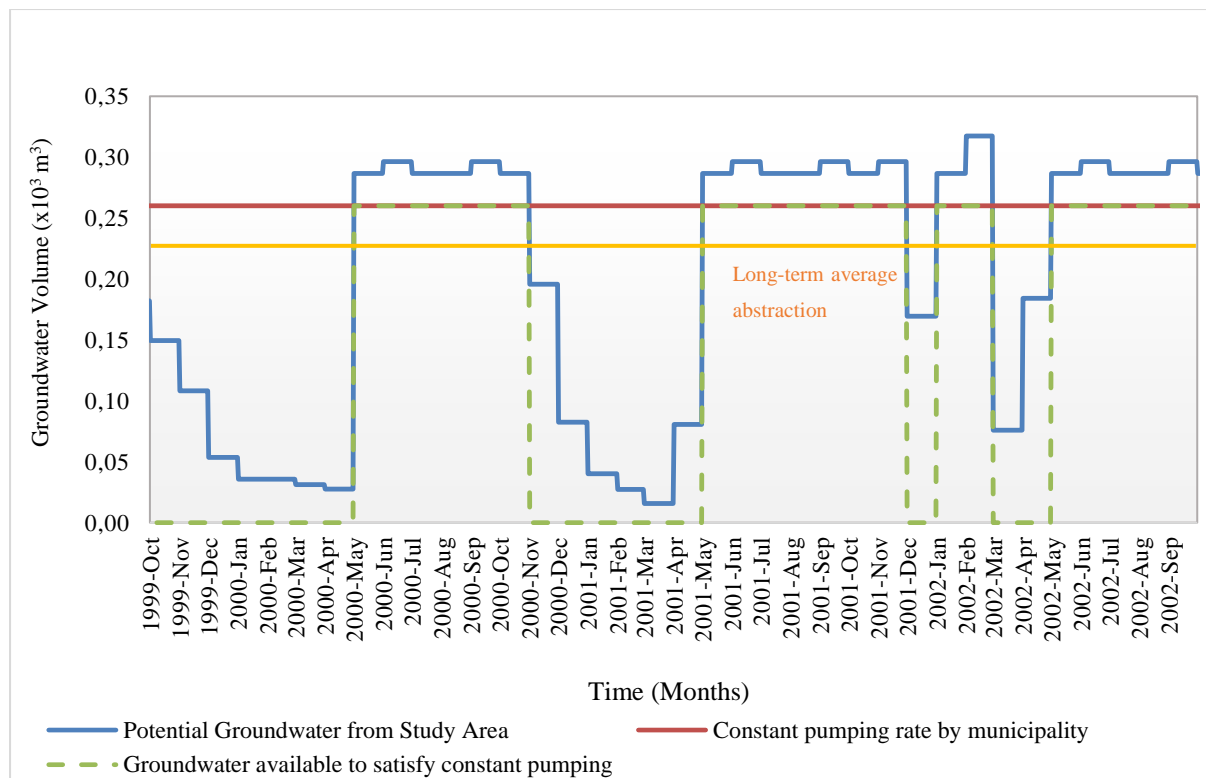


Figure 4-16: Combined pumping rate larger than average long-term potential abstraction rate

4.9.1.2 Short-Term Analysis

For the short-term analysis, the combined yield of the boreholes in the aquifer underlying the central area of Stellenbosch is determined by the borehole yield pumping tests. The results of the pumping tests indicate the amount of water that is available towards satisfying the demand, regardless of the calculated long-term potential average abstraction available for a specific sequence. The Cloeteville, Die Braak and Van der Stel boreholes were developed and tested for potential contribution to the municipal supply. Their combined pumping rate is 29 ℓ/s (2 506 m^3/day). The short-term management period for Stellenbosch is 2 years. Over this 2-year period, it is assumed that 2 506 m^3/day will be available for the yield, and that the respective boreholes will not fail.

4.9.2 Inter-Basin Transfer from WCWSS

The inter-basin transfer from the WCWSS is assumed to be a constant surface water supply as dictated by its allocation (3 000 $M\ell/a$). The allocation is associated with a 98% assurance of supply. For the long-term analysis, the total amount of water supplied by the allocation is assumed to be available for the yield. For the short-term analysis, the percentage of the allocation delivered over the 2-year period can be altered to investigate different scenarios. If the amount of water supplied by the WCWSS is only 50% of the allocation, only 1 500 $M\ell/a$ is available over the 2-year period.

4.9.3 Surface Water

Groundwater sources and the inter-basin transfer scheme by the WCWSS are primarily utilized to satisfy the municipal demand, before the surface water from the Eerste River (Idas Valley WTW) and Idas Valley Dams are utilized. For the long-term analysis, the capacity of the Idas Valley Dams is set at 100% at the commencement of the simulation, however; for the short-term analysis, the starting capacity of the Idas Valley Dams can be set at the actual capacity at the beginning of the 2-year analysis period. For the short-term analysis, conducted towards planning and then managing resources for the next two years, storage capacity at commencement of the analysis can be set to 85%.

4.10 Yield Analysis and Discussion

The conjunctive use model developed in Microsoft Excel (2016) is used to perform a historical yield analysis, as well as a long-term and short-term stochastic yield analysis on the water resources of Stellenbosch. To gain an overview of the functionality of the developed conjunctive use model as well as gauge the supply capability of the Stellenbosch system, different scenarios are used to evaluate the yield capability for different physical constraints. This is undertaken to compare the capability of the current water supply system to that of a system using more available water sources in a conjunctive manner under different conditions. To gain an overview of the functionality of the model, as well as evaluate the supply capability of the current Stellenbosch system, different scenarios are simulated, under which the yields of the different water resources are assessed under different physical circumstances and constraints. A sensitivity analysis on the historical firm yield is also performed by considering these different scenarios.

4.10.1 Historical Firm Yield

The Stellenbosch municipality only introduced groundwater as an augmentation measure to supplement surface water in 2017, due to persisting drought conditions, therefore; the base scenario for evaluating the historical firm yield only takes surface water resources into consideration, as this is the typical set-up of the water supply system. The base scenario is simulated with input data obtained from the WR2012 database, namely the naturalized historical streamflow. The base scenario is presented in Table 4-12, and the dam capacity is set at 100% upon commencement of the simulation (Basson et al, 1994). The capacity-time graph for the Idas Valley dams, for the base scenario, is used to identify the critical period. A draft-yield curve is also generated for the base scenario to establish the firm yield point, which indicates the supply capability of the system to satisfy a given target draft. The historical yield for the base scenario is determined as 7 561 Mℓ/a (section 1.1.1.2). A sensitivity analysis is performed on the historical firm yield (firm yield of the historical streamflow sequence) by simulating 5 different scenarios based on different physical circumstances or constraints, discussed in greater detail in section 4.10.3.

Table 4-12: Input values of the historical yield analysis for the base scenario

Idas Valley dams combined capacity	2 380 Mℓ
Dead storage capacity of Idas Valley dams	0 %
MAR of Stream 1 (from Eerste River into Idas Valley dams)	22 300 Mℓ/a (22.3 mil m ³ /a)
Pipeline Capacity (abstraction capacity from Eerste River into Idas Valley dams)	470 ℓ/s (14.8 Mℓ/a)
MAR of Stream 2 (runoff from contributing catchment into Idas Valley dams)	29 Mℓ/a
Allocation from the WCWSS	3 000 Mℓ/a

4.10.1.1 Capacity-Time Graph

The capacity-time graph for the historical inflow sequence, during simulation of the base scenario (presented in Appendix C.6.1). The capacity-time graph is generated by plotting daily dam capacities for a target draft equal to the historical firm yield of 7 561 Mℓ/a for the period spanning from the 1st of October 1920 to the 30th of September 2010 (entire historical streamflow sequence), to assess the amount of daily dam failures that might occur. The capacity-time graph for the period between the 1st of October 1990 and the 30th of September 2002 is presented in Figure 4-17, to identify the critical period with ease. The first failure (day) of the existing water supply system (only surface water in use), would occur on the 25th of May 2000 when the dam level would fall to 0% of the full storage capacity. Therefore, the critical period spans the 7 months between the 16th of October 1999 (last full dam level before failure), and the 25th of May 2000 (failure before the dam starts to recover).

The failure occurs as a result of the lowest streamflow volumes recorded between August 1999 and April 2000 (Figure 4-17). To compare the 9-month flow over a total yearly flow, the period with which the 9-month flow is compared is from August to July (12-month period starting in August, not October). The streamflow volume recorded during this 9-month period (August 1999 to July 2000) comprised only 29.6% of the total streamflow contribution of the total streamflow contribution from August 1999 to July 2000. The average streamflow contribution from August to April over the total streamflow contribution from August to July (12-month) for the naturalized historical streamflow sequence is 57%, almost double what was experienced during the low flow period that resulted in the failure. A second failure would have occurred on 25th of May 1994, if the target draft were further increased (Figure 4-17).

It can be deducted from the time-capacity graph, that in the years when the inflow stream from the Eerste river increased from April onwards, the Idas Valley dams were able to recover, however; with

late rainfall (end of May) the Idas Valley dams have the potential to fail. Additionally, if the low flow period started in August or September, the Idas Valley dams are more likely to fail.

The highest overflow volume during the simulation of the base scenario, namely 42 Mℓ/day occurred on the 30th of September 2010. If the overflow were to be utilized for artificial aquifer recharge, 42 Mℓ would be the maximum daily volume which could be used as artificial recharge. Furthermore, the average overflow over the record length (October 1920 to September 2010) is 9 Mℓ/day, which if utilized, could form part of a secondary yield. However, no artificial aquifer recharge schemes have been implemented in Stellenbosch and no downstream storage facilities are available, therefore the overflow volume spills into the tributary of the Kromme River.

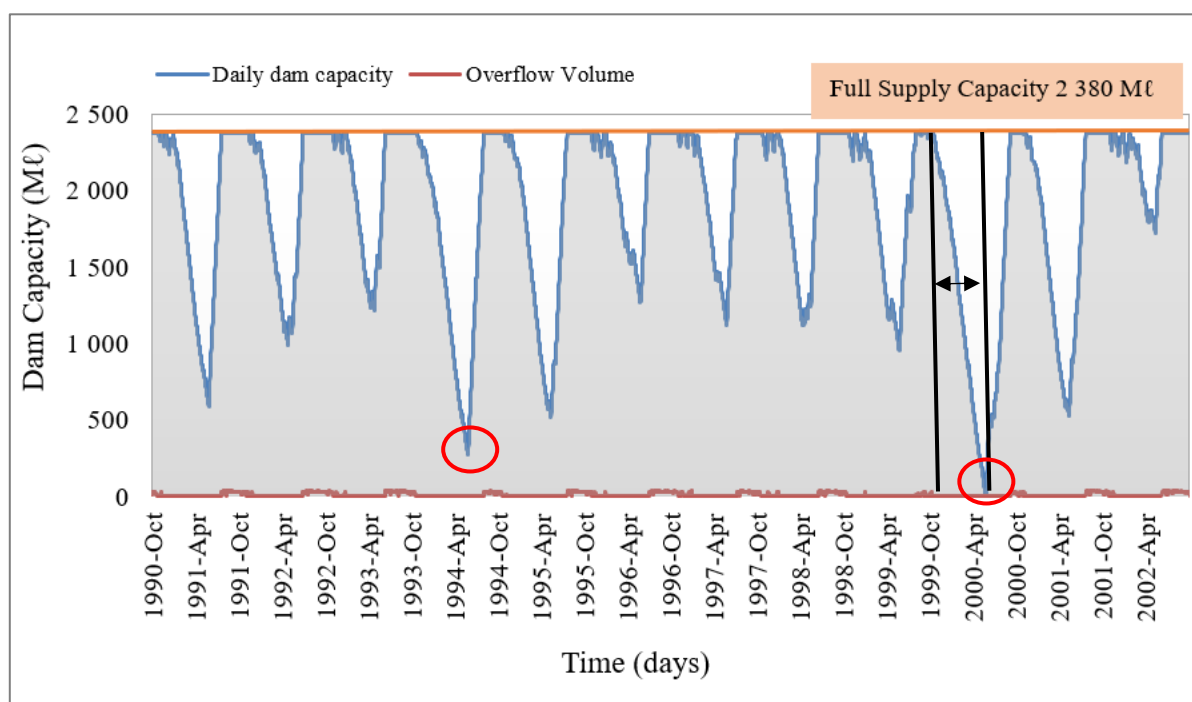


Figure 4-17: Daily Idas Valley dams' time-capacity graph with critical period for base scenario

4.10.1.2 Draft-Yield Curve

The historical firm yield for the base scenario (Table 4-12) is determined as 7 561 Mℓ/a. The historical firm yield, depicted in Figure 4-18, indicates that a target draft of 7 561 Mℓ/a can be provided, without a single daily dam failure, when simulating the historical streamflow sequence for the base scenario. If two years in the sequence are allowed to fail over the span of the historical record (90 years), the target draft that can be supplied is 8 382 Mℓ/a with an annual risk of failure of 2% (1:50 year recurrence interval).

The relationship between the target draft and the associated yield for the base scenario is depicted in Figure 4-18. After reaching the maximum amount of base yield, which is the historical firm yield point, the base yield displays a gradual decline, asymptotically approaching the minimum flow rate over a 12-month period. For the base scenario, the asymptote of the historical streamflow sequence is 6 660 Mℓ/a,

which suggests that the 3 000 Mℓ/a allocation by the WCWSS and the 3 600 Mℓ/a from the Idas Valley resources (dams and Eerste River inflow) are the minimum inflow rates for a 12-month period.

The non-firm yield indicates the yield range in which the target draft can still be satisfied frequently, but not continuously. The average yield is close to the target draft until it breaks away at around 9 400 Mℓ/a, which suggests that up to 9 400 Mℓ/a can be supplied frequently, in periods where no low flow periods are experienced. At a target draft of 9 400 Mℓ/a, 28 years fail out of the 90-year historical inflow sequence evaluated, indicating a risk of failure of 31% (1:3 year recurrence interval).

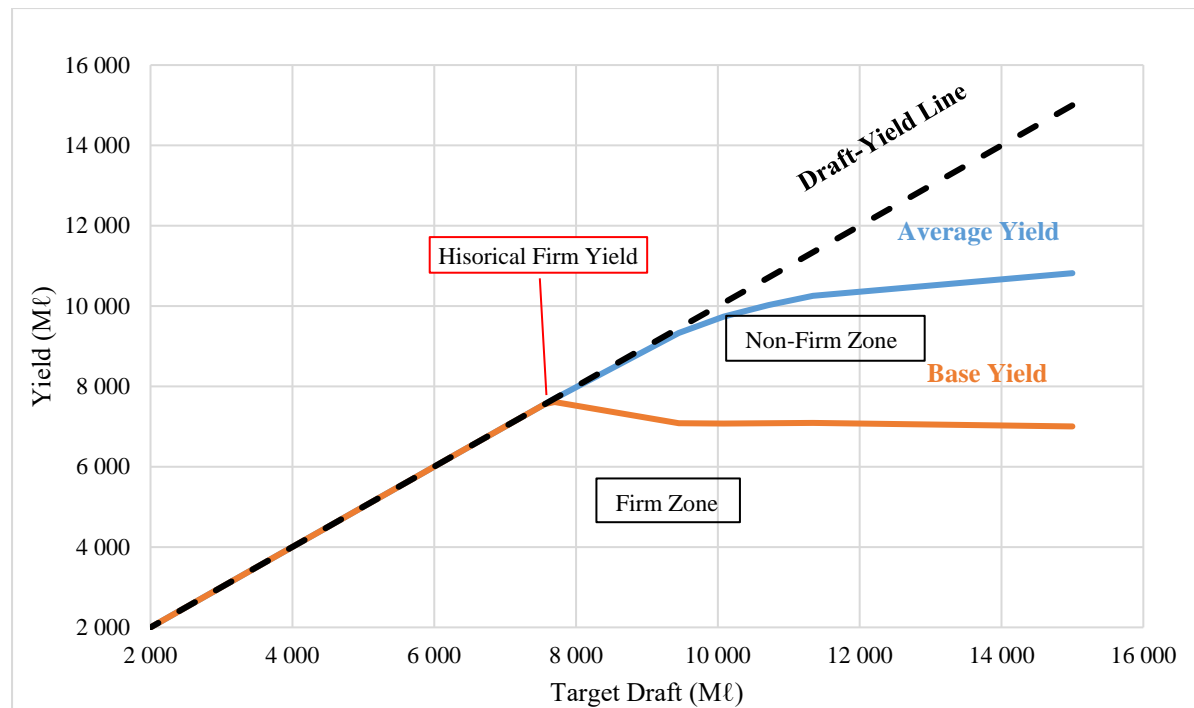


Figure 4-18: Base scenario Draft-Yield curve with firm yield point for historical sequence

4.10.1.3 Sensitivity Analysis

The sensitivity analysis performed on the historical firm yield investigates the impact of variance in different components on the capability of the water supply system to satisfy the target draft. For the sensitivity analysis on the historical firm yield the results of the following 5 scenarios are analysed in addition, and in comparison, to the base scenario discussed in section 4.10.1.2. These scenarios comprise the following:

Scenario 1- Addition of groundwater abstraction to current surface water sources. The combined pumping rate of the boreholes is set to the daily groundwater abstraction rate, as per the long-term potential average available abstraction of 81 Mℓ/a, previously determined as 222 m³/day (section 4.9.1.1).

Scenario 2 - Increase of 25% in storage capacity of the Idas Valley dams (increase from 2 380 Mℓ to 2 980 Mℓ).

Scenario 3 - Increase of 25% in allocation from the WCWSS (increase from 3 000 Mℓ/a to 3 750 Mℓ/a).

Scenario 4 - Varying the capacity of the current pipe facilitating abstraction of water from the Eerste River to the Idas Valley WTP between 80%, 100% and 120%.

Scenario 5 - Varying the streamflow diversion efficiency at 60%, 80% and 100% of the streamflow volume (runoff) from the Eerste River.

The historical firm yield values for the base scenario, as well as scenario 1, 2, and 3 are summarized in Table 4-13. The historical firm yield curves for scenario 1, 2 and 3 are presented in Appendix C.6.2, Appendix C.6.3 and Appendix C.6.4, respectively. The respective draft-yield curves are similar to that of the base scenario (Figure 4-18).

Table 4-13: Sensitivity analysis results for Scenario 1, 2 and 3

Scenario	Water Sources (Components)	Input values	Firm yield	Percentage increase from base scenario
Base Scenario	Groundwater abstraction	0 Mℓ/a		
	Interbasin-transfer allocation	3 000 Mℓ/a	7 561 Mℓ/a	NA
	Idas Valley dams	2 380 Mℓ		
	Groundwater abstraction	82 Mℓ/a		
Scenario 1	Interbasin-transfer allocation	3 000 Mℓ/a	7 638 Mℓ/a	1 %
	Idas Valley dams	2 380 Mℓ		
	Groundwater abstraction	0 Mℓ/a		
	Interbasin-transfer allocation	3 000 Mℓ/a	8 172 Mℓ/a	8 %
Scenario 2	Idas Valley dams	2 975 Mℓ		
	Groundwater abstraction	0 Mℓ/a		
	Interbasin-transfer allocation	3 750 Mℓ/a	8 261 Mℓ/a	9 %
	Idas Valley dams	2 380 Mℓ		

The results of the analysis of scenarios 1, 2 and 3, demonstrates that the largest impact on the historical firm yield occurs when the allocation from the WCWSS is increased by 25%. The WCWSS allocation is modelled as a constant inflow, thus; it is expected to make the most reliable contribution to the firm yield. The 25% increase in the WCWSS allocation results in an increase of 9 % in the firm yield when compared to the base scenario. In scenario 2 the storage capacity of the Idas Valley dams is increased by 25%, resulting in an increase of 8 % in the firm yield when compared to the base scenario.

Scenarios 4 and 5 were combined to analyse different combinations of the structural capacity and diversion efficiency in terms of the firm yield. The combinations were selected according to the matrix in Table 4-14 and the firm yields for each combination were determined. The calculated firm yield values for the different combinations are summarized in the sensitivity matrix Table 4-14.

Table 4-14: Sensitivity matrix of the historical firm yield for the base scenario

Structural Capacity → Diversion Efficiency ↓	80 %	100 %	120 %
60 %	6 664 Mℓ/a	6 864 Mℓ/a	7 016 Mℓ/a
80 %	7 119 Mℓ/a	7 306 Mℓ/a	7 308 Mℓ/a
100 %	7 500 Mℓ/a	7 561 Mℓ/a	7 574 Mℓ/a

The structural capacity of the pipeline transporting water from the Eerste River to the Idas Valley dams is 470 ℓ/s. If the pipe capacity was to be increased to 120 % (564 ℓ/s) of its actual capacity, assuming that the streamflow diversion is 100% efficient, the firm yield would increase by 0.2 %. If the pipe capacity was to be decreased to 80% (376 ℓ/s) of its actual capacity, due to a potential blockage, the firm yield would decrease by 0.8%. These marginal increases to the historical firm yield, illustrated by the green line in Figure 4-19, could occur as a result of the pipe capacity already being the optimum size. In other words, the pipe capacity is large enough to cater for peak daily flows. In Figure 4-19 it is also indicated that for a diversion efficiency of 60%, the pipe capacity has a greater effect on the firm yield, with a firm yield increase of 2.2% at a capacity of 120%.

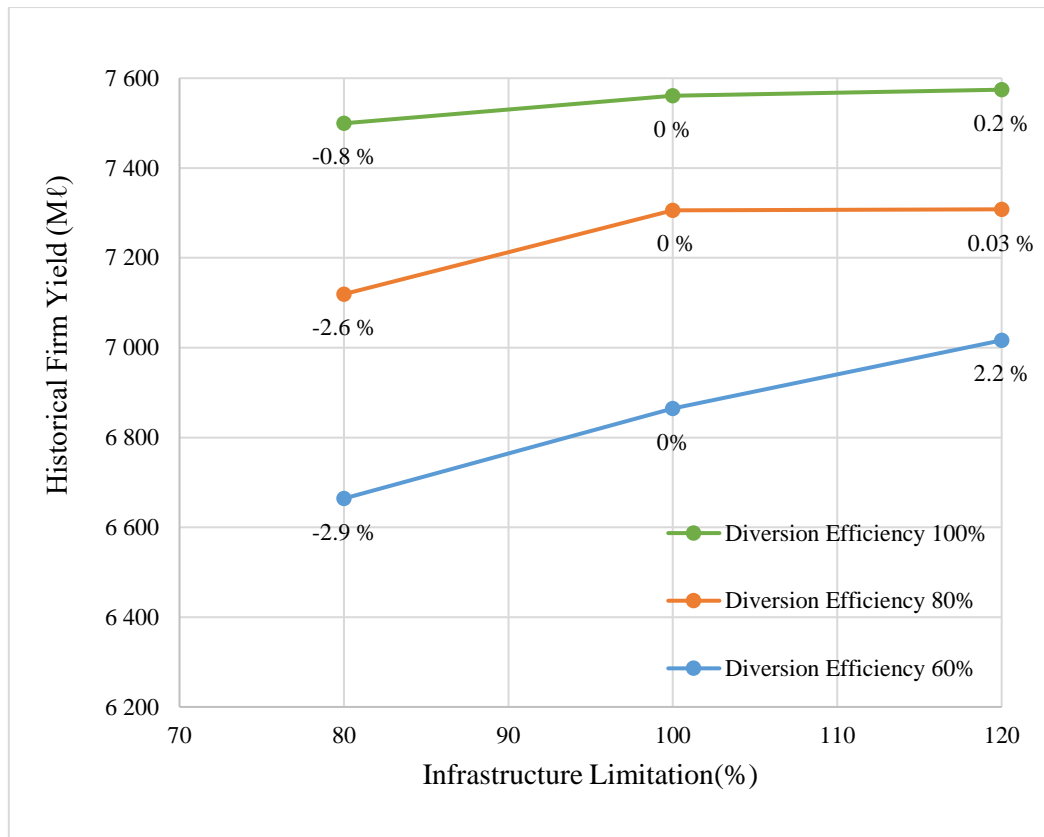


Figure 4-19: Percentage increases and decreases in the yield at 100% structural capacity

Diversion efficiency refers to the level of effectiveness in diverting the streamflow (Section 2.2.2). If the pipe capacity is at 100% (470 l/s) and the streamflow diversion was 60% efficient, the historical firm yield would decrease by 9.2%. The firm yield seems to be significantly impacted when the diversion efficiency of 60% is coupled with a smaller structural capacity (80%), resulting in the historical firm yield being reduced by 11.1 %. It is evident that the historical firm yield values are more sensitive to diversion efficiency than the structural capacities, as indicated in Figure 4-20. The diversion weir in the Eerste River should be cleared of material and debris on a regular basis to avert obstruction of diverted flow.

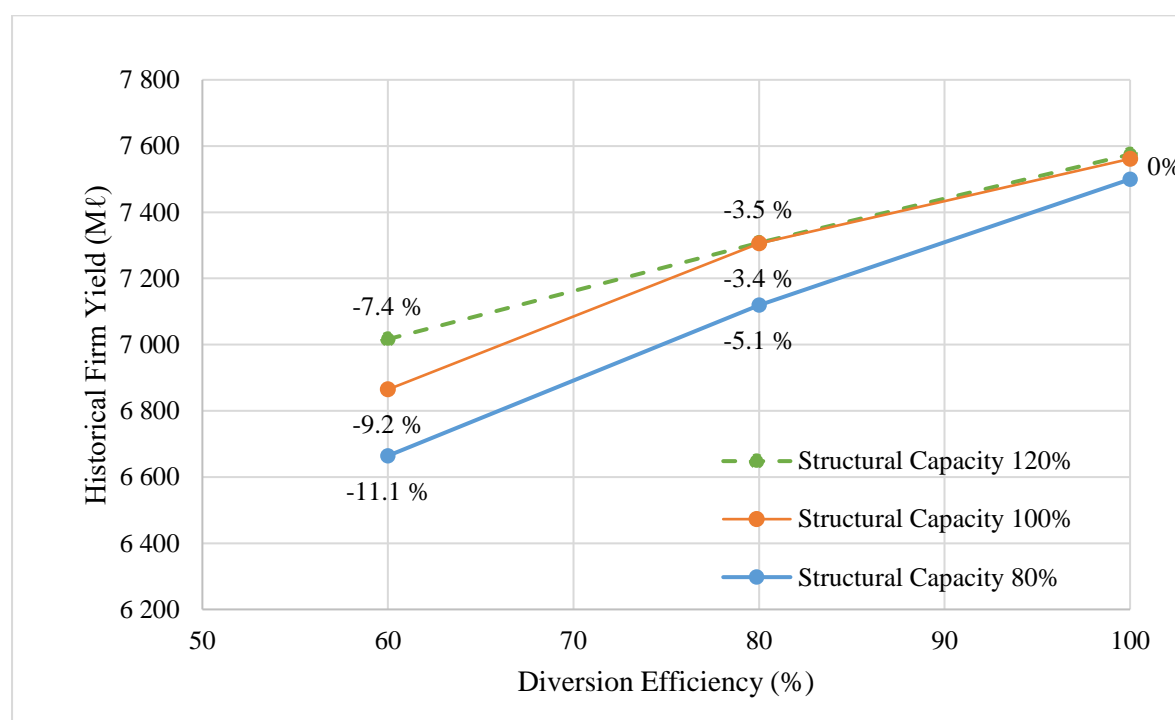


Figure 4-20: Percentage increases and decreases in the yield at 100% diversion efficiency

Of the 5 different scenarios simulated, the parameters which have the most significant impacts on the historical firm yield, is the diversion efficiency and the value of the WCWSS allocation. A diversion efficiency of 60% causes the historical firm yield to decrease by 9.2 %, while an increase of 25% in the WCWSS allocation increases the yield by 9%.

4.10.2 Long-term Reliability

To determine the probability of a failure with a satisfactory level of confidence, more than one streamflow sequence has to be evaluated for its ability to supply the given target draft (section 2.1.2). Stochastic streamflow sequences (amount: 101) are available to perform a long-term reliability analysis at different target drafts. The Stellenbosch municipality is in the process of expanding its water supply system to include groundwater and a possible increase in the allocation from the WCWSS. Therefore, scenarios 1, 2 and 3 (as discussed in section 4.10.1.3) are considered for performing the long-term reliability analysis and generating the long-term reliability curves. The reliability of supply for a higher

target draft is also determined using the long-term reliability curves generated for each scenario, as future demand is expected to increase, due to a predicted population growth of 8% over the 5-year period from 2018 to 2023 (Stellenbosch Socio-economic Profile, 2017). As no information on the increase of demand in the near future is currently available, it is assumed that the demand of 8 000 Mℓ/a (section 4.7) increases by 8% by the year 2023 linearly, due to the projected population growth, therefore 8 250 Mℓ/a is the higher target draft that the stochastic sequences can be evaluated at.

The water supply system components of scenario 1 consists of 2 380 Mℓ from the Idas Valley dams and Eerste River inflow, as well as the 3 000 Mℓ/a allocation from the WCWSS. The target draft, at which the 101 stochastic sequences are first evaluated, is equal to the historical firm yield of 7 638 Mℓ/a. The safe yield of each sequence is calculated and ranked in descending order in Figure 4-21 to indicate the breakpoint. The breakpoint indicates that twelve sequences failed to supply the target draft, therefore; the long-term risk of failure is 12 % and the long-term reliability of supply is 88 %, calculated by applying Equation 2-1. The record length used for the calculation is 90 years, therefore, the recurrence interval of failure is calculated as 1: 712 years by applying Equation 2-2.

$$\text{Reliability of Supply (\%)} = 1 - \frac{\text{Number of Failure Sequences}}{\text{Total Number of Sequences}}$$

$$\text{Reliability of Supply (\%)} = 1 - \frac{12}{101} = 88 \%$$

$$\text{Recurrence Interval of Failure} = \frac{1}{\left[1 - (\text{Reliability of Supply})^{\frac{1}{\text{record length}}}\right]}$$

$$\text{Recurrence Interval of Failure} = \frac{1}{\left(1 - \left(\frac{88}{100}\right)^{\frac{1}{90}}\right)} = 712 \text{ years}$$

For a single streamflow record of 90 years, the recurrence interval associated with a single failure is 1:100 years. However, when analysing a number of stochastic sequences, the recurrence interval is expected to be less than 1:100 years, as the risk of failure will increase. A recurrence interval of failure is customarily expected to be within the vicinity of 1:100 years, as analysing more stochastic sequences increases the risk of failure, therefore; the calculated recurrence interval of 1:712 years seems highly unlikely. Possible reasons for this are explored in the following paragraphs.

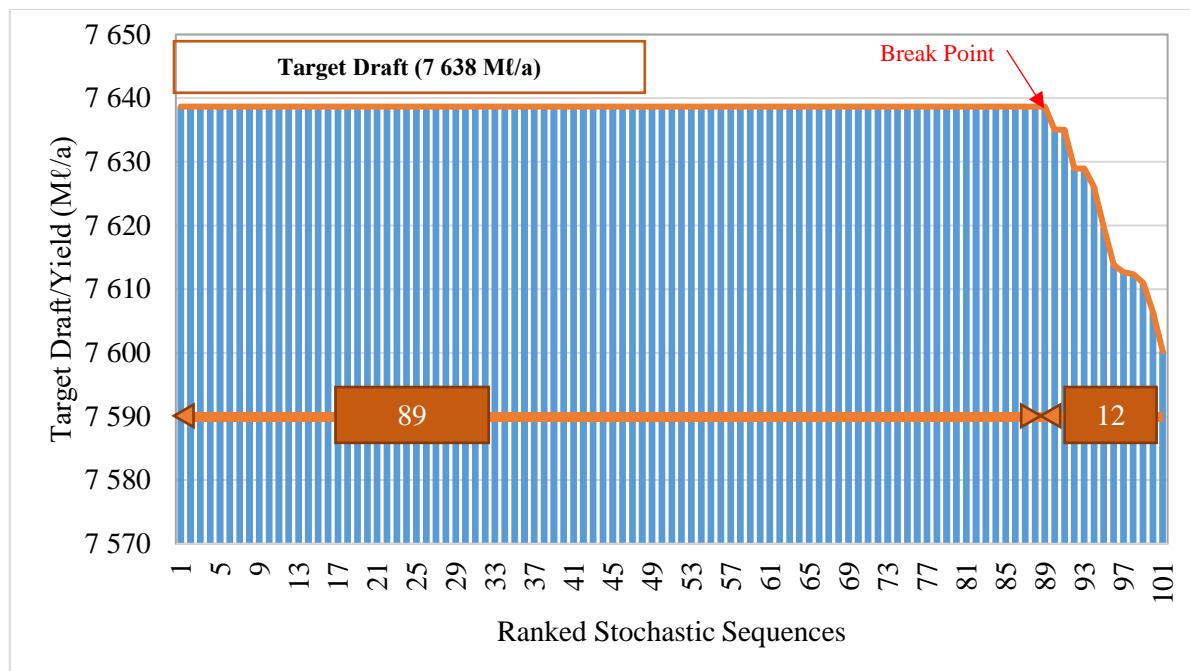


Figure 4-21: Yields of 101 stochastic sequences for a target draft of 7 638 Mℓ/a

The critical period for the historical streamflow sequence, identified in section 4.10.1.1, indicated that the lowest streamflow volumes occurred over the 9-month period leading up to the dam failure, affecting the total (annual) streamflow volumes of 2 hydrological years (1998/1999 and 1999/2000) negatively. What is significant about the 1998/1999 and 1999/2000 hydrological years is that their annual streamflow volumes are 17.5 mil m³ and 20.46 mil m³ respectively, and that these two streamflow volumes are the two lowest annual streamflow volumes in the historical streamflow sequence. The particular order in which the two low flow volumes appear is the lowest volume first, followed by the second lowest volume. The cumulative monthly streamflow distributions of the historical sequence for years 1 to 90 is depicted in Figure 4-22. The lowest streamflow volume (1998/1999) is indicated by the dotted red line and the second lowest (1999/2000) is indicated by the thick blue line. The dotted red line has a very flat slope for July to September (low streamflow for these months), which does not seem to occur in any other any other yearly historical sequence yearly historical sequence (Figure 4-22).

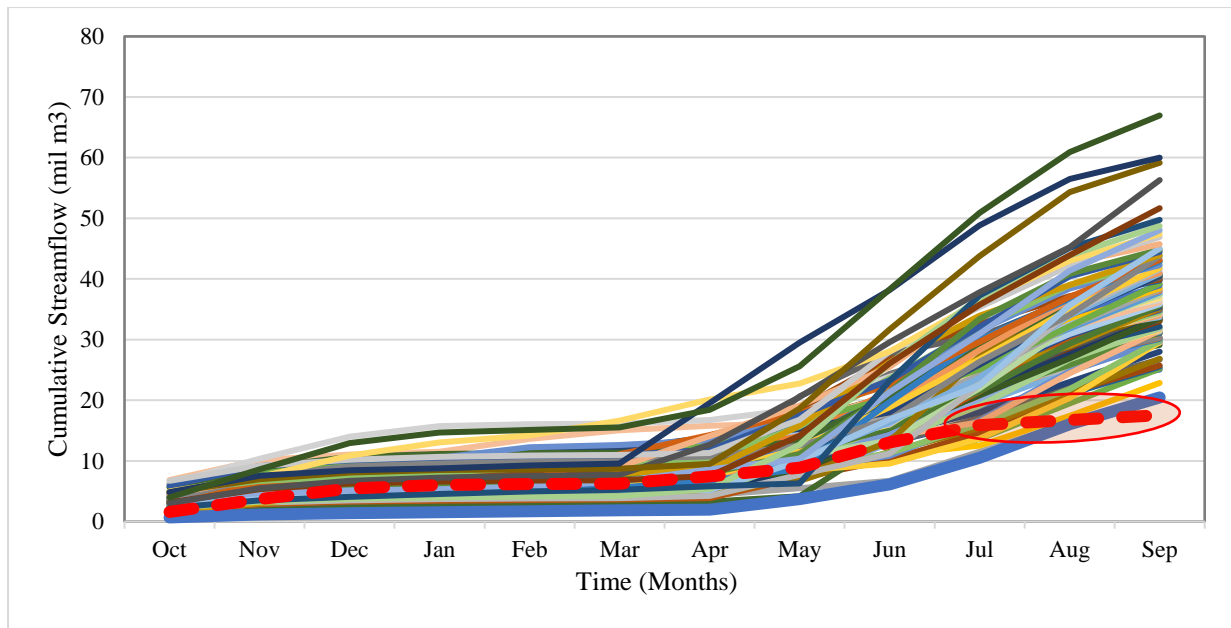


Figure 4-22: Cumulative monthly flows for the naturalized historical streamflow sequence

STOMSA generates monthly stochastic sequences by disaggregating the stochastic annual streamflow volumes, into monthly streamflow distributions which resemble that of the annual streamflow volumes in the historical streamflow sequence (Van Rooyen & McKenzie, 2004) (section 2.1.3). This means that for all stochastic annual streamflow volumes smaller than, or equal to, 19 mil m³ (average of 17.5 mil m³ and 20.46 mil m³), the lowest historical monthly streamflow distribution is automatically chosen by STOMSA to disaggregate the stochastic sequence into monthly distributions, indicated in Figure 4-22. Out of the 101 stochastic sequences generated by STOMSA, 27 sequences have been disaggregated according to lower annual flows than 19 mil m³. Thus, 26.7% of the stochastic sequences generated have the monthly streamflow distribution associated with the lowest annual streamflow volume (17.5 mil m³) of the historical naturalized sequence. If the stochastic sequence does not have an annual streamflow volume lower than 19 mil m³, it will only fail at a higher target draft than the determined historical firm yield. The firm yield of a stochastic sequence depends on the annual streamflow volume of the year that follows on that specific stochastic sequence with the lower totalled annual distribution of 19 mil m³.

Upon analysing the yields of the stochastic sequences for a number of different target drafts, it can be distinguished that the worst failure (lowest yield not able to supply the chosen target draft) occurs when evaluating sequence 21, indicated in Figure 4-24. Stochastic sequence 21 has a similar succession of low flows when compared to the historical streamflow sequence, namely: the lowest annual flow volume of 16.5 mil m³ is followed by the 3rd lowest annual flow volume of 19.65 mil m³. The two consecutive annual stochastic streamflow volumes are less than those appearing in the historical streamflow sequence for the same period, which explains why the failures for sequence 21 at different target drafts are the most severe out of all the stochastic sequences evaluated.

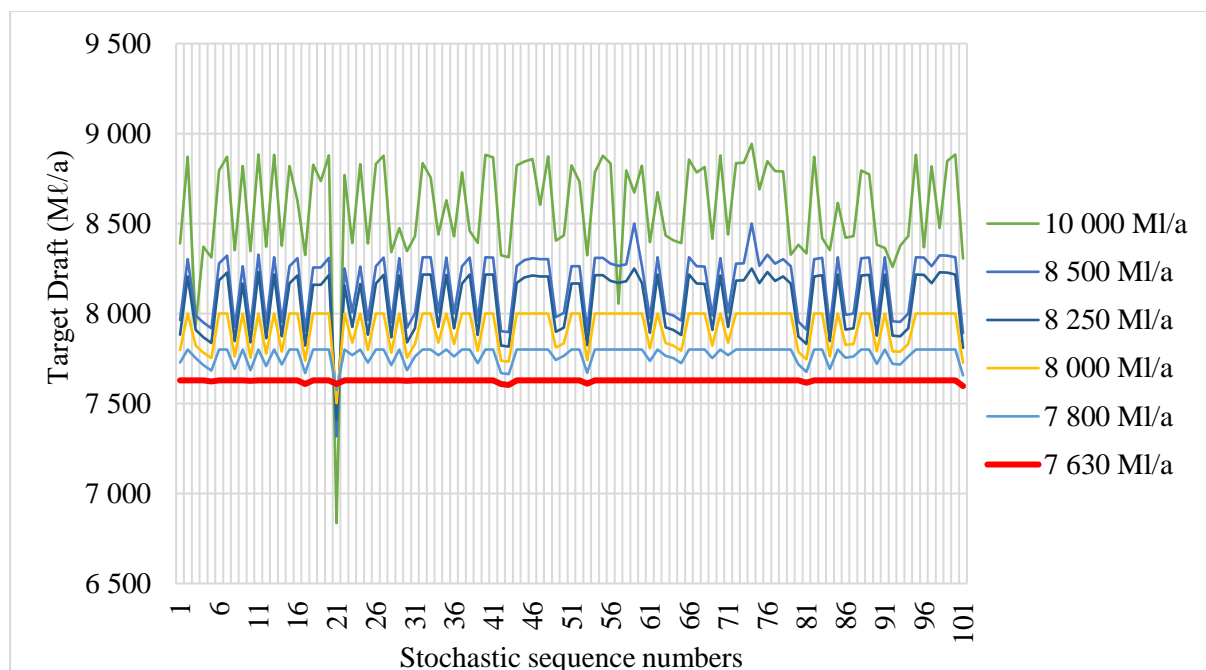


Figure 4-23: Base yields for stochastic sequences at different target drafts

The yields of the stochastic sequences at the target drafts for scenario 1 (Figure 4-23) are plotted according to their reliability of supply in Figure 4-24. The yield lines for each of the target drafts in the graph do not display the trend customarily expected from a long-term reliability curve, as suggested in Figure 2-5 (Basson et al., 1994). Instead of decreasing yield lines after the break point, the lines show a terraced effect. From the point where the firm yields fail to supply the target drafts, a rapid decline in yields are observed, after which it gradually declines again. This indicates that the capability of the yields take on two possibilities. In other words, the evaluation of the stochastic sequences that were disaggregated by STOMSA, according to an historical annual flow volume lower than 19 mil m^3 (26.7%), depicted in Figure 4-24, resulted in similar yield values. The rest of the stochastic sequences (73.3%) disaggregated by STOMSA according to historical annual flows larger than 20.5 mil m^3 were able to supply higher yields. The transition between the stochastic sequences with annual flow volumes lower than 19 mil m^3 and the stochastic sequences with annual flow volumes larger than 20.5 mil m^3 causes the rapid decrease in yield at a 63 % reliability of supply.

From Figure 4-24, the reliability of supply for a specific target draft can be read off of the graph, or inversely, the target draft can be determined for a specific recurrence interval or reliability of supply (indicated with (a) in Figure 4-24). The reliability of supply for a target draft of $8\,250 \text{ Mℓ/a}$ (8% increase from $8\,000 \text{ Mℓ/a}$) is 2%. The target draft that can be supplied at a 1:100 year recurrence interval is $8\,105 \text{ Mℓ/a}$, as indicated with (a) in Figure 4-24. In other words, the graph indicates that the long-term stochastic analysis results in a firm yield with a higher reliability, in comparison to the historical firm yield when evaluating the historical streamflow sequence. data is used. This is a highly unlikely occurrence, as an increase in stochastic sequences, customarily results in a decrease in the firm yield,

when performing the long-term reliability of supply (Basson et al., 1994). However, only one stochastic sequence resembles the historical annual low flow distribution (less than 19 mil m³), while the other sequences (100) do not show this unique distribution, which makes the percentages of the reliability of supply at different target drafts highly unlikely, but plausible. The assumption that the WCWSS is 100% assured also increases the reliability of supply for scenario 1, and the fact that groundwater is used in conjunction with the rest of the sources in the water supply system, also increases the reliability of supply.

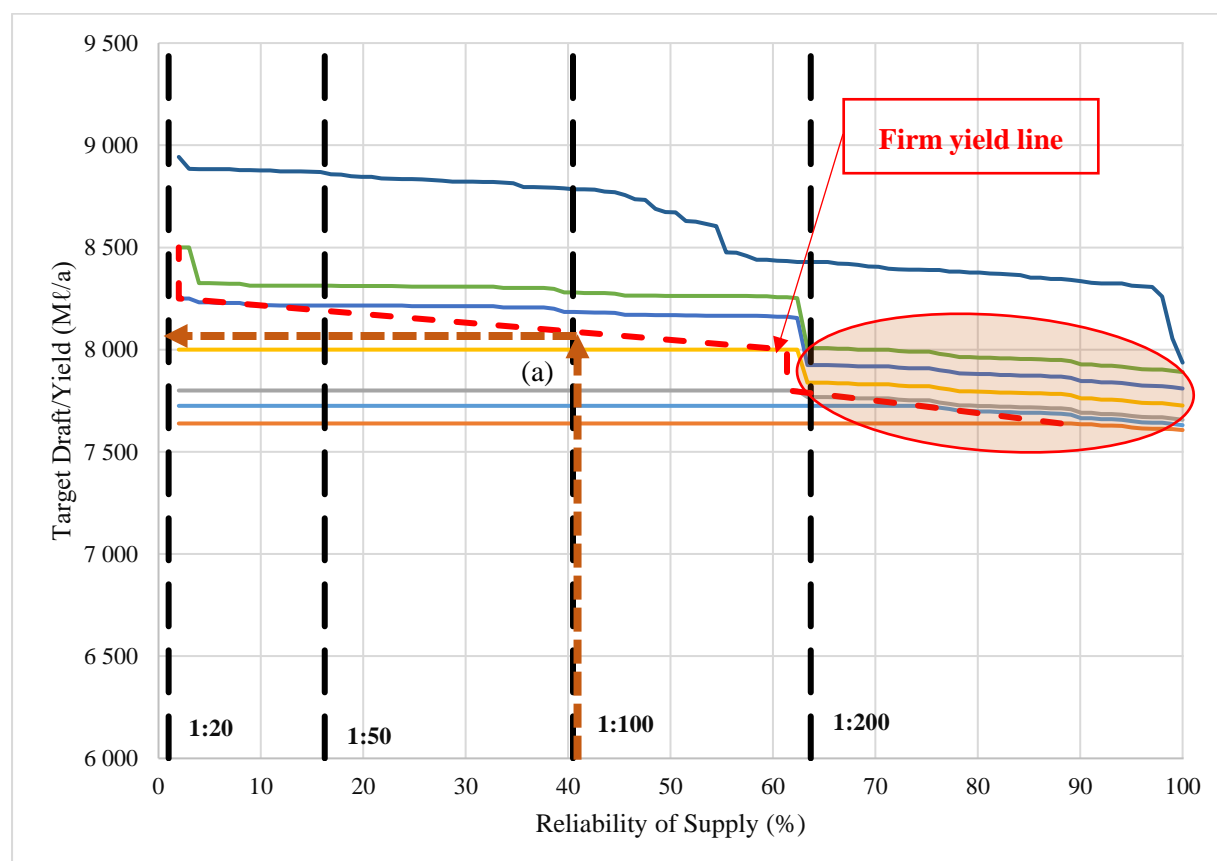


Figure 4-24: Reliability of supply and firm yield line for scenario 1

The long-term reliability curves were generated for scenarios 2 and 3 and are presented in Appendix C.6.4 and Appendix C.6.5 respectively. The long-term reliability curves for scenario 2 and 3 reveal a similar trend to that of scenario 1, which is terrace shaped, similar to Figure 4-24. The respective curves were used to determine the reliability of supply for a target draft of 8 250 Mℓ/a, as well as to determine the target draft that can be supplied with a 1:100 year recurrence interval. The results for scenarios 1, 2 and 3 are summarized in Table 4-15. The values displayed in bold represent the known figures.

Table 4-15: Long-term analysis results for scenario 1, 2 and 3

Scenario	Target Draft	Long-term risk of failure	Reliability of Supply	Recurrence Interval of failure
Scenario 1	Historical firm yield 7 638 Mℓ/a	88 %	12 %	1:712 year
	Target draft 8 250 Mℓ/a	98 %	2 %	1:23 year
	Target draft with 1:100 year return period: 8 102 Mℓ/a	60 %	40 %	1:100 year
Scenario 2	Historical firm yield 8 172 Mℓ/a	1%	99%	1:9045 year
	Target draft 8 250 Mℓ/a	2 %	98 %	1: 4 455 year
	Target draft with 1:100 year return period: 9 020 Mℓ/a	60 %	40 %	1:100 year
Scenario 3	Historical firm yield 8 261 Mℓ/a	1%	99%	1:9045 year
	Target Draft 8 250 Mℓ/a	10 %	90%	1:855 year
	Target draft with 1:100 year return period: 8 102 Mℓ/a	60 %	40 %	1:100 year

It is expected that scenario 3 should provide the best long-term reliability, because the WCWSS allocation is modelled as a constant inflow stream with no climate dependence. However, from Table 4-15 it can be concluded that the scenario with the best long-term reliability of supply is scenario 2, in which the capacity of the Idas Valley dams (modelled as a single dam) is increased by 25%. The long-term reliability recurrence intervals are highly unlikely, especially for a target draft of 8 172 Mℓ/a for scenario 1, and the target draft 8 261 Mℓ/a for scenario 2. As discussed for the recurrence interval associated with the historical firm yield, the possible reason for the extreme values is the unique historical streamflow distribution for the hydrological year 1998/1999 which was only reflected in one stochastic sequence out of the 101 stochastic sequences generated.

The unique succession of low flow periods in the historical sequence (specifically 1998/1999 hydrological year) caused the disaggregation of the stochastic sequences to be skewed. Thereby resulting in higher probabilities for reliability of supply associated with different target drafts, than is

expected from literature. Therefore, it is deemed necessary to check the naturalized streamflow data for catchment G22F against observed data of streamflow gauge G2H037, to identify any possible discrepancies in the naturalized streamflow data, which could be corrected, findings are discussed in section 4.10.2.1.

4.10.2.1 Simulation with Patched Data

Observed (recorded) monthly streamflow data for the streamflow gauge G2H037 is obtained from the DWS hydrology website (online database) from the hydrological year 1989/1990 to 2018/2019 (30 years). The naturalized streamflow sequence for the quaternary catchment G22F was simulated by the WRS2000 and obtained from the WR2012 online database, from the hydrological year 1920/1921 to 2009/2010 (90 years). To ensure that naturalized streamflow data, used for generating stochastic sequences, does not contain streamflow volumes too excessive or insufficient, resulting in calculation or disaggregation errors, correlation between the observed data of G2H037 and simulated data for G22F has to be established. Figure 4-25 depicts the monthly simulated streamflow data for G22F, and the monthly observed streamflow data of G2H037, for the 1998/1999 hydrological year. It is evident from the graph that the simulated streamflow volume is significantly less than the observed streamflow volume, between August and September of 1999.

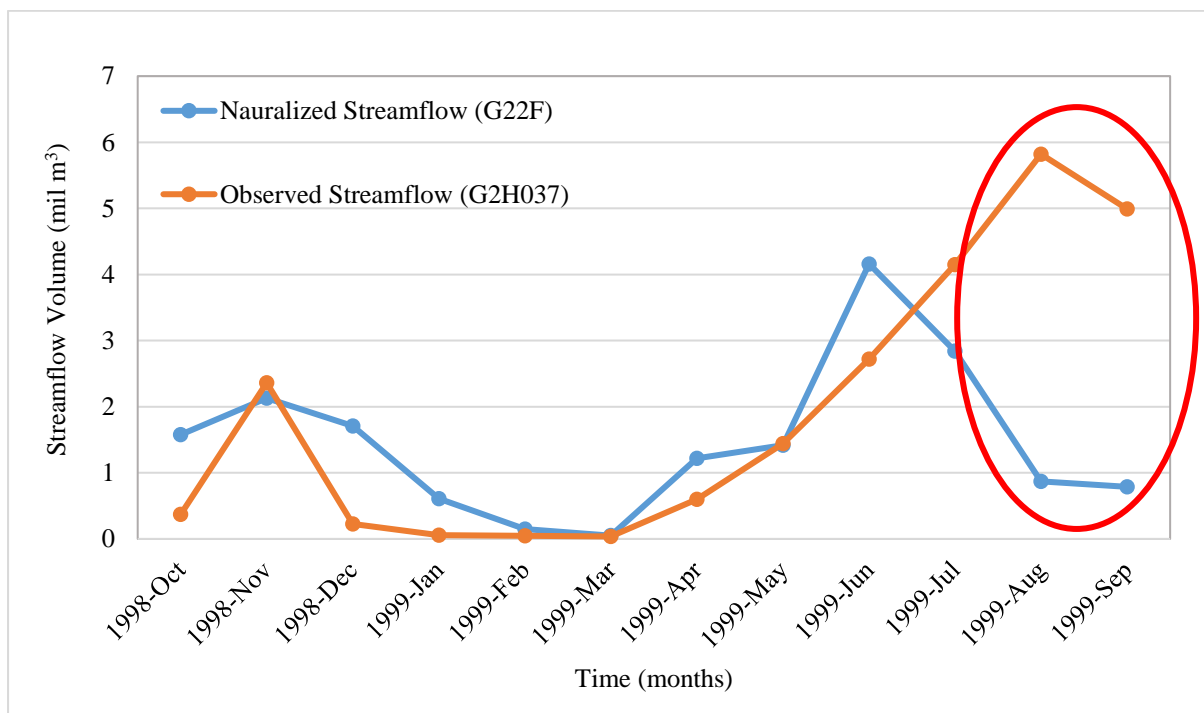


Figure 4-25: Observed streamflow and naturalized streamflow

To determine whether the occurrence in Figure 4-25 is a one-time event or whether it continues throughout the simulated naturalized streamflow sequence, the ratios between the observed monthly streamflow and simulated monthly streamflow volumes were determined over a period when data was available for both, namely from the 1989/1990 hydrological year to 2009/2010 (20 years). The area contributing to the streamflow of G2H037 is only a portion of the entire quaternary catchment, thus, the result of the monthly ratios are expected to be less than 1. The streamflow gauge G2H037 is situated in the Jonkershoek nature reserve, stream-up of the plantation area, therefore limited (negligible) human impacts affect the streamflow, making it comparable with the simulated naturalized streamflow sequence.

The results of the abovementioned ratios for the 20-year period are depicted in Figure 4-26, in the form of coloured dots. The ratio results (dots) of two consecutive hydrological years were connected in the graph, to demonstrate the difference between adequate correlation in the 1999/2000 hydrological year and outliers in the 1998/1999 hydrological year. It is evident that the correlation between the observed streamflow data and the simulated streamflow data for August and September of 1999 is not within the same range as the correlation for the other months in the 20-year period examined. Thus, the simulated streamflow values for those two months should be replaced by more realistic values, which reflect a more sound correlation between the two streamflow distribution data sets (G2H037 and G22F).

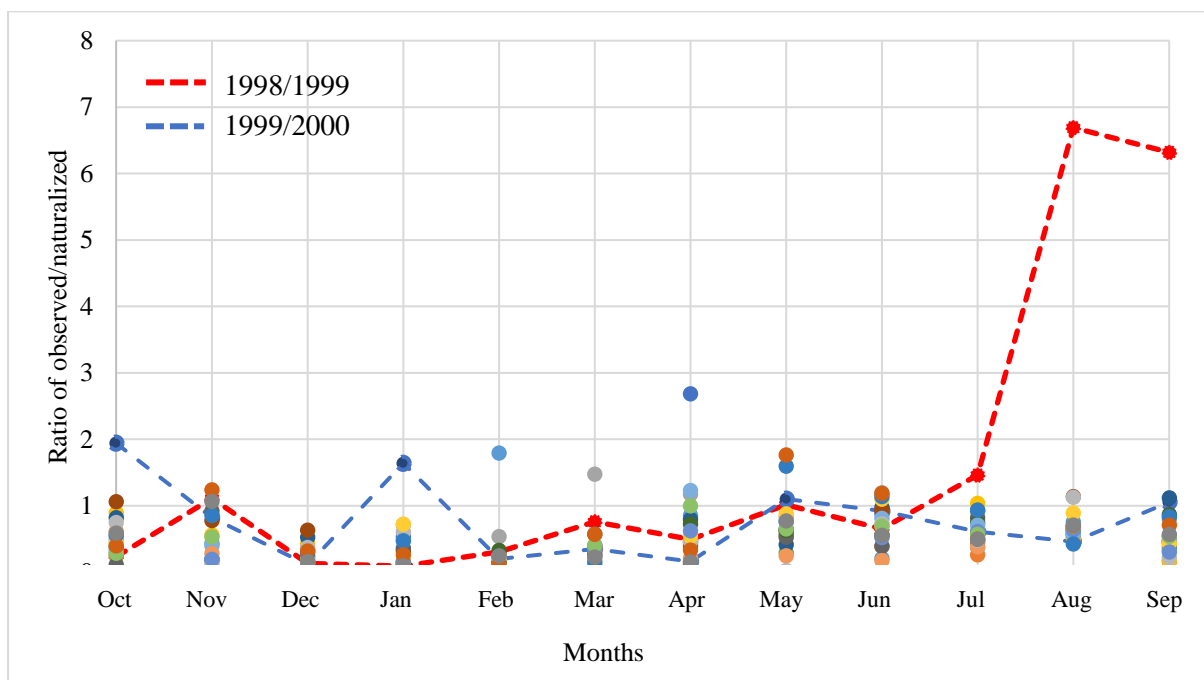


Figure 4-26: Ratio results of observed flow and naturalized streamflow before patching

The naturalized streamflow sequence is patched, by replacing the two lowest monthly streamflow values (August and September of 1999), with the second lowest monthly streamflow values, appearing in the same months, but during different hydrological years of the 90-year sequence. In other words, from the 90 sets of values for August appearing in the 90-year sequence, the 2nd lowest streamflow value is chosen to replace the lowest value of August 1999, and the same is applied for September. This is a conservative approach, as only the two insufficient values far outside of the correlation range have been replaced, and they have been replaced in such a way as to have two low flow sequences still appearing consecutively in the 90-year sequence. However, after patching, the order of low flows is the 3rd lowest flow (20.74 mil m³) followed by the lowest flow (20.46 mil m³), which is different to the original data (lowest followed by 2nd lowest). The monthly distribution of the patched monthly low flow sequence now follows the same trend as the other monthly low flow sequences in the naturalized streamflow sequence, attached as Appendix C.6.6. This particular distribution order now changes the

historical firm yield for the base scenario to 7 672 Mℓ/a (increase of 1.5%). The correlation between the observed and simulated monthly streamflow volumes also reflect correlations closer to the average correlation as seen in Figure 4-27.

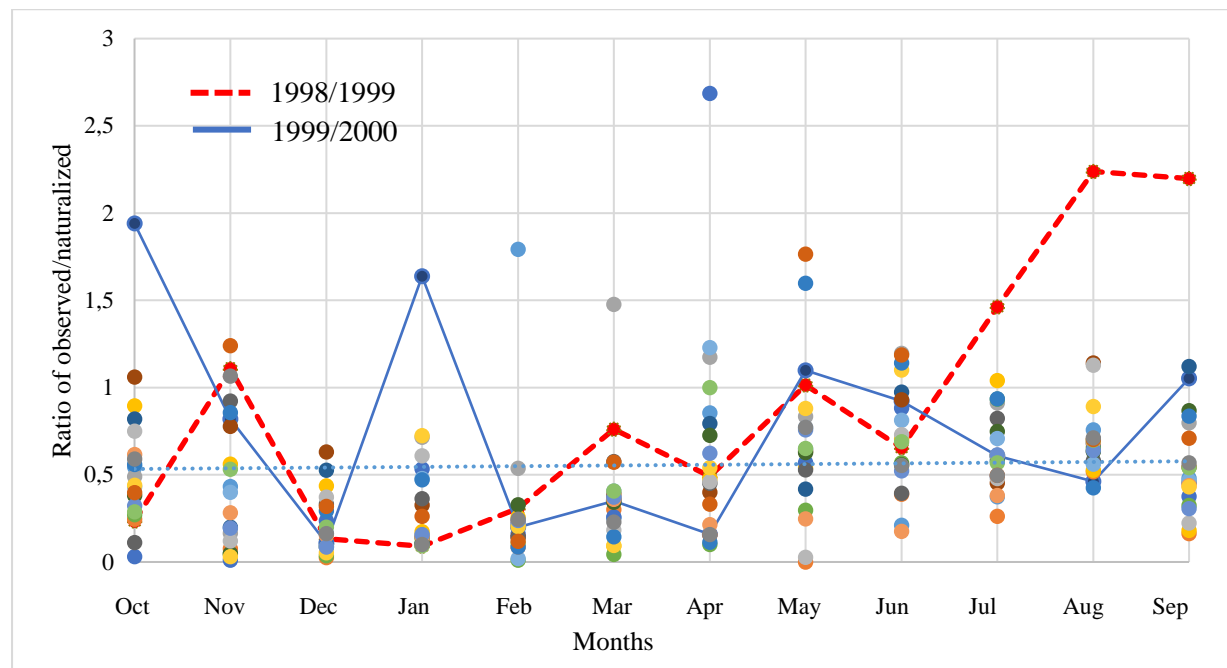


Figure 4-27: Ratio results of observed flow and naturalized streamflow after patching

By patching the historical naturalized streamflow data, which STOMSA and subsequently the conjunctive use model relies on for simulating a variety of scenarios, the changed volumes and order of the low flow periods will impact the stochastic sequences generated with STOMSA. Therefore, the simulation process needs to be repeated from the beginning with the newly patched data. New stochastic sequences are generated, which are disaggregated into daily streamflow sequences. Furthermore, new RAIN-RUNOFF ratios are determined and the stochastic groundwater simulation is repeated by following the steps discussed in sections 4.3 to 4.9.

The historical firm yield of scenario 1 increases to 7 725 Mℓ/a (1.14 % increase) when applying the patched data. The stochastic sequences generated with the patched data show a significant change to those previously generated, as 50 of the sequences have an annual low flow volume of less than 20.5 mil m³ (average between lowest and second lowest flow). The yields for the stochastic sequences were determined for scenario 1 at different target drafts, and are included as Appendix C.6.7.

A new long-term reliability curve is generated for scenario 1 as illustrated in Figure 4-28. The yield curves for the different target drafts still display a terraced effect, but it is less pronounced than in Figure 4-24. The sharp decrease in the yields for the target drafts now occur at around 53% reliability of supply, which suggests that if sequences have annual low flow volumes of less than 20.5 mil m³, the yield is less when compared to the sequences with higher low flow volumes. The reliability of supply associated

with the historical firm yield for scenario 1 is 53.5% (47 stochastic sequences fail) and the recurrence interval is 1:144 years, which is a more realistic reliability of supply than what was determined with the unpatched data. The recurrence interval is larger than 1:100 years, which can be ascribed to the assumption that the WCWSS allocation is supplied at a 100% reliability of supply. Furthermore, the addition of groundwater contributes to the water supply, which also extends the recurrence interval of failure.

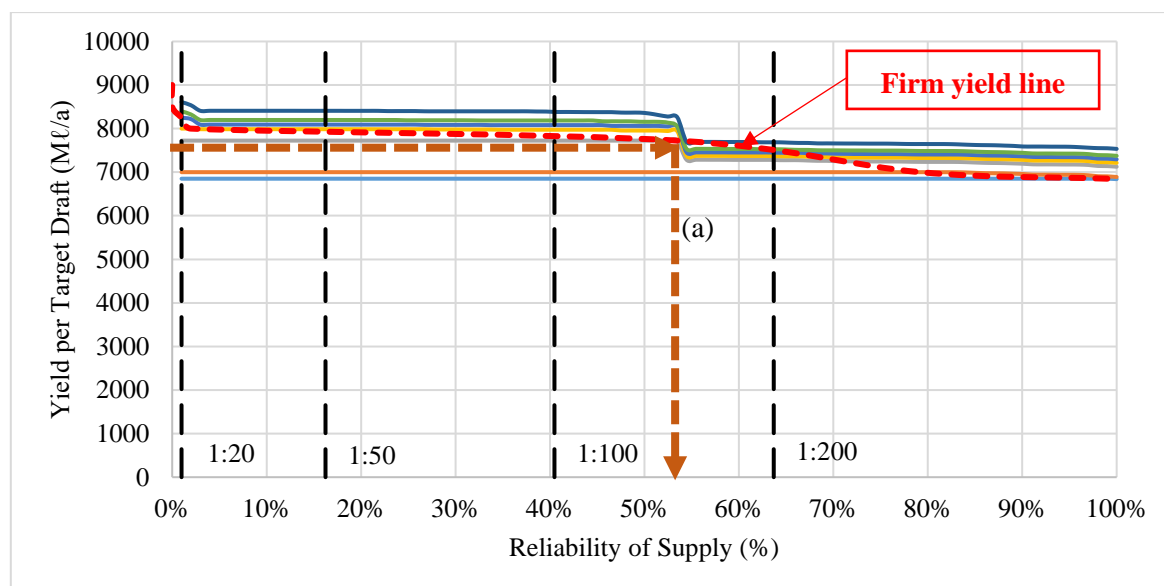


Figure 4-28: Reliability of supply curve for scenario 1 with patched streamflow

The reliability of supply associated with the historical firm yield for scenario 1 is 53.5% (47 daily stochastic sequences fail) and the recurrence interval of failure is 1:144 years, which is a more realistic reliability of supply than what was determined with the unpatched data. The recurrence interval is larger than 1:100 years, which can be ascribed to the assumption that the WCWSS allocation is supplied at a 100% reliability of supply. Furthermore, the addition of groundwater contributes to the water supply, which also extends the recurrence interval of failure.

4.10.3 Short-term Management

The short-term management curve of Stellenbosch is generated for a two-year period using probabilistic storage projections of the Idas Valley dams. The probabilistic storage projections are used to simulate stochastic exceedance probabilities of possible future events (section 2.1.2.2) with regard to the current water resource situation. The water resource manager can generate these curves at the beginning of a decision period. The storage capacity, water resource allocation from inter-basin transfer schemes, groundwater abstraction rate, as well as the demand, should reflect the current situation and these values are fixed at the commencement of the decision period. The probabilistic storage projections give an indication of plausible system storage behaviour over the decision period, given the current situation. The water resource manager can gauge the real-time storage by comparing it with the probabilistic

storage projections, so that management decisions regarding restrictions and augmentation resources can be taken to avert possible crisis situations.

To simulate the probabilistic storage projections of the Stellenbosch water supply system, different commencement situations are evaluated, based on events that have occurred in the past (which could again occur in the future). The first situation includes simulating the drought scenario where no water from the WCWSS was supplied to the Paradyskloof WTW during November 2017, because Theewaterskloof dam was empty (GLS, 2018). At that time, the storage level of the Idas Valley dams were at approximately 50%, the demand is assumed to have remained at the average rate of 8 000 Mℓ/a (section 4.7) and no groundwater for augmentation purposes have been implemented yet. Using the conjunctive use model, the probabilistic storage projections for a two-year period, starting at the beginning of November 2017, can be generated. The situation at commencement of the short-term management period is summarized in Table 4-16.

Table 4-16: Input data of a drought situation for a short-term management graph

Start Capacity	50	%
Target Draft	8 000	Mℓ/a
Start Date	1 st November 2017	
Number of years evaluated	2	
WCWSS percentage supply	0	%
Groundwater Abstraction	0	Mℓ/day

Storage trajectories are generated for every stochastic inflow sequence (101 stochastic sequences) over a 2-year period. For each month, a box plot with exceedance probabilities is generated to represent specific storage trajectories for the situation indicated in Table 4-16. The exceedance probabilities evaluated are: 5%, 25%, 50%, 75% and 95%, which are the same percentages as in Figure 2-6 and Figure 3-19. Instead of plotting the box plots for every month to represent the different storage trajectories, lines are used (Figure 4-29). An exceedance probability of 5% is associated with the 95th percentile of all the storage trajectories simulated; indicating that only the 5 best performing stochastic sequences (out of the 101) resulted in a storage trajectory of at least 5% or higher. In other words, there is a 5% chance that the storage level of the Idas Valley dams follows or exceeds the storage trajectory indicated by the 5% line (best storage trajectory). Conversely, the 95% exceedance probability indicates the storage trajectory followed by the 5 lowest performing stochastic sequences (5th percentile), therefore there is a 95% chance that the storage level will at least follow the 95% exceedance line or be higher.

Figure 4-29 illustrates the probabilistic storage projection for the commencement situation as summarized in Table 4-16. The water resource manager is able to attach different percentages of demand reductions to the different probabilistic trajectories and test their effect on the future storage

trajectories so that approval for the reductions can be granted. By reducing the demand, the risk of failure should decrease.

From Figure 4-29 it is distinguished that there is only a slight difference in storage level between the 95% exceedance probability line and the 5% exceedance probability line over the period from March to June 2018, which indicates that there is a high risk of dam failure within the 6 months from November 2017. All exceedance probabilities show that the storage level of the Idas Valley dams will reach a critical level by April 2018. There is only a 5% exceedance probability associated with the dam narrowly averting failure during the 8-month period from November 2017 to July 2018.

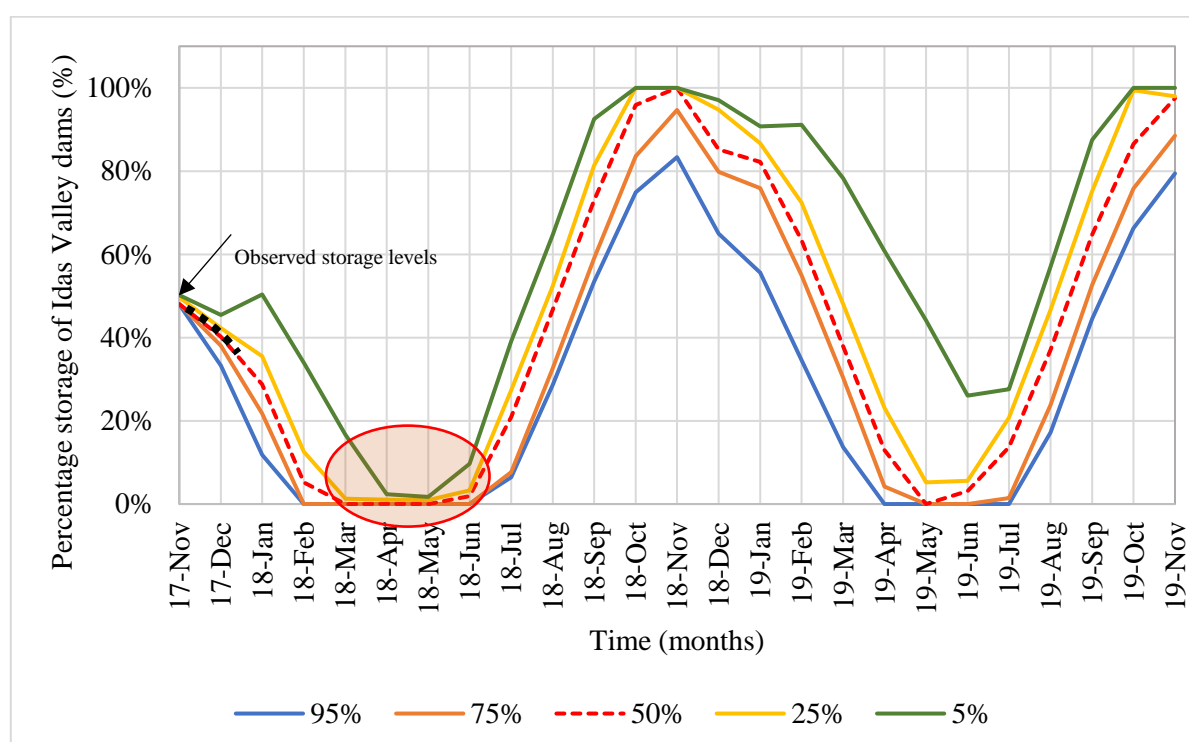


Figure 4-29: Probabilistic storage projection for Idas Valley dams with starting level at 50%

After a month from the time of having drawn up the probabilistic storage projections (Figure 4-29), the water resource manager adds real-time storage levels (black dotted line) observed until December 2017. The real-time storage level follows the 50% exceedance probability storage projection. At this point the system manager implements water restrictions of approximately 37% to reduce the demand to 5 000 Mℓ/a, and introduces abstracted groundwater to the municipal water supply system to avert the crisis situation. The drought demand of Stellenbosch can be reduced to 5 000 Mℓ/a (section 4.7) and the combined abstraction rate for Cloeteville, die Braak and Van der Stel boreholes (section 4.8) is 1.4 Mℓ/day. The storage projections are simulated from the beginning of December in Figure 4-30. The starting storage level of the Idas Valley dams is 40% (as determined from the previous projections in Figure 2-28) and the specific situation summarized in Table 4-17.

Table 4-17: Input data of a drought mitigation situation for a short-term management graph

Start Capacity	40	%
Target Draft	5 000	Ml/a
Start Date	1 st December 2017	
Number of years evaluated	2	
WCWSS percentage supply	0	%
Groundwater Abstraction	1.43	Ml/day

Figure 4-30, indicates that the risk of system storage failure is reduced. There is now a 50% chance that the system storage trajectory follows the 50% (median) line, indicating that the Idas Valley dams might narrowly avert failure. There is a 5% chance that the dam levels will not fall below 30% during the next 6-month period (from December 2017 to May 2018). Using these probabilistic storage projections, the water resources manager can motivate that the restrictions imposed on the demand and the augmentation of the water supply system with groundwater are necessary.

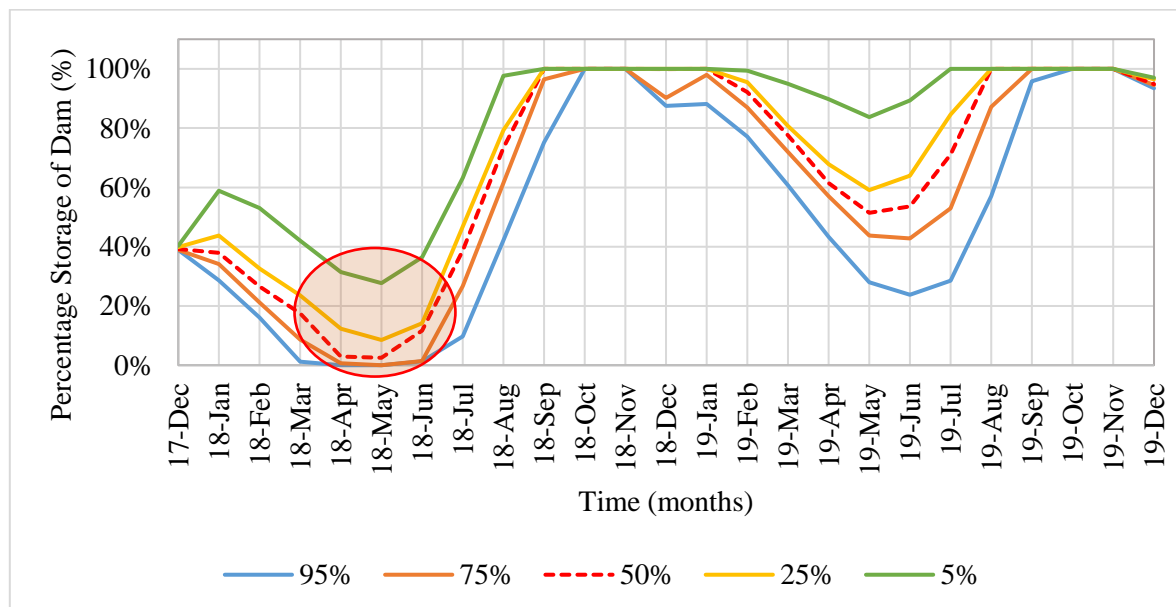


Figure 4-30: Probabilistic storage projection for Idas Valley dams with starting level at 40%

The short-term management curves can be used to simulate possible future scenarios at the start of the 2-year planning or decision periods. The storage trajectories associated with the different starting situations (storage levels) aid operational management decisions regarding water restrictions on demand and short-term augmentation of the water supply system at any point in time.

After performing a historical, long-term and short-term yield analysis, it is concluded that even though the total current water resource allocation for Stellenbosch amounts to a yield of 10 224 Ml/a (3 000 Ml/a from WCWSS and 7 224 Ml/a from the Eerste River), the water resources that can be safely supplied to satisfy the demand is estimated at 7 500 Ml/a, after evaluation of the historical streamflow sequence together with the WCWSS allocation (modelled as a constant inflow source).

4.11 Critical Evaluation of the Model

The accurate computation of the results of the conjunctive use model is dependent on the quality of input data. A separate data check has not been incorporated into the model; therefore, the user is responsible for cross-checking results with input data. In section 4.10.2.4, the streamflow data, as retrieved from the WR2012 online data base, portrayed a dry period, while the observed data portrayed average streamflow values. It is therefore necessary for the user to verify the simulated data with observed data and patch the simulated data if necessary, to generate more reliable results. If another simulation is performed for the same catchment, results might differ, as STOMSA generates different stochastic sequences for every simulation. This is due to the random generator incorporated in a stochastic sequence generator.

The conjunctive use model is a scenario-based model, which does not incorporate changing scenarios, or incremental demand increases, during a simulation. It does, however, make provision for the user to define different starting scenarios at the beginning of the simulation, for them be analysed and compared in order to aid decision-making processes. The computational time associated with opening and running the different components of the conjunctive use model might seem excessive, but it is still considered a user-friendly software, which is widely applicable.

5 CONCLUSION

Municipalities, who are the water providers of urban users in cities and towns across South Africa, are faced with population growth and changing climate conditions impacting on finite resources and limited internal management capacity. To relieve some of these challenges, a stochastic, daily time-step conjunctive water resource model was developed, using the Microsoft Excel application. The purpose of the conjunctive use model is to act as a planning and management tool, which can be applied to analyse the yield, and associated reliability of supply, of resources included in a municipal supply system or distribution network.

Modelling principles were identified during the literature review, which guided the process of developing the model for the conjunctive use of surface water, groundwater and desalination and reuse. Monthly streamflow data obtained from WR2012 was used as input to STOMSA software to generate monthly stochastic streamflow. The stochastic monthly streamflow sequences were disaggregated into daily flow sequences using high-, medium- and low-flow classes. The challenge in combining the different water resources was to establish the stochastic links between surface water and groundwater. Groundwater is a recharge dependent resource driven by rainfall events. Rainfall, being stochastic in nature, could be generated from stochastic streamflow sequences (STOMSA output) using a calculable runoff-rainfall relationship. The SVF method was used to describe water level fluctuations, due to recharge over a quaternary catchment area. The catchment aquifer was simulated as a lumped-parameter

box-model, similar to the AFYM, which assumes that inflow and outflow are equal to balance the system, and abstraction rates were evaluated using maximum allowable water level drawdown restrictions. Surface water storage capacity simulation was governed by the dam balancing equation developed for daily time-steps, using both historic and stochastic streamflow, disaggregated into daily streamflow. Desalination and reuse were incorporated by modelling them as constant supply of inflow, depending on the monthly operational capacity, as percentage of total desalination plant or reuse plant capacity. The priority ranking in which water resources are utilized to satisfy demand is as follows: (1) desalination and reuse, (2) groundwater, (3) surface water (should the alternative water resources not be able to meet the demand). A series of operational scenarios were suggested in order to incorporate the different water resources.

Daily time-step simulations assist municipalities in managing water resources on a daily basis, which is especially helpful during critical periods. Yield and associated reliability of supply analyses are performed to evaluate the system capacity and assurance of supply, which facilitates improved planning and operational management strategies to be implemented before municipalities experience water supply deficits.

A case study on the water supply system of the Stellenbosch Municipality, for urban users, is presented to illustrate the application of the conjunctive use model. A yield analysis on the current water resources in the distribution network, as well as the anticipated potential expansion thereof, which could include an increase in storage dam capacity and introduction of new resources, is performed. It was found that even though Stellenbosch has a current water allocation of 10 244 Mℓ/a on record (Eerste River and WCWSS), the historical firm yield indicates that only 7 5617 Mℓ/a can be supplied. The historical firm yield analysis of the Eerste River and the WCWSS allocation, on a daily basis, results in a yield of 7 561 Mℓ/a, which is 26% less than the current annual water budget. The combined borehole yields (determined through borehole yield tests) of those boreholes that the municipality has access to (Cloetesville, Die Braak and Van der Stel), amount to 1 426 m³/day. This yield is estimated at 6 times larger than the long-term average potential abstraction calculated at 222 m³/day through the application of the AFYM. Furthermore, the interference between the boreholes within the central Stellenbosch area was calculated and indicated that the boreholes do influence each other, and that the abstraction rates from the Die Braak and Van Der Stel boreholes should be reduced to minimise the impact of interference and curb over-abstraction. The long-term reliability of the Stellenbosch water supply system was determined for 3 scenarios:

Scenario 1 - Water resources from the Eerste River (transferred to the Idas Valley dams and WTW), combined the WCWSS allocation, as well as the long-term average potential groundwater abstraction;

Scenario 2 - An increased storage capacity for the Idas Valley dams (modelled as one dam); and

Scenario 3 - An increased WCWSS allocation.

Increasing the Idas Valley dams storage capacity, resulted in a yield of 9 020 Mℓ/a, which could be supplied at a 1:100 year recurrence interval. An increase WCWSS system resulted in a yield of 8 102 Mℓ/a. Thus, scenario 2 proved to result in the most significant yield increase, while performing the system simulation with the original naturalized streamflow data. Due to a unique monthly distribution in a unique monthly distribution scenario in the original naturalized streamflow data, which caused the disaggregation of STOMSA to be skewed, the recurrence intervals determined for specific target drafts were unrealistic. The data was patched according to observed data from a streamflow gauge and the historical yield analysis as well as the long-term reliability analysis of the base scenario were generated with the patched data. The long-term reliability of the new calculated historical firm yield of 7 672 Mℓ/a was determined as 1:144 years.

Short-term management curves for the probabilistic storage trajectory were generated for a plausible drought scenario in which the starting capacity of the Idas Valley dams was 40% at commencement of the 2-year decision period, and the WCWSS allocation was 0%. The storage protectories indicated high risk of non-supply. Upon introducing groundwater and demand reductions, the possible drought scenario could be averted with a lower risk of failure.

The conjunctive use model developed in this thesis proved to be a user-friendly, planning and management tool used to simulate to conjunctive use system of Stellenbosch Municipality.

6 RECOMMENDATIONS

The conjunctive use model presents a management tool for the conjunctive use of surface water, groundwater, as well as desalination and water reclamation, depending on the components of a municipality's water supply system. The model is limited to the assumptions made, based on the relationships between the different components. Furthermore, the conjunctive use model utilised input data, identified to be readily available to municipalities, such as the GRA II and Hydrology (from the DWS websites), as well as the WR2012 online data bases to render it user friendly. However, if streamflow records or rainfall records are obtained from other sources, they will have to be presented in a similar format to those used in the model. The conjunctive use model does not include a cost analysis on the different water resources, as the aim was to develop a tool to establish the potential amount of water available from different resources, but utilized in a conjunctive manner, through considering the way in which they interaction.

To further enhance the range of its applicability and accuracy, the following recommendations are proposed when using the model:

- Incorporate a data patching worksheet in which simulated data from the WR2012 database can be cross checked with observed data from the DWS database, so that future disaggregation discrepancies by STOMSA are avoided.
- Incorporating the changing of operational rules within the analysis period.
- Considering the effects of population growth on the demand during the analysis period.
- Allowing for desalination and water reclamation to be triggered by low dam levels, while still remaining operational at a constant capacity over 3-month blocks.

Recommendations which can aid in further development of the groundwater component of the model are as follows:

- Investigating artificial aquifer recharge schemes and incorporating it into the conjunctive use model for increased yield, through an improved understanding of managing water transfers between surface water and groundwater.
- Incorporating stochastic groundwater estimation specific to different localized aquifer systems.
- Calibrating the aquifer storage parameters, as well as lag-time, by incorporating monitoring data from boreholes in the wellfield. However, this can only be undertaken when more monitoring data is readily available to the municipalities.
- Incorporating evapotranspiration computations which are applicable to localized aquifers and their associated data, especially if riparian zones make up a significant percentage of the aquifer in question.

7 REFERENCES

- AQTESOLV, 2018. *AQTESOLV Is The World's Leading Aquifer Test Analysis Software*. [Online] Available at: <http://www.aqtesolv.com> [Accessed on 08 March 2018].
- Aurecon, 2011. Development of a Reconciliation Strategy for the Olifants River Water Supply System-Future Water Reuse and other Marginal Water Use Possibilities, Pretoria: Aurecon.
- Aurecon, 2012. Report on the third safety inspection of Idas Valley No 1 Dam and Idas Valley Dam No 2, Cape Town: Aurecon South Africa (Pty) Ltd.
- Bailey, A., Pitman, W. & Kakebeeke, J. 2019. *Water Resources of South Africa, 2012 Study (WR2012)*. [Online] Available at: <http://www.waterresourceswr2012.co.za/> [Accessed on 10 June 2019].
- Basson, G. 2005. *Considerations for the Design of River Abstraction Works in South Africa*, Stellenbosch : Ninham Shand.
- Bredenkamp, D., Botha, L., van Tonder, G. & Van Rensburg, H. 1995. *Manual on Quantitative Estimation of Groundwater Recharge and Aquifer Storativity*, Pretoria: Water Research Commission.
- Buenaventura, A. 2019. *A short history on desalination*. [Online] Available at: <http://www.theenergyofchange.com/short-history-of-desalination>. [Accessed on 20 July 2019].
- Catherine Blersch, J.d.P. 2017. Planning for desalination in the context of the Western Cape water supply sytem. *Journal of the South African Institution of Civil Engineering*, 59(1), pp. 11-21.
- Chang, W. & Chen, X. 2018. Monthly Rainfall-Runoff Modeling at Watershed Scale: A comparative study of Data-Driven and Theory-Driven Approaches. *Water*, 1116(10), pp. 1-21.
- Chapman, A. 2015. *Managing Water Resources in Time of Climate Change*, Cape Town: Cape Town University, Stellenbosch University.
- Chris Swartz Water Utilization Engineers, 2010. *Operations and Maintenacne Manual for Idas Valley Water Treatment Plant*. Mossel Bay: Stellenbosch Municipality.
- Consulting, G. 2017. *Municipality of Stellenbosch Water Consumption* [Interview] (11 September 2017).
- Critchley, W. & Siegret, K. 1991. *A Manual for the Design and Construction of Water Harvesting Schemes for Plant Production*. 1st ed. Rome: Food and Agriculture Organization of the United Nations.

De Villiers, J. 2018. *Namibia solved Cape Town's water crisis 50 years ago- using sewage water*. [Online] Available at: <https://www.businessinsider.co.za/namibia-knows-how-to-survive-without-water-2018-2> [Accessed on 15 March 2019].

Department of Water Affairs, 2010. *National Groundwater Strategy*, Pretoria: Department of Water Affairs.

Department of Water Affairs, 2011. *Groundwater Dictionary*. [Online] Available at: http://www.dwa.gov.za/Groundwater/Groundwater_Dictionary/. [Accessed on 20 April 2018].

Department of Water Affairs, 2013. *National Water Resource Strategy*. 2nd ed. Pretoria: Department of Water Affairs.

Department of Water and Sanitation, 2016. *National Groundwater Strategy*. Pretoria : Department of Water and Sanitation.

Department of Water and Sanitation, 2018. *Department of Water and Sanitation*. [Online] Available at: <http://www.dwa.gov.za/Hydrology/Weekly/SumProvince.aspx>. [Accessed on 4 April 2019].

Department of Water and Sanitation, 2018. *Dual Strategy for Desalination of Groundwater and Surface (sea) water*. Johannesburg, DWS.

Department of Water and Sanitation, 2019. *Hydrological Services - Surface Water (Data, Dams, Floods and Flows)*. [Online] Available at: <http://www.dwa.gov.za/Hydrology/Default.aspx> [Accessed on 4 May 2019].

Du Plessis, J. 2016. Integrated Water Management at Local Government Level for South Africa. In: V.P. Singh, ed. *Water Resources Management*. Texas: Springer, pp. 209-231.

Du Plessis, J. 2018. *A Water Crisis: What about the next drop?*, Stellenbosch: University of Stellenbosch.

Du Plessis, J., Burger, A., Schwartz, C. & Musee, N. 2006. *A desalination guide for South African municipal engineers*, Pretoria: Department of Water Affairs and Forestry.

Engelbrecht, C. 2017. *Geohydrological assessment of groundwater development at Atlantis Beach Estate, Melkbosstrand*, Stellenbosch: GEOSS (Pty) Ltd.

Food and Agriculture Organization of United Nations, 2003. *Review of World Water Resources by Country*, Rome: United Nations.

Fourie, F., Dennis, I., Dennis, D., Veltman, S., Titus, R. & Parsons, R. 2011. *The Groundwater Dictionary*. 2nd ed. Bloemfontein(Free State): University of Free State.

- G. Mackintosh, U.J. 2008. *Assesment of the Occurence and Key Causes of Drinking-Water Quality Failures within the non-metropolitan Water Supply Systems in South Africa, and Guidelines for the Practical Management Thereof*, Gezina: Water Research Commission.
- Gelhar, L. 1993. *Stochastic Subsurface Flow*. New Jersey: Massachusettes Instute of Technology.
- GEOSS, 2018. *Groundwater Development for Stellenbosch Municipality Drought Relief-Stellenbosch Central Area*, Stellenbosch: GEOSS.
- GLS, 2018. *Bulk Water Resources: Drought Intervention Projects*, Stellenbosch: Stellenbosch Municipality.
- Gorelick, J. & Serjak, C. 2018. *Water reuse gets a new take in South Africa*. [Online] Available at: <https://www.globalwaters.org/resources/blogs/wash-fin/water-reuse-gets-new-take-south-africa>. [Accessed on 1 July 2019].
- Hagen, D. 2019. *Embankment Dam Design*. Stellenbosch, Ingerop, Cape Town.
- Heath, R. 2004. *Basic Ground-Water Hydrology*. 10th ed. North Carolina: U.S. Geological Survey Water-Supply Paper 2220.
- Hoffman, J. 2019. *Development of a Daily Stochastic Streamflow Model for Probabilistic Water Resource Management*. Stellenbosch, University of Stellenbosch, Water Resource Management Course.
- Huizenga, J. M., Silberbauer, M., Dennis, R. & Dennis, I., 2013. An inorganic water chemistry dataset (1972-2011) of rivers, dams and lakes in South Africa. *Water SA*, 39(2), pp. 335-340.
- Jacobus, J. 2017. *Idas Valley Water Treatment Plant* [Interview] (12 September 2017).
- Klaasen, B. 2018. *Witzenberg Municipality Annual Report*, s.l.: Witzenberg Municipality.
- Lund, J.R., Jenkins, M. & Kalman, O. 1998. *Integrated Planning and Management for Urban Water Supplies Considering Multiple Uncertainties*, California: University of California Water Resources Center.
- Maas, L. & Du Plessis, J. 2017. *Comparison of Stochastic Streamflow Generators and the use thereof within the Water Resources Yield Model and MIKE Hydro Basin*, Stellenbosch: Stellenbosch University.
- Maddaus Water Management, 2003. *Water Conservation, Reuse and Recycling Master Plan*, County of Santa Clara: Standford University.
- Mahjoub, H., Mohammadi, M.M. & Parsinejad, M. 2011. Conjunctive Use Modeling of Groundwater and Surface Water. *Journal of Water Resource and Protection*, pp. 726-734.

- Marais, P. & Von Dückheim, F. 2011. Beaufort West Reclamation Plant: First Direct (Toilet-to Tap) Water Reclamation Plant in South Africa. *IMESA Conference Paper*, Volume 75th.
- Murray, R., Baker, K., Ravenscroft, P., Musekiwa, C. & Dennis, R. 2012. *A Groundwater Planning Toolkit for the Main Karoo Basin: Identifying and quantifying groundwater development options incorporating the concept of wellfield and aquifer firm yields*, Somerset West: Water Resource Commission, WRC Report No: 1763/1/11.
- Murray, R., Baker, K., Ravenscroft, P., Musekiwa, C., & Dennis, R., 2012. A groundwater-planning toolkit for the main Karoo basin: Identifying and quantifying groundwater-development options incorporating the concept of wellfield yields and aquifer firm yields. *Water South Africa*, Volume 38th No.3.
- Naude, H. 2017. *Stellenbosch Water Distribution System* [Interview] (11 August 2017).
- Nel, M. 2017. *Groundwater: The myths, the truth and the basics*, Pretoria: Water Research Commission.
- Nkwonta, O., Dzwauro, B., Otieno, F. & Adeyemo, J. 2017. A Review on Water Resources Yield Model. *South African Journal of Chemical Engineering*, Issue 23, pp. 107-115.
- Oduro-Kwarteng, S., Nyarko, K., Odai, S. & Aboagye-Sarfo, P. 2009. Water conservation potential in educational institutions in developing countries: case study of a university campus in Ghana. *Urban Water Journal*, 6(6), pp. 449-455.
- Onta, P.R., Gupta, A.D. & Harboe, R. 1991. Multistep Planning Model for Conjunctive use of Surface- and Ground-Water Resources. *Journal of Water Resources Planning and Management*, pp. 662-678.
- Onta, P.R., Gupta, A.D. & Richardo, H. 1991. Multistep Planning Model for Conjunctive Use of Surface- and Ground-Water Resources. *Journal of Water Resource Planning and Management*, 117(6), pp. 662-678.
- Patel, M., 2018. *Desalination in South Africa: Panacea or Peril for Industrial Development?*, Pretoria: Department of Trade and Industry.
- Pavelic, P., Giordano, M., Keraita, B., Ramesh, V., Rao, T., 2012. *Groundwater availability and use in sub-saharan Africa: A review of 15 countries*, Sri Lanka: International Water Management Institute.
- Pitman, W. 2011. *Overview of water resource assessment in South Africa: Current state and future challenges*. Kempton Park, Water Resource Commission.
- Ponce, V.M. 2007. *Sustainable Yield of Groundwater*. [Online] Available at: http://ponce.sdsu.edu/groundwater_sustainable_yield.html. [Accessed on 1 June 2019].

- Pulido-Velázquez, M., Andreu, J. & Sahuquillo, A. 2006. Economic Optimization of Conjunctive Use of Surface Water and Groundwater at Basin Scale. *Journal of Water Resources Planning and Management*, pp. 454-467.
- Purnama, S. & Marfai, M. 2012. Saline water intrusion towards groundwater: Issues and its control. *Journal of Natural Resources and Development*, Volume 2, pp. 25-32.
- Van Rooyen, P. & McKenzie, R. 2004. *Monthly Multi-Site Stochastic Streamflow Model*, Pretoria: Water Research Commission.
- Rayne of the Valley, 2015. *Australia and Israel Lead The Way On Water Conservation*. [Online] Available at: <https://www.raynedrops.com/australia-israel-lead-way-water-conservation/> [Accessed on 23 July 2019].
- SANCOLD, 2019. *Dams in South Africa*. [Online] Available at: <http://www.sancold.org.za/index.php/about/about-dams/dams-in-south-africa>.
- Schutte, F. 2006. *Handbook for the Operation of Water Treatment Works*. 1st ed. Pretoria: Water Research Commission.
- Seago, C. & McKenzie, R. 2008. *An Overview of Water Resources System Modelling in South Africa*. Pretoria, IAHS Publications-Series of Proceedings.
- Stellenbosch Municipality, 2017. *2017 Socio-economic Profile: Stellenbosch Municipality*, Stellenbosch: Western Cape Government.
- Sun, X. & Xu, Y., 2005. *A Water Balance Approach to Groundwater Recharge Estimation in Montagu Area of the Western Klein Karoo*, Bellville: University of Western Cape.
- Tarback, E., Lutgens, F. & Tasa, D. 2014. *An Introduction to Geology*. 11th ed. Harlow: Pearson Education Limited.
- Van Tonder, G., Bardenhagen, I., Riemann, K., Van Bosch, J., Dzanga, P. & Xu, Y. 2002. *Manual on pumping test analysis in fractured-rock aquifers*, Bloemfontein: Water Research Commission, WRC Report No 1116/1/02.
- Waldron, M. & Archfield, S. 2006. *Factors Affecting Firm Yield and the Estimation of Firm Yield for Selected Streamflow-Dominated Drinking-Water-Supply Reservoirs in Massachusetts*, Reston, Virginia: U.S. Geological Survey.
- Watkins, D.A. 1993. *The Relationship between Daily and Monthly Pan Evaporation and Rainfall Totals in Southern Africa*, Rhodes: Rhodes University.

- Wessels, P. & Rooseboom, A. 2009. Flow-gauging structures in South African rivers Part 1: An Overview. *Water SA*, 35(1).
- Withuser, K., Cobbing, J. & Titus, R. 2009. *National Groundwater Strategy: Review of GRA1, GRA2 and international assessment methodologies*, Pretoria: Department of Water Affairs.
- Wolski, P. 2018. *How severe is Cape Town's drought? A detailed look at the data*. [Online] Available at: <https://m.news24.com/SouthAfrica/News/how-severe-is-cape-towns-drought-a-detailed-look-at-the-data-20180123>. [Accessed on 16 July 2019].
- Woodford, A. & Rosewarne, P. 2005. *How much groundwater does South Africa have?*, Pretoria: Department of Water Affairs and Forestry.
- Woodford, A., Rosewarne, P. & Girman, J. 2005. *How much groundwater does South Africa have?*, Pretoria: Department of Water Affairs and Forestry .
- WWF-SA, 2016. *Water: Facts&Futures*, Cape Town: WWF-SA.
- Xu, C. 2002. *Hydrolic Models*. s.l.:Textbooks of Uppsala University. Department of Earth Sciences Hydrology.
- Xu, Y. & and Beekman, H. 2003. *Groundwater recharge estimation in Southern Africa*. Cape Town: UNESCO International Hydrological Programme (IHP).
- 5th World Water Forum, 2009. *Perspectives on Water and Climate Change Adaption*, s.l.: 5th World Water Forum.

APPENDIX A – USER GUIDE

**STOCHASTIC DAILY TIME-STEP MODEL FOR CONJUNCTIVE
USE OF SURFACE WATER, GROUNDWATER, DESALINATION
AND WATER RECLAMATION**

USER MANUAL

By Erika Gertrud Braune

Supervisor: Prof J.A. du Plessis

Stellenbosch University

October 2019

TABLE OF CONTENTS

Table of Contents	i
List of Figures	iii
1 Background	1
1.1 Minimum System Requirements.....	1
1.2 Installation of Software	2
1.3 Running of Software	2
1.4 Municipal Water Supply System	3
1.5 Overview of the Conjunctive Use Model.....	3
2 Streamflow Classification workbook.....	5
2.1 Input Daily Streamflow Data	6
2.1.1 Identify Streamflow Gauge	6
2.1.2 Retrieve Daily Streamflow from DWS website.....	7
2.1.3 Populate “RAW_DFLOW” sheet	10
2.2 Choose a Daily Distribution.....	10
2.3 Monthly Streamflow Ranges and Daily Distributions	11
2.4 Input Rainfall and Streamflow	11
2.4.1 WR2012 Rainfall Data.....	11
2.4.2 Populating the “HIST_RAIN” and “HIST_FLOW” worksheets.....	13
2.5 Rainfall-Runoff ratio.....	14
3 STOMSA	15
3.1 STOMSA Application	15
3.2 STOMSA File Combiner	17
4 Streamflow Disaggregation.....	19
5 Groundwater Simulation Workbook.....	21
5.1 Groundwater Resource Assessment Phase II data	22
5.2 Aquifer System Water Balance.....	22
5.3 Borehole Interference Test.....	24
6 Conjunctive System Simulation Workbook.....	26

6.1	Input Sheets.....	28
6.1.1	“EVAP” Worksheet	28
6.1.2	“AREA_CAPACITY” Worksheet.....	30
6.1.3	“DESAL” worksheet.....	32
6.1.4	“USE_1” Worksheet	32
6.1.5	“USE_2” Worksheet	33
6.1.6	“SIMULATION” Sheet	34
6.2	Time Series Graphs.....	39
6.2.1	“DAM_CAPACITY” Worksheet.....	39
6.2.2	“GW_CAPACITY” Worksheet	41
6.2.3	“CONJ_CAPACITY” Worksheet.....	41
6.3	Output Analysis Worksheets.....	42
6.3.1	“DRAFT_YIELD” Worksheet.....	42
6.3.2	“RELIABILITY” Worksheet.....	42
6.3.3	“SHORT_MNG” Worksheet	43

LIST OF FIGURES

Figure 1-1: “Enable Content” button	2
Figure 1-2: Example of a water supply system of a municipality	3
Figure 1-3: Setup of the conjunctive use model.....	4
Figure 2-1: “ <i>Streamflow Classification</i> ” workbook user interface	5
Figure 2-2: DWS website menu for downloading streamflow gauging stations’ files	7
Figure 2-3: Streamflow gauging stations file opened with <i>Google Earth</i>	7
Figure 2-4: DWS website – <i>Hydrology-verified</i> interface (DWS, 2019).....	8
Figure 2-5: Streamflow gauging station database on the DWS hydrology website.....	8
Figure 2-6: Daily streamflow data set displayed on the DWS hydrology website	9
Figure 2-7: Daily streamflow input (“RAW_DLOW”) worksheet.....	10
Figure 2-8: Daily distributions in streamflow classes in the “DISTR_CHOOSER” worksheet	11
Figure 2-9: The Water Resource Centre (WR2012 online database) and its folders	12
Figure 2-10: The “HIST_RAIN” worksheet with rainfall data inputs	13
Figure 2-11: “HIST_FLOW” worksheet with naturalized streamflow data inputs	14
Figure 3-1: STOMSA new project user interface steps 2 and 3	15
Figure 3-2: STOMSA user interface steps 4 and 5	16
Figure 3-3: STOMSA user interface step 6	16
Figure 3-4: “ <i>STOMSA File Combiner</i> ” user interface	17
Figure 3-5: File Explorer window to navigate to required folder	17
Figure 3-6: “Text to Columns” button in the “STOMSA_Superfile” worksheet	18
Figure 3-7: “Convert Text to Columns” user interface	18
Figure 3-8: Saving the “STOMSA_Superfile” as an Excel file with “.xlsx” extension	19
Figure 4-1: “Streamflow Disaggregation” workbook User Interface	19
Figure 4-2: Selection window upon selecting the “copy” buttons	20
Figure 5-1: “ <i>Groundwater Simulation</i> ” workbook user interface.....	21
Figure 5-2: GRAII page of the DWS groundwater website.....	22
Figure 5-3: Information boxes for the “Calcs_Balance_1” sheet	24
Figure 5-4: “Borehole Information” box	25
Figure 5-5: Calculated radius of influence and borehole interference	25
Figure 6-1: The “ <i>Conjunctive System Simulation</i> ” workbook user interface	26
Figure 6-2: “Browse for workbook” window to navigate to required workbook	27
Figure 6-3: Links to different input worksheets for each system component.....	28
Figure 6-4: Evaporation coefficients for the “EVAP” input worksheet.....	29
Figure 6-5: Monthly S-pan evaporation percentages of MAE per evaporation zone	29
Figure 6-6: “AREA_CAPACITY” worksheet with graphs	30

Figure 6-7: Adding a trendline to the Surface Area-Capacity curve or the Depth-Capacity curve	31
Figure 6-8 "Format Trendline" window	31
Figure 6-9: "DESAL" worksheet with capacity and unit amount options	32
Figure 6-10: "USE_1" downstream abstraction requirements input worksheet	33
Figure 6-11: "USE_2" worksheet for municipal demand distributions	33
Figure 6-12: "SIMULATION" worksheet overview.	34
Figure 6-13: "Catchment of Origin Hydrology" information box	34
Figure 6-14: "Dam Characteristics" information box	35
Figure 6-15: "Inflow Characteristics" information box (Streams 1, 2, and 3)	36
Figure 6-16: Conjunctive use components information box	37
Figure 6-17: "System Yield for Long Term Yield Analysis" information box	37
Figure 6-18: Firm yield point information boxes and buttons	38
Figure 6-19: Progress bar for firm yield calculations	38
Figure 6-20: "DAM_CAPACITY" worksheet with graphs	39
Figure 6-21: Pop up menu with "Format Axis" option	40
Figure 6-22: "Format Axis" tab with options for selection	40
Figure 6-23: "GW_CAPACITY" worksheet with groundwater-time graph	41
Figure 6-24: "CONJ_CAPACITY" worksheet with conjunctive use capacity graph	41
Figure 6-25: "DRAFT_YIELD" worksheet with historical firm yield point	42
Figure 6-26: "RELIABILITY" Worksheet with long-term reliability graph	43
Figure 6-27: "SHORT_MNG" worksheet with Short-Term Management Curve	44

1 BACKGROUND

The stochastic, daily time-step model for the conjunctive use of water resources was developed as a tool to aid municipalities in planning and management decisions regarding their water supply systems and the use thereof. The water sources (components) incorporated into the model include: surface water, groundwater, desalination and water reclamation. The stochastic interrelationships between the different water resources were also incorporated into the model. The model performs a historical yield analysis, a long-term planning analysis, as well as a short-term management analysis. The conjunctive use model was developed in Microsoft Office Excel (2016) and programmed with Visual Basic Application (VBA) for the convenience of the user.

The conjunctive use model consists of 4 Microsoft Excel workbooks, which make use of 3 databases (available online) to populate its initial input data fields. The model also requires the use of a stochastic sequence generator called STOMSA (Stochastic Model of South Africa) and a text file processing program, Visual Studio application for preparing STOMSA output, as required for Excel input.

The purpose of this document is to guide the user through the processes involving this model, from data retrieval and data preparation, to populating the required workbooks, which makes use of automated computations when performing a yield analysis.

Disclaimer:

Although every effort has been made to ensure accuracy and applicability contained in this software and supporting databases, the Stellenbosch University and the developer cannot accept any legal responsibility or liability for any errors or omissions or for any other reason whatsoever. Copy right © 2019 Stellenbosch University. All rights reserved.

1.1 Minimum System Requirements

The minimum system requirements for running the model on a computer:

- 2 GB of RAM;
- 500 Mb Hard Disk capacity;
- Windows 2016/2016XP or more recent Windows operating system;
- Microsoft Office 2016; and
- CD ROM drive

Note: This model and its programming is not compatible with versions earlier than Microsoft Office 2010 products. The unprotected, white cells in the worksheets are primarily used for input data, manually inserted by the user, and must be free of data before commencing with a new yield analysis. Thus, any contents previously entered into these specific cells are to be cleared by the user or by a clear button if provided.

1.2 Installation of Software

The conjunctive use model is installed on the CD accompanying this report. The CD contains the following files:

- STOMSA stochastic generator program and STOMSA user guide
- STOMSA File combiner program
- Streamflow Classification.xlsm (Excel 2016 Macro-enabled workbook, 4.3 MB)
- Streamflow Disaggregation.xlsm (Excel 2016 Macro-enabled workbook, 92 MB)
- Groundwater Simulation.xlsm (Excel 2016 Macro-enabled workbook, 5.7 MB)
- Conjunctive System Simulation (Excel 2016 Macro-enabled workbook, 66.5 MB)
- Conjunctive_use_model_UserManual.pdf (Adobe Acrobat document).

It is suggested that these files are saved in the following created location:
C:\Conjunctive_use_model\directory

The instructions in this manual automatically assume that files are stored at that location.

1.3 Running of Software

Once these files are stored in the applicable directory, the user has to open the first Excel workbook namely: “*Streamflow Classification*” workbook. The user has to follow the sections outlined in this document for each of the 4 Excel workbooks forming part of the conjunctive use model. Upon opening the “*Streamflow Classification*” workbook, a security warning will appear, notifying the user that the macros in the workbook have been disabled (Figure 1-1). The user has to click on the “Enable Content” button. Upon clicking the “Enable Content” button another message appears where the user has to press “OK”. The macros have to be enabled for every workbook, upon opening the workbook.

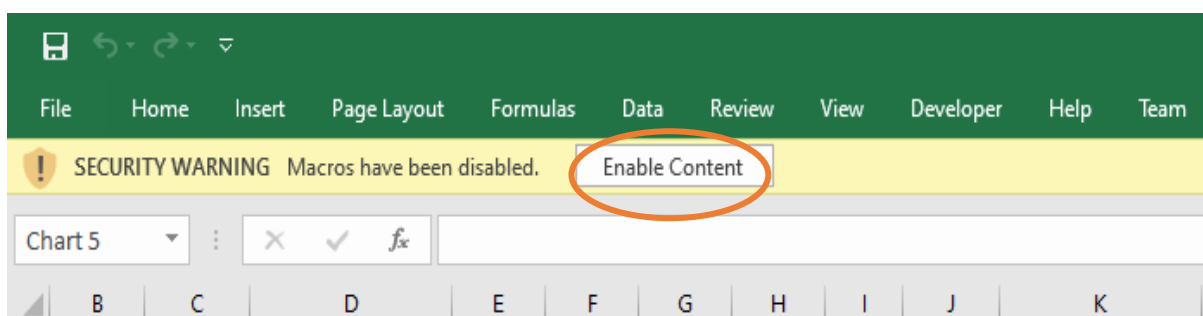


Figure 1-1: “Enable Content” button

1.4 Municipal Water Supply System

The setup of a municipal water supply system, for which this model was developed, is illustrated in Figure 1-2. If the municipality has 2 or more storage dams in the system, they will be modelled as 1 storage dam with multiple inflow streams (off-channel and in-channel). Desalination and groundwater directly contribute to the supply system without being stored.

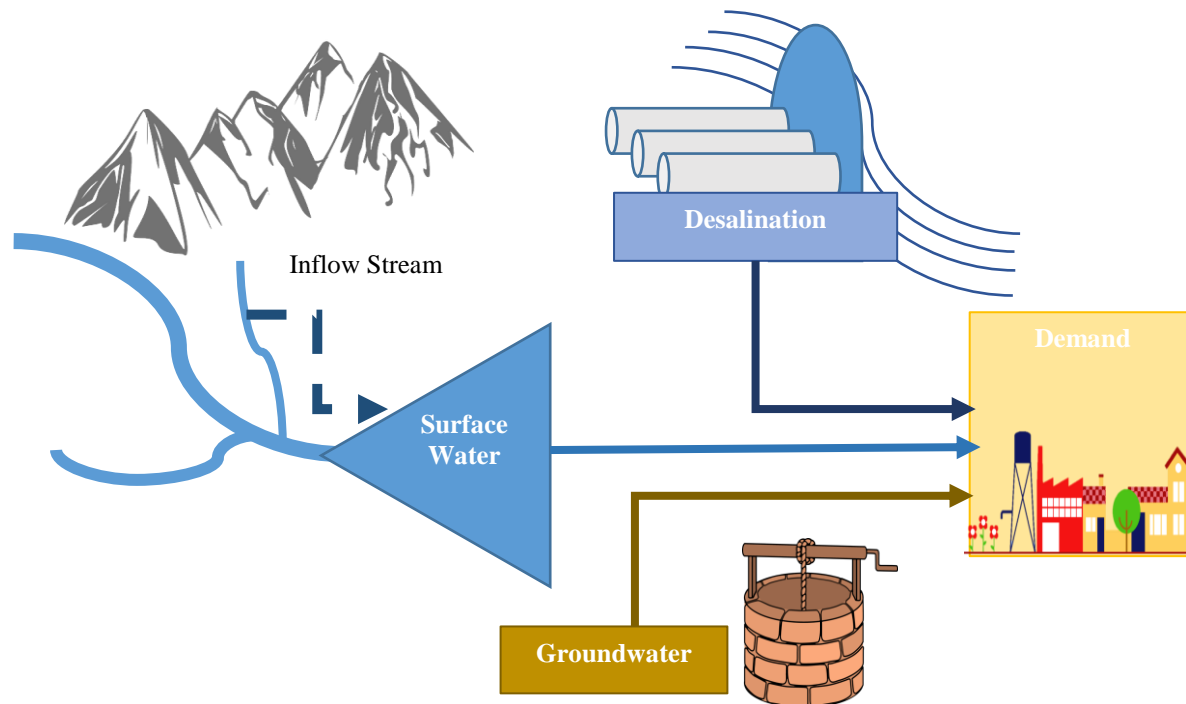


Figure 1-2: Example of a water supply system of a municipality

1.5 Overview of the Conjunctive Use Model

A flow diagram of the setup of the conjunctive use model is illustrated in Figure 1-3. The databases (available online) used for initial input data are that of the Department of Water and Sanitation (DWS) (hydrology and groundwater), as well as the Water Resources (WR2012) database. Streamflow data recorded at various streamflow gauging stations are retrieved from the DWS hydrology website and online database, while the Groundwater Resource Assessment Phase II (GRA II) data, pertaining to groundwater recharge and aquifer parameters are obtained from the DWS groundwater database. Rainfall data for the catchment in the study area is obtained from the WR2012 database. STOMSA is used to generate stochastic sequences and a “STOMSA File Combiner” program combines the output (text files). Results of borehole yield tests are obtained from the municipality.

The 4 Excel workbooks are: *Streamflow Classification*, *Streamflow Disaggregation*, *Groundwater Simulation* and *Conjunctive System Simulation*. This user manual covers the data retrieval and preparation process required for each workbook, as well as the instructional steps taken to start the automated computations of the model.

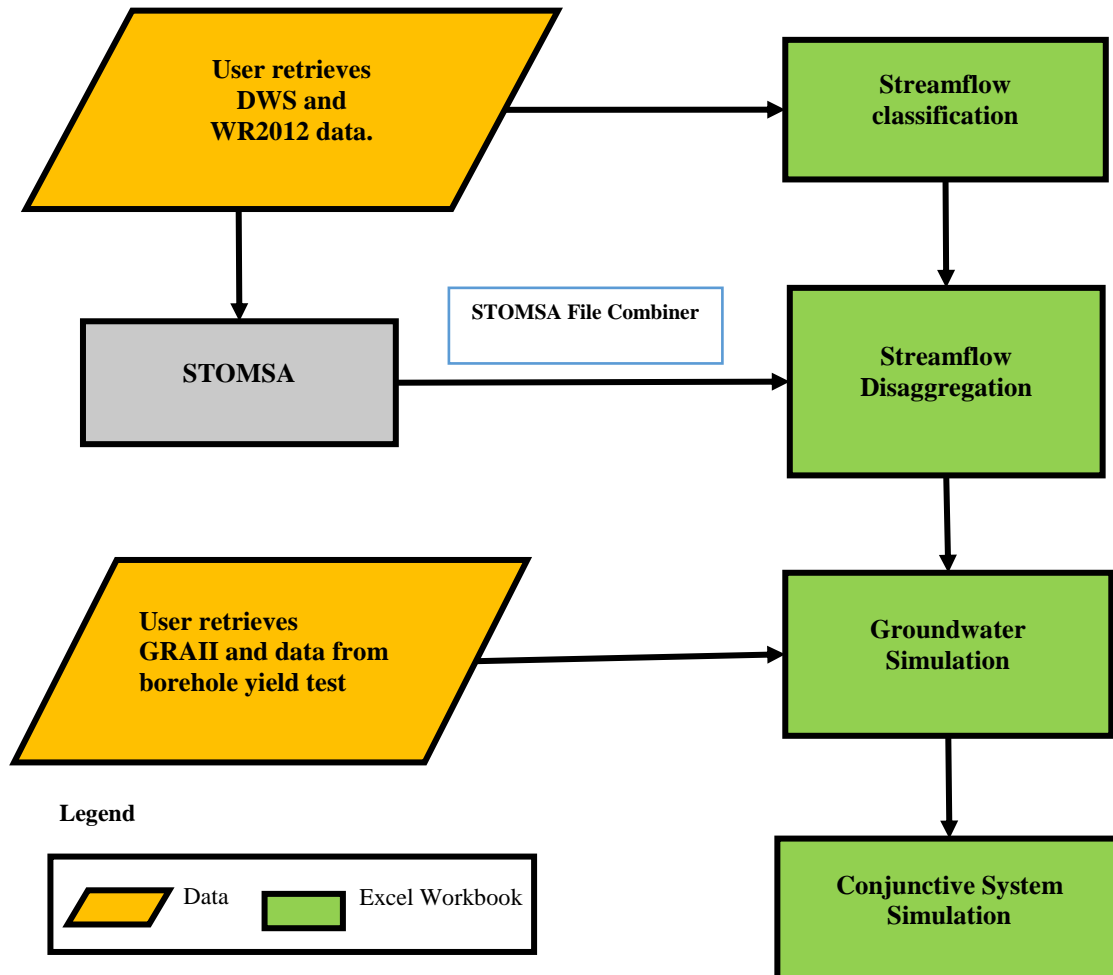


Figure 1-3: Setup of the conjunctive use model

The data retrieval process from the DWS website and online database to obtain gauging station (streamflow) information, as well as data retrieval from the WR2012 database to obtain catchment-based rainfall and streamflow information, is discussed in section 2. The “*Streamflow Classification*” workbook, its required input data and its user interface, is discussed in section 2. The preparation of data for input into STOMSA and the processing of output data files are outlined in section 3. Section 4 describes the steps taken in the “*Streamflow Disaggregation*” workbook. Data retrieval from the GRA II (DWS groundwater database), as well as the “*Groundwater Simulation*”, is discussed in section 5. The “*Conjunctive System Simulation*” workbook is discussed in section 6.

Every workbook has a start page displaying a user interface, where the instructions are outlined and the user is required to select the associated buttons in numerical order.

2 STREAMFLOW CLASSIFICATION WORKBOOK

The first workbook in the conjunctive use model is the “*Streamflow Classification*” workbook. The “START” sheet of the “*Streamflow Classification*” workbook is illustrated in Figure 2-1, where an overview of the procedures, performed in this workbook, are outlined in the user interface. The flow diagram prompts the user through a number of steps to be taken (in numerical order), during the streamflow classification process. There are specific buttons to select for each step, which upon selection, transfers the user to the respective worksheets, where input data is required. The input (orange) and output (green) worksheets are colour coded for the convenience of the user. There are 4 worksheets in this workbook which require user input, namely: “RAW_DFLOW”, “DISTR_CHOOOSE”, “HIST_RAIN”, and “HIST_FLOW”. There are 2 output worksheets, which do not require user input, but display results, namely: “RANGES”, “DISTR” and “RAIN_RUNOFF”.

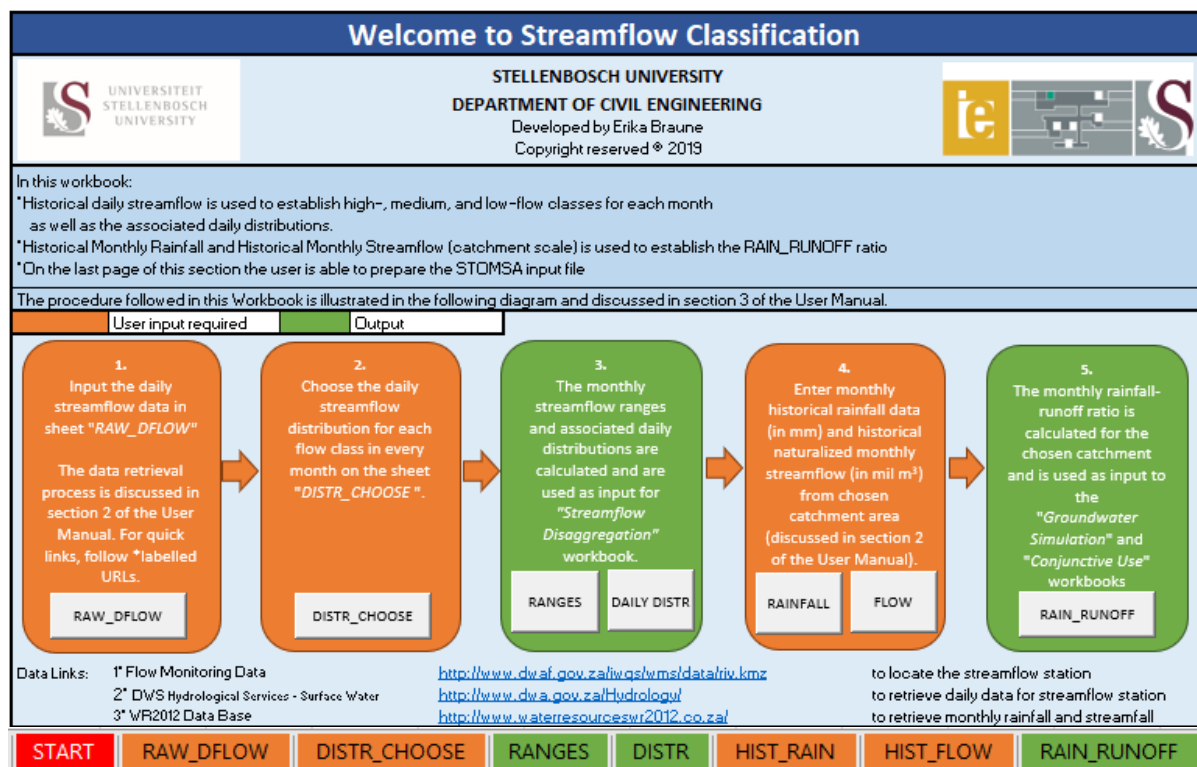


Figure 2-1: “*Streamflow Classification*” workbook user interface

The steps followed during the streamflow classification process are as follows:

Step1 - Historical streamflow data recorded at the applicable gauging station is obtained from the DWS online database and then used to populate the “RAW_DFLOW” worksheet. The streamflow data is processed to obtain a variety of daily streamflow distributions. This step is explained in section 2.1.

Step 2 – The most suitable daily distribution is chosen from a number of daily distributions within each monthly flow category (low, medium and high flow) for every month in the “DISTR_CHOOOSE” worksheet. This step is explained in section 2.2

Step 3 – The streamflow classes have ranges which are automatically generated in the “RANGES” sheet. The chosen daily distributions are automatically summarized for every flow class in every month in a summary sheet called “DISTR”. Both of these sheets consist of output data used to later populate the “*Streamflow Disaggregation*” workbook. This step is explained in section 2.3.

Step 4 – Historical monthly rainfall and naturalized historical monthly streamflow data is retrieved from the WR2012 database and used to populate the “HIST_RAIN” sheet and the “HIST_FLOW” sheet respectively. This step is explained in section 2.4.

Step 5 – The monthly historical rainfall-runoff relationships are automatically determined for the catchment included in the analysis in the “RAIN_RUNOFF” worksheet, by using both the monthly rainfall data and monthly streamflow data. This step is explained in section 2.4

2.1 Input Daily Streamflow Data

The first type of input data required for the “*Streamflow Classification*” workbook is the daily streamflow data, recorded at a streamflow gauging station. The user identifies the applicable streamflow gauging station according to the criteria discussed in section 2.1.1. The streamflow gauging station number is then used to retrieve the daily data in the DWS online database, after which the “RAW_DFLOW” worksheet is populated.

2.1.1 Identify Streamflow Gauge

To enable the user to search for an applicable streamflow gauging station on the DWS online database, the station should satisfy the following criteria:

- It should be situated in the quaternary catchment where the abstraction or diversion takes place, in other words where the water supply is sourced from;
- It should be located in close proximity to the point of abstraction or diversion;
- It should have a record of at least 20 years of daily streamflow data, preferably continuous.

To select the applicable streamflow gauging station, a *Google Earth* file (.kml file), containing all the stations across South Africa, is downloaded from the following website (Figure 2-2): <http://www.dwa.gov.za/iwqs/wms/data/000keyh.asp>. Once the website is opened, the user navigates to the menu on the left of the page and selects the “rivers” link under the “Hydrological sites” section, as indicated in Figure 2-2. The *Google Earth* file downloads automatically.

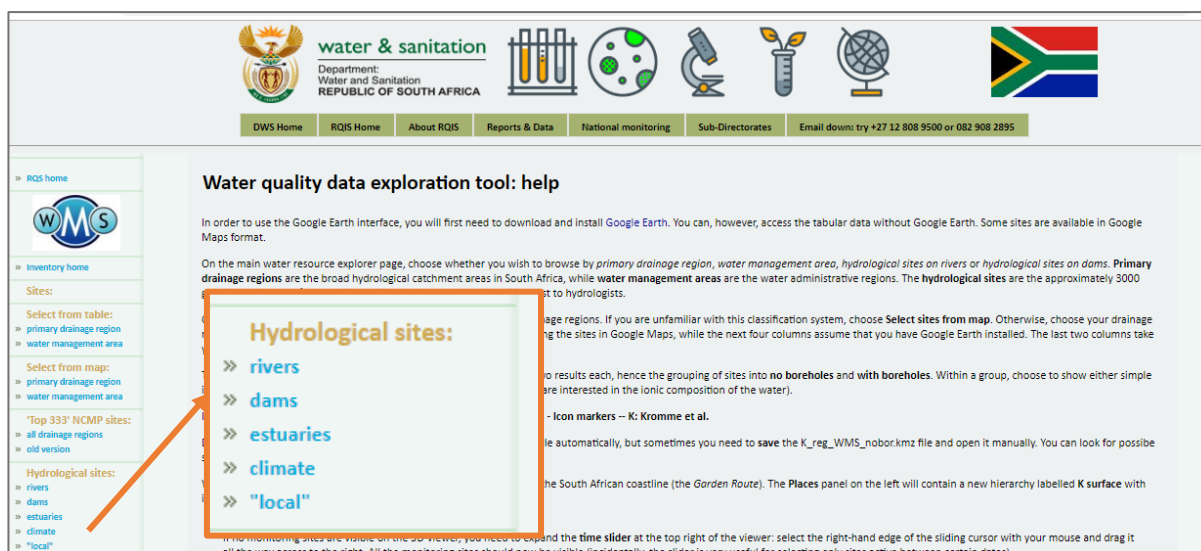


Figure 2-2: DWS website menu for downloading streamflow gauging stations' files

After downloading the file, it is opened with the *Google Earth* application and the location of the streamflow gauging stations are displayed on a satellite image of the earth's surface, as enlarged in Figure 2-3. Upon selecting the specific station, a pop-up will appear, indicating the date of commencement of operation, as well as other information related to streamflow recording.



Figure 2-3: Streamflow gauging stations file opened with *Google Earth*

2.1.2 Retrieve Daily Streamflow from DWS website

After the applicable streamflow gauging station is identified, the DWS *Hydrology* website can be opened using this link: <http://www.dwa.gov.za/Hydrology/Verified/hymain.aspx>

In the event that the user experiences technical difficulties with the abovementioned link, an alternative link is provided: <http://intertest.dwa.gov.za/Hydrology/hymain.aspx>.

The DWS hydrology website which serves as an online database displays options for selection and fields to be populated. By selecting “River” as the “Station type” and populating the “Station no.” field with the applicable gauging station number, as indicated in Figure 2-4, the recorded streamflow data can be accessed by selecting the “Access station data” button.

Figure 2-4: DWS website – *Hydrology-verified* interface (DWS, 2019)

The website directs the user to the data sheet for the gauging station, as indicated in Figure 2-5. The user is required to click on the “Daily Avg. Flow” button, which opens a page containing a text file with daily streamflow flow rates in cubic meters per second (m^3/s). This online text file serves as the input data to the “*Streamflow Classification*” workbook. On occasion more than one data retrieval attempt is necessary to obtain the complete available streamflow record, as only 20 years of the historical record is available at a time. The second and third data retrievals can be performed by changing the start date according to the next data set required.

Station Number-Type	Variable	Component	Start Date	End Date	Volume (Multiples of m^3)	Flow (m^3/s)	Primary Data
G2H037-RIV	100.00	Jonkershoek @ Kleinp	1989-06-15	2019-02-26	Monthly Volume	Daily Avg. Flow	Primary Data

Figure 2-5: Streamflow gauging station database on the DWS hydrology website

The data can be directly copied from the webpage to populate the “RAW_DFLOW” worksheet of the “*Streamflow Classification*” workbook, as illustrated in Figure 2-7.

It is required that the streamflow record in use starts on the 1st of October in the first year of the available historical record, as October is regarded as the start of the hydrological year. The data set of the daily streamflow record displayed on the webpage can be selected by pressing “Ctrl+Shift+End” buttons on the keyboard, which will copy the information.

Data are continuously updated and reviewed.
The format of this file is as follows:
POS. 1-8 = Date of daily flow CCYYMMDD
POS. 10-18 = Daily avg flow rate in cubic metres/sec 99999.999
POS. 20-24 = Quality code

G2H037
Variable 100.00 Surface Water Level

DATE	D	AVG	F/R	QUAL
19891001		0.543		1
19891002		0.598		1
19891003		0.533		1
19891004		0.539		1
19891005		1.635		1
19891006		0.760		1
19891007		0.554		1
19891008		4.462		1
19891009		1.945		1
19891010		0.944		1
19891011		0.670		1
19891012		0.589		1
19891013		0.488		1
19891014		0.435		1
19891015		1.757		1
19891016		0.887		1
19891017		0.548		1
19891018		0.450		1
19891019		1.066		1
19891020		0.654		1
19891021		1.888		1
19891022		1.024		1
19891023		1.482		1
19891024		0.619		1
19891025		0.516		1
19891026		0.516		1

Select data from the 1st of October until the end of the data set and copy.

Figure 2-6: Daily streamflow data set displayed on the DWS hydrology website

2.1.3 Populate “RAW_DFLOW” sheet

The user clicks on the “RAW_DFLOW” button on the user interface page of the “*Streamflow Classification*” workbook, which will redirect to the “RAW_DFLOW” worksheet. Select the “Clear Data” button to ensure that no data from previous modelling attempts remain in the worksheet, before populating it. The daily streamflow text retrieved from the DWS online database (Figure 2-6) is pasted into the indicated field under the “*Input text string*” heading (Figure 2-7). The input data starts on the 1st of October in the first year of the available streamflow record. The end date of the first data set is automatically indicated in the “RAW_DFLOW” worksheet and the date after that is used to indicate the start date of the second data retrieval. This retrieval procedure is repeated until the complete historical record available is obtained. The user enters the streamflow gauging station number in the block indicated in orange.

Raw Historical Daily Flow Rate Data (DWS)									
Clear Data		Flow Gauge Number	G2H037	Start Date	1989/10/01	End Date	2019/01/31	MAR	22.1651 mil m ³
Input text string		Date String	Year	Month/day	Month	Day	Concatenate Reference	Flow Rate (m ³ /s)	Count
19891001	0.543 1	19891001	1989	1001	10	1	1989101	0.543	10715
19891002	0.598 1	19891002	1989	1002	10	2	1989102	0.598	1
19891003	0.533 1	19891003	1989	1003	10	3	1989103	0.533	1
19891004	0.539 1	19891004	1989	1004	10	4	1989104	0.539	1
19891005	1.635 1	19891005	1989	1005	10	5	1989105	1.635	1
19891006	0.760 1	19891006	1989	1006	10	6	1989106	0.76	1
19891007	0.554 1	19891007	1989	1007	10	7	1989107	0.554	1

Figure 2-7: Daily streamflow input (“RAW_DFLOW”) worksheet

2.2 Choose a Daily Distribution

In the “*DISTR_CHOUSE*” worksheet (Figure 2-8) the low, medium and high streamflow classes for 12 months are displayed. The user chooses the most appropriate daily distribution in each flow class for every month according to the following criteria:

- The streamflow distribution should reflect the dominant trend within the month.
- If a daily distribution reflects the number of daily spikes which are repeated throughout the other daily distributions in the month, the respective distribution is chosen.
- If a daily distribution reflects the magnitude of the daily spike which is repeated a number of times, it is chosen.

Upon examination of the graphs in the worksheet and considering the abovementioned criteria, the appropriate distributions for each streamflow class are selected by either changing the values in the white fields (see option 1 in Figure 2-8), or the user can select a value within the specific range, and click on a button to assign that value to all the streamflow classes of all the months (see option 2 in Figure 2-8).

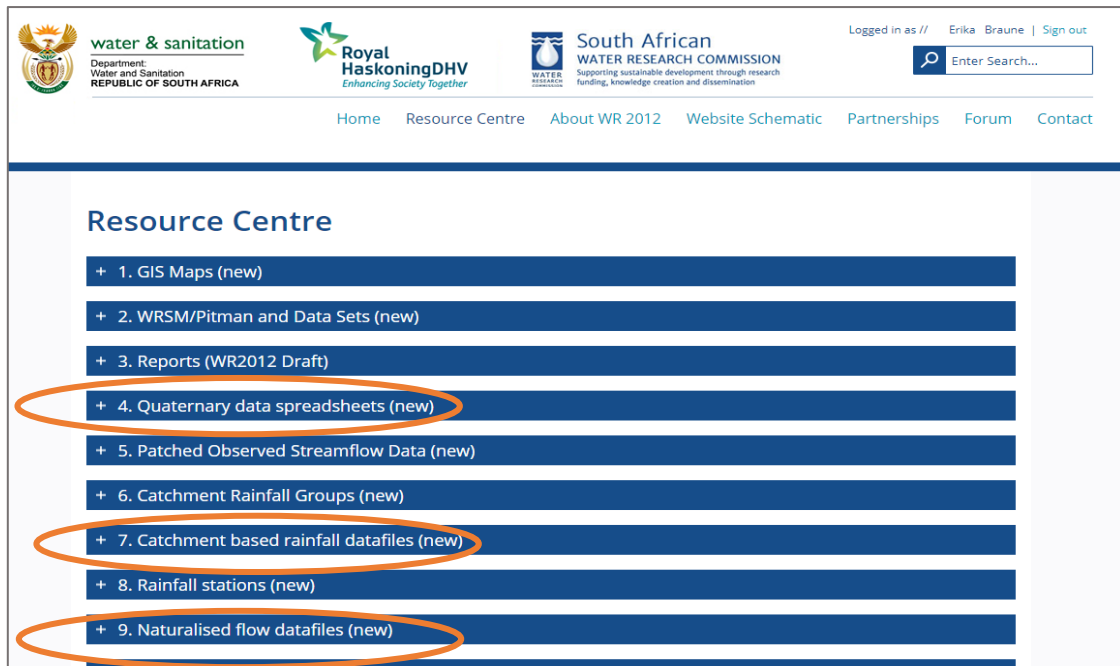


Figure 2-9: The Water Resource Centre (WR2012 online database) and its folders

The folders of interest to the user are: “*Quaternary data spreadsheets*”, “*Catchment based rainfall datafiles*” and “*Naturalized flow datafiles*”, as indicated in Figure 2-9. It is required that the user knows in which Water Management Area (WMA) the catchment of interest (where the abstraction or diversion point is located) falls, as the subfolders are arranged according to the WMAs.

The “*Quaternary data spreadsheets*” folder contains quaternary catchments’ information for the listed WMAs. The user clicks on the folder and selects the applicable WMA, after which an Excel file is automatically downloaded. The user opens the Excel file and expands the worksheet to access information specific to the quaternary catchments in the WMA, such as: area, S-pan evaporation, evaporation zone, rainfall zone, Mean Annual Precipitation (MAP), and Mean Annual Runoff (MAR). This information pertaining to the quaternary catchment in the study area, is required to populate a number of fields in worksheets, during the use of the Excel workbooks of the conjunctive use model.

The rainfall zone for the quaternary catchment where abstraction or diversion takes place (water is sourced from) is identified and used during the next step.

The “*Catchment based rainfall datafiles*” folder contains rainfall data in percentages of MAP for the rainfall zones (stations) located within the listed WMAs. The user selects the applicable WMA and a list of rainfall stations appear. Upon selecting the applicable rainfall station (as identified during the previous step), a text file is automatically downloaded. The text file can be opened with the Microsoft Notepad application. This data is used to populate the “HIST_RAIN” worksheet in the “*Streamflow Classification*” workbook.

The “*Naturalized flow datafiles*” folder contains simulated monthly streamflow volumes expressed in million cubic meters per month (mil m³/month). The user selects the “*individual naturalized flow datafiles*” option provided under the folder (not the “download complete set” option), after which a list of quaternary catchment numbers will appear. The user selects the applicable quaternary catchment number, and the text files are automatically downloaded, to be opened with Microsoft Notepad. Data can be retrieved in this manner for various catchments as necessary. The naturalized flow data of the selected quaternary catchment is copied into the “HIST_FLOW” worksheet of the “*Streamflow Classification*” workbook.

2.4.2 Populating the “HIST_RAIN” and “HIST_FLOW” worksheets

In the user interface on the “START” page of the “*Streamflow Classification*” workbook, the “RAINFALL” and “FLOW” buttons redirect the user to the “HIST_RAIN” and “HIST_FLOW” worksheets respectively. These worksheets are equipped with 2 instruction buttons, which aid the user-input process. In the “HIST_RAIN” sheet the user is required to fill out the blank fields with the quaternary catchment number, the rainfall station number and the MAP, as indicated in Figure 2-10. In the top left corner of the worksheet, a “Clear Data” button is selected to clear any residual data of previous yield analyses, for new data to be inserted. The rainfall data, as downloaded from the WR2012 online database, is pasted into the “Paste Raw text data in” field as text, after which the “Text to Columns” button is selected to populate the respective fields. These steps are numbered 1 to 3, for the convenience of the user, on the buttons and sheet. The user selects the “YES” option after being prompted about the population of the worksheet.

1. Clear Data		3.Text To Columns		Catchment Based Rainfall (WR2012)							
Quaternary catchment		G22F	Rainfall Class		G2C	MAP	1465 (mm)				
Mean Monthly Precipitation (MMP)		86.57	61.43	46.00	31.00	38.44	42.84	111.13	205.14	268.00	
2. Paste Raw text data in		Year	OCT	NOV	DEC	JAN	FEB	MAR	APR	MAY	JUN
g1c		1920	161.2	68.1	161.0	93.3	179.5	0.0	138.1	19.6	680.6
g1c		1921	74.3	72.8	68.0	216.8	10.8	10.8	198.9	107.2	410.6
g1c		1922	48.5	10.3	0.0	46.3	0.0	35.3	93.8	422.2	586.9
g1c		1923	106.4	114.3	33.0	31.6	27.2	38.2	98.4	27.7	373.0
g1c		1924	169.1	252.0	0.0	87.2	11.3	27.2	0.0	133.6	947.3

Figure 2-10: The “HIST_RAIN” worksheet with rainfall data inputs

The “HIST_FLOW” sheet requires the user to fill out the blank fields with the quaternary catchment number and the MAR, as indicated in Figure 2-11, after which the user follows the same procedure (numbers 1 to 3) as used in the “HIST_RAIN” worksheet, except this time the naturalized streamflow data is pasted in the “Paste Raw text data in” field, and not the rainfall data. Once the data is distributed over the respective columns by selecting the “Text to Columns” button, the naturalized streamflow data can be prepared as input for generating stochastic sequences with STOMSA. This is done by clicking

on the “Prepare Streamflow data for STOMSA” button. Upon selecting the button a new Excel worksheet (outside of the “*Streamflow Classification*” workbook) is automatically created with the streamflow data already inserted and column width set to 8 pixels (as required for STOMSA input). The user then saves and stores this new Excel file at a convenient location on an electronic or portable device (PC or USB) and closes the file. The user then clicks on the closed file to change the file extension to “.INC”, which renders it ready for STOMSA input. Processes involving STOMSA are discussed in section 4.

1. Clear Data		3.Text To Columns		Naturalized Catchment Data (WR2012)												START	
Quaternary catchment:		G22F		MAR		36.58 mil m ³		Units in:		mil m ³ /month							
Mean Monthly Precipitation (MMP)		3.24	1.98	1.03	0.55	0.41	0.46	1.42	3.59	5.89	6.67	6.46	4.87	36.58			
2. Paste Raw text data in A5 as instructed in comment		OCT	NOV	DEC	JAN	FEB	MAR	APR	MAY	JUN	JUL	AUG	SEP	Year Total			
1920		2.26	1.25	0.54	0.5	0.41	0.3	0.6	0.5	16.9	14.1	7.9	4.6	49.8			
1921		2.25	1.06	0.78	1.65	0.94	0.8	0.8	1.8	9.9	7.0	6.5	5.0	38.5			
1922		2.22	1.04	0.48	0.24	0.12	0.1	1.2	7.3	13.4	10.8	7.0	4.9	48.7			
1923		3	2.79	1.59	0.6	0.39	0.5	0.5	2.2	6.5	6.0	6.1	4.3	34.4			
1924		2.83	3.05	1.5	0.45	0.23	0.1	0.1	1.3	10.3	10.7	6.2	3.1	39.8			

Figure 2-11: “HIST_FLOW” worksheet with naturalized streamflow data inputs

After filling in the input data in the “*Streamflow Classification*” workbook, it has to be saved as a macro-enabled workbook (section 1.1.3), preferably with a name starting with *Streamflow Classification* and the quaternary catchment.

2.5 Rainfall-Runoff ratio

The “RAIN_RUNOFF” button under step 5 on the user interface of the “*Streamflow Classification*” workbook redirects the user to the “RAIN_RUNOFF” worksheet. The rainfall-runoff relationship is automatically calculated and updated after the user has filled out the “HIST_RAIN” and “HIST_FLOW”. The rainfall-runoff ratio will be used at a later stage as input to the “*Groundwater Simulation*” and “*Conjunctive Use*” workbooks, discussed in sections 5 and 6 respectively.

After populating the fields in the worksheets with input data, the “*Streamflow Classification*” workbook, is saved (and stored at a convenient location) as a macro-enabled workbook, preferably with a name containing the terms “*Streamflow Classification*” and the number of the quaternary catchment in the study area.

3 STOMSA

The STOMSA application generates 101 stochastic streamflow sequences using the historical naturalized streamflow sequences, previously prepared, as discussed in section 2.4.2. The stored “.INC” file containing the prepared monthly naturalized streamflow data is used as input into STOMSA. An outline of the steps followed for generating stochastic sequences with STOMSA and the steps followed to use the “*STOMSA File Combiner*” are discussed in sections 3.1 and 3.2.

3.1 STOMSA Application

The STOMSA application is installed on the CD which accompanies this user manual. The STOMSA start page is provided in Figure 3-1. The process followed when using STOMSA, can be divided into 6 steps, as outlined below and indicated in Figure 3-1:

1. Open the STOMSA application.
2. Click on the “Create a new project” file icon and choose the folder, after which the file containing the previously saved “.INC” file is selected (Figure 3-1).
3. Select the “.INC” file and click on the “Add>>” button (Figure 3-1).
4. Select the yellow key icon to and select the key gauge (Figure 3-2).
5. Select the green “GO” button (Figure 3-2).
6. Tick the box to “save data in file” (6.1), select all streamflow gauges (6.2), then generate the sequences (6.3) and then select an appropriate folder (6.4) to save the stochastic sequences in. (Figure 3-3).

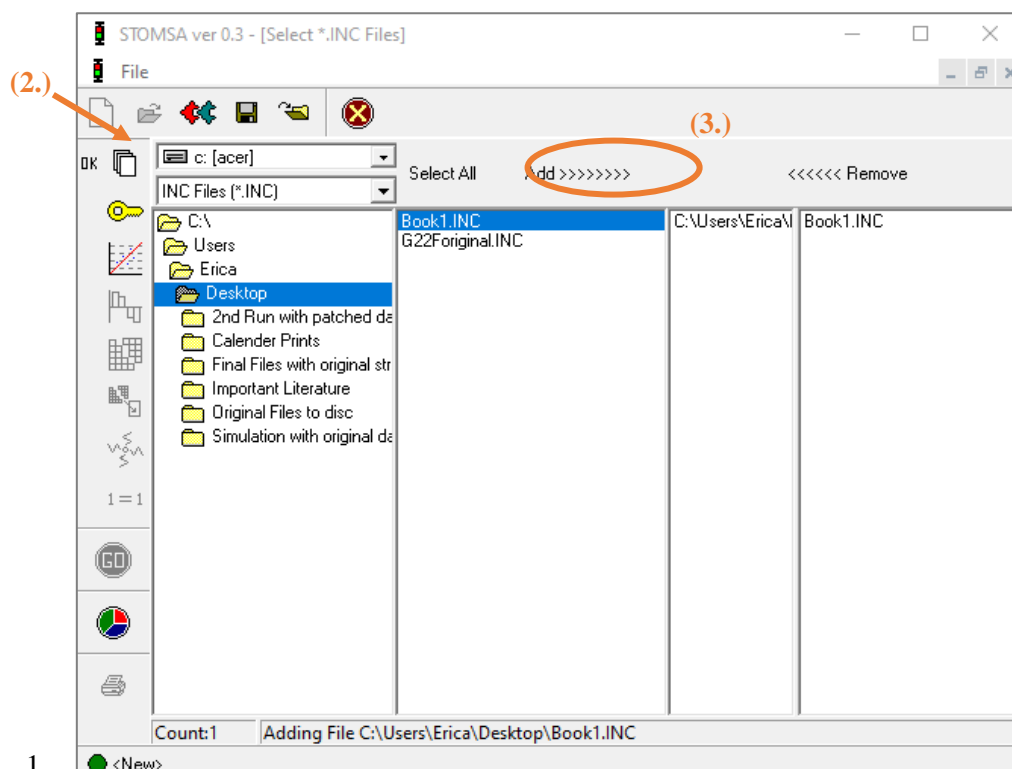


Figure 3-1: STOMSA new project user interface steps 2 and 3

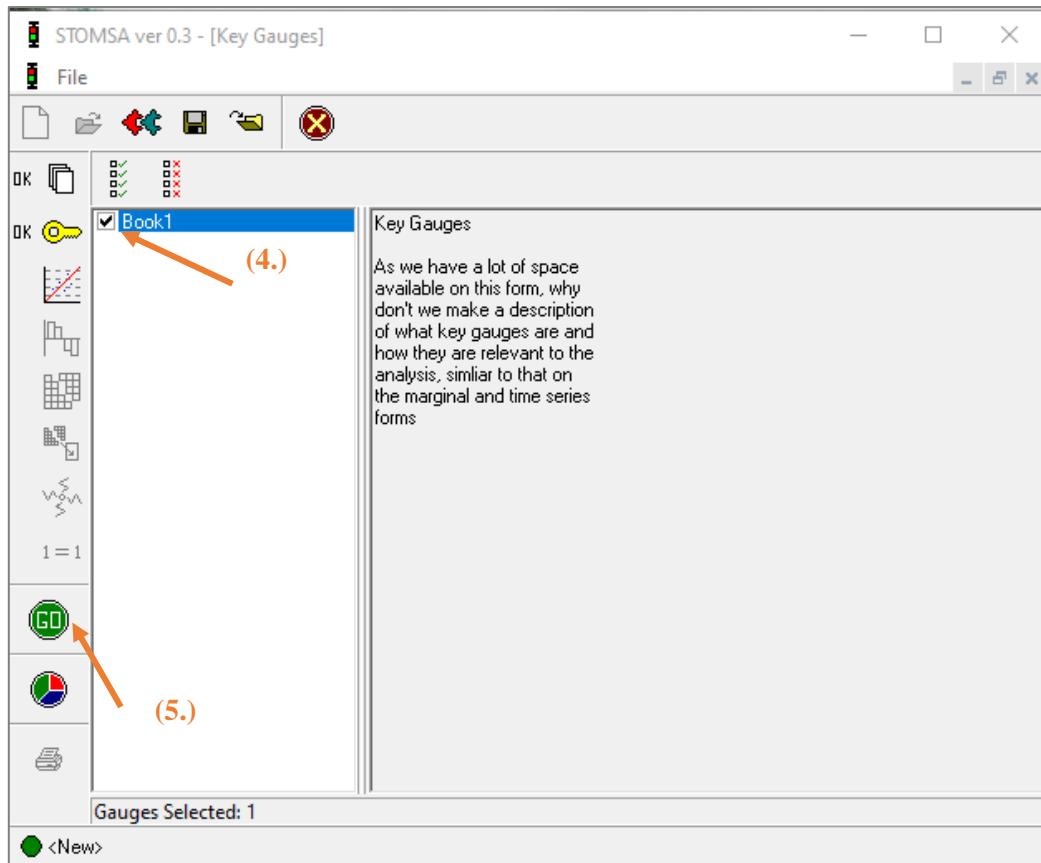


Figure 3-2:STOMSA user interface steps 4 and 5

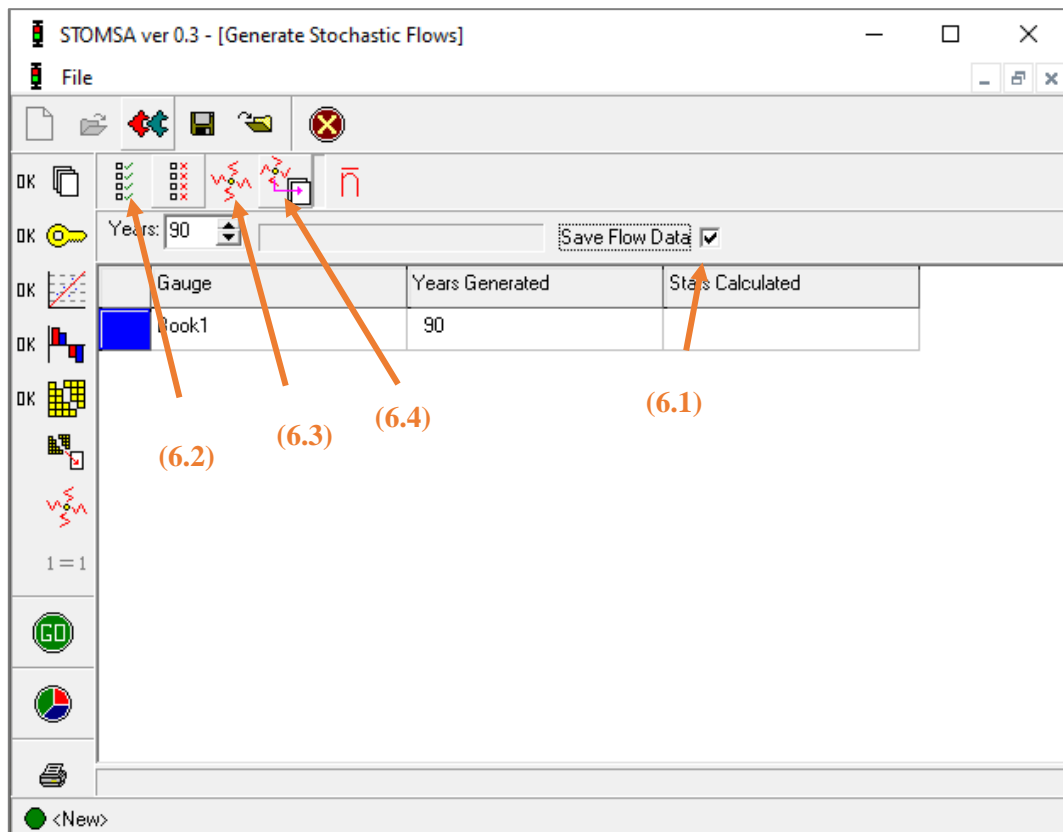


Figure 3-3:STOMSA user interface step 6

3.2 STOMSA File Combiner

Upon opening the STOMSA File Combiner (also installed on the CD accompanying this user manual), the user interface (Figure 3-4) displays a “Start” prompt for the user to select, which opens a file explorer (Figure 3-5). The file explorer is used to navigate to the stored file containing the 101 stochastic sequences (text files) generated by STOMSA. Once the stochastic sequences-containing file is selected, the file combiner program combines all the text files and creates a new Excel file called “*STOMSA Super File*” in a new folder called “Combine”.

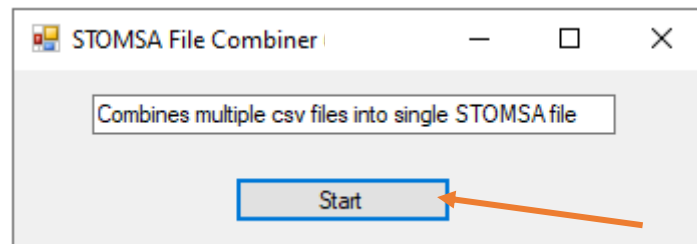


Figure 3-4: “*STOMSA File Combiner*” user interface

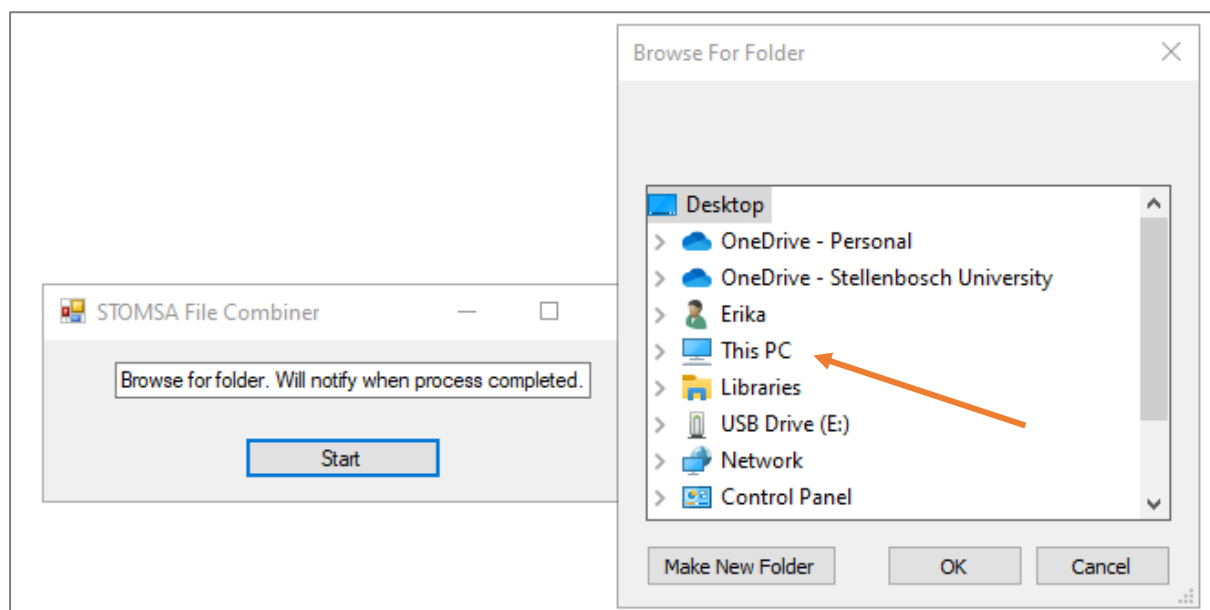


Figure 3-5: File Explorer window to navigate to required folder

The user opens the “*STOMSA Super File*” and selects the entire first column, after which the “Text to Columns” button under the “Data” tab within the “Data Tools” is selected (Figure 3-6). Upon selecting the “Text to Columns” button the user chooses the “fixed width delimited” option and then selects “finish” (Figure 3-7). The “*STOMSA Super File*” is saved and stored as an Excel file (Figure 3-8). The newly-saved Excel file is used as input for the “*Streamflow Disaggregation*” workbook of the conjunctive use model.

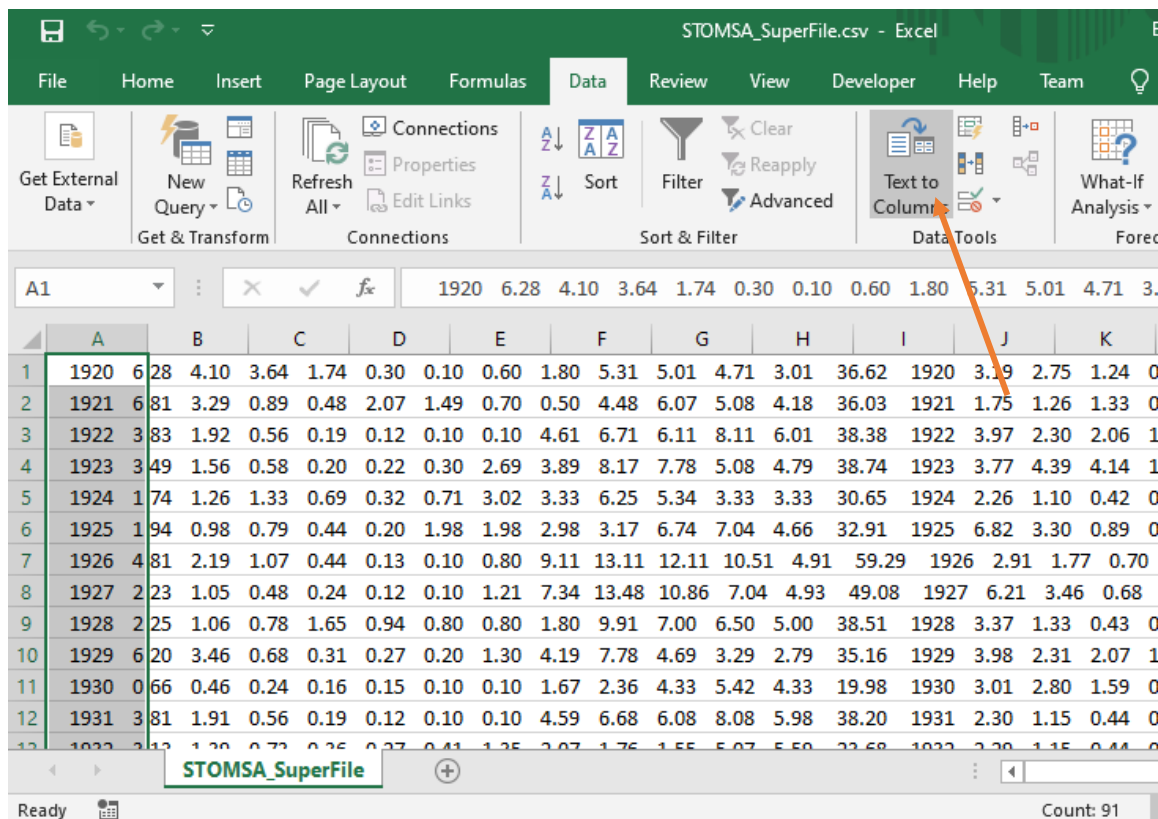


Figure 3-6: “Text to Columns” button in the “STOMSA_Superfile” worksheet

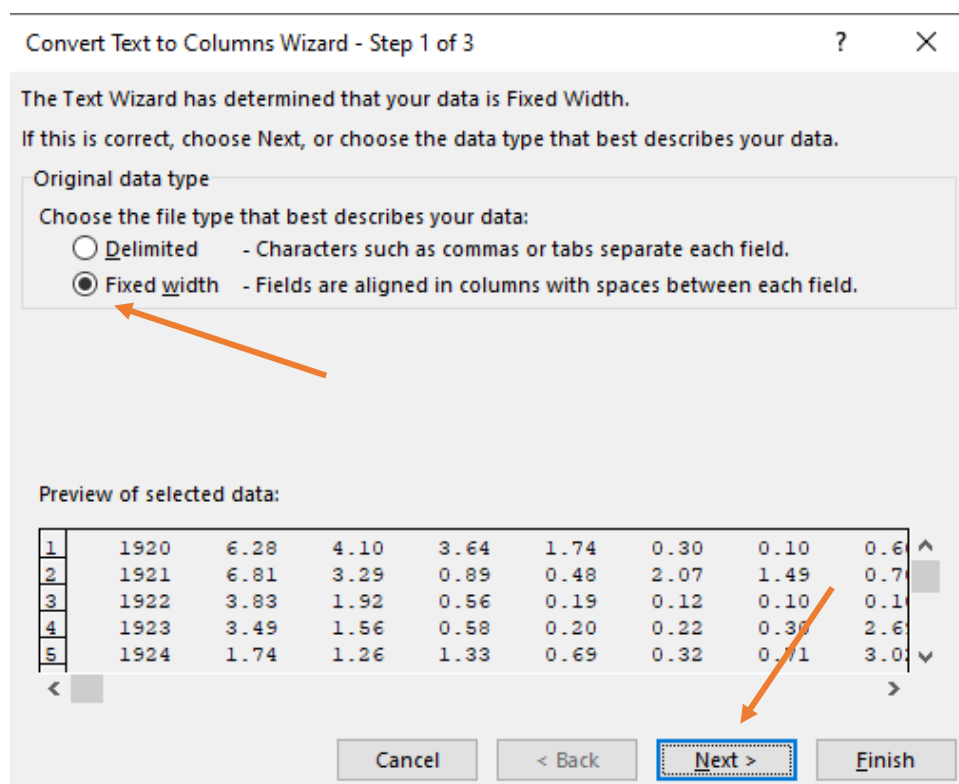


Figure 3-7: “Convert Text to Columns” user interface

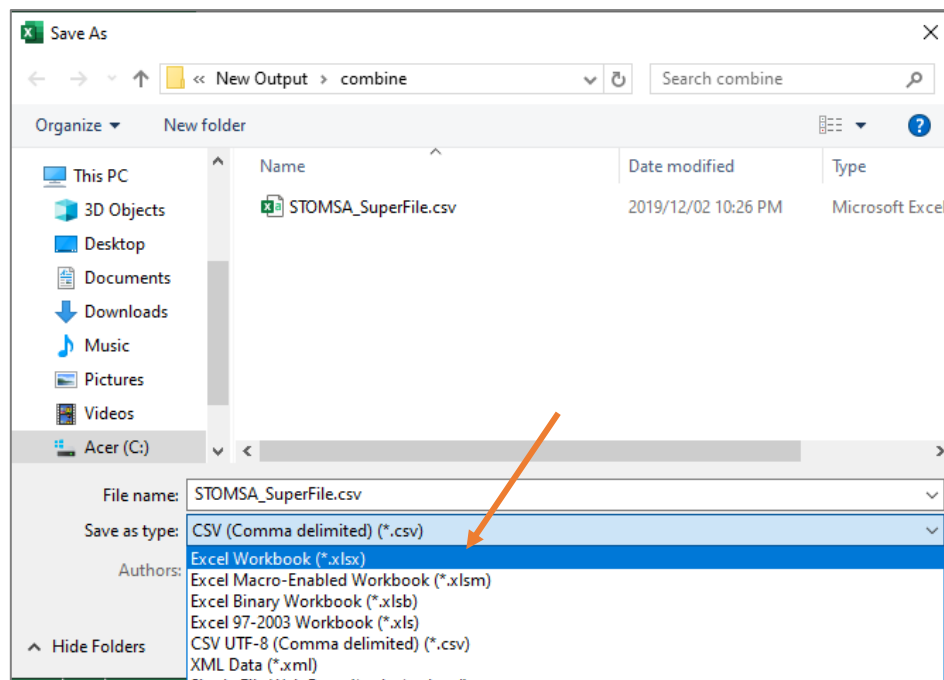


Figure 3-8: Saving the “STOMSA_Superfile” as an Excel file with “.xlsx” extension

4 STREAMFLOW DISAGGREGATION

The second workbook of the conjunctive use model is the “*Streamflow Disaggregation*” workbook. This is a large workbook which requires a couple of minutes to open. An overview of the procedures performed in this workbook appears in the user interface, which is on the “START” sheet of the workbook and is illustrated in Figure 4-1.

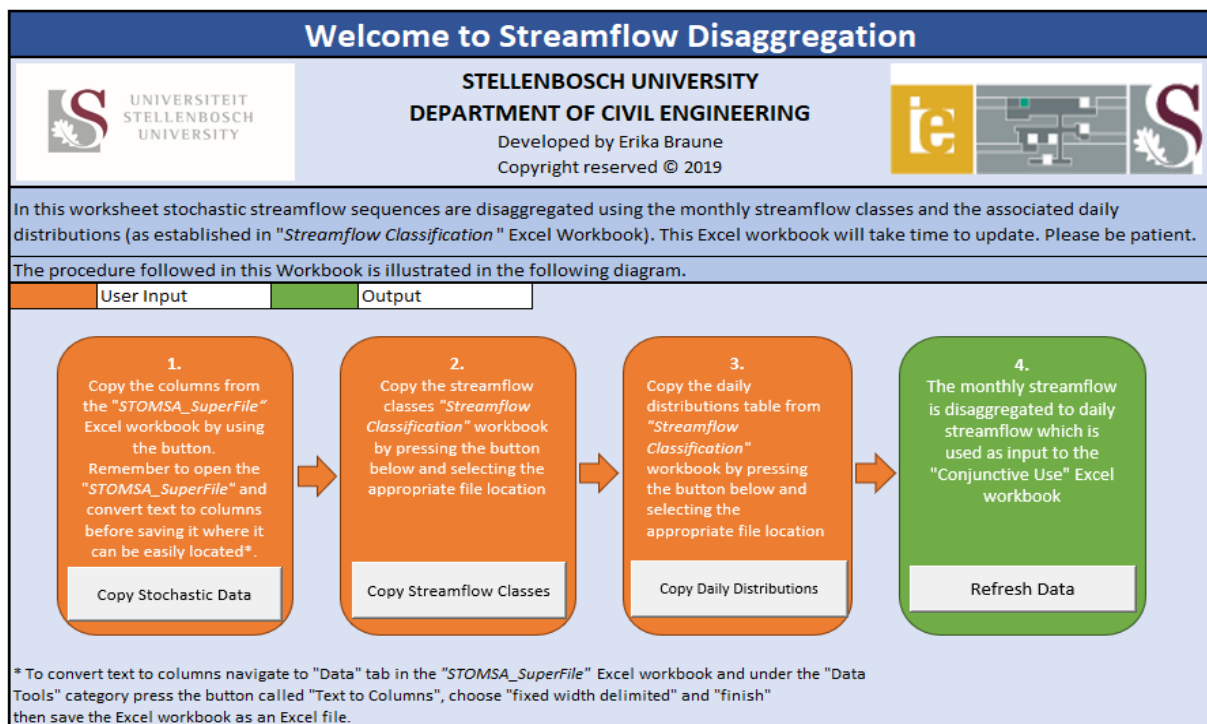


Figure 4-1: “Streamflow Disaggregation” workbook User Interface

The flow diagram prompts the user through a number of steps to be taken in numerical order, and their associated buttons for selection. Upon selecting a button, the applicable data in the “*Streamflow Classification*” workbooks are automatically copied and pasted into the “*Streamflow Disaggregation*” workbook. If the user decides to cancel the process the “Esc” button on the keypad has to be selected twice and then a pop-up message will appear where the user has to choose “End”.

The following steps are taken by the user in the “*Streamflow Disaggregation*” workbook:

Step 1 – Select the “Copy Stochastic Data” button and navigate to the “*STOMSA Super File*” as discussed in section 3.2 (Figure 4-2);

Step 2 – Select the “Copy Streamflow Classes” button and navigate to the “*Streamflow Classification*” workbook (as indicated in Figure 4-2);

Step 3 – Select the “Copy Daily Distributions” button and navigate to the “*Streamflow Classification*” workbook (as indicated in Figure 4-2); and

Step 4 - Select the “Refresh Data” button so that the data can be automatically updated by letting the workbook calculate.

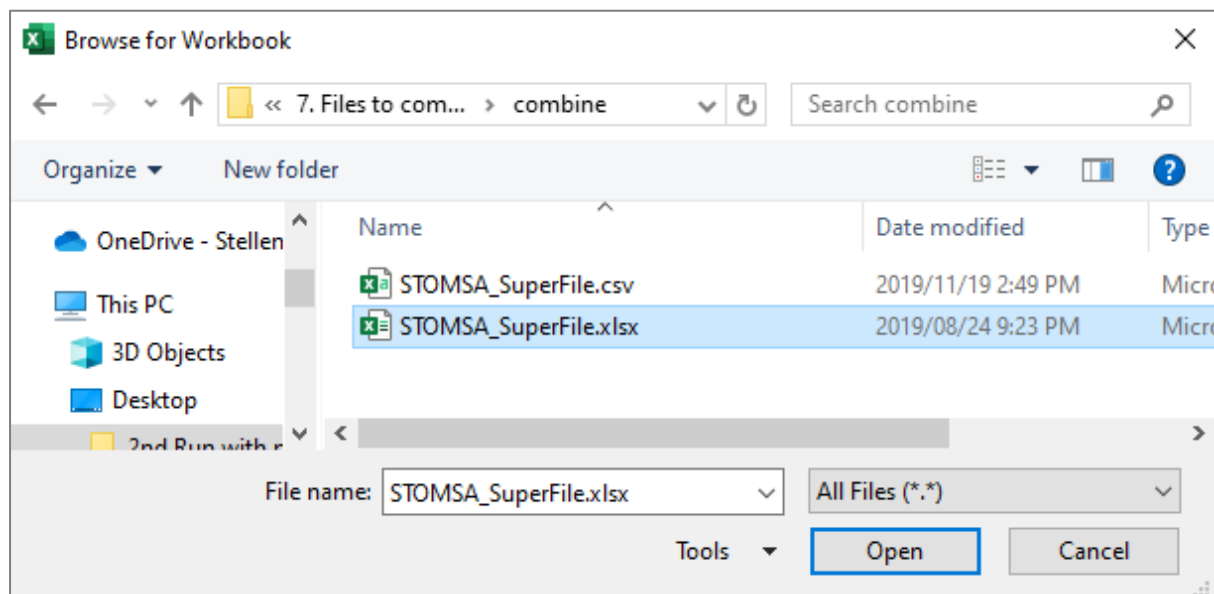


Figure 4-2: Selection window upon selecting the “copy” buttons

Each of the actions associated with the buttons are performed on the “START” sheet (Figure 4-1) and each action will require patience while the sheet updates. The daily data from the “SUM” sheet is the input data for the “*Conjunctive System Simulation*” Excel workbook.

5 GROUNDWATER SIMULATION WORKBOOK

The third workbook of the conjunctive use model is the “*Groundwater Simulation*” workbook. Groundwater modelling consists of two parts, namely: the aquifer system water balance and the borehole interference test. The aquifer system water balance requires input data from the GRAII database of the DWS, and output data from the “*Streamflow Classification*” and “*Streamflow Disaggregation*” workbooks, while the borehole interference test requires data from borehole yield tests, customarily obtained from the municipality. The “START” page of the “*Groundwater Simulation*” workbook (Figure 5-1) serves as the user interface, which outlines the procedures (in numerical steps) included in the two phases of groundwater modelling, and the associated buttons for selection during each step. The groundwater simulation is limited to 2 quaternary catchments. Data retrieval is discussed in section 5.1, while the aquifer system water balance is discussed in section 5.2 and borehole interference tests are discussed in section 5-3.

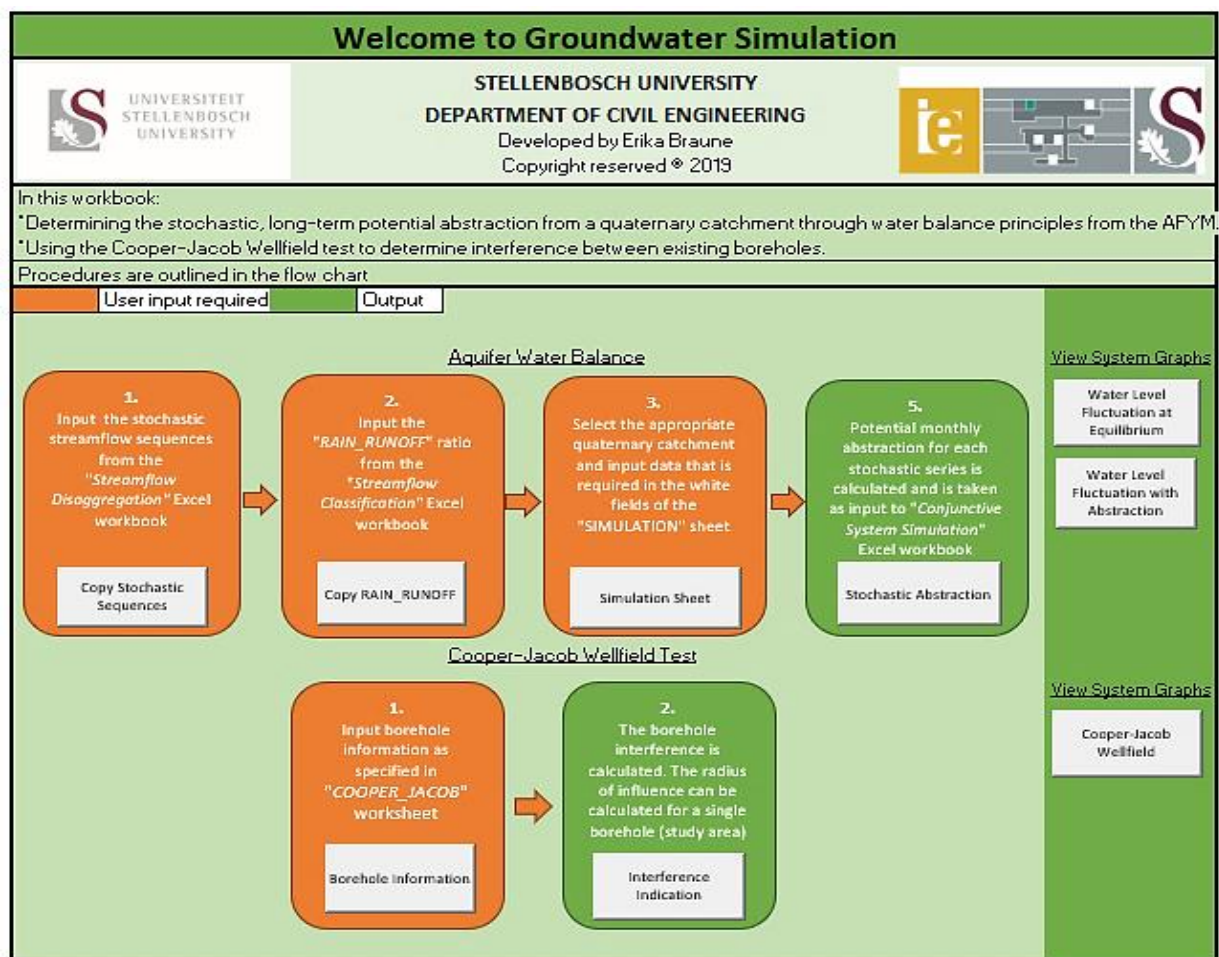


Figure 5-1: “*Groundwater Simulation*” workbook user interface

5.1 Groundwater Resource Assessment Phase II data

The GRAII database can be accessed through the DWS groundwater website by following the link: <http://www.dwa.gov.za/groundwater/GRAII.aspx>. An information or document request is then sent to the following e-mail address: georequests@dws.gov.za. The GRAII website displays the documents available upon request, as illustrated in Figure 5-2.

For the convenience of the user, the applicable groundwater related information of all the existing quaternary catchments were already incorporated (built-in) into the “*Groundwater Simulation*” workbook for selection, according to workbook instructions, thus; the user is not required to download a personal copy. This information includes the monthly recharge percentages of MAP, the average groundwater levels of the quaternary catchments, and the average specific yields of the quaternary catchments, as well as the quaternary catchment areas.



Figure 5-2: GRAII page of the DWS groundwater website

5.2 Aquifer System Water Balance

The aquifer is modelled to the size of the entire quaternary catchment, which is scaled according to the geology maps of the Council for Geoscience. If only one borehole is available to the municipality, for contributing to the water supply system, the radius of influence discussed in section 5.3) is used as the aquifer’s scaled size for the borehole yield calculation. The aquifer system water balance requires two main procedures, namely: adding the specific data and running the simulation.

To determine the long-term potential average abstraction rate of the boreholes in municipal use for each month, using every stochastic sequence, the output of STOMSA becomes the input data for the first step in the “*Groundwater Simulation*” workbook.

Recharge for each month is determined as percentages of monthly rainfall, after which the rainfall-runoff ratio is necessary to generate stochastic rainfall sequences from every stochastic sequence generated by STOMSA.

On the “START” page of the workbook the user is prompted to navigate to the “*Streamflow Disaggregation*” and “*Streamflow Classification*” workbooks respectively, after which the applicable buttons will copy the correct ranges into the “*Groundwater Simulation*” workbook automatically. The user undertakes the following steps to populate applicable fields with input data:



1. Click on the “Copy Stochastic Sequences” button and select the “*Streamflow Disaggregation*” workbook (the same user window will appear as in Figure 4-2);
2. Click on the “Copy RAIN_RUNOFF” button and select the “*Streamflow Classification*” workbook (Figure 4-2);
3. Click on the “Simulation Sheet” button and populate the required field in the “Calcs_Balance_1” sheet. The information boxes of the “Calcs_Balance_1” sheet are illustrated in Figure 5-3.
4. If more than one quaternary catchment contributes to the aquifer system from which abstraction is done, the required fields in the “Calcs_Balance_2” sheet is also populated. Otherwise, if no second catchment is available, the study area in the “Calcs_Balance_2” sheet has to be set to 0 km².

After populating the required fields in the “Calcs_Balance_1” sheet (and if necessary, the “Calcs_Balance_2” sheet), the user clicks on the “Refresh Sequence” button so that the “STOCH_ABSTRACT” sheet automatically recalculates. Thereafter the user selects the “Stochastic Abstraction”, which allows the user to view the “STOCH_ABSTRACT” sheet.

The colour coding of the information boxes works as follows: If the field is coloured, the user is not required to populate it, if the field is blank, the user is required to populate it with the indicated information.

The “Quaternary catchment 1” information box requires data of the quaternary catchment that stochastic sequences were generated for. The quaternary catchment number is selected from a dropdown list and so is the stochastic sequence number. All the numbers up to 101 in the dropdown list are stochastic sequences, while number 102 is the historical naturalized streamflow sequence obtained from WR2012. The size of the study area, required in the green “Hydrogeology Catchment Information” box, is the area of the aquifer from which abstraction is taking place. This is obtained through geology maps of the Council for Geoscience, which indicates alluvial or fractured aquifer systems. However, if there is only one borehole available to the municipality for use, the size of the study area is obtained through examining the cone of depression during the Cooper-Jacob wellfield interference test (section 5.3). The deepest and most shallow static water levels of the borehole, required in the “Borehole Data”

information box, are the rest water levels of a borehole in use within the aquifer system, but excluding pumping.

Quaternary Catchment 1 (Origin)		
Selected Quaternary	G22F	
Rainfall Zone	G2C	
Start Year	1920	year
Stochastic Sequence	102	
Historical MAR	36.6	mil m ³
Historical MAP	1 465.0	mm

Hydrogeology Catchment Information		
Initial Specific Yield	0.001231	(0 < S _y < 1)
Adjusted Specific Yield	0.02226793	
Avg Static Water Level	7.8	mbgl
Recharge	11.21	%
Catchment Area	65.7	km ²
Study Area	25	km ²

Borehole Data		
Deepest BH static WL	25	mbgl
Lowest BH static WL	3.9	mbgl
Deepest simulated WL	25.00	mbgl
Lowest simulated WL	-2.55	mbgl

Figure 5-3: Information boxes for the “Calcs_Balance_1” sheet

5.3 Borehole Interference Test

The borehole interference test is performed by applying the Cooper-Jacob wellfield equation to the data available for the boreholes used by the municipality. This data is obtained through borehole yield tests. The cumulative drawdown at a specific borehole within the wellfield is determined as result of other boreholes in the wellfield impacting upon that specific borehole. Up to 10 boreholes can be analysed in this manner.

The user navigates to the “Cooper_Jacob” sheet by selecting the “Borehole information” button in the user interface on the “START” sheet. The user will be required to populate the blank cells in the “Borehole Information” box (Figure 5-4). The following information is required and is obtained through borehole yield tests:

- borehole coordinates (latitude and longitude) in decimal degrees;

- name of the borehole;
- the pumping rate recommended for the borehole in litres/second (ℓ/s);
- the hours in a day which the borehole is being pumped in hours/day;
- the diameter of the borehole in millimetres (mm), in other words the pipe diameter that is used in the borehole;
- the depth at which the pump is installed, which indicates the allowable drawdown of the borehole;
- the rest water level when the borehole is not being pumped (has recovered fully);
- the storativity (value between 0 and 1) and transmissivity describing the hydrogeology of the borehole and surroundings.

Borehole Information										Number of Boreholes: 6		
Latitude (S)	Longitude (E)	South Latitude	Easting	Long Zone	Name	Recommended pump rate (L/s)	Pumping Duration per day (hours)	Diameter (mm)	Depth or Pump Spec drawdown level (mbgl)	Rest Water Level (mbgl)	Storativity (0< ratio <1)	Transmissivity (m2/day)
-33.91	18.85	6245925	301194	34	1. Cloetessville_BH	8.5	12	200	70	2.6	0.006	12.1
-33.94	18.86	6242713	302070	34	2. Die_Braak_BH	8.5	12	160	50	4.9	0.007	24.2
-33.93	18.86	6242990	301882	34	3. Van_der_Stel_BH	12.0	16	180	70	4	0.007	20
-33.92	18.85	6241767	301415	34	4. Kayamandi	10.0	12	160	100	6.23	0.02	15
-33.93	18.88	6244442	303762	34	5. Jan-Marais Nature Reserve	1.0	12	168	25	3.2	0.01	2.3
-33.93	18.89	6243193	304728	34	6. Municipal Nursery	2.0	12	180	50	3	0.03	2.1

Figure 5-4: “Borehole Information” box

Upon populating the above-mentioned fields with the applicable data, a coordinate transformation system (UTM) is used to change the coordinates from the spherical coordinates to cartesian coordinates so that the distance between boreholes can be accurately calculated. Thereafter, drawdown at each borehole (caused by its own pumping), is automatically calculated, as well as the radius of influence (Figure 5-5). The user clicks on the “Cumulative Drawdown” button so that the drawdown from all boreholes can be automatically calculated.

Radius of Influence and Borehole Interference			
Drawdown at own BH	Radius of Influence	Cumulative Drawdown	Interference
88	910	88	NO
46	1191	57	YES
79	1251	85	YES
81	555	81	YES
49	307	49	NO
99	170	99	NO

Figure 5-5: Calculated radius of influence and borehole interference

6 CONJUNCTIVE SYSTEM SIMULATION WORKBOOK

The final workbook in the conjunctive use model is the “*Conjunctive System Simulation*” workbook. At this point the user should have completed all previously discussed steps for the preceding workbooks. The “START” sheet of the “*Conjunctive System Simulation*” workbook is illustrated in Figure 6-1, where an overview of the procedures, performed in this workbook, are outlined in the user interface. The flow diagram prompts the user through a number of steps to be taken (in numerical order), during the conjunctive system simulation process. There are specific buttons to select for each step, which upon selection, transfers the user to the respective worksheets, where input data is required. The input (orange) and output (green) worksheets are colour coded for the convenience of the user. There are 9 worksheets in this workbook which require user input, namely: “RAIN_RUN”, “STREAM1_DAILY”, “GW_STOCH”, “USE_1”, “USE_2”, “EVAP”, “AREA_CAPACITY”, “DESAL”, and “SIMULATION”. The user can navigate between input worksheets through links discussed in section 6.1. There are 3 worksheets which show the time-series graphs for different components, namely: “DAM_CAPACITY”, “GW_CAPACITY”, and “CONJ_CAPACITY”, discussed in section 6.2. There are 3 output worksheets, which require minimal user input, namely: “DRAFT_YIELD”, “RELIABILITY” and “SHORT_MNG”, discussed in section 6.3. The user navigates to the output and graphs worksheets through the use of buttons. Where the user is required to navigate to a worksheet or an automated computation an applicable button, labelled in ***Bold Italics***, is selected and the user waits for the model to respond.

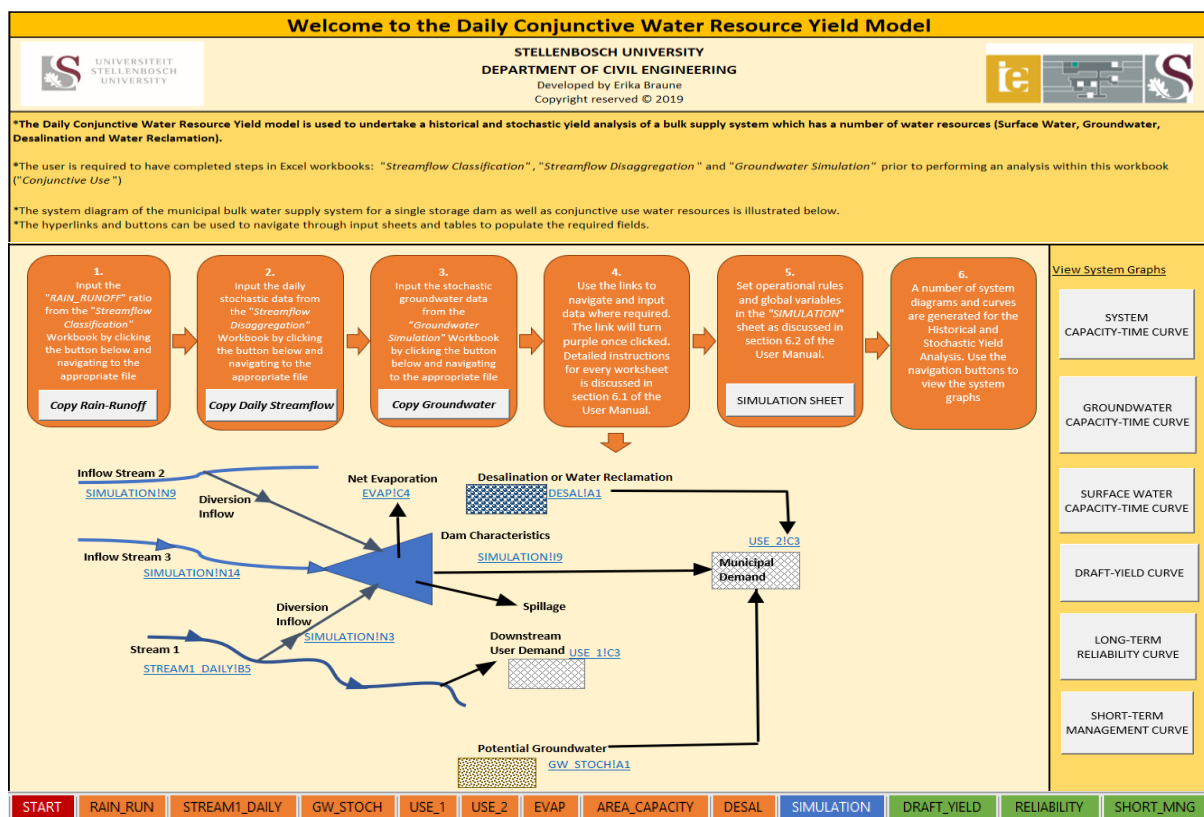


Figure 6-1: The “*Conjunctive System Simulation*” workbook user interface

The steps followed during the conjunctive system simulation process are as follows:

Step1 – Select the “Copy Rain-Runoff” button and navigate to the “*Streamflow Classification*” workbook using the “Browse for Workbook” interface (Figure 6-2), which opens when the button is selected. The RAIN-RUNOFF ratios are automatically copied from the “*Streamflow Classification*” workbook into the “RAIN_RUN” worksheet.

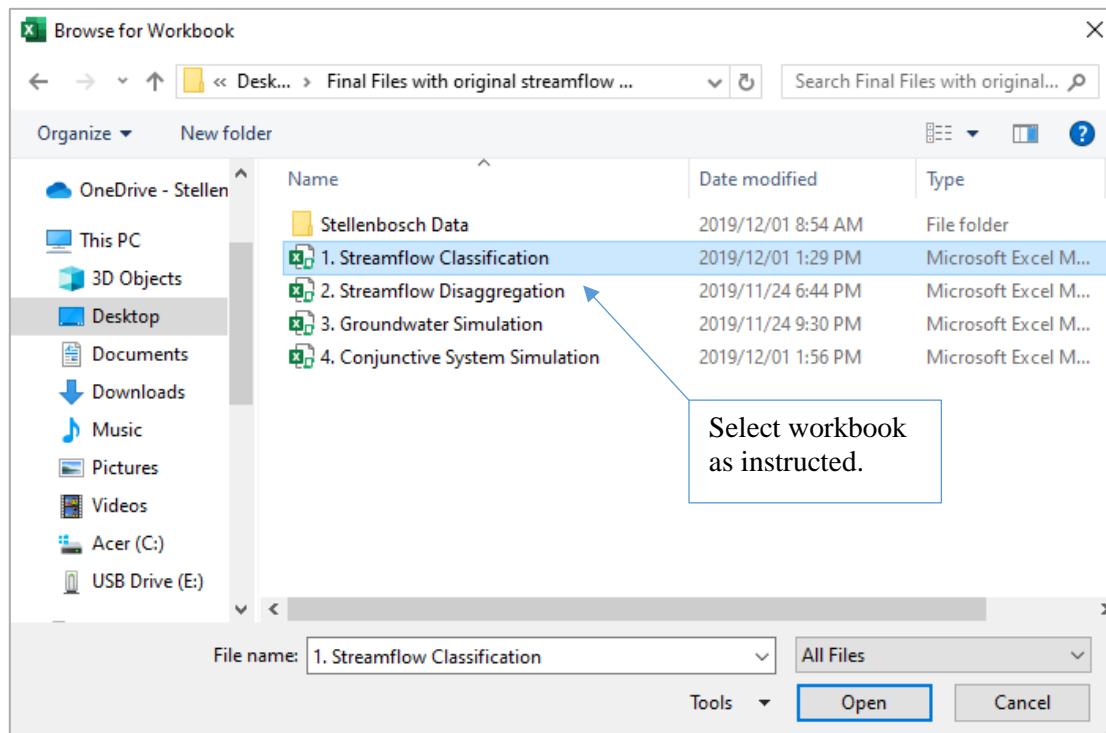


Figure 6-2: “Browse for workbook” window to navigate to required workbook

Step 2 – Select the “Copy Daily Streamflow” button and navigate to the “*Streamflow Disaggregation*” workbook using the “Browse for Workbook” interface (Figure 6-2), which opens when the button is selected. The daily streamflow is automatically copied from the “*Streamflow Disaggregation*” workbook into the “STREAM1_DAILY” worksheet. This process takes long as this workbook contains a large amount of information.

Step 3 – Select the “Copy Groundwater” button and navigate to the “*Groundwater Simulation*” workbook using the “Browse for Workbook” interface (Figure 6-2), which opens when the button is selected. The stochastic groundwater abstraction rate for the study area is automatically copied from the “*Groundwater Simulation*” workbook into the “GW_STOCH” worksheet. This process takes long as this workbook contains a large amount of information.

Step 4 – Populate the blank fields, as required for the different system inputs, by following the links indicated on the “START” page of this workbook. The links take the user to the required input fields and turn purple after being selected. A detailed discussion of the input sheets follows in section 6.1.

Step 5 – Set variables for the different system inputs and operational scenarios in the “SIMULATION” worksheet. There are a number of buttons to select to run the simulation, detailed in section 6.2.

Step 6 – Set target drafts to generate the firm yield curve, as well as the reliability of supply curve, in the “DRAFT_YIELD” and “RELIABILITY” worksheets respectively. Set variables and operational scenarios for the short-term management curve in the “SHORT_MNG” worksheet. Each of these worksheets display the respective output graphs after the buttons have been selected to generate them. A detailed discussion on step 6 follows in section 6.3.

6.1 Input Sheets

At this point it is assumed that the user had already used the following buttons to populate their associated worksheets: “Copy Rain-Runoff”, “Copy Daily Streamflow” and “Copy Groundwater”, as discussed in steps 1 to 3. The user now selects the links (blue) to navigate between input worksheets for different components (Figure 6-3).

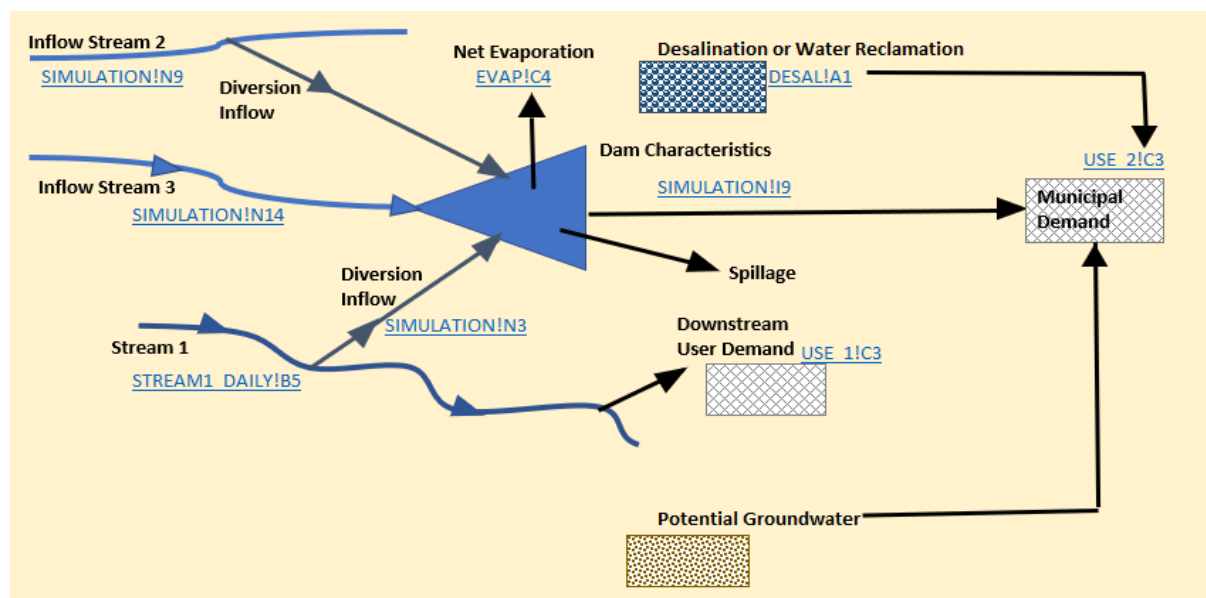


Figure 6-3: Links to different input worksheets for each system component

6.1.1 “EVAP” Worksheet

The S-pan factors and the open water pan coefficients are both set in the “EVAP” worksheet (Figure 6-4) by populating the blank cells for every month. The user retrieves the evaporation zone from the “*Quaternary data spreadsheets*” folder containing the quaternary catchments’ information for the listed WMAs from the WR2012 online database (section 2.4.1). The S-pan factors are available from the WR90 online database, which was provided to water resource officials through as printed documents. For the convenience of the user, the monthly evaporation as percentages of MAE for all evaporation zones are given in Figure 6-5. The user enters the values, corresponding to the identified evaporation zone, into the cells indicated. The “Start” link is followed back to the “START” worksheet upon completion of the information required.

Evaporation											
	Oct	Nov	Dec	Jan	Feb	Mar	Apr	May	Jun	Jul	Sep
S-pan factor (%)	8.76	12.23	14.38	14.73	12.43	10.86	6.76	3.9	3	3.52	3.9
Open water pan coefficient	0.81	0.82	0.83	0.84	0.88	0.88	0.88	0.87	0.85	0.83	0.81
Combined coefficient	0.07	0.10	0.12	0.12	0.11	0.10	0.06	0.03	0.03	0.03	0.05

Back to Start [START!A1](#)

Figure 6-4: Evaporation coefficients for the “EVAP” input worksheet

(VOLUME IV) APPENDIX 3.2 : MONTHLY EVAPORATION AS A PERCENTAGE OF MAE FOR EVAPORATION ZONE

EVAP ZONE	OCT	NOV	DEC	JAN	FEB	MAR	APR	MAY	JUN	JUL	AUG	SEP
1A	11.13	10.49	10.70	10.26	8.81	8.65	6.96	6.02	4.84	5.38	7.31	9.45
1B	10.46	10.03	10.68	10.43	8.49	8.49	6.94	6.55	5.40	6.08	7.42	9.03
1C	11.08	10.29	10.96	11.00	9.15	8.89	6.89	5.72	4.65	5.04	7.02	9.31
1D	11.60	10.78	10.78	10.72	8.94	8.45	6.63	5.63	4.65	5.23	7.03	9.56
2A	11.16	11.21	11.59	11.08	8.90	8.38	6.58	5.50	4.48	5.03	6.94	9.15
2B	11.15	11.01	11.35	11.10	9.03	8.61	6.57	5.44	4.56	5.05	6.93	9.20
3A	11.52	11.54	11.86	11.20	9.20	8.50	6.38	5.07	3.99	4.62	6.78	9.34
3B	10.92	10.37	11.28	10.70	8.93	8.66	6.83	5.81	4.78	5.30	7.02	9.40
4A	10.78	10.17	11.20	11.00	9.17	9.05	6.96	5.86	4.76	5.21	6.90	8.94
5A	9.50	9.48	10.77	11.28	9.67	9.49	7.20	6.28	5.16	5.57	7.05	8.55
6A	9.63	11.72	13.66	13.74	10.87	9.27	6.50	4.78	3.66	3.94	5.22	7.01
6B	10.02	11.56	12.87	12.65	9.90	8.91	6.60	5.24	4.27	4.69	5.71	7.58
7A	10.07	11.90	13.71	13.60	10.45	9.02	6.30	4.54	3.45	3.99	5.44	7.53
8A	11.47	12.08	12.53	11.78	8.93	8.22	6.13	4.88	3.87	4.51	6.54	9.06
9A	11.14	12.09	12.59	11.89	9.10	8.13	6.15	4.88	3.99	4.64	6.50	8.90
9B	10.96	12.05	13.16	12.75	9.87	8.47	6.06	4.68	3.59	4.20	5.83	8.38
10A	11.11	11.46	11.87	11.48	8.98	8.13	6.33	5.28	4.17	4.91	6.97	9.31
11A	10.97	11.39	12.37	12.23	9.86	8.96	6.55	4.94	3.78	4.22	6.12	8.61
12A	10.85	10.88	11.71	11.36	9.37	8.76	6.62	5.37	4.36	4.71	6.83	9.18
13A	9.79	10.19	10.91	10.98	9.39	9.09	7.07	5.88	4.94	5.54	7.15	9.07
13B	10.35	10.20	11.00	10.87	9.38	8.94	6.88	5.85	4.82	5.29	7.26	9.16
14A	9.50	11.22	12.82	13.06	10.99	10.30	7.40	4.96	3.74	3.66	5.12	7.23
14B	9.58	11.40	12.32	12.64	10.23	9.57	6.92	5.41	4.76	4.52	5.53	7.12
15A	9.21	11.38	13.37	14.22	11.48	10.38	6.69	4.63	3.47	3.62	4.77	6.78
15B	9.22	12.03	14.48	14.94	11.98	10.36	6.24	4.08	2.80	3.18	4.44	6.25
16A	9.84	12.07	14.13	14.40	10.97	9.56	6.23	4.24	3.11	3.48	4.89	7.08
17A	10.19	12.43	14.64	14.41	10.67	8.89	5.91	4.12	2.99	3.38	5.05	7.32
17B	10.30	11.94	13.88	13.96	11.19	9.28	6.10	4.26	2.97	3.53	5.08	7.51
18A	10.32	11.61	13.46	13.07	9.83	8.54	6.08	4.78	3.77	4.44	6.10	8.00
19A	10.59	11.93	13.51	12.83	10.05	8.94	6.21	4.48	3.47	4.01	5.82	8.16
19B	10.52	12.36	14.06	13.62	10.44	8.62	6.10	4.29	3.23	3.62	5.30	7.84
19C	10.68	12.05	13.81	13.51	10.15	8.81	5.94	4.37	3.16	3.74	5.52	8.26
20A	10.61	12.17	13.81	13.19	10.09	8.66	6.00	4.34	3.37	3.86	5.75	8.15
20B	10.83	11.69	13.48	12.72	9.86	8.56	5.94	4.64	3.50	4.09	6.00	8.69
21A	9.93	10.38	11.07	10.76	9.36	9.01	7.25	6.00	5.06	5.56	7.17	8.45
21B	10.23	9.39	9.77	9.57	8.02	7.93	7.00	6.88	5.64	6.45	9.01	10.11
21C	10.16	10.21	11.37	11.19	9.50	8.93	6.93	5.70	4.82	5.29	7.26	8.64
22A	8.95	10.36	11.63	12.05	10.33	10.01	7.22	5.83	4.79	5.17	6.18	7.48
22B	10.66	9.75	10.78	10.63	8.84	8.76	6.67	6.03	5.16	5.63	7.90	9.19
22C	9.22	10.24	11.71	12.46	10.73	10.13	7.12	5.63	4.40	4.67	6.10	7.59
23A	9.19	11.46	14.11	14.78	12.40	11.16	7.05	4.34	2.94	2.96	3.83	5.78
23B	8.67	12.08	14.83	15.09	12.45	11.51	7.06	4.00	2.62	2.55	3.57	5.57
23C	8.76	12.23	14.38	14.73	12.43	10.86	6.76	3.90	3.00	3.32	3.90	5.73
23D	8.77	12.40	15.47	16.12	13.44	11.29	6.12	3.24	2.40	2.21	3.24	5.30
23E	9.65	12.36	14.97	14.98	11.88	9.81	6.36	3.91	2.69	2.94	4.09	6.36
24A	9.31	11.56	13.89	14.21	11.62	10.18	6.77	4.51	3.30	3.50	4.68	6.47
24B	9.21	10.91	13.29	12.96	10.16	8.77	6.59	5.41	4.95	5.06	5.92	6.77
24C	9.19	11.10	13.74	13.97	11.09	9.72	6.91	4.85	3.95	3.94	4.87	6.67
25A	9.73	11.36	13.67	13.60	10.57	9.02	6.30	4.78	3.88	4.27	5.62	7.20
26A	9.51	11.23	13.45	13.79	11.06	9.54	6.92	4.88	3.54	3.83	5.23	7.02
27A	9.94	11.37	13.38	13.09	10.45	9.07	6.28	4.81	3.61	4.09	6.05	7.86
28A	9.75	11.15	13.07	13.17	10.49	9.05	6.53	4.86	3.99	4.41	5.92	7.61
28B	10.06	11.43	13.07	13.17	10.46	9.25	6.81	4.96	3.66	4.09	5.52	7.52
28C	9.24	9.56	10.92	10.81	8.77	8.28	6.82	6.36	6.04	6.91	7.78	8.51
28D	9.58	10.89	12.43	12.40	10.17	9.19	6.73	5.31	4.65	4.66	6.18	7.81
29A	10.32	11.20	12.03	11.61	9.58	8.82	6.46	5.10	4.31	4.85	6.99	8.73
29B	10.06	10.82	12.60	12.62	10.20	8.97	6.82	4.77	3.82	4.43	6.49	8.40
30A	9.39	9.65	10.56	10.49	9.37	9.26	7.58	6.40	5.60	5.99	7.24	8.47
30B	9.47	9.57	11.27	10.69	9.41	9.62	7.23	6.03	5.14	5.78	7.41	8.38
30C	8.70	8.76	11.18	12.02	10.41	9.95	7.71	6.34	4.74	5.24	7.22	7.73

Figure 6-5: Monthly S-pan evaporation percentages of MAE per evaporation zone

6.1.2 “AREA_CAPACITY” Worksheet

The depth-capacity and area-capacity relationships for the storage dam are determined in the “AREA_CAPACITY” worksheet, indicated in Figure 6-6. The user is required to input the water depth and the corresponding capacity, and surface area if available, at various depth levels (in ascending order). The minimum information that should be available is either the capacity at different depths, or the surface area for different capacities. This information is obtained from dam safety reports (which should be prepared for storage dams), or from the individuals who performed the dam safety investigation. After the user has populated the required columns, the Capacity-Depth curve and the Surface Area-Capacity curve are automatically generated.

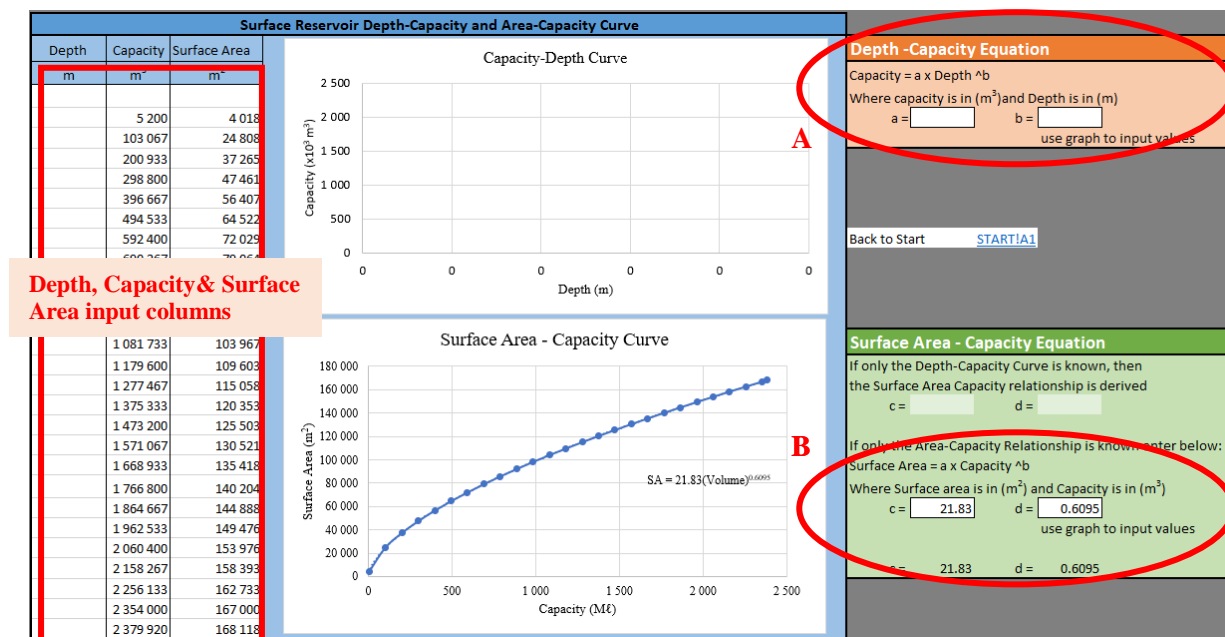


Figure 6-6: “AREA_CAPACITY” worksheet with graphs

The user is required to populate the blank cells as indicated by the red circles (A and B) in Figure 6-6. The coefficients, ‘a’ and ‘b’, have to be set in a manner that describes the depth-capacity curve as follows in Equation 6-1:

$$Volume = a (Depth^b) \quad (6-1)$$

The user determines the coefficients by plotting a trendline and displaying the trendline equation as a power function. This is done by clicking on the chart and selecting the “chart elements” button (green cross). The user ticks the box next to ‘trendline’ (Figure 6-7) and then right clicks on the trendline, which appears in the graph, and selects the “Format Trendline” option. The “Format Trendline” tab opens and the user selects the “Power” option by ticking the box next to the “Display the Equation on chart” option (Figure 6-8).

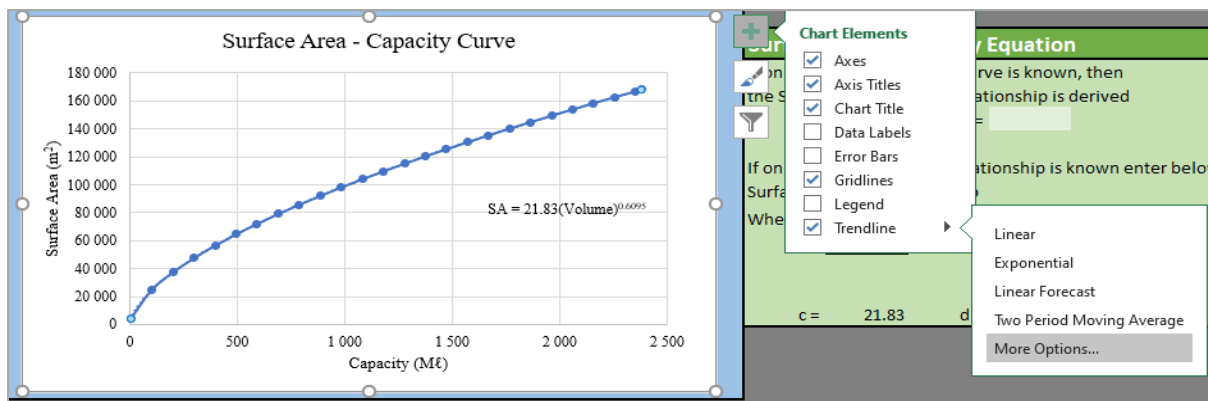


Figure 6-7: Adding a trendline to the Surface Area-Capacity curve or the Depth-Capacity curve

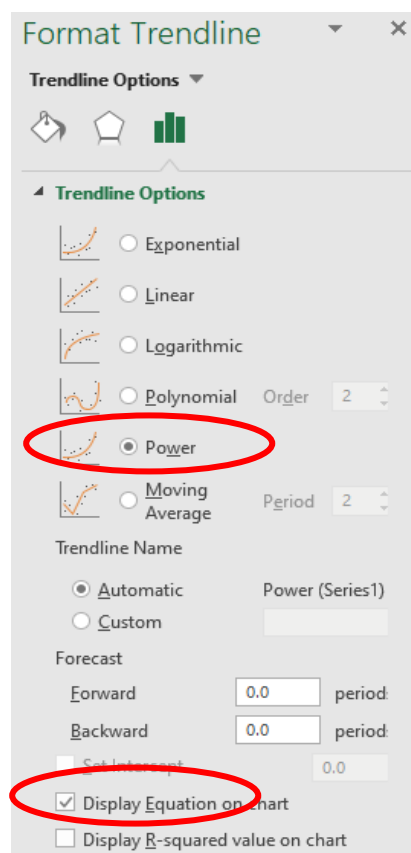


Figure 6-8 "Format Trendline" window

If the depth-capacity relationship is known only, then the Surface Area-Capacity relationship is automatically generated. However, if the Surface Area-Capacity relationship is known only, then coefficients 'c' and 'd', have to be set. The user determines the coefficients by generating a trendline as previously explained (Figure 6-7 and Figure 6-8). The coefficients, 'c' and 'd', have to be set in a manner that describes the Surface Area-Capacity curve as follows in Equation 6-2:

$$\text{Surface Area} = a (\text{Volume}^b) \quad (6-2)$$

The "Start" link is used to navigate back to the "START" worksheet upon completion of the information required.

6.1.3 “DESAL” worksheet

Information pertaining to two desalination or water reclamation plants can be set in the “DESAL” worksheet indicated in Figure 6-9. If more than 2 desalination plants (or water reclamation plants) are available then the capacities have to be totalled before it is used as input data. The user chooses between the available options, and populates the related fields, indicated with bold red characters and shapes in Figure 6-9. The user is then required to populate the field related to the plant capacity, for the respective plants, and select the number of reverse osmosis units that the plants have available. Up to 5 reverse osmosis units are allowed per plant.

The user is then required to populate the blank column with the monthly percentages that the plant is functional at. The user must choose for the available options (percentages), indicated with the red shapes in Figure 6-9 so that 3-month blocks of the same capacity are reflected. In other words, the plant capacity has to stay the same for at least 3-months. The “Start” link is used to navigate back to the “START” worksheet upon completion of the information required.

Desalination or Water Reclamation Plant 1				Desalination or Water Reclamation Plant 2			
Desalination Plant?	NO	0	The desalination plant capacity of :	Desalination?	NO	0	The desalination plant capacity of :
Total plant capacity	0	MI/day	100%	Total plant capacity	0	MI/day	100%
Number of modules?	2	RO units	for all of the time.	Number of modules?	5	RO units	for all of the time.
Percentage Capacities to chose from (%):				Percentage Capacities to chose from (%):			
0 50 100				0 20 40 60 80 100			
Distribution of Desalination Plant Capacity			Operational Rules	Distribution of Desalination Plant Capacity			Operational Rules
Month	Distribution % of Capacity for each month	Water produced per day (MI/day)	Desalination plant capacities have to be fixed for at least 3 monthly periods.	Month	Distribution % of Capacity for each month	Water produced per day (MI/day)	Desalination plant capacities have to be fixed for at least 3 monthly periods.
OCT	50%	0.00		OCT	20%	0.00	
NOV	50%	0.00		NOV	20%	0.00	
DEC	50%	0.00		DEC	20%	0.00	
JAN	100%	0.00		JAN	40%	0.00	
FEB	100%	0.00		FEB	40%	0.00	
MAR	100%	0.00		MAR	40%	0.00	
APR	50%	0.00		APR	60%	0.00	
MAY	50%	0.00		MAY	60%	0.00	
JUN	50%	0.00		JUN	60%	0.00	
JUL	100%	0.00	JUL	100%	0.00		
AUG	100%	0.00	AUG	100%	0.00		
SEP	100%	0.00	SEP	100%	0.00		
Back to Start				START!A1			

Figure 6-9: “DESAL” worksheet with capacity and unit amount options

6.1.4 “USE_1” Worksheet

Provision is made that Stream 1 can be modelled with downstream abstraction requirements. The downstream abstraction requirements from Stream 1 are inserted into the “USE_1” worksheet (Figure 6-10). Monthly streamflow from Stream 1 is required in mil m³ per month, from October to September. The “Start” link is followed back to the “START” worksheet upon completion of the information required. The user should have the data on record in municipal planning reports.

USE_1 Downstream Requirements		
October	0	mil m ³
November	0	mil m ³
December	0	mil m ³
January	0	mil m ³
February	0	mil m ³
March	0	mil m ³
April	0	mil m ³
May	0	mil m ³
June	0	mil m ³
July	0	mil m ³
August	0	mil m ³
September	0	mil m ³

Back to Start [START!A1](#)

Figure 6-10: “USE_1” downstream abstraction requirements input worksheet

6.1.5 “USE_2” Worksheet

The monthly municipal demand (urban users) as percentages of the total yearly demand is inserted into the “USE_2” worksheet, illustrated in Figure 6-11. The municipality should have these percentages available in municipal water infrastructure planning reports.

USE_2 Municipal demand distribution		
October	8.56	%
November	9.11	%
December	9.02	%
January	9.54	%
February	9.05	%
March	9.50	%
April	8.54	%
May	7.77	%
June	6.80	%
July	7.25	%
August	7.38	%
September	7.47	%

Back to Start [START!A1](#)

Figure 6-11: “USE_2” worksheet for municipal demand distributions

6.1.6 “SIMULATION” Sheet

After having populated the input sheets discussed in section 6.1, the “SIMULATION” worksheet (Figure 6-12) is a summary sheet of all the input values that have yet to be set by the user. Information pertaining to the following subject matter is filled out in the “SIMULATION” worksheet:

- Catchment of origin (the catchment for which daily streamflow data is observed at a gauging station) hydrological characteristics;
- Storage dam characteristics;
- Inflow streams hydrological characteristics (Stream 1, Stream 2 and Stream 3); and
- Conjunctive use components including: inter-basin transfer schemes, long-term potential groundwater abstraction and desalination or water reclamation.

CATCHMENT OF ORIGIN HYDROLOGY	
Historical MAP	1465 mm
Historical MAE	1450 mm
Historical MAR	36.61 mil m ³
Stochastic Sequence MAR	36.3 mil m ³
Stochastic Sequence Number	101 choose
DAM CHARACTERISTICS	
Full Supply Capacity (Volume)	2.38 mil m ³
Start Capacity Percentage	50 %
Failure Capacity	0 %
Demand Distributions of Draft	USE_2
Historical MAP of Dam Catchment	754 mm
Historical MAE of Dam Catchment	1455 mm
Historical MAR of Dam Catchment	14.32 mil m ³
Surface Area (m ²) =	2183 x Volume(m ³) ^{0.61}
INFLOW CHARACTERISTICS	
Stream 1 Downstream demand & infrastructural capacity	
Downstream Demand	NO
Infrastructure Capacity	470 l/s
Infrastructure Capacity Limitation	100 %
Diversion Efficiency	100 %
Historical MAR	22.30 mil m ³
Stream 2 Infrastructural capacity	
Infrastructure Capacity	0 l/s
Infrastructure Capacity Limitation	100 %
Diversion Efficiency	100 %
Historical MAR of Stream 2	0 mil m ³
Stream 3 Total inflow stream, no infrastructure	
Historical MAR of Stream 3	0.26 mil m ³
INTERBASIN TRANSFER	
Constant inflow	3000 Ml/annum
Percentage Reduction	0 %
LONG-TERM POTENTIAL GROUNDWATER ABSTRACTION	
Are there boreholes available?	YES
Study Area	35 km ²
Average available abstraction for sequence	161 m ³ /day
BOREHOLE ABSTRACTION	
Total combined long-term pumping rate	0 m ³ /day
For short term abstraction rate	0
DESALINATION AND/OR WATER RECLAMATION	
Is there a desalination or reuse plant available?	NO

Figure 6-12: “SIMULATION” worksheet overview.

6.1.6.1 Catchment of Origin Hydrology

The catchment of origin is the catchment where daily streamflow data was available for the main inflow stream into the system by means of observed volumes at a gauging station. Furthermore, the naturalized streamflow of the catchment of origin is used to generate stochastic streamflow sequences using STOMSA (section 3.1). The user is required to populate the blank cells indicated in Figure 6-13. The Mean Annual Precipitation (MAP) and Mean Annual Evaporation (MAE) for the quaternary catchment are both obtained from the WR2012 database under the “*Quaternary data spreadsheets*” folder (section 2.4.1). The coloured cells below the above-mentioned information are automatically filled. The user is required to choose a stochastic sequence number as highlighted in red in Figure 6-13. Number 102 is the historical sequence, while sequences 1 to 101 are stochastic sequences.

CATCHMENT OF ORIGIN HYDROLOGY		
Historical MAP	1465	mm
Historical MAE	1450	mm
Historical MAR	36.61	mil m ³
Stochastic Sequence MAR	36.3	mil m ³
Stochastic Sequence Number	101	choose

Figure 6-13: “Catchment of Origin Hydrology” information box

6.1.6.2 Storage Dam Characteristics

The full supply capacity of the storage dam, storage percentage at the start of a simulation, and the failure level or minimum operational capacity, are all set in the “SIMULATION” worksheet under the “Dam Characteristics” information box (Figure 6-14). If the dam is situated in the catchment of origin, the MAP, MAE and MAR are filled out according to the information in the “Catchment of Origin Hydrology” box. The dam might be in a different catchment than the catchment of origin. The user will then have to retrieve the MAP, MAE and MAR for the applicable quaternary catchment from the WR2012 database under the “*Quaternary data spreadsheets*” folder (section 2.4.1).

DAM CHARACTERISTICS			
Full Supply Capacity (Volume)	2.38	mil m ³	
Start Capacity Percentage	50	%	
Failure Capacity	0	%	
Demand Distributions of Draft	USE_2		
Historical MAP of Dam Catchment	754	mm	
Historical MAE of Dam Catchment	1455	mm	
Historical MAR of Dam Catchment	14.92	mil m ³	
Surface Area (m ²) =	21.83	x Volume(m ³)^	0.61

Figure 6-14: “Dam Characteristics” information box

6.1.6.3 Inflow streams hydrological characteristics

Provision is made for 3 different inflow streams into the storage dam, namely: Stream 1, Stream 2 and Stream 3. Hydrological characteristics and capacity limitations are set in the “Inflow Characteristics” information box (Figure 6-15) of the “SIMULATION” worksheet.

Stream 1 is the main stream for which daily streamflow data is observed at a gauging station, and the quaternary catchment of Stream 1 is the one used for generating stochastic sequences. Provision is made that Stream 1 not only has downstream abstraction (section 6.1.4) to be satisfied, but that an abstraction pipeline capacity can also be specified. The user sets this capacity in the “Inflow Characteristics” information box (Figure 6-15). Furthermore, the user has the option to select the percentage increase or decrease in infrastructural (pipeline) capacity, and diversion efficiency. Options for selection from a drop-down list are 80%, 100% or 120% for infrastructural capacity and 60%, 80% or 100% for diversion efficiency. The user sets the Mean Annual Runoff (MAR) of Stream 1 (mil m³), as calculated in the “*Streamflow Classification*” workbook in the “RAW_DFLOW” sheet. It can also be calculated manually using data retrieved from the DWS hydrology database for the specific streamflow gauging station, which is located in close proximity to Stream 1.

Stream 2 is an inflow stream representing abstraction through a pipeline. Provision is made for an infrastructural (pipeline) capacity. The user has the option to select the percentage increase or decrease

in infrastructural (pipeline) capacity, and diversion efficiency. Options for selection form a drop-down list are 80%, 100% or 120% for infrastructural capacity and 60%, 80% or 100% for diversion efficiency. The MAR of Stream 2 is also set.

Stream 3 is not limited by infrastructural capacity; it flows directly into the storage dam. Therefore, only the MAR of Stream 3 is set.

INFLOW CHARACTERISTICS		
Stream 1 Downstream demand & infrastructural capacity		
Downstream Demand	NO	
Infrastructure Capacity	470	l/s
Infrastructure Capacity Limitation	100	%
Diversion Efficiency	100	%
Historical MAR	22.30	mil m ³
Stream 2 Infrastructural capacity		
Infrastructure Capacity	0	l/s
Infrastructure Capacity Limitation	100	%
Diversion Efficiency	100	%
Historical MAR of Stream 2	0	mil m ³
Stream 3 Total inflow stream, no infrastructure		
Historical MAR of Stream 3	0.26	mil m ³

Figure 6-15: “Inflow Characteristics” information box (Streams 1, 2, and 3)

6.1.6.4 Conjunctive Use Components

Information pertaining to inter-basin transfer schemes, groundwater and desalination or water reclamation is set in different information boxes in the “SIMULATION” worksheet, namely: the “Interbasin Transfer”, “Long-Term Potential Groundwater Abstraction” and “Desalination and/or Water Reclamation” information boxes respectively (Figure 6-16).

Water entering the supply system through an inter-basin transfer scheme is modelled as a constant inflow stream with a capacity in Mega liters per annum (Mℓ/a). If the inter-basin transfer scheme cannot provide water for any reason, or provides less water than the standard allocation, the percentage of supply has to be set.

For a firm yield analysis and a long-term yield analysis, the long-term potential groundwater abstraction value in cubic meters per day (m³/day) is automatically set using the stochastic groundwater abstraction in the “SIMULATION” worksheet. The user selects a “YES” or “NO” option from a drop-down list, which indicates whether groundwater will be utilized or not. The user inserts the study area size where groundwater abstraction can potentially take place. The study area was previously required as input to the “Groundwater Simulation” workbook and is discussed in section 5.2.

If the water supply system incorporates desalination or a water reclamation plant, the user selects “YES” from a drop-down list. However, if neither desalination nor water reclamation plants are available or in

use during a specific simulation, the user selects “NO”. The desalination and water reclamation plant parameters and operational rules are set in the “DESAL” worksheet as discussed in section 6.1.3.

INTERBASIN TRANSFER		
Constant inflow	3000	ML/annum
Percentage Supplied	100	%

LONG-TERM POTENTIAL GROUNDWATER ABSTRACTION		
Are there boreholes available?	NO	
Study Area	35	km ²
Average available abstraction for sequence	0	m ³ /day

BOREHOLE ABSTRACTION		
Total combined long-term pumping rate	0	m ³ /day

DESALINATION AND/OR WATER RECLAMATION		
Is there a desalination or reuse plant available?	NO	0

Figure 6-16: Conjunctive use components information box

6.1.6.5 Target Draft/Demand

The target draft or demand is set in the blank cell found in the “System Yield for Long Term Yield Analysis” information box (Figure 6-17). Information on the number of sequences evaluated and the length of each sequence is automatically supplied in this information box. After setting the values in all the input sheets and information boxes, including setting the target draft, the “Refresh Data” button is selected. The “Conjunctive System Simulation” workbook will update and calculate the base yield, average yield, as well as the annual probability of failure, based on the 90-year naturalized streamflow sequence. Furthermore, the number of days, months and years that the system fail to supply the specific target draft when evaluating the historical sequence are also automatically updated in the “SIMUALTION” worksheet within the “System Yield for Long Term Yield Analysis” information box.

SYSTEM YIELD FOR LONG TERM ANALYSIS			
Number of Years available		90 years	
Start year	1920	start date	1920/10/01
End year	2010	end date	2010/09/30
Number of years to evaluate		90 years	
Sequences from		1 to	101
Yearly Failures		0 yearly	
Monthly Failures		0 months	
Daily Failures		0 days	
Target Draft		7671.88	x10 ³ m ³ /annum
Average Yield		7672	x10 ³ m ³ /annum
Base Yield		7672	x10 ³ m ³ /annum
Probability of Failure		0 %	
Reliability of Supply		100 %	
Refresh Data			

Figure 6-17: “System Yield for Long Term Yield Analysis” information box

To determine the historical firm yield of the historical sequence (naturalized streamflow record of 90 years), or the firm yield of any stochastic sequence, the user enters an initial target draft in the “Firm Yield Point” information box (Figure 6-18). The user then specifies the increment size by which the initially guessed target draft should be increased. The user chooses the stochastic sequence number from the drop-down list (number 102 is the historical sequence). The “Calculate Firm Yield Point” button is selected and the computation is automatically completed. The user then selects the “Historical Firm Yield Point” button, so that the historical firm yield point can be automatically calculated. Upon selection of either of the above-mentioned buttons, a progress bar will appear (Figure 6-19), which gives the user an indication of the amount of time the automated simulation is expected to be completed within, as well as the increment size and the number of target drafts that the sequences are evaluated at. The progress bar will disappear when the automated simulation is completed and the user can only make changes in the “Conjunctive System Simulation” workbook by then. Navigation buttons in the “Yield Analysis Curves” box are used to navigate to the desired analysis worksheet, discussed in sections 6.2, 6.3 and 6.4.

FIRM YIELD POINT			
Initial Guess of target draft	500	$\times 10^3 \text{ m}^3/\text{annum}$	Calculate Firm Yield point
Initial increment	1000	$\times 10^3 \text{ m}^3$	
smallest increment	1	$\times 10^3 \text{ m}^3$	
Sequence number	102		
Firm Yield Point	7672.00	$\times 10^3 \text{ m}^3$	

HISTORICAL FIRM YIELD POINT			
Sequence Number	102		Calculate Historical Firm Yield
Historical Firm Yield Point	7672	$\times 10^3 \text{ m}^3$	

Yield Analysis Curves		
Draft-Yield Curve	Long-term Reliability Curve	Short-term Management Curve

Figure 6-18: Firm yield point information boxes and buttons

Progress Bar

The firm yield of the sequence is determined iteratively.
Please be patience this can take a couple of minutes.

50 % complete. Increment Size: 500

Number of target drafts evaluated: 2

Progress bar showing 50% completion.

Figure 6-19: Progress bar for firm yield calculations

6.2 Time Series Graphs

Time-series graphs are generated for surface water (storage dam and its inflows), groundwater and a conjunctive contribution. The graphs automatically update, if the user changes input values and selects the “Refresh data” button in the “SIMULATION” worksheet.

6.2.1 “DAM_CAPACITY” Worksheet

The “DAM_CAPACITY” worksheet is illustrated in Figure 6-20. The daily storage capacity for the 90-year sequence is plotted on a graph to identify the critical period. Accompanying the dam capacity-time graph, is the inflow stream-time graph, which shows the daily inflows into the dam, namely: Stream 1, Stream 2 and Stream 3. Navigation buttons in the “DAM_CAPACITY” worksheet can be used to navigate between the different worksheets.

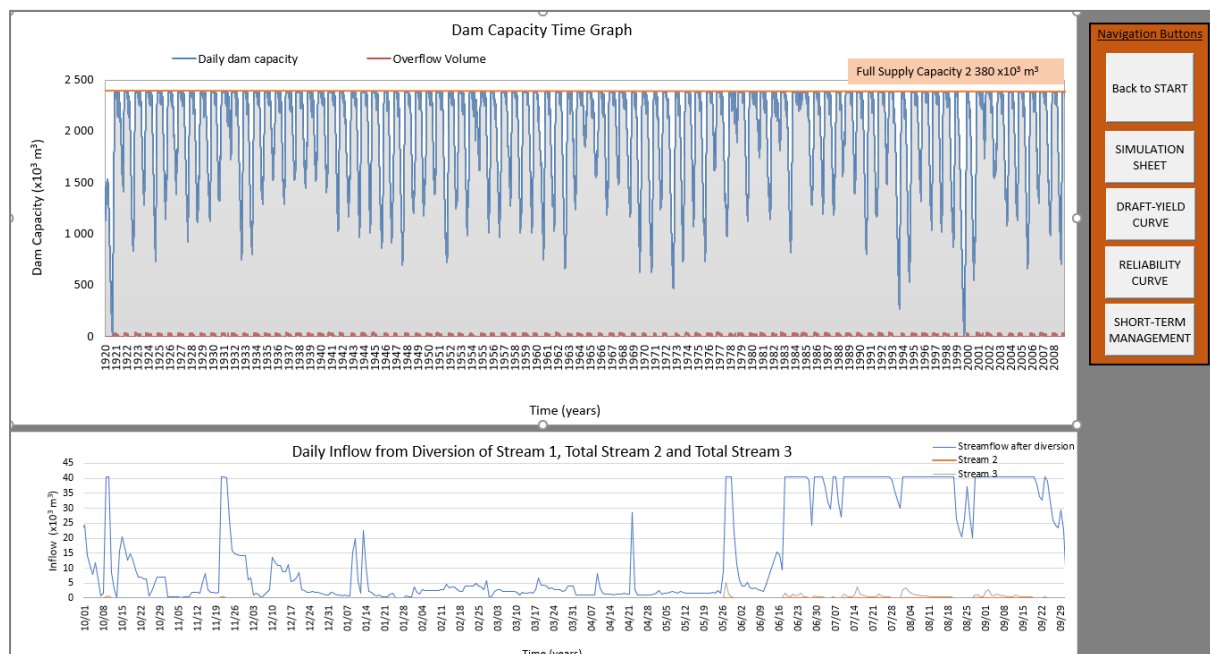


Figure 6-20: “DAM_CAPACITY” worksheet with graphs

The user can change the period over which the graph is generated by right clicking on the bottom time-axis and selecting the “Format Axis” option from the menu that will appear (Figure 6-21). The “Format Axis” tab is automatically opened on the right side of the screen. The user enters the customized dates as illustrated in Figure 6-22. This procedure can be followed to adjust the starting and ending dates of any graph in any of the different worksheets. The process can also be followed to change the bounds of the vertical axis by right clicking on the vertical axis and following the exact same procedure.

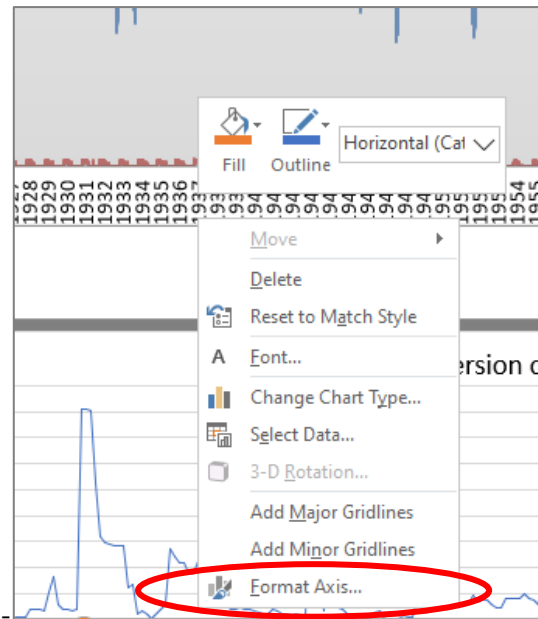


Figure 6-21: Pop up menu with “Format Axis” option

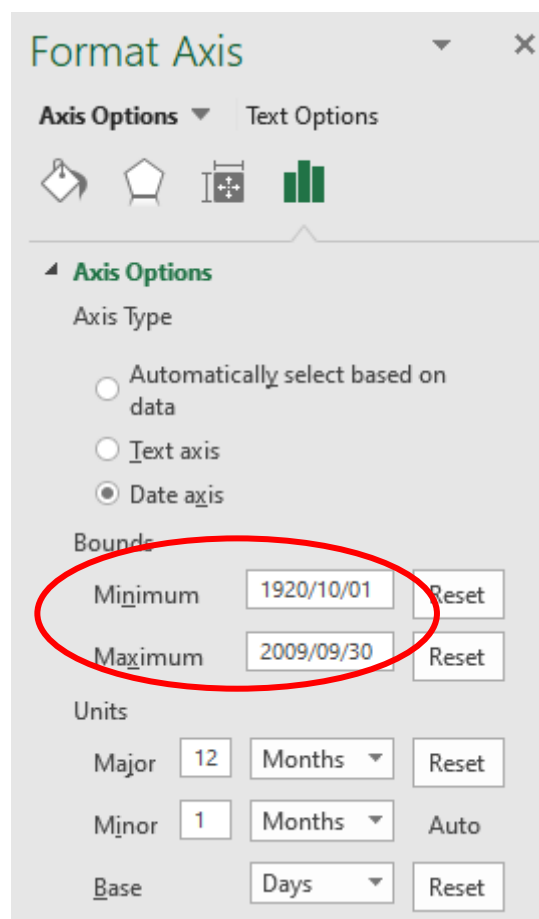


Figure 6-22: “Format Axis” tab with options for selection

6.2.2 “GW_CAPACITY” Worksheet

The “GW_CAPACITY” worksheet is illustrated in Figure 6-23. In the groundwater-time graph, the daily long-term groundwater abstraction volume is indicated, as well as the actual abstraction volume per month. The user can use the time-series groundwater abstraction graph to identify prominent trends, as well as identify the months in which potential over-abstraction is taking place. The time-axis can be adjusted by following the steps discussed in section 6.2.1 (Figure 6-21 and Figure 6-22).

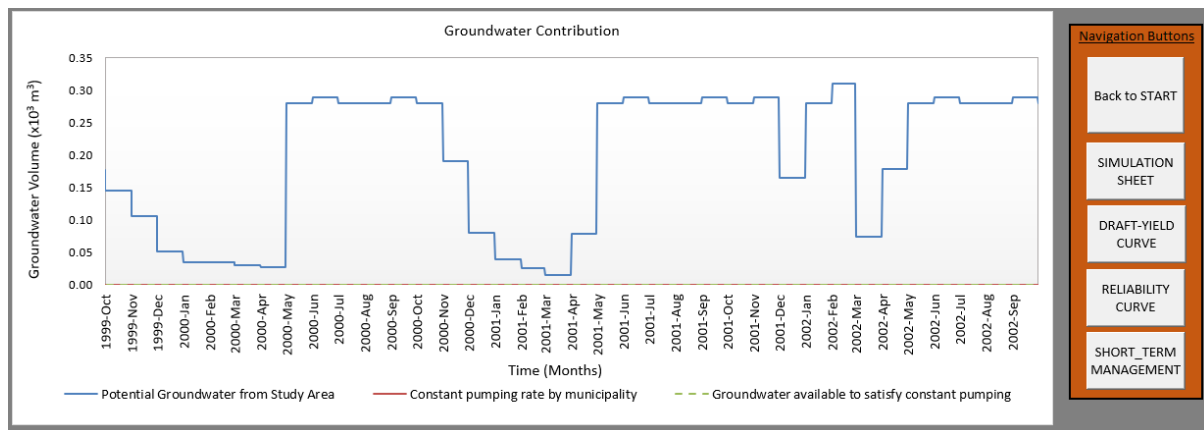


Figure 6-23: “GW_CAPACITY” worksheet with groundwater-time graph

6.2.3 “CONJ_CAPACITY” Worksheet

The “CONJ_CAPACITY” worksheet is illustrated in Figure 6-24. In the conjunctive use capacity graph, the daily contribution of each component in satisfying the demand is depicted. Daily bar charts are stacked for surface water, groundwater, inter-basin transfer, desalination and water reclamation, as well as demand for the user to identify the dominant water contributions with ease. The time-axis can be adjusted by following the steps discussed in section 6.2.1 (Figure 6-21 and Figure 6-22).

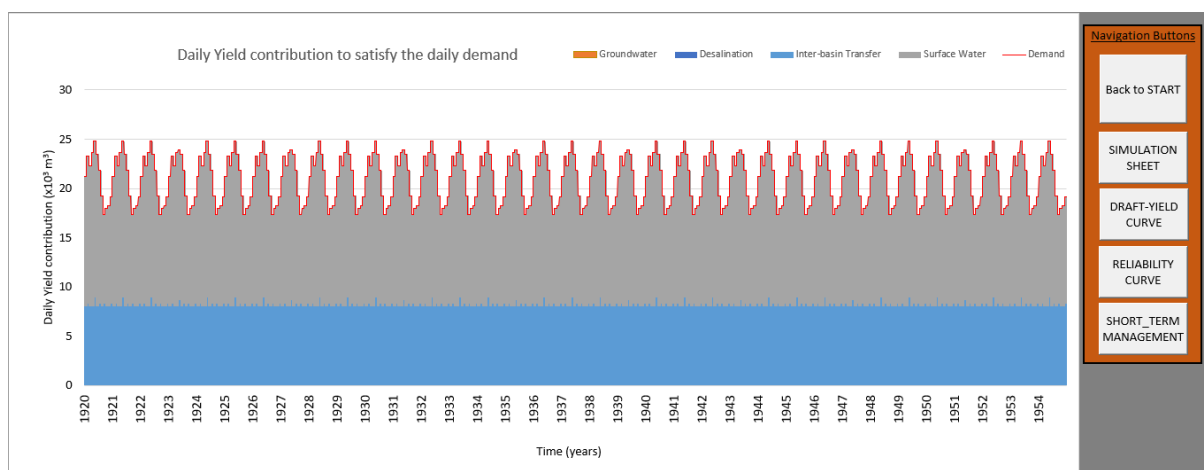


Figure 6-24: “CONJ_CAPACITY” worksheet with conjunctive use capacity graph

6.3 Output Analysis Worksheets

The output analysis worksheets, are the worksheets in which the target drafts are set to enable the model to generate the following graphs: draft-capacity graph; long-term reliability graph; and short-term management curve.

6.3.1 “DRAFT_YIELD” Worksheet

The “DRAFT_YIELD” worksheet, illustrated in Figure 6-25, is the worksheet in which the draft-yield curve is generated for a specific sequence. The user ensures that the firm yield point and historical firm yield point are calculated (section 6.1.6.5), after which the user is required to select the “Refresh Curve” button. This will automatically update the average and base yield values for each target draft, as well as the number of failures per day, month and year associated with the target draft. A progress bar similar to that indicated in Figure 6-19 is available for selection. The user can select the navigation buttons to navigate to the desired sheets.

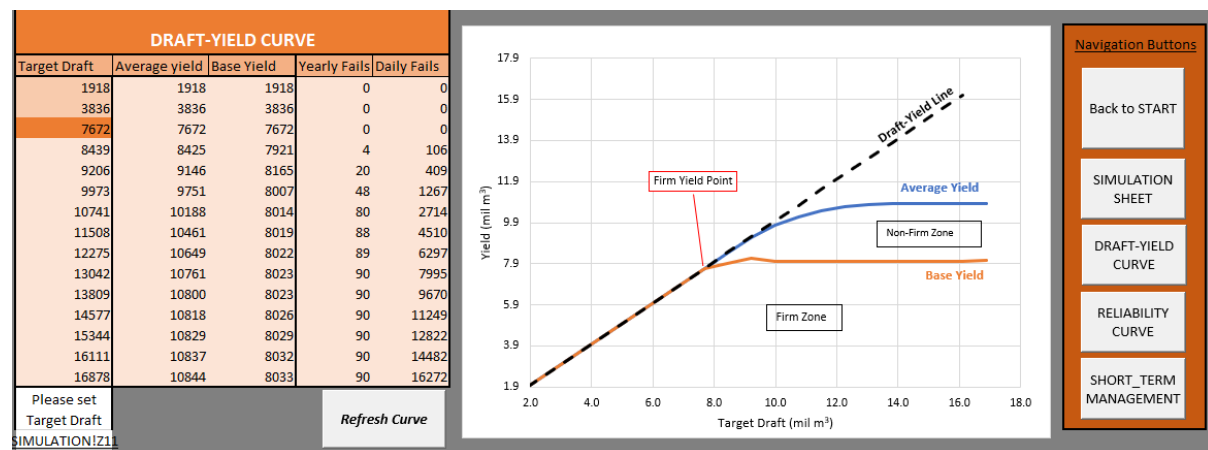


Figure 6-25: “DRAFT_YIELD” worksheet with historical firm yield point

6.3.2 “RELIABILITY” Worksheet

The long-term reliability of the supply system is calculated in the “RELIABILITY” worksheet in Figure 6-26. To generate long-term reliability yield curves, 7 target drafts are set. Provision has been made to evaluate 2 target drafts which are smaller than the historical firm yield and 4 which are larger than the historical firm yield. The user has to ensure that all information inserted into the “SIMULATION” sheet is correctly done before proceeding.

The user has to set increment values for the different target drafts. The increments are from the historical firm yield point. In other words, the historical firm yield point is automatically updated and the target drafts larger than the historical firm yield are evaluated to the right of the historical firm yield, and smaller drafts are evaluated to the left of the historical firm yield. After setting the target draft increments, the user selects the “Evaluate Long-Term Reliability” button. A progress bar will appear similar to the one indicated in Figure 6-19, specific to the long-term simulation. This process will take

up to 40 minutes, due to the 101 sequences that have to be evaluated for 7 different target drafts, every simulation takes roughly 4 seconds. No Microsoft Excel workbook may be used or opened at this stage of the analysis. After the simulation is completed, the progress bar will automatically disappear, and the user selects the “Sort” button. The yields that result from the 101 stochastic sequences, evaluated at different target drafts, are automatically sorted in descending order. And the Long-term reliability curve is automatically updated.

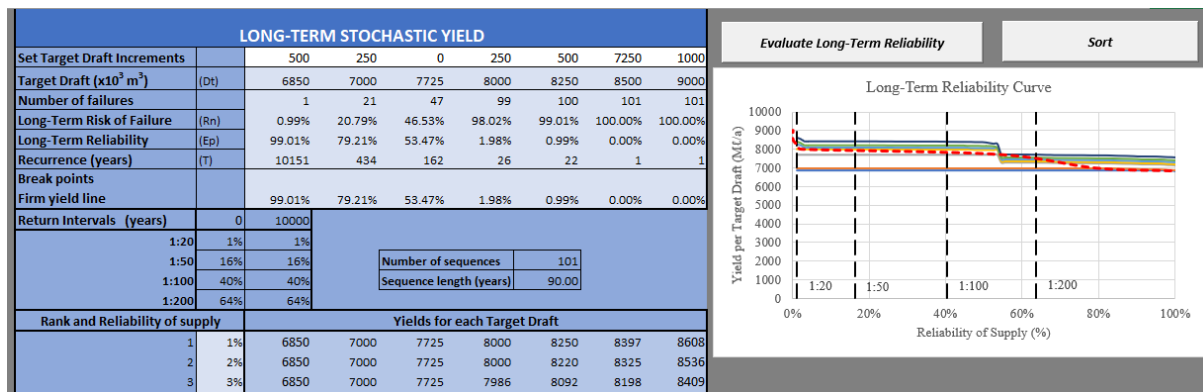


Figure 6-26: “RELIABILITY” Worksheet with long-term reliability graph

6.3.3 “SHORT_MNG” Worksheet

The Short-term management curves are generated through the use of probabilistic storage projections in the “SHORT_MNG” worksheet, illustrated in Figure 6-27. The user sets the short-term variables in this worksheet. The short-term variables are user defined according to the water supply system in use. The start capacity of the storage dam and the target draft/demand is set, after which the start year for commencement of the simulation period is selected from a drop-down list. The user selects the number of years to be evaluated from a drop-down menu (3 years max) as well. The percentage of the allocation that the inter-basin transfer scheme supplies to the system is also set, and if no inter-basin transfer scheme contributes to the system, the value should be set to 0. The user specifies the amount of groundwater that can be abstracted on a short-term basis, which is the combined yield of all the boreholes that a municipality has access to. The yield per borehole is retrieved from borehole yield tests. Furthermore, the user has to select “YES” if a desalination or water reclamation plant is available and ensure that the short-term management of that plant is set in the “DESAL” worksheet, before proceeding.

Upon having populated all the required fields with the correct information, the user has to select the “Refresh Short-Term Management Curve” button. A progress bar is automatically started, similar to the one indicated in Figure 6-19. When the progress bar closes the short-term management curve is automatically updated. During this simulation, no other Microsoft Excel workbook in the model should be opened or used. Navigation buttons aid the user to move between the different worksheets.

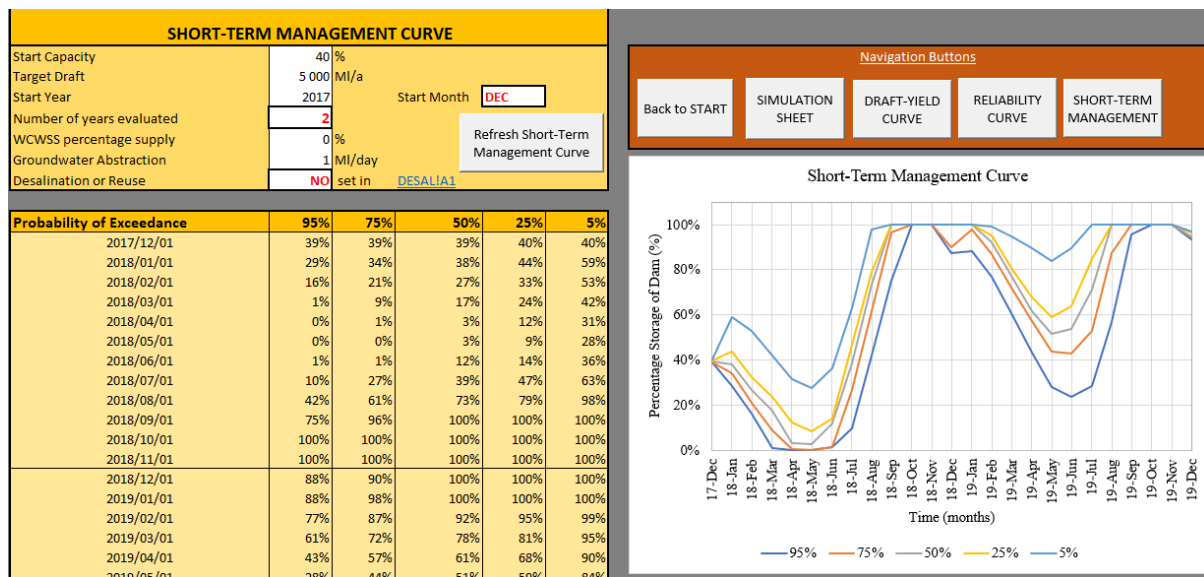


Figure 6-27: “SHORT_MNG” worksheet with Short-Term Management Curve

APPENDIX B – METHODOLOGY APPENDIX

B.1 Quality codes (DWS)

Qual code	Print code	Description
1		Good continuous data
2		Good edited data
3		Preserved historical data
4	Q	Unaudited
5		Height derived from flow
6	D	Drops
7	Q	Good edited unaudited
25	Q	Unaudited Gauge Plate Readings / dip level readings
26	\$	Audited Gauge Plate Readings / dip level readings
27	&	Good monthly reading
50	S	Gap filled data
58	H	Hb not available - assume no submergence
59	V	Static or reverse flow due to backwater submergence conditions
60	A	Above Rating
64	E	Audited Estimate
65	E	Unaudited Estimate
66	*	Program Estimate
70	?	Unknown
78	U	Not Accumulated Unreliable
79	%	Accumulated Unreliable
80	+	Accumulated Reliable
81	#	Wet day within accumulated rainfall period
90	<	GW: Water level below instrument
91	>	Minimum Value
92	<	Maximum Value
93	<	Dry borehole
94	>	Artesian borehole level
95	<	Borehole Seepage
100	?	Flag Boshielo Dam under construction. New FSL not yet implemented.
<hr/>		
130	E	Used previous week's level as an estimate for this week
140	!	Data not yet checked
150	^	Rating table extrapolated - flows estimated
151	M	Data Missing
152	~	Negative
153	F	No height data - Flow data only
154	[Reversal start
155]	Reversal end
160	Z	No info for stage/discharge determination (zero dt loaded)
161	T	Rating missing
162	R	Rating unreliable
163	G	Gate(s) in operation - no spillway discharge
164	B	Continuously variable submergence flow derivation DT in operation
165	P	Estuarine water level recording only - no flow calculated
170	M	Permanent Gap
172	M	Temporary Gap
173	?	Data Unreliable
201	[Data not recorded or incomplete
245	V	Undefined submergence flow calc program exception
246	M	No cross-sectional area upstream of notch/structure
247	V	ha > rating table limit - no calculation performed
248	V	No hb data
249	V	No ha data
250	V	Structural submergence > 97.7%
251	V	Static or reverse flow possibilities
252	V	Froude number > 0.8 at inlet section
253	V	Flow not converging to constant val after max # iterations
254	A	Rating Table Exceeded
255	M	Data Missing

B.2 Derivation of General Equation for Surface Area-Capacity relationship

The depth-capacity curve, using a power function, is derived to describe the area-capacity relationship of a reservoir. The derivation process is followed from Equation B-1 to Equation B-6.

The depth-capacity power function is given as Equation B-1:

$$Volume = a (Depth^b) \quad (B-1)$$

From which it follows that *Depth* can be written as Equation B-2:

$$Depth = \sqrt[b]{\frac{Volume}{a}} \quad (B-2)$$

The derivative of *Volume* in terms of *Depth* expresses surface area (*SA*) as written in Equation B-3:

$$\frac{d(Volume)}{d(Depth)} = SA \quad (B-3)$$

Therefore, the derivative of Equation B-1 in terms of *Depth* is written as Equation B-4:

$$SA = \frac{d(Volume)}{d(Depth)} = a \times b \times (Depth)^{(b-1)} \quad (B-4)$$

To express the area-capacity relationship in terms of volume, Equation B-2 is substituted into Equation B-4, leading to Equation B-5:

$$SA = \frac{d(Volume)}{d(Depth)} = a \times b \times \left(\sqrt[b]{\frac{Volume}{a}} \right)^{(b-1)} \quad (B-5)$$

Equation B-5 is rearranged as Equation B-6:

$$SA = a \times b \times \left(\frac{Volume}{a} \right)^{\left(\frac{1}{b}\right) \times (b-1)} \quad (B-6)$$

APPENDIX C – STELLENBOSCH CASE STUDY DATA AND PROCESSING

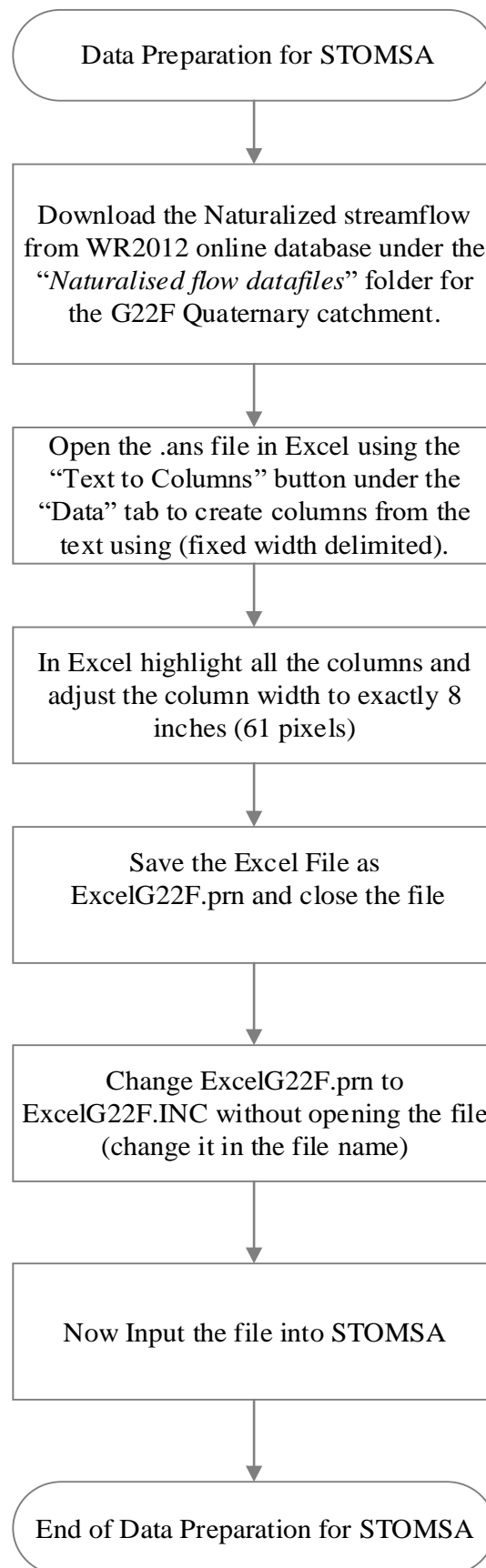
Appendix C.1 Generating Stochastic Monthly Streamflow

C.1.1 NATURALIZED STREAMFLOW SEQUENCE FOR G22F (MIL M3/MONTH)

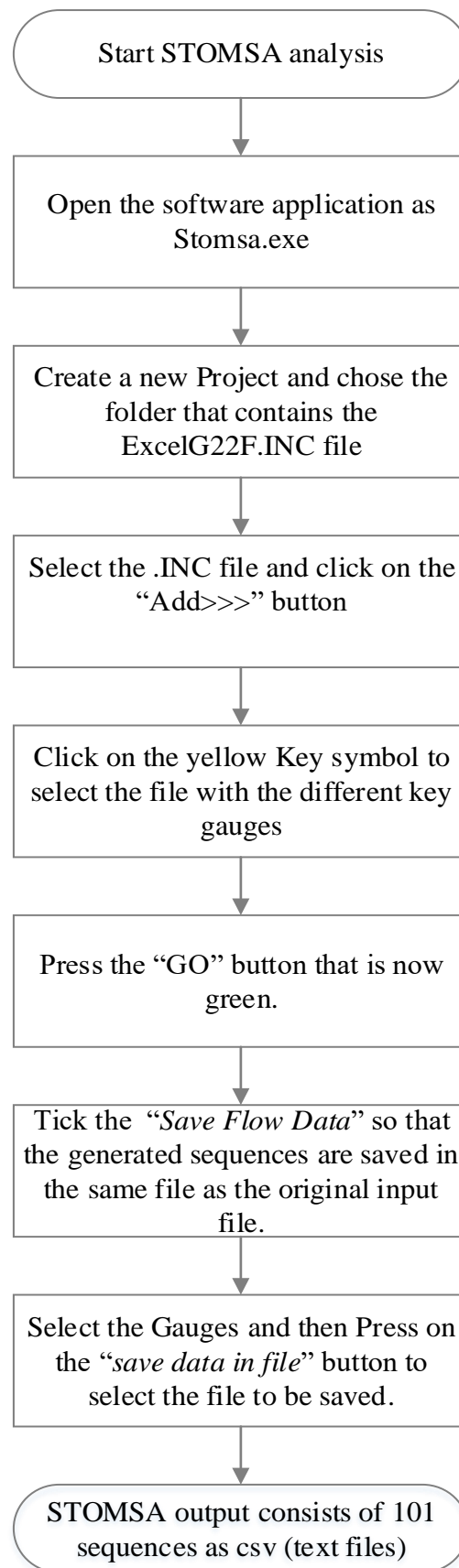
Year	Oct	Nov	Dec	Jan	Feb	Mar	Apr	May	Jun	Jul	Aug	Sep	Total
1920	2.26	1.25	0.54	0.50	0.41	0.29	0.56	0.49	16.85	14.11	7.86	4.63	49.75
1921	2.25	1.06	0.78	1.65	0.94	0.79	0.79	1.84	9.87	7.01	6.54	4.95	38.47
1922	2.22	1.04	0.48	0.24	0.12	0.06	1.24	7.28	13.40	10.81	7.00	4.85	48.74
1923	3.00	2.79	1.59	0.60	0.39	0.46	0.48	2.22	6.52	5.97	6.09	4.32	34.43
1924	2.83	3.05	1.50	0.45	0.23	0.09	0.10	1.28	10.25	10.68	6.15	3.14	39.75
1925	4.39	3.56	1.34	0.39	0.31	0.24	0.34	3.62	3.74	5.96	6.69	4.26	34.84
1926	5.01	3.06	0.81	0.24	0.90	0.61	0.68	3.15	3.42	3.53	5.84	4.38	31.63
1927	1.97	2.10	1.71	0.80	0.30	0.26	0.32	0.46	6.59	6.29	6.11	6.72	33.63
1928	3.72	1.39	0.72	0.33	0.13	0.08	2.44	4.37	3.95	6.09	6.97	4.12	34.31
1929	1.89	1.12	1.84	1.19	0.50	0.52	0.62	0.69	1.20	4.09	6.72	9.22	29.60
1930	5.64	2.71	1.19	0.32	0.23	0.17	2.34	3.98	3.69	4.83	7.08	7.05	39.23
1931	6.84	3.31	0.89	0.48	2.08	1.45	0.72	0.50	4.50	6.14	5.09	4.20	36.20
1932	2.69	1.26	0.67	0.40	0.25	0.17	0.22	1.68	5.55	6.88	7.64	4.45	31.86
1933	2.34	1.32	0.47	0.17	0.15	0.34	0.34	4.39	4.87	3.61	5.00	5.00	28.00
1934	3.76	3.03	1.38	0.42	0.22	0.31	1.42	4.51	4.05	5.54	6.30	4.90	35.84
1935	3.07	2.99	1.54	0.99	0.62	1.12	0.79	3.28	3.27	3.32	4.83	5.44	31.26
1936	3.12	1.49	0.97	0.58	0.26	0.43	1.13	3.17	10.22	12.07	7.42	3.97	44.83
1937	2.90	1.77	0.70	1.06	0.68	0.21	2.43	5.65	4.66	4.26	4.63	6.27	35.22
1938	4.35	2.05	0.87	0.26	0.62	0.44	1.74	3.87	2.98	3.25	5.34	3.76	29.53
1939	1.73	1.25	1.32	0.68	0.32	0.72	2.98	3.30	6.15	5.27	3.27	3.27	30.26
1940	3.00	2.51	1.21	0.49	0.31	0.21	4.93	7.87	9.02	8.26	7.42	11.08	56.31
1941	6.71	2.45	1.03	0.49	0.22	0.10	0.30	5.50	11.23	7.33	6.84	4.73	46.93
1942	2.26	1.10	0.42	0.57	0.52	0.43	1.19	3.09	3.74	5.77	7.68	5.19	31.96
1943	3.17	2.16	0.96	0.32	0.13	0.08	0.67	6.66	11.92	9.67	8.20	7.73	51.67
1944	4.80	2.19	1.07	0.44	0.13	0.07	0.78	9.14	13.06	12.09	10.54	4.85	59.16
1945	2.63	1.88	0.86	0.33	0.13	0.29	0.71	1.82	2.64	4.75	5.83	7.95	29.82
1946	5.03	1.75	0.65	0.24	0.08	0.47	0.79	3.38	3.60	9.35	7.65	3.85	36.84
1947	2.29	1.15	0.44	0.15	0.07	0.18	0.69	3.45	5.46	7.69	6.00	6.01	33.58
1948	4.89	2.12	0.86	0.43	0.18	0.08	1.87	2.24	2.40	4.31	5.51	4.62	29.51
1949	2.76	1.99	1.01	0.29	0.09	0.06	4.78	3.23	1.82	10.13	6.71	4.46	37.33
1950	3.30	2.27	1.54	0.79	0.32	0.11	2.68	3.09	7.44	7.88	4.88	3.74	38.04
1951	2.75	1.90	0.87	0.24	0.09	0.14	0.55	1.53	1.78	3.77	5.87	5.71	25.20
1952	3.50	2.73	1.35	0.33	0.12	0.11	3.37	5.04	4.17	5.05	4.80	2.72	33.29
1953	1.43	1.52	0.85	0.27	0.14	0.15	1.10	4.66	4.20	7.89	8.16	4.20	34.57
1954	2.11	1.20	0.59	0.25	2.20	1.37	0.43	0.53	2.14	5.86	8.09	4.95	29.72
1955	3.22	2.78	1.25	0.35	0.13	0.13	0.58	2.92	5.59	5.20	5.38	3.49	31.02
1956	1.85	0.98	0.47	0.23	0.41	0.37	0.50	4.36	6.08	6.22	5.25	3.39	30.11
1957	4.76	2.79	0.63	0.18	0.87	0.64	0.76	5.20	5.05	2.60	4.95	3.71	32.14
1958	2.11	1.20	0.42	0.20	0.13	0.17	4.54	11.87	7.15	2.83	5.01	4.62	40.25
1959	4.07	2.16	0.70	0.37	0.19	0.33	0.80	4.56	8.13	4.78	2.60	2.36	31.05
1960	1.60	0.74	0.34	1.28	0.79	0.17	0.18	1.62	4.78	3.93	5.62	5.80	26.85
1961	3.37	1.33	0.43	0.21	0.39	0.87	1.99	1.74	11.00	9.60	10.44	6.66	48.03
1962	5.09	3.12	0.96	0.40	0.18	0.08	0.10	0.78	2.67	8.56	10.17	5.23	37.34
1963	1.90	1.67	1.44	0.60	0.51	0.32	0.32	2.35	5.94	6.84	7.00	4.36	33.25
1964	2.82	2.44	1.14	0.41	0.59	2.20	2.96	3.97	3.22	2.85	4.34	3.40	30.34
1965	1.96	0.99	0.80	0.44	0.20	1.96	1.99	2.95	3.18	6.80	7.10	4.66	33.03

1966	2.32	1.10	0.58	0.37	0.18	0.15	3.97	3.90	7.31	6.37	4.32	3.40	33.97
1967	3.82	2.53	0.89	0.86	0.70	0.28	1.22	5.38	7.90	8.36	7.06	3.83	42.83
1968	3.47	2.02	0.84	0.92	0.62	0.38	0.89	0.88	3.01	3.48	4.49	4.53	25.53
1969	3.82	1.92	0.56	0.19	0.12	0.07	0.07	4.59	6.66	6.10	8.13	6.03	38.26
1970	3.02	1.44	0.79	0.39	0.14	0.09	0.12	1.20	2.98	4.43	6.77	4.36	25.73
1971	2.22	1.20	0.47	0.33	0.30	0.21	3.83	5.74	4.66	3.78	4.74	3.87	31.35
1972	2.13	0.93	0.59	0.31	0.09	0.14	0.14	1.16	1.20	4.81	4.77	4.29	20.56
1973	2.70	1.20	0.69	0.33	0.13	0.07	0.07	4.78	6.88	5.60	13.23	9.35	45.03
1974	5.90	3.23	0.95	0.48	0.26	0.12	0.86	5.71	5.76	8.81	8.37	4.00	44.45
1975	2.63	1.76	0.68	0.21	0.08	0.26	1.13	1.91	11.05	10.29	6.77	6.10	42.87
1976	3.97	4.62	4.35	1.71	0.45	0.42	2.91	7.19	12.64	12.61	10.03	6.06	66.96
1977	3.02	1.34	0.71	0.35	0.26	0.42	1.25	1.95	1.68	1.54	4.89	5.44	22.85
1978	3.69	1.70	0.92	0.56	2.23	1.36	0.26	3.74	5.52	4.61	3.59	3.41	31.59
1979	6.22	3.47	0.68	0.31	0.27	0.15	1.34	4.15	7.75	4.70	3.27	2.78	35.09
1980	1.96	3.12	2.19	2.76	1.46	0.57	1.82	1.40	2.71	7.87	8.18	6.46	40.50
1981	3.37	1.58	0.95	0.66	0.32	0.13	2.19	1.95	3.35	4.01	3.97	2.57	25.05
1982	1.68	1.36	1.41	0.71	1.38	1.32	0.65	7.31	10.42	7.72	5.05	4.93	43.94
1983	2.98	1.06	0.44	0.22	0.11	0.51	1.12	6.01	5.08	4.25	3.47	4.30	29.55
1984	4.96	2.40	3.53	2.16	1.14	2.43	3.48	2.66	5.27	8.22	6.76	4.41	47.42
1985	2.56	1.16	0.49	0.23	0.26	1.02	2.17	2.45	6.03	7.33	10.32	6.85	40.87
1986	2.80	1.28	0.56	0.83	0.54	0.23	0.97	5.08	6.55	7.90	8.32	6.77	41.83
1987	3.49	1.33	1.06	0.58	0.15	0.13	1.46	2.94	4.26	6.07	7.88	6.26	35.61
1988	3.84	1.86	0.71	0.26	0.17	4.23	3.21	3.63	4.62	7.11	7.44	6.06	43.14
1989	4.49	2.68	1.05	0.36	0.28	0.17	5.09	4.99	6.41	10.39	6.68	3.15	45.74
1990	1.84	1.09	0.71	0.33	0.12	0.08	0.20	2.99	5.85	13.99	8.49	4.77	40.46
1991	3.50	1.56	0.58	0.20	0.22	0.29	2.72	3.90	8.22	7.83	5.14	4.78	38.94
1992	4.84	2.69	0.90	0.33	0.48	0.33	9.96	9.96	8.67	10.68	7.67	3.49	60.00
1993	1.49	0.69	0.34	0.30	0.18	0.07	0.20	0.92	9.54	8.20	4.22	2.96	29.11
1994	1.91	0.95	0.40	0.19	0.10	0.07	0.22	3.44	6.31	7.86	8.62	4.92	34.99
1995	3.98	2.31	2.07	1.11	0.69	0.72	0.89	0.90	6.00	7.05	6.11	5.94	37.77
1996	6.27	4.09	3.63	1.74	0.30	0.11	0.62	1.83	5.26	4.98	4.70	3.00	36.53
1997	1.31	3.61	2.16	0.41	0.14	0.08	1.09	9.85	8.15	5.75	4.60	2.77	39.92
1998	1.58	2.13	1.71	0.61	0.15	0.05	1.22	1.42	4.16	2.84	0.87	0.79	17.53
1999	0.67	0.47	0.24	0.16	0.15	0.14	0.12	1.74	2.42	4.41	5.51	4.43	20.46
2000	2.28	0.85	0.37	0.18	0.11	0.07	0.35	3.49	3.50	11.34	11.86	7.18	41.58
2001	4.64	2.25	0.76	2.87	1.75	0.34	0.80	3.43	6.28	8.38	6.95	3.83	42.28
2002	2.47	1.59	0.74	0.30	0.13	2.62	1.93	2.04	2.17	2.38	8.09	7.05	31.51
2003	3.48	1.43	0.88	0.57	0.22	0.17	2.16	1.51	2.48	4.18	5.55	4.08	26.71
2004	3.80	2.08	0.57	0.47	0.32	0.19	1.22	3.07	6.73	5.60	6.65	4.63	35.33
2005	2.15	1.16	0.48	0.16	0.08	0.07	0.65	5.43	5.53	6.76	7.65	4.46	34.58
2006	2.24	1.72	1.00	0.37	0.32	0.33	1.24	4.20	7.55	9.32	8.20	4.51	41.00
2007	3.69	3.67	1.73	0.56	0.41	0.36	0.31	1.76	4.35	9.48	7.78	9.64	43.74
2008	5.70	3.18	1.77	0.49	0.16	0.07	0.22	1.66	7.44	8.23	6.19	5.66	40.77
2009	3.64	3.97	2.09	0.40	0.22	0.18	0.46	5.73	6.72	4.61	3.42	2.27	33.71
AVERAGE	3.24	1.98	1.03	0.55	0.41	0.46	1.42	3.59	5.89	6.67	6.46	4.87	36.58

C.1.2 Preparation of STOMSA streamflow Input file



C.1.3 Process followed in STOMSA program



C.1.4 Stochastic Sequence generated with STOMSA (ExcelG22F003) (mil m³/month)

1920	1.95	0.99	0.80	0.44	0.20	1.95	1.98	2.94	3.17	6.77	7.07	4.64	32.90
1921	3.51	2.74	1.35	0.33	0.12	0.11	3.38	5.06	4.18	5.07	4.81	2.73	33.39
1922	2.80	1.28	0.56	0.83	0.54	0.23	0.97	5.08	6.55	7.90	8.32	6.77	41.85
1923	3.27	1.53	0.92	0.64	0.31	0.13	2.12	1.89	3.25	3.89	3.85	2.49	24.30
1924	6.27	4.09	3.63	1.74	0.30	0.11	0.62	1.83	5.26	4.98	4.70	3.00	36.51
1925	2.81	1.28	0.56	0.83	0.54	0.23	0.97	5.10	6.57	7.93	8.35	6.79	41.98
1926	3.50	2.73	1.35	0.33	0.12	0.11	3.37	5.04	4.17	5.05	4.80	2.72	33.30
1927	2.31	1.10	0.58	0.37	0.18	0.15	3.96	3.89	7.29	6.35	4.31	3.39	33.86
1928	2.26	1.06	0.78	1.65	0.94	0.79	0.79	1.84	9.90	7.03	6.56	4.96	38.57
1929	3.01	1.33	0.71	0.35	0.26	0.42	1.24	1.94	1.67	1.53	4.87	5.42	22.75
1930	0.65	0.46	0.23	0.16	0.15	0.14	0.12	1.69	2.35	4.28	5.35	4.30	19.85
1931	1.67	1.35	1.40	0.70	1.37	1.31	0.64	7.25	10.33	7.65	5.01	4.89	43.56
1932	1.68	1.36	1.41	0.71	1.38	1.32	0.65	7.30	10.41	7.71	5.04	4.92	43.88
1933	4.76	2.17	1.06	0.44	0.13	0.07	0.77	9.06	12.94	11.98	10.44	4.81	58.62
1934	2.75	1.90	0.87	0.24	0.09	0.14	0.55	1.53	1.78	3.77	5.87	5.71	25.18
1935	2.32	1.31	0.47	0.17	0.15	0.34	0.34	4.35	4.82	3.58	4.95	4.95	27.73
1936	3.20	2.77	1.24	0.35	0.13	0.13	0.58	2.91	5.56	5.17	5.35	3.47	30.86
1937	2.25	1.06	0.78	1.65	0.94	0.79	0.79	1.84	9.87	7.01	6.54	4.95	38.46
1938	3.51	1.56	0.58	0.20	0.22	0.29	2.73	3.91	8.24	7.85	5.15	4.79	39.04
1939	0.67	0.47	0.24	0.16	0.15	0.14	0.12	1.73	2.41	4.39	5.48	4.41	20.35
1940	2.79	1.28	0.56	0.83	0.54	0.23	0.97	5.07	6.53	7.88	8.30	6.75	41.73
1941	2.11	1.20	0.42	0.20	0.13	0.17	4.54	11.88	7.15	2.83	5.01	4.62	40.28
1942	3.29	1.54	0.93	0.65	0.31	0.13	2.14	1.91	3.28	3.92	3.88	2.51	24.49
1943	5.91	3.23	0.95	0.48	0.26	0.12	0.86	5.72	5.77	8.82	8.38	4.01	44.52
1944	2.97	1.32	0.70	0.34	0.26	0.41	1.23	1.92	1.65	1.51	4.81	5.35	22.48
1945	2.83	1.29	0.57	0.84	0.55	0.23	0.98	5.13	6.62	7.98	8.41	6.84	42.28
1946	1.89	1.12	1.84	1.19	0.50	0.52	0.62	0.69	1.20	4.09	6.72	9.22	29.61
1947	1.95	0.98	0.79	0.44	0.20	1.95	1.98	2.93	3.16	6.75	7.05	4.63	32.79
1948	3.49	1.33	1.06	0.58	0.15	0.13	1.46	2.94	4.26	6.07	7.88	6.26	35.61
1949	3.13	1.39	0.74	0.36	0.27	0.44	1.30	2.02	1.74	1.60	5.07	5.64	23.68
1950	1.96	0.99	0.80	0.44	0.20	1.96	1.99	2.94	3.17	6.79	7.09	4.65	32.97
1951	3.18	2.17	0.96	0.32	0.13	0.08	0.67	6.69	11.97	9.71	8.24	7.76	51.90
1952	1.61	0.75	0.34	1.29	0.80	0.17	0.18	1.63	4.82	3.96	5.66	5.84	27.06
1953	1.67	1.35	1.40	0.70	1.37	1.31	0.64	7.25	10.34	7.66	5.01	4.89	43.60
1954	3.20	2.77	1.24	0.35	0.13	0.13	0.58	2.90	5.56	5.17	5.35	3.47	30.85
1955	4.52	2.70	1.06	0.36	0.28	0.17	5.13	5.03	6.46	10.47	6.73	3.17	46.09
1956	4.78	2.80	0.63	0.18	0.87	0.64	0.76	5.22	5.07	2.61	4.97	3.73	32.29
1957	5.67	2.72	1.20	0.32	0.23	0.17	2.35	4.00	3.71	4.85	7.11	7.08	39.42
1958	4.76	2.79	0.63	0.18	0.87	0.64	0.76	5.20	5.05	2.60	4.95	3.71	32.11
1959	3.06	2.98	1.54	0.99	0.62	1.12	0.79	3.27	3.26	3.31	4.82	5.43	31.18
1960	3.97	2.30	2.06	1.11	0.69	0.72	0.89	0.90	5.98	7.03	6.09	5.92	37.64
1961	2.76	1.99	1.01	0.29	0.09	0.06	4.78	3.23	1.82	10.13	6.71	4.46	37.32
1962	2.69	1.26	0.67	0.40	0.25	0.17	0.22	1.68	5.54	6.87	7.63	4.44	31.81
1963	4.79	2.81	0.63	0.18	0.88	0.64	0.76	5.23	5.08	2.62	4.98	3.73	32.33
1964	1.89	1.12	1.84	1.19	0.50	0.52	0.62	0.69	1.20	4.09	6.72	9.22	29.60
1965	3.01	1.34	0.71	0.35	0.26	0.42	1.25	1.95	1.68	1.54	4.88	5.43	22.79
1966	1.49	0.69	0.34	0.30	0.18	0.07	0.20	0.92	9.54	8.20	4.22	2.96	29.11
1967	2.27	1.26	0.54	0.50	0.41	0.29	0.56	0.49	16.92	14.17	7.89	4.65	49.97
1968	6.83	3.30	0.89	0.48	2.08	1.45	0.72	0.50	4.49	6.13	5.08	4.19	36.13
1969	6.74	2.46	1.04	0.49	0.22	0.10	0.30	5.53	11.29	7.37	6.88	4.75	47.17
1970	2.92	2.45	1.18	0.48	0.30	0.20	4.80	7.67	8.79	8.05	7.23	10.79	54.86

1971	2.80	1.28	0.56	0.83	0.54	0.23	0.97	5.08	6.55	7.89	8.31	6.77	41.80
1972	3.00	2.79	1.59	0.60	0.39	0.46	0.48	2.22	6.52	5.97	6.09	4.32	34.44
1973	5.91	3.23	0.95	0.48	0.26	0.12	0.86	5.72	5.77	8.82	8.38	4.00	44.49
1974	2.96	2.47	1.19	0.48	0.31	0.21	4.86	7.75	8.89	8.14	7.31	10.92	55.48
1975	2.90	1.77	0.70	1.06	0.68	0.21	2.43	5.66	4.67	4.27	4.64	6.28	35.27
1976	2.16	0.94	0.60	0.31	0.09	0.14	0.14	1.18	1.22	4.88	4.84	4.36	20.88
1977	3.50	1.56	0.58	0.20	0.22	0.29	2.72	3.90	8.22	7.83	5.14	4.78	38.96
1978	5.05	1.76	0.65	0.24	0.08	0.47	0.79	3.39	3.61	9.39	7.68	3.87	36.99
1979	3.50	2.73	1.35	0.33	0.12	0.11	3.37	5.04	4.17	5.05	4.80	2.72	33.32
1980	1.94	0.98	0.79	0.44	0.20	1.94	1.97	2.93	3.15	6.75	7.04	4.62	32.77
1981	1.47	0.68	0.34	0.30	0.18	0.07	0.20	0.91	9.41	8.09	4.16	2.92	28.72
1982	3.97	2.30	2.06	1.11	0.69	0.72	0.89	0.90	5.98	7.03	6.09	5.92	37.64
1983	2.30	1.30	0.46	0.17	0.15	0.33	0.33	4.31	4.78	3.54	4.91	4.91	27.49
1984	2.28	0.85	0.37	0.18	0.11	0.07	0.35	3.50	3.51	11.36	11.88	7.19	41.66
1985	2.82	3.04	1.50	0.45	0.23	0.09	0.10	1.28	10.23	10.65	6.14	3.13	39.65
1986	2.36	1.33	0.47	0.17	0.15	0.34	0.34	4.43	4.91	3.64	5.04	5.04	28.24
1987	1.94	0.98	0.79	0.43	0.20	1.94	1.96	2.91	3.14	6.71	7.01	4.60	32.61
1988	2.63	1.88	0.86	0.33	0.13	0.29	0.71	1.82	2.64	4.76	5.84	7.96	29.87
1989	2.28	1.15	0.44	0.15	0.07	0.18	0.69	3.44	5.44	7.66	5.98	5.99	33.46
1990	1.96	0.99	0.80	0.44	0.20	1.96	1.99	2.95	3.18	6.79	7.09	4.65	32.99
1991	3.21	2.78	1.25	0.35	0.13	0.13	0.58	2.92	5.58	5.19	5.37	3.48	30.97
1992	2.33	1.10	0.58	0.37	0.18	0.15	3.99	3.92	7.34	6.40	4.34	3.41	34.12
1993	6.84	3.31	0.89	0.48	2.08	1.45	0.72	0.50	4.50	6.14	5.09	4.20	36.18
1994	1.67	1.35	1.40	0.71	1.37	1.31	0.65	7.28	10.38	7.69	5.03	4.91	43.76
1995	6.87	3.32	0.89	0.48	2.09	1.46	0.72	0.50	4.52	6.16	5.11	4.22	36.33
1996	2.82	1.29	0.56	0.84	0.54	0.23	0.98	5.12	6.60	7.96	8.39	6.82	42.16
1997	3.37	1.58	0.95	0.66	0.32	0.13	2.19	1.95	3.35	4.01	3.97	2.57	25.03
1998	3.96	4.61	4.34	1.70	0.45	0.42	2.90	7.17	12.60	12.57	10.00	6.04	66.76
1999	3.05	1.45	0.80	0.39	0.14	0.09	0.12	1.21	3.01	4.47	6.84	4.40	25.98
2000	5.64	2.71	1.19	0.32	0.23	0.17	2.34	3.98	3.69	4.83	7.08	7.05	39.25
2001	1.96	0.99	0.80	0.44	0.20	1.96	1.99	2.95	3.18	6.80	7.10	4.66	33.04
2002	2.83	1.29	0.57	0.84	0.55	0.23	0.98	5.13	6.61	7.97	8.40	6.83	42.22
2003	3.00	2.79	1.59	0.60	0.39	0.46	0.48	2.22	6.52	5.97	6.09	4.32	34.44
2004	2.82	3.04	1.50	0.45	0.23	0.09	0.10	1.28	10.23	10.66	6.14	3.13	39.67
2005	6.24	4.07	3.61	1.73	0.30	0.11	0.62	1.82	5.24	4.96	4.68	2.99	36.37
2006	1.59	0.74	0.34	1.27	0.79	0.17	0.18	1.61	4.75	3.91	5.59	5.77	26.71
2007	2.33	1.32	0.47	0.17	0.15	0.34	0.34	4.38	4.86	3.60	4.99	4.99	27.92
2008	6.65	2.43	1.02	0.49	0.22	0.10	0.30	5.45	11.13	7.27	6.78	4.69	46.52
2009	3.71	1.39	0.72	0.33	0.13	0.08	2.43	4.36	3.94	6.07	6.95	4.11	34.21

Appendix C.2 Streamflow Disaggregation

C.2.1 Daily Streamflow Data for Flow Gauge G2H037 (DWS)

Data are continuously updated and reviewed.

The format of this file is as follows:

POS. 1-8 = Date of daily flow CCYYMMDD

POS. 10-18 = Daily avg flow rate in cubic metres/sec

POS. 20-24 = Quality code

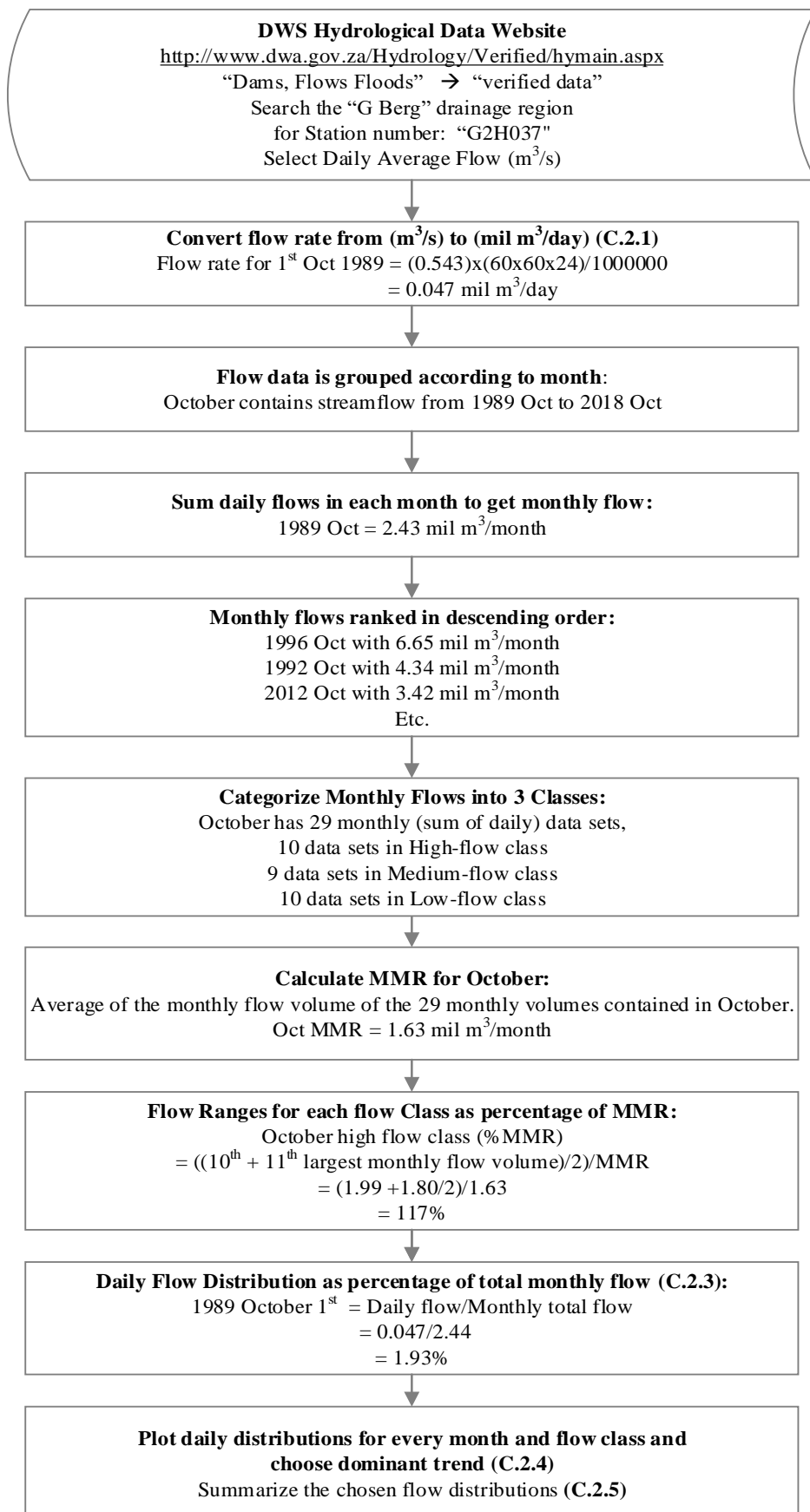
G2H037

Variable 100.00 Surface Water Level

DATE	D AVG F/R	QUAL
------	-----------	------

19891001	0.543	1
19891002	0.598	1
19891003	0.533	1
19891004	0.539	1
19891005	1.635	1
19891006	0.760	1
19891007	0.554	1
19891008	4.462	1
19891009	1.945	1
19891011	0.670	1
19891010	0.944	1
19891012	0.589	1
19891013	0.488	1
19891014	0.435	1
19891015	1.757	1
19891016	0.887	1
19891017	0.548	1
19891018	0.450	1
19891019	1.066	1
19891020	0.654	1
19891021	1.888	1
19891022	1.024	1
19891023	1.482	1
19891024	0.619	1
19891025	0.516	1
19891026	0.516	1
19891027	0.625	1
19891028	0.470	1
19891029	0.374	1
19891030	0.338	1
19891031	0.290	1
19891101	0.316	1
19891102	0.291	1
19891103	0.209	1
19891104	0.190	1
19891105	0.158	1
19891106	0.118	1
19891107	0.096	1
19891108	0.101	1

C.2.2 Streamflow Classification Process of Streamflow Gauge G2H037

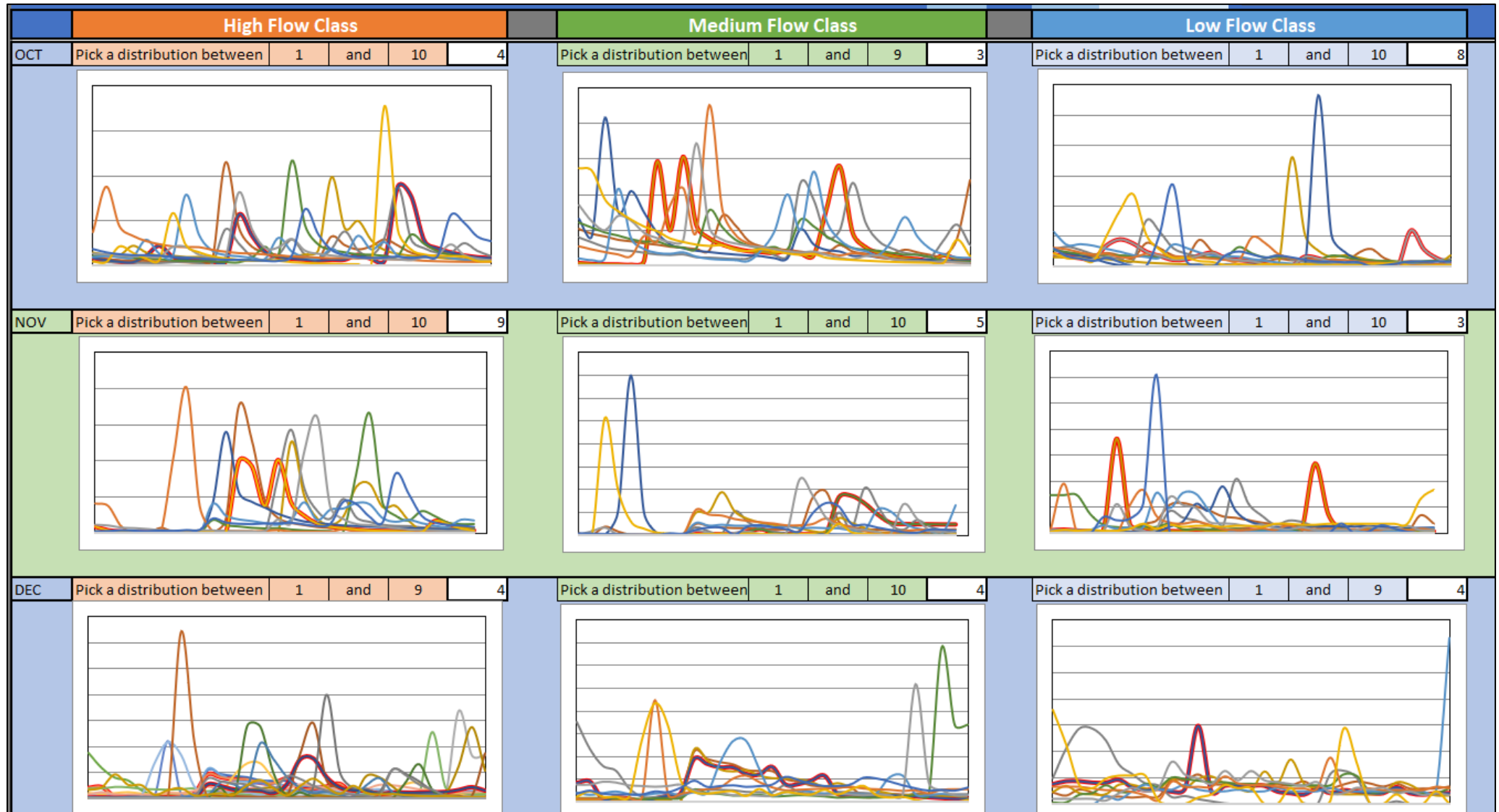


C.2.3 High-Flow and Medium-Flow Class for October with daily distribution as percentage of total monthly volume

Year	Month	Monthly Volume (mil m ³ /month)	1	2	3	4	5	6	7	8	9	10	11	12	13	14	15
1996	Oct	6.65	1.92%	1.48%	1.20%	1.17%	1.10%	0.97%	0.87%	0.77%	0.69%	1.30%	23.07%	8.56%	4.23%	3.01%	2.33%
1992	Oct	4.34	0.85%	0.72%	0.65%	0.59%	0.55%	0.53%	0.71%	0.80%	0.54%	0.45%	8.02%	4.84%	1.91%	1.25%	2.41%
2012	Oct	3.42	2.90%	2.41%	2.28%	4.40%	2.93%	2.18%	2.19%	1.89%	1.92%	1.77%	1.48%	1.27%	1.14%	1.06%	1.27%
1995	Oct	3.26	1.57%	1.12%	0.76%	0.65%	2.08%	4.32%	1.89%	1.25%	0.97%	0.85%	0.77%	11.24%	6.54%	2.90%	1.86%
2003	Oct	2.61	2.23%	2.22%	1.95%	1.67%	1.68%	1.47%	1.16%	1.06%	0.99%	0.95%	0.82%	0.75%	1.81%	4.22%	2.42%
1989	Oct	2.44	1.93%	2.12%	1.89%	1.91%	5.80%	2.70%	1.96%	15.82%	6.90%	3.35%	2.38%	2.09%	1.73%	1.54%	6.23%
2008	Oct	2.27	7.44%	17.64%	8.74%	6.60%	5.43%	4.72%	4.22%	4.06%	4.05%	3.45%	3.02%	2.72%	2.62%	2.40%	2.15%
2009	Oct	2.15	2.76%	2.58%	2.29%	2.13%	2.11%	2.01%	4.18%	4.24%	2.51%	1.99%	2.02%	16.21%	8.06%	3.95%	4.13%
2007	Oct	2.06	0.91%	0.79%	4.28%	2.86%	1.59%	1.24%	11.67%	4.61%	2.97%	2.09%	1.57%	1.24%	1.06%	1.09%	1.07%
2001	Oct	2.00	3.60%	2.88%	2.46%	2.26%	2.26%	2.14%	1.88%	1.75%	1.55%	1.36%	1.23%	1.23%	1.11%	0.99%	0.98%

Year	Month	Monthly Volume (mil m ³ /month)	1	2	3	4	5	6	7	8	9	10	11	12	13	14	15
2013	Oct	1.80	5.22%	4.53%	4.18%	3.70%	3.49%	3.19%	3.01%	2.73%	2.59%	2.40%	2.21%	7.09%	5.73%	3.56%	2.78%
1991	Oct	1.72	3.92%	3.23%	2.56%	2.19%	2.04%	1.76%	1.53%	1.45%	1.54%	1.14%	1.08%	0.98%	0.89%	0.98%	2.15%
2004	Oct	1.67	0.33%	0.20%	0.15%	0.13%	0.09%	0.63%	14.6%	4.95%	15.3%	5.72%	3.82%	2.93%	2.38%	2.01%	1.90%
2002	Oct	1.52	6.54%	4.17%	20.78%	7.59%	10.4%	7.44%	4.57%	2.95%	2.40%	2.06%	1.87%	1.67%	1.51%	1.40%	1.28%
1999	Oct	1.30	6.05%	5.34%	4.67%	4.24%	3.73%	3.40%	3.41%	2.79%	2.57%	2.47%	7.79%	5.40%	3.66%	2.86%	2.49%
2017	Oct	1.16	0.96%	0.71%	1.02%	10.80%	3.80%	2.29%	1.73%	1.61%	1.82%	1.20%	0.90%	0.78%	0.73%	0.58%	2.13%
2016	Oct	0.91	2.66%	2.21%	1.83%	1.51%	1.28%	4.14%	3.36%	8.46%	10.89%	4.64%	22.60%	7.84%	4.30%	3.06%	2.49%
2000	Oct	0.87	8.47%	6.15%	4.95%	6.93%	6.27%	4.56%	3.82%	3.24%	3.54%	17.15%	5.29%	3.61%	3.06%	2.71%	2.55%
2018	Oct	0.77	13.71%	13.35%	9.29%	7.64%	6.45%	5.47%	4.80%	3.78%	3.29%	2.92%	2.73%	2.81%	2.14%	2.00%	2.28%

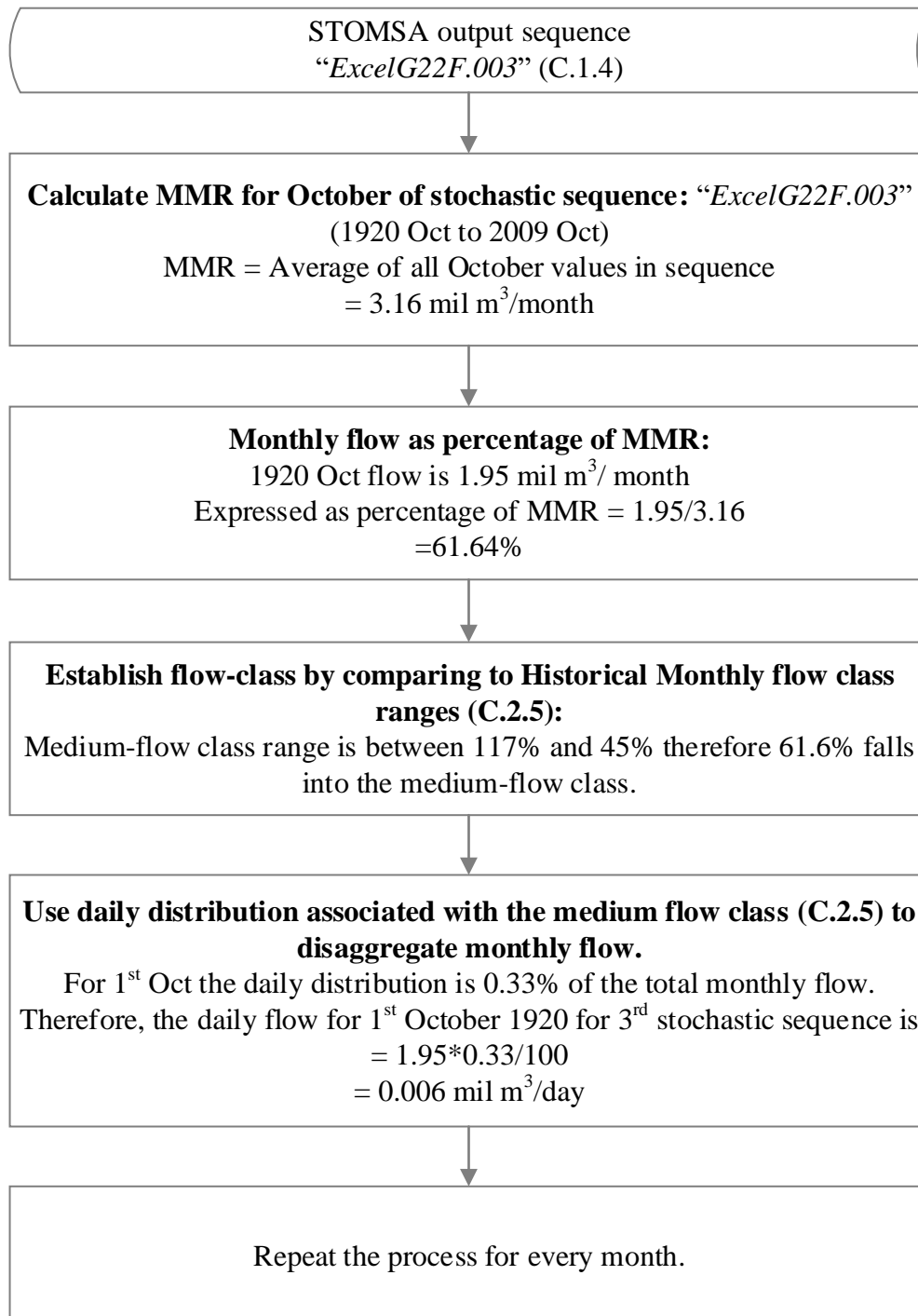
C.2.4 Daily distribution graphs for each flow class for October, November and December



C.2.5 Summary Table for Daily Distributions for months October to July for High-, Medium- and Low- Flow Class

Daily Flow Distributions (% total monthly flow)																	START
Month	Class % of MMR		1	2	3	4	5	6	7	8	9	10	11	12	13	14	
OCT	>117	high	1.57%	1.12%	0.76%	0.65%	2.08%	4.32%	1.89%	1.25%	0.97%	0.85%	0.77%	11.24%	6.54%	2.90%	1.86%
OCT	117-45	medium	0.33%	0.20%	0.15%	0.13%	0.09%	0.63%	14.69%	4.95%	15.38%	5.72%	3.82%	2.93%	2.38%	2.01%	1.90%
OCT	<45	low	4.16%	3.44%	2.93%	2.65%	7.21%	9.14%	7.77%	5.02%	3.67%	2.39%	2.56%	3.84%	4.72%	2.91%	2.33%
NOV	>106	high	1.74%	0.73%	0.39%	0.17%	0.15%	0.15%	0.17%	0.15%	0.19%	0.17%	0.16%	19.99%	18.46%	7.50%	20.26%
NOV	106-17	medium	0.15%	0.18%	0.18%	0.15%	0.18%	0.08%	0.13%	0.13%	0.15%	0.69%	0.67%	0.64%	0.62%	1.77%	2.88%
NOV	<17	low	1.03%	1.29%	0.95%	0.77%	1.20%	36.49%	3.36%	2.07%	0.95%	0.77%	0.69%	1.20%	0.77%	0.77%	1.03%
DEC	>76	high	0.26%	0.30%	0.16%	0.23%	0.00%	0.00%	0.37%	0.00%	0.00%	5.34%	4.69%	3.37%	3.16%	3.02%	2.00%
DEC	76-22	medium	4.15%	4.51%	0.71%	1.07%	0.77%	0.12%	0.77%	1.42%	2.02%	9.37%	8.30%	7.53%	7.53%	6.11%	5.99%
DEC	<22	low	3.71%	4.29%	4.29%	4.00%	4.00%	4.57%	3.14%	2.57%	2.86%	2.29%	2.86%	14.86%	2.29%	3.43%	3.43%
JAN	>85	high	0.39%	0.33%	0.46%	0.43%	0.39%	3.44%	41.33%	11.49%	3.34%	0.98%	0.59%	0.39%	0.36%	0.29%	0.39%
JAN	107-24	medium	2.08%	1.68%	1.04%	0.98%	0.69%	0.93%	0.87%	0.75%	15.51%	20.43%	6.02%	1.62%	23.09%	10.88%	2.31%
JAN	<24	low	2.84%	13.40%	7.47%	3.87%	4.64%	3.61%	3.09%	3.09%	3.61%	2.32%	2.32%	2.32%	3.35%	2.84%	1.80%
FEB	>74	high	2.05%	2.99%	2.56%	1.83%	1.24%	1.83%	3.51%	3.51%	3.87%	2.19%	1.83%	3.87%	3.21%	3.51%	4.09%
FEB	74-46	medium	2.76%	4.02%	3.27%	3.27%	3.02%	2.76%	2.76%	2.76%	3.77%	3.27%	12.56%	3.02%	2.26%	2.26%	2.26%
FEB	<46	low	3.96%	2.16%	1.44%	3.24%	2.88%	2.88%	2.88%	2.88%	2.88%	2.88%	3.24%	3.24%	5.04%	3.60%	3.96%
MAR	>52	high	0.61%	3.31%	2.32%	0.78%	0.78%	0.78%	0.96%	0.93%	0.93%	0.82%	0.78%	0.89%	0.78%	0.86%	0.71%
MAR	52-34	medium	3.65%	3.84%	3.84%	3.84%	3.84%	3.84%	3.84%	3.45%	1.73%	3.07%	3.84%	1.73%	2.11%	3.65%	7.10%
MAR	<34	low	0.87%	2.62%	3.21%	3.21%	2.62%	2.62%	2.62%	2.62%	2.62%	2.33%	1.17%	2.33%	1.75%	2.04%	2.33%
APR	>79	high	4.45%	25.27%	3.33%	1.07%	0.33%	0.05%	0.05%	0.66%	1.06%	0.64%	0.09%	0.10%	0.05%	0.05%	0.06%
APR	79-38	medium	0.13%	0.17%	0.10%	0.06%	0.10%	0.10%	1.24%	3.13%	3.10%	2.79%	2.62%	37.36%	23.58%	11.62%	5.94%
APR	<38	low	1.31%	1.31%	1.31%	1.55%	1.31%	1.31%	1.31%	1.31%	11.19%	4.52%	2.14%	1.90%	1.90%	1.90%	1.55%
MAY	>133	high	0.32%	0.04%	0.51%	0.78%	2.61%	4.42%	1.15%	0.38%	0.07%	0.01%	0.00%	0.01%	0.00%	0.00%	0.00%
MAY	133-56	medium	0.02%	0.02%	2.34%	17.43%	6.00%	3.46%	4.43%	1.73%	8.28%	3.13%	1.20%	0.36%	0.06%	0.03%	0.04%
MAY	<56	low	0.16%	0.25%	0.13%	0.15%	0.15%	0.20%	0.21%	0.18%	0.16%	0.21%	0.18%	0.15%	0.15%	0.15%	0.15%
JUN	>112	high	6.45%	4.68%	13.60%	6.56%	3.31%	1.98%	1.95%	4.15%	2.53%	1.61%	1.20%	4.02%	6.35%	10.75%	4.18%
JUN	112-74	medium	8.19%	3.55%	5.95%	2.15%	1.10%	0.69%	0.48%	0.37%	3.73%	2.19%	1.05%	0.69%	0.52%	5.30%	6.93%
JUN	<74	low	0.41%	0.28%	0.28%	0.35%	0.24%	0.21%	0.23%	0.19%	0.16%	0.16%	0.31%	0.49%	0.67%	0.86%	1.04%
JUL	>107	high	1.90%	0.83%	0.58%	0.48%	0.79%	0.49%	1.64%	2.55%	17.08%	7.44%	2.81%	1.84%	1.31%	1.04%	0.77%
JUL	107-80	medium	0.56%	0.47%	0.53%	0.43%	0.34%	12.80%	3.53%	1.63%	1.14%	0.85%	0.69%	3.66%	2.50%	6.29%	6.62%
JUL	<80	low	2.53%	1.62%	1.38%	1.19%	1.11%	1.98%	1.54%	1.18%	1.01%	6.25%	3.75%	2.52%	1.80%	5.69%	20.33%

C.2.6 Flow Diagram for disaggregation of stochastic streamflow



Appendix C.3 Rainfall Runoff Relationship for G22F

C.3.1 Rainfall data in mm/month (%MAP x MAP)

1920	125.6	38.4	61.8	77.1	57.1	48.5	84.7	16.7	705.4	266.9	214.0	100.2
1921	45.1	29.9	87.0	144.2	25.1	105.6	68.3	142.1	436.9	104.5	257.3	101.7
1922	37.8	43.8	30.9	41.0	0.9	22.9	143.3	367.4	450.3	242.6	176.7	129.9
1923	77.9	144.9	56.3	59.8	53.9	74.1	55.2	169.6	299.3	159.0	219.8	94.5
1924	110.6	153.5	14.1	60.4	23.6	3.2	40.1	138.7	467.0	267.7	142.8	60.7
1925	210.8	121.4	40.4	22.0	67.2	29.7	68.3	239.7	128.2	262.1	195.0	103.3
1926	217.4	63.6	0.0	23.9	122.2	18.6	100.1	203.3	129.9	146.8	232.6	99.2
1927	32.4	142.3	100.4	60.9	17.6	64.0	49.2	60.4	357.9	159.8	226.5	216.1
1928	60.7	48.3	62.8	17.7	22.0	25.3	202.5	208.0	145.3	253.3	211.1	76.5
1929	39.1	69.1	146.9	62.3	63.3	75.4	71.1	60.5	95.1	217.6	249.8	319.5
1930	104.6	116.8	23.9	0.0	63.3	18.3	196.0	191.5	142.1	198.2	248.2	210.7
1931	230.7	21.8	55.8	59.5	174.9	61.7	75.7	0.0	281.3	216.5	158.7	137.0
1932	74.7	37.9	67.8	49.8	42.8	33.4	49.8	151.8	274.2	228.2	252.9	60.1
1933	98.6	32.7	0.0	30.6	47.3	73.5	41.2	279.5	162.8	126.7	203.5	156.0
1934	127.9	138.4	25.5	49.2	35.7	68.3	138.1	242.5	125.1	236.3	192.5	142.1
1935	89.1	156.0	22.1	110.8	41.3	126.6	24.9	225.6	114.4	149.1	188.1	185.5
1936	51.3	83.7	77.2	60.8	15.5	86.1	115.7	190.6	422.7	325.1	146.5	99.3
1937	104.6	64.0	6.2	124.7	31.4	35.7	196.7	265.6	137.3	162.5	155.6	235.1
1938	98.3	84.2	22.6	0.0	104.9	19.9	162.9	204.2	93.6	151.6	212.1	76.2
1939	40.1	91.4	109.6	30.6	60.2	100.6	201.6	139.9	278.1	127.2	94.3	129.5
1940	113.7	124.2	36.5	64.2	42.5	40.6	310.9	295.9	304.9	218.3	215.4	329.3
1941	116.8	73.3	52.6	50.8	12.6	20.7	72.4	324.4	404.9	126.7	252.0	81.7
1942	63.9	10.1	25.1	94.6	61.1	67.4	122.2	182.4	151.3	237.8	252.7	113.8
1943	112.2	95.8	29.3	31.4	12.3	25.5	107.1	358.0	408.1	225.6	245.5	211.5
1944	113.5	63.9	70.6	6.3	5.1	21.4	115.6	447.3	397.0	324.1	238.5	24.6
1945	122.5	80.3	41.2	29.9	9.5	74.4	93.3	137.0	131.7	211.7	194.7	290.4
1946	94.8	41.9	36.0	11.6	0.0	97.3	89.2	215.1	129.7	393.1	149.1	101.1
1947	68.3	30.0	13.9	11.9	20.7	61.7	98.6	217.8	220.0	278.8	143.3	221.7
1948	137.4	30.0	70.9	38.5	11.1	18.3	174.6	118.4	127.6	194.6	192.5	140.5
1949	78.4	111.9	35.6	11.4	11.4	26.8	311.0	57.7	115.7	444.5	62.0	187.5
1950	84.1	121.2	90.2	67.2	11.0	12.0	214.6	138.4	342.4	210.8	117.6	126.7
1951	85.7	97.4	11.3	11.3	25.3	50.5	90.8	126.3	90.5	193.5	220.8	182.5
1952	94.6	142.0	25.9	21.2	21.4	38.5	244.2	212.1	146.9	201.3	143.3	30.6
1953	57.1	113.2	22.4	37.8	31.6	45.0	128.3	259.9	126.9	333.6	211.3	67.5
1954	73.5	45.4	48.8	8.9	191.3	20.7	67.0	58.0	156.6	267.4	267.5	93.8
1955	133.2	126.6	30.6	23.3	17.7	44.4	95.7	195.4	241.4	159.2	194.3	58.2
1956	73.5	21.1	54.4	23.6	84.8	45.3	79.1	266.6	220.5	210.1	152.2	86.3
1957	217.6	27.0	0.0	20.2	121.7	40.0	99.6	294.5	147.4	50.8	238.4	60.7
1958	97.9	30.2	5.1	48.9	25.9	52.9	294.0	457.4	106.7	70.3	221.8	121.6
1959	160.0	17.1	56.3	48.5	24.8	75.4	97.9	265.6	306.5	58.2	97.6	86.3
1960	41.3	8.5	47.0	139.9	19.8	30.2	47.3	150.6	241.6	104.9	244.2	170.7
1961	87.3	0.6	30.9	42.9	79.7	105.2	149.3	81.3	491.5	186.6	361.7	96.5
1962	201.9	70.3	22.1	51.1	1.9	21.8	33.7	108.6	170.5	369.3	286.3	74.0
1963	29.0	118.1	98.9	10.1	88.6	5.9	71.5	180.3	272.3	220.8	226.0	82.8
1964	115.6	118.7	26.1	54.9	89.8	172.6	157.0	191.0	102.0	115.0	178.6	79.8

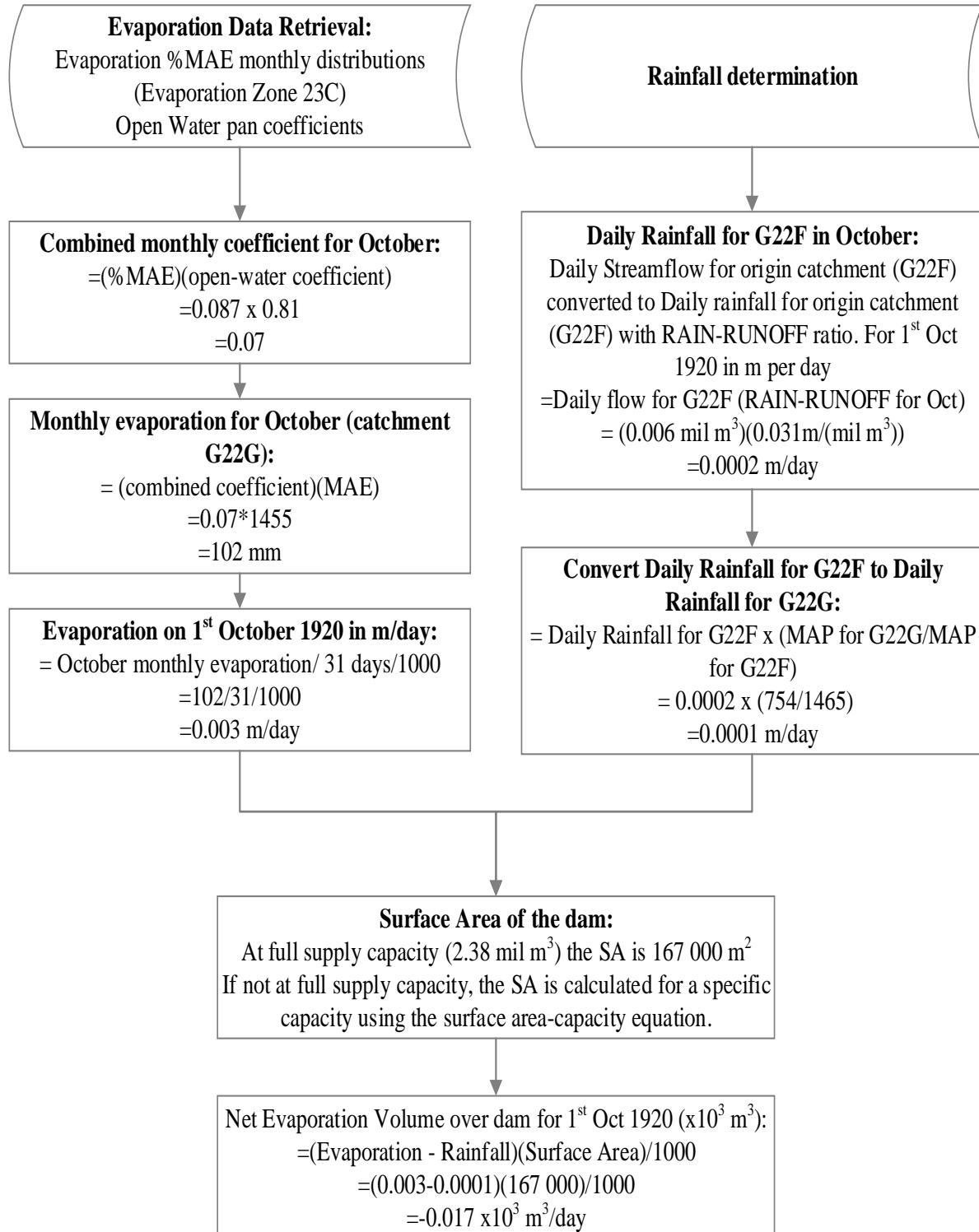
1965	69.1	17.3	94.8	16.3	51.4	175.2	108.1	173.7	124.2	295.9	191.6	124.8
1966	22.1	65.3	45.7	56.8	0.7	53.5	270.1	137.0	329.6	144.0	134.5	101.7
1967	164.5	81.6	23.9	106.9	65.9	0.3	138.1	289.9	282.9	254.6	190.3	52.0
1968	161.2	13.3	79.5	100.9	53.8	55.7	106.4	50.8	193.4	126.4	188.4	147.2
1969	143.0	31.9	20.9	27.5	30.3	11.3	24.2	299.9	247.0	201.1	285.1	133.2
1970	79.1	41.0	72.5	27.2	3.8	35.6	33.0	133.2	171.3	186.1	257.7	73.7
1971	91.1	31.9	34.7	63.0	53.8	33.3	263.4	231.3	154.4	128.0	181.1	103.9
1972	51.4	0.6	79.5	14.9	4.0	54.2	23.1	131.9	57.9	268.1	135.2	168.0
1973	56.4	65.0	63.9	29.3	17.1	25.6	18.0	308.5	252.0	173.2	484.3	149.6
1974	203.6	63.7	21.1	66.5	21.1	23.6	117.9	313.4	171.3	339.9	205.8	36.8
1975	124.8	66.5	10.7	1.5	22.1	72.1	124.1	124.5	482.6	221.7	191.0	193.4
1976	97.3	221.5	173.7	38.1	49.4	67.5	209.6	317.8	431.9	297.5	226.9	137.4
1977	59.0	30.3	65.2	25.3	57.9	74.4	124.8	122.2	68.3	74.6	246.6	169.8
1978	122.5	35.9	88.6	53.6	184.4	14.9	25.9	256.2	214.2	149.0	111.3	128.2
1979	268.5	19.6	12.6	58.0	51.6	7.9	146.8	230.7	310.9	54.2	140.2	79.8
1980	81.0	180.3	94.5	186.3	4.1	87.3	150.7	47.0	172.9	335.3	216.1	192.6
1981	41.5	86.0	67.1	76.2	9.1	26.1	188.7	82.5	192.2	144.0	145.2	35.3
1982	90.2	86.3	115.1	22.7	144.0	93.3	41.6	391.7	331.8	183.9	132.4	172.3
1983	24.9	20.4	38.7	29.3	19.9	97.0	110.2	321.1	125.7	166.9	88.9	183.3
1984	180.0	16.0	228.5	63.3	113.4	169.2	180.0	104.5	253.3	276.6	167.7	118.8
1985	57.9	14.4	44.5	26.7	65.0	121.6	151.2	126.1	284.6	222.1	352.2	117.3
1986	53.2	37.9	33.4	109.0	28.6	45.0	118.7	281.6	226.0	271.5	242.6	185.6
1987	46.4	33.5	102.1	15.1	0.9	48.5	149.3	167.3	189.6	231.2	263.0	161.6
1988	113.4	46.1	38.5	11.3	45.7	284.6	99.2	202.9	174.5	271.3	209.8	176.1
1989	136.5	97.0	12.5	43.2	57.6	4.8	322.6	161.7	275.9	345.0	107.8	72.7
1990	34.6	64.8	66.4	14.1	14.8	29.6	56.8	217.0	251.0	498.7	96.4	172.7
1991	93.6	31.9	27.4	6.3	63.6	56.0	206.7	174.6	349.4	193.1	137.0	165.0
1992	169.4	69.1	33.7	29.7	87.3	16.7	499.9	267.8	292.3	314.5	156.3	23.6
1993	11.9	20.2	40.0	60.4	12.2	6.7	64.0	109.4	450.6	171.1	115.1	94.9
1994	53.9	33.4	28.4	37.4	9.5	28.6	63.6	236.7	259.0	269.4	264.7	72.4
1995	174.0	32.4	153.5	7.2	99.6	78.7	92.4	60.9	322.6	209.6	194.0	192.9
1996	219.8	122.2	189.1	14.4	11.3	13.5	104.3	140.8	259.6	141.8	172.0	37.2
1997	31.2	228.4	37.2	34.9	0.9	33.7	133.2	463.2	178.3	189.9	124.2	54.9
1998	44.1	145.3	96.4	8.1	5.1	0.9	144.6	92.7	234.5	0.0	0.0	79.5
1999	27.4	55.5	4.0	52.3	41.3	40.3	20.5	163.3	125.6	211.5	191.9	136.7
2000	31.1	24.8	42.2	19.3	33.0	7.0	84.2	233.8	122.3	470.6	284.6	170.5
2001	142.4	39.3	36.6	213.3	38.2	32.5	106.9	211.4	257.7	281.0	175.7	75.0
2002	97.3	66.4	41.8	28.1	18.8	212.3	70.0	146.1	92.1	113.1	353.9	160.9
2003	94.1	4.4	93.6	55.8	2.1	53.5	183.1	18.8	176.1	182.4	210.4	102.0
2004	165.1	20.1	36.0	80.0	34.0	41.8	134.3	181.1	293.4	137.7	254.3	82.6
2005	60.7	49.4	9.7	2.2	33.5	19.6	107.2	308.4	168.3	263.1	230.3	77.9
2006	73.7	98.4	58.7	17.6	69.6	52.7	130.7	233.5	296.7	289.9	217.4	76.2
2007	156.6	153.5	46.9	51.7	64.6	52.3	42.8	153.4	215.9	366.1	171.1	352.3
2008	57.6	156.6	59.3	6.4	16.8	11.6	65.8	150.0	354.1	233.2	175.9	187.5
2009	87.6	199.4	21.4	4.7	55.4	34.6	83.9	326.3	212.6	134.3	106.4	42.8

C.3.2 Monthly Rainfall-Runoff Ratios

Month	RAIN-RUNOFF ratio (m/mil m3)	MMP (Rain) (m)	MMR (Runoff) (mil m3)
OCT	0.031	0.10	3.24
NOV	0.036	0.07	1.98
DEC	0.051	0.05	1.03
JAN	0.081	0.05	0.55
FEB	0.108	0.04	0.41
MAR	0.117	0.05	0.46
APR	0.087	0.12	1.42
MAY	0.055	0.20	3.59
JUN	0.040	0.24	5.89
JUL	0.032	0.22	6.67
AUG	0.031	0.20	6.46
SEP	0.026	0.13	4.87

Appendix C.4 Net Evaporation

C.4.1 Net Evaporation Flow Diagram for Idas Valley Dams



Appendix C.5 Groundwater Simulation

C.5.1 G22F simulated aquifer in Equilibrium

Time	Avg WL	Rainfall in month	Rainfall in month	Recharge Volume	Discharge Volume	Water level
Year-month	mbgl	mm	m	m ³	m ³	mbgl
1920-OCT	7.80	69.03	0.07	510 716	903 455	8.07
1920-NOV	8.07	44.96	0.04	332 630	903 455	8.46
1920-DEC	8.46	27.80	0.03	205 651	903 455	8.93
1921-JAN	8.93	40.68	0.04	300 944	903 455	9.34
1921-FEB	9.34	44.27	0.04	327 511	903 455	9.73
1921-MAR	9.73	33.99	0.03	251 464	903 455	10.18
1921-APR	10.18	48.51	0.05	358 903	903 455	10.55
1921-MAY	10.55	26.88	0.03	198 897	903 455	11.03
1921-JUN	11.03	681.15	0.68	5 039 593	903 455	8.21
1921-JUL	8.21	457.24	0.46	3 382 955	903 455	6.52
1921-AUG	6.52	240.82	0.24	1 781 724	903 455	5.93
1921-SEP	5.93	120.58	0.12	892 095	903 455	5.93
1921-OCT	5.93	68.72	0.07	508 456	903 455	6.20
1921-NOV	6.20	38.12	0.04	282 070	903 455	6.63
1921-DEC	6.63	40.15	0.04	297 051	903 455	7.04
1922-JAN	7.04	134.23	0.13	993 116	903 455	6.98
1922-FEB	6.98	101.49	0.10	750 879	903 455	7.08
1922-MAR	7.08	92.59	0.09	685 022	903 455	7.23
1922-APR	7.23	68.43	0.07	506 310	903 455	7.50
1922-MAY	7.50	100.95	0.10	746 877	903 455	7.61
1922-JUN	7.61	398.99	0.40	2 951 975	903 455	6.21
1922-JUL	6.21	227.16	0.23	1 680 689	903 455	5.68
1922-AUG	5.68	200.38	0.20	1 482 503	903 455	5.29
1922-SEP	5.29	128.91	0.13	953 751	903 455	5.26

C.5.2 G22G simulated aquifer in Equilibrium

Month	Avg WL of Aquifer	Rainfall in month	Rainfall in month	Recharge Volume	Discharge Volume	Water level response to recharge and average discharge
	mbgl	mm	m	m³	m³	mbgl
1920-OCT	7.90	28.15	0.03	272 907	482 801	8.17
1920-NOV	8.17	18.34	0.02	177 745	482 801	8.55
1920-DEC	8.55	11.34	0.01	109 892	482 801	9.02
1921-JAN	9.02	16.59	0.02	160 813	482 801	9.43
1921-FEB	9.43	18.06	0.02	175 009	482 801	9.82
1921-MAR	9.82	13.86	0.01	134 373	482 801	10.26
1921-APR	10.26	19.79	0.02	191 784	482 801	10.63
1921-MAY	10.63	10.96	0.01	106 283	482 801	11.10
1921-JUN	11.10	277.82	0.28	2 692 967	482 801	8.31
1921-JUL	8.31	186.50	0.19	1 807 723	482 801	6.63
1921-AUG	6.63	98.22	0.10	952 085	482 801	6.04
1921-SEP	6.04	49.18	0.05	476 702	482 801	6.05
1921-OCT	6.05	28.03	0.03	271 700	482 801	6.32
1921-NOV	6.32	15.55	0.02	150 728	482 801	6.74
1921-DEC	6.74	16.38	0.02	158 733	482 801	7.14
1922-JAN	7.14	54.75	0.05	530 684	482 801	7.08
1922-FEB	7.08	41.39	0.04	401 241	482 801	7.19
1922-MAR	7.19	37.76	0.04	366 050	482 801	7.33
1922-APR	7.33	27.91	0.03	270 553	482 801	7.60
1922-MAY	7.60	41.17	0.04	399 103	482 801	7.71
1922-JUN	7.71	162.74	0.16	1 577 423	482 801	6.33
1922-JUL	6.33	92.65	0.09	898 096	482 801	5.80
1922-AUG	5.80	81.73	0.08	792 193	482 801	5.41
1922-SEP	5.41	52.58	0.05	509 649	482 801	5.38

C.5.3 G22F Baseflow Separation

Time	Total Flow Qi	Surface water contribution Qsi	Decay	Growth	G_Gmax	Groundwater contribution Qgi = Qi-Qsi
Year-month	m ³ /month	m ³ /month	ratio	ratio	m ³ /month	m ³ /month
1920-OCT	2 260 000	1 103 563	0.5	5	1 156 437	1 156 437
1920-NOV	1 250 000	93 563	0.5	5	1 156 437	1 156 437
1920-DEC	540 000	0	0.5	5	1 156 437	540 000
1921-JAN	500 000	0	0.5	5	1 156 437	500 000
1921-FEB	410 000	0	0.5	5	1 156 437	410 000
1921-MAR	290 000	0	0.5	5	1 156 437	290 000
1921-APR	560 000	0	0.5	5	1 156 437	560 000
1921-MAY	490 000	0	0.5	5	1 156 437	490 000
1921-JUN	16 850 000	15 693 563	0.5	5	1 156 437	1 156 437
1921-JUL	14 110 000	12 747 103	0.5	5	1 362 897	1 362 897
1921-AUG	7 860 000	6 541 197	0.5	5	1 318 803	1 318 803
1921-SEP	4 630 000	3 473 563	0.5	5	1 156 437	1 156 437
1921-OCT	2 250 000	1 093 563	0.5	5	1 156 437	1 156 437
1921-NOV	1 060 000	0	0.5	5	1 156 437	1 060 000
1921-DEC	780 000	0	0.5	5	1 156 437	780 000
1922-JAN	1 650 000	493 563	0.5	5	1 156 437	1 156 437
1922-FEB	940 000	0	0.5	5	1 156 437	940 000
1922-MAR	790 000	0	0.5	5	1 156 437	790 000
1922-APR	790 000	0	0.5	5	1 156 437	790 000
1922-MAY	1 840 000	683 563	0.5	5	1 156 437	1 156 437
1922-JUN	9 870 000	8 713 563	0.5	5	1 156 437	1 156 437
1922-JUL	7 010 000	5 853 563	0.5	5	1 156 437	1 156 437
1922-AUG	6 540 000	5 383 563	0.5	5	1 156 437	1 156 437
1922-SEP	4 950 000	3 793 563	0.5	5	1 156 437	1 156 437

C.5.4 G22G Baseflow Separation

Time	Total Flow Qi	Surface water contribution Qsi	Decay	Growth	G_Gmax	Groundwater contribution Qgi = Qi-Qsi
Year-month	m ³ /month	m ³ /month	ratio	ratio	m ³ /month	m ³ /month
1920-OCT	921 793	258 970	0.5	5	662 823	662 823
1920-NOV	509 841	0	0.5	5	662 823	509 841
1920-DEC	220 252	0	0.5	5	662 823	220 252
1921-JAN	203 937	0	0.5	5	662 823	203 937
1921-FEB	167 228	0	0.5	5	662 823	167 228
1921-MAR	118 283	0	0.5	5	662 823	118 283
1921-APR	228 409	0	0.5	5	662 823	228 409
1921-MAY	199 858	0	0.5	5	662 823	199 858
1921-JUN	6 872 663	6 209 840	0.5	5	662 823	662 823
1921-JUL	5 755 090	5 092 267	0.5	5	662 823	662 823
1921-AUG	3 205 883	2 543 060	0.5	5	662 823	662 823
1921-SEP	1 888 453	1 225 630	0.5	5	662 823	662 823
1921-OCT	917 715	254 892	0.5	5	662 823	662 823
1921-NOV	432 346	0	0.5	5	662 823	432 346
1921-DEC	318 141	0	0.5	5	662 823	318 141
1922-JAN	672 991	10 168	0.5	5	662 823	662 823
1922-FEB	383 401	0	0.5	5	662 823	383 401
1922-MAR	322 220	0	0.5	5	662 823	322 220
1922-APR	322 220	0	0.5	5	662 823	322 220
1922-MAY	750 487	87 664	0.5	5	662 823	662 823
1922-JUN	4 025 708	3 362 885	0.5	5	662 823	662 823
1922-JUL	2 859 191	2 196 368	0.5	5	662 823	662 823
1922-AUG	2 667 490	2 004 667	0.5	5	662 823	662 823
1922-SEP	2 018 972	1 356 149	0.5	5	662 823	662 823

C.5.5 Stressed aquifer system G22F calculation table

Time	Start WL of Aquifer	Recharge Volume of Aquifer	Baseflow Volume of Aquifer	End Water Level	Abstraction Volume available
Year-month	mbgl	m ³ /month	m ³ /month	mbgl	m ³ /month
1920-OCT	7.80	510 716	1 182 101	8.26	25 664
1920-NOV	8.26	332 630	1 182 101	8.83	25 664
1920-DEC	8.83	205 651	551 984	9.07	11 984
1921-JAN	9.07	300 944	511 096	9.21	11 096
1921-FEB	9.21	327 511	419 099	9.28	9 099
1921-MAR	9.28	251 464	296 436	9.31	6 436
1921-APR	9.31	358 903	572 428	9.45	12 428
1921-MAY	9.45	198 897	500 874	9.66	10 874
1921-JUN	9.66	5 039 593	1 182 101	7.03	25 664
1921-JUL	7.03	3 382 955	1 393 142	5.68	30 246
1921-AUG	5.68	1 781 724	1 348 071	5.38	29 267
1921-SEP	5.38	892 095	1 182 101	5.58	25 664
1921-OCT	5.58	508 456	1 182 101	6.04	25 664
1921-NOV	6.04	282 070	1 083 524	6.58	23 524
1921-DEC	6.58	297 051	797 310	6.92	17 310
1922-JAN	6.92	993 116	1 182 101	7.05	25 664
1922-FEB	7.05	750 879	960 861	7.20	20 861
1922-MAR	7.20	685 022	807 532	7.28	17 532
1922-APR	7.28	506 310	807 532	7.48	17 532
1922-MAY	7.48	746 877	1 182 101	7.78	25 664
1922-JUN	7.78	2 951 975	1 182 101	6.58	25 664
1922-JUL	6.58	1 680 689	1 182 101	6.24	25 664
1922-AUG	6.24	1 482 503	1 182 101	6.03	25 664
1922-SEP	6.03	953 751	1 182 101	6.19	25 664

C.5.6 Stressed aquifer system G22G calculation table

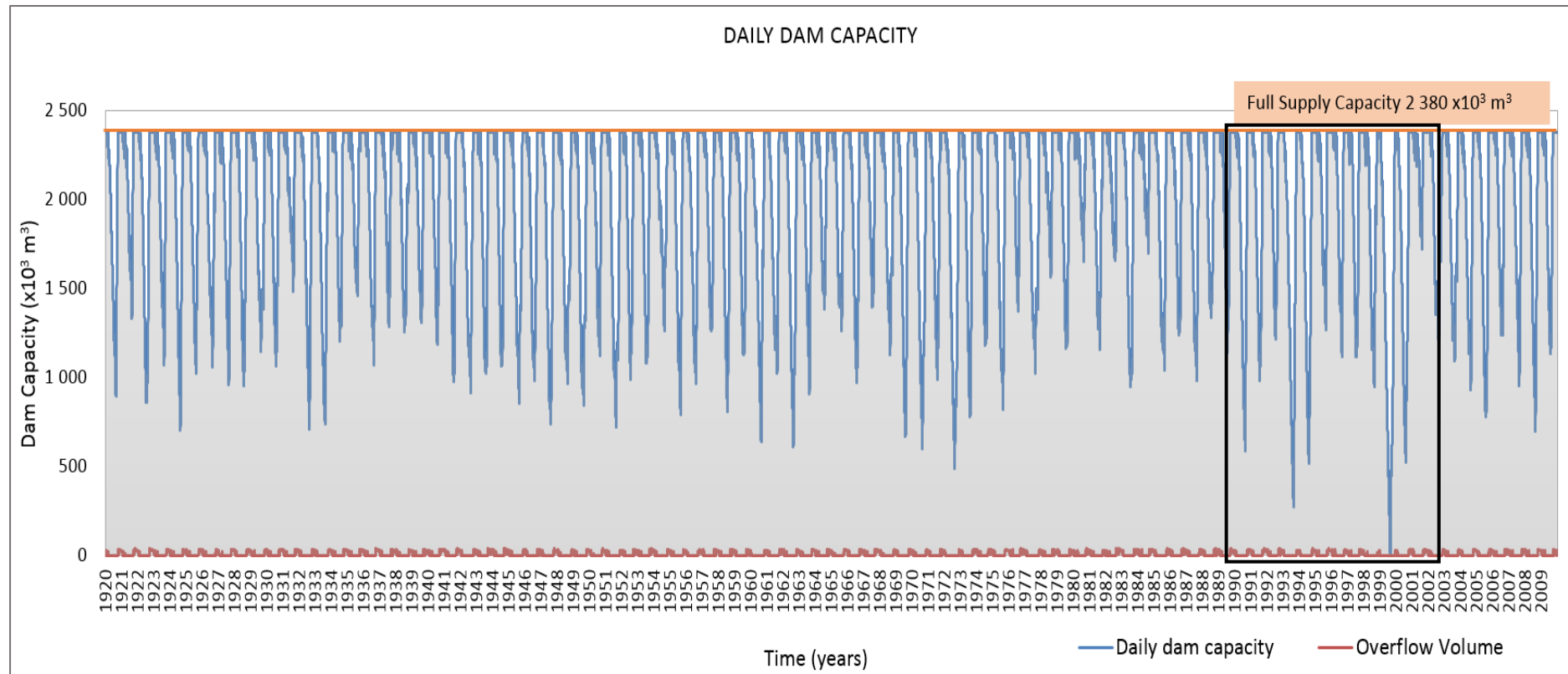
Time	Start WL of Aquifer	Recharge Volume of Aquifer	Baseflow Volume of Aquifer	End Water Level	Abstraction Volume available
Year-month	mbgl	m ³ /month	m ³ /month	mbgl	m ³ /month
1920-OCT	7.90	272 907	680 355	8.42	17 532
1920-NOV	8.42	177 745	523 327	8.85	13 485
1920-DEC	8.85	109 892	226 077	9.00	5 826
1921-JAN	9.00	160 813	209 331	9.06	5 394
1921-FEB	9.06	175 009	171 651	9.06	4 423
1921-MAR	9.06	134 373	121 412	9.04	3 129
1921-APR	9.04	191 784	234 450	9.09	6 041
1921-MAY	9.09	106 283	205 144	9.22	5 286
1921-JUN	9.22	2 692 967	680 355	6.67	17 532
1921-JUL	6.67	1 807 723	680 355	5.25	17 532
1921-AUG	5.25	952 085	680 355	4.91	17 532
1921-SEP	4.91	476 702	680 355	5.16	17 532
1921-OCT	5.16	271 700	680 355	5.68	17 532
1921-NOV	5.68	150 728	443 781	6.05	11 435
1921-DEC	6.05	158 733	326 556	6.26	8 415
1922-JAN	6.26	530 684	680 355	6.45	17 532
1922-FEB	6.45	401 241	393 542	6.44	10 141
1922-MAR	6.44	366 050	330 742	6.40	8 523
1922-APR	6.40	270 553	330 742	6.47	8 523
1922-MAY	6.47	399 103	680 355	6.83	17 532
1922-JUN	6.83	1 577 423	680 355	5.69	17 532
1922-JUL	5.69	898 096	680 355	5.42	17 532
1922-AUG	5.42	792 193	680 355	5.28	17 532
1922-SEP	5.28	509 649	680 355	5.49	17 532

C.5.7 Combined monthly abstraction (scaled G22F and scaled G22G)

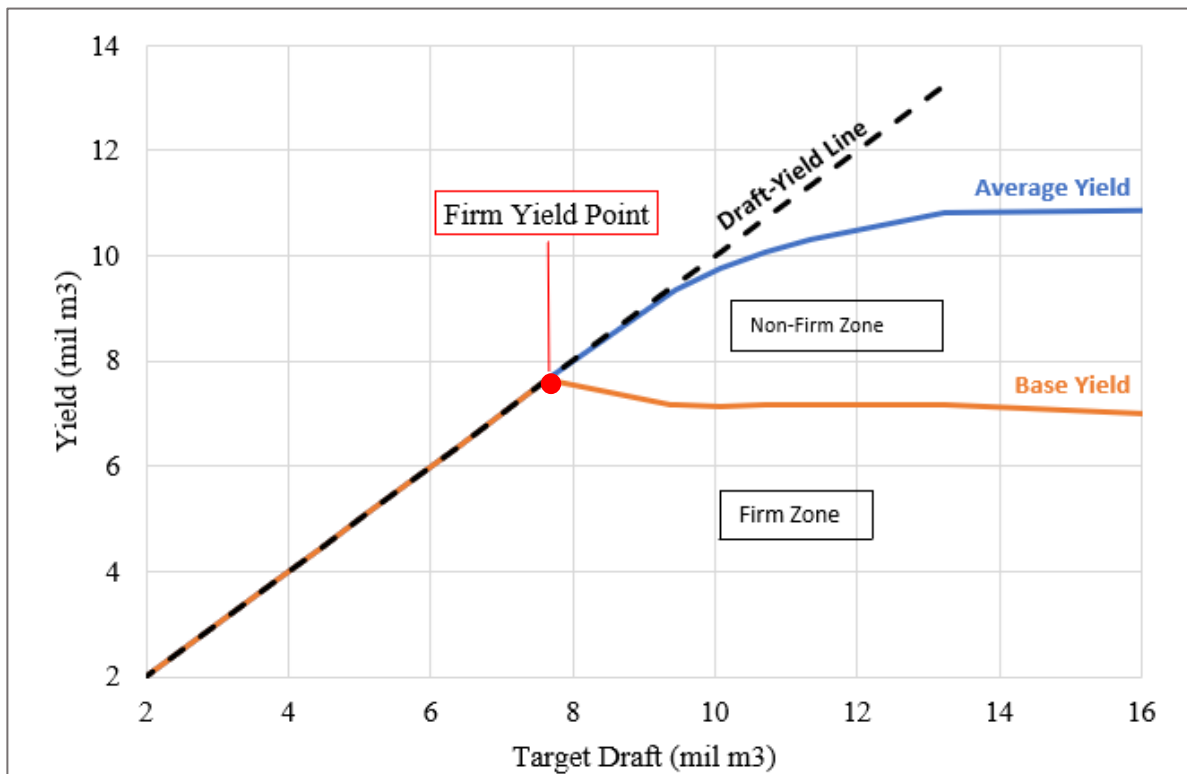
Sequence Number	97	98	99	100	101	Historical
Average potential long-term abstraction of sequence (m³/month)	4 544	8 278	8 352	14 229	4 923	6 930
1920-OCT	5 997	10 741	10 703	18 635	6 657	9 088
1920-NOV	5 326	10 741	10 703	18 021	6 657	8 325
1920-DEC	2 231	10 741	9 974	11 111	4 341	3 813
1921-JAN	1 047	10 741	3 048	5 093	2 171	3 531
1921-FEB	1 184	9 755	1 132	2 006	909	2 895
1921-MAR	4 689	10 741	1 132	1 235	404	2 048
1921-APR	5 997	10 741	5 051	18 635	6 657	3 955
1921-MAY	5 997	10 741	10 703	18 635	6 657	3 460
1921-JUN	5 997	10 741	10 703	18 635	6 657	9 088
1921-JUL	5 997	10 741	10 703	18 635	6 657	10 144
1921-AUG	5 997	10 741	10 703	18 635	6 657	9 930
1921-SEP	5 997	10 741	10 703	18 635	6 657	9 088
1921-OCT	5 997	10 524	10 703	18 635	6 657	9 088
1921-NOV	5 997	5 930	10 157	18 635	6 131	7 486
1921-DEC	5 413	2 922	9 232	14 660	2 827	5 508
1922-JAN	1 457	2 578	5 051	7 407	4 190	9 088
1922-FEB	1 047	1 547	1 306	4 012	2 726	6 638
1922-MAR	774	602	1 132	1 852	1 161	5 579
1922-APR	5 997	1 719	10 454	13 271	4 896	5 579
1922-MAY	5 997	7 992	10 703	18 635	6 657	9 088
1922-JUN	5 997	10 741	10 703	18 635	6 657	9 088
1922-JUL	5 997	10 741	10 703	18 635	6 657	9 088
1922-AUG	5 997	10 741	10 703	18 635	6 657	9 088
1922-SEP	5 997	10 741	10 703	18 635	6 657	9 088

Appendix C.6 Conjunctive Use System Yield Analysis

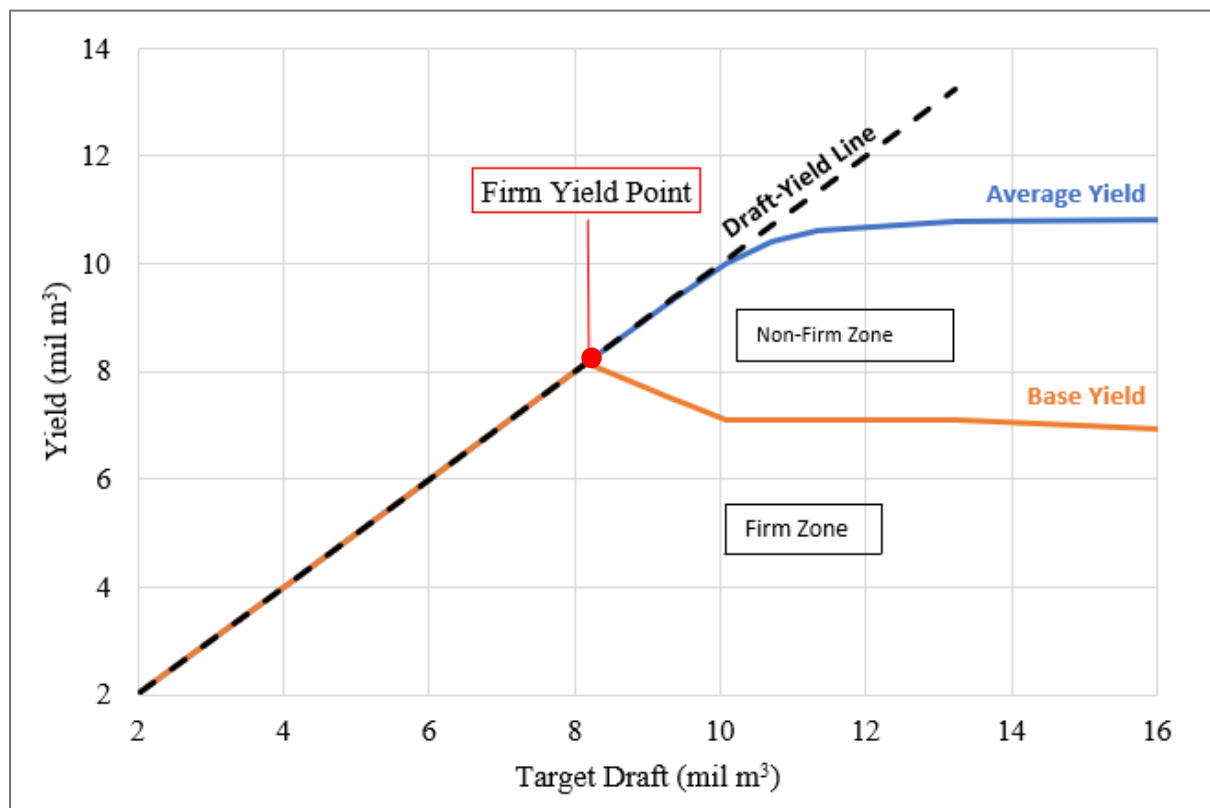
C.6.1 Time-Capacity curve for Idas Valley Dams (1920 to 2010)



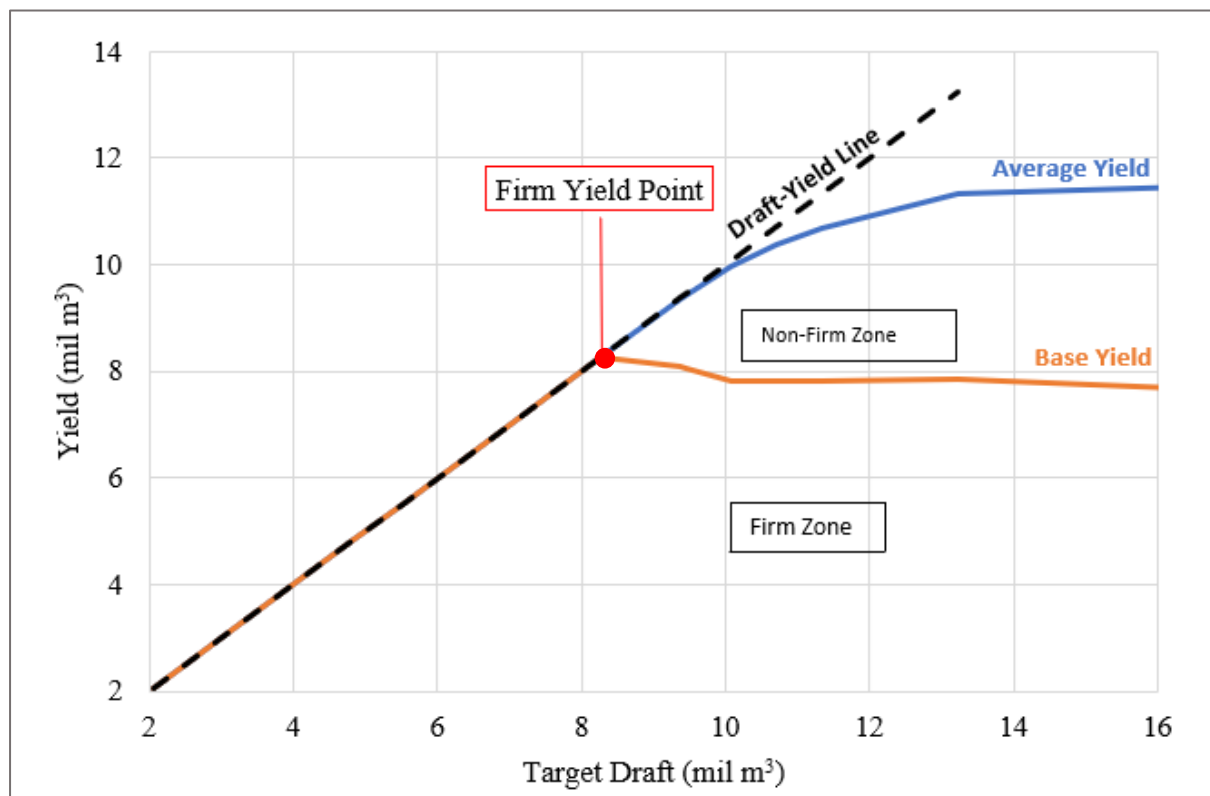
C.6.2 Draft-Yield Curve for Scenario 1



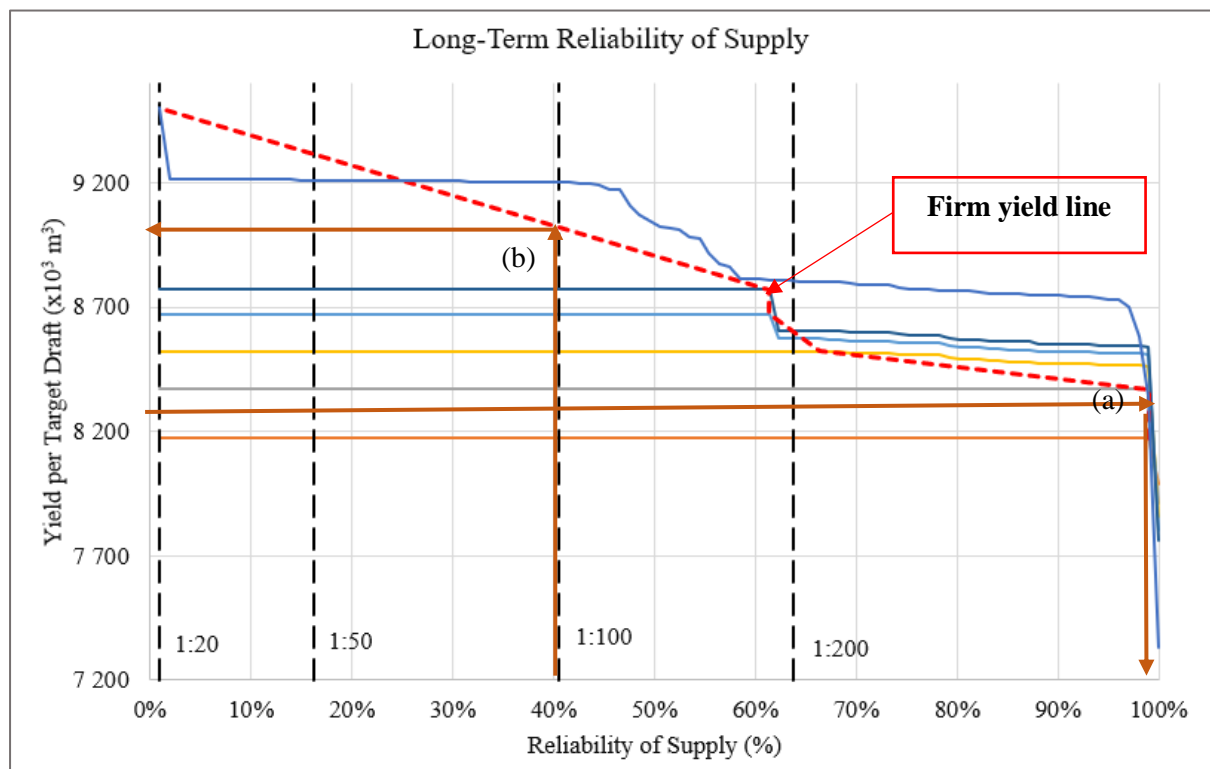
C.6.3 Draft-Yield Curve for Scenario 2



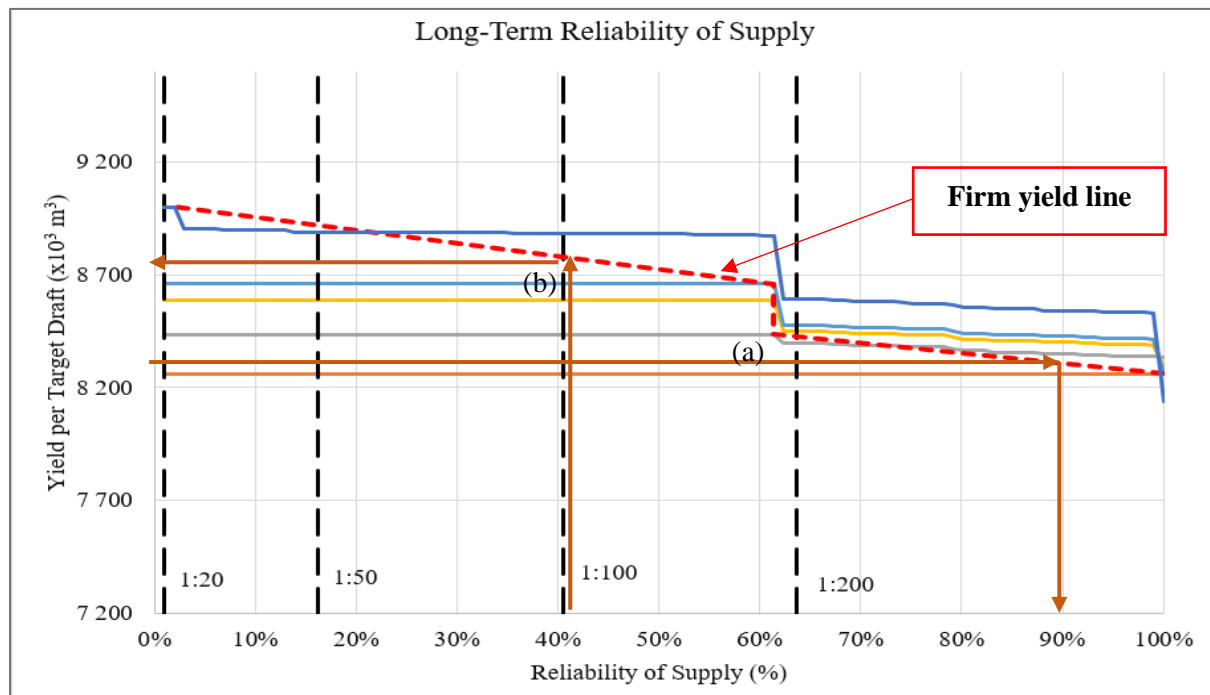
C.6.4 Draft-Yield Curve for Scenario 3



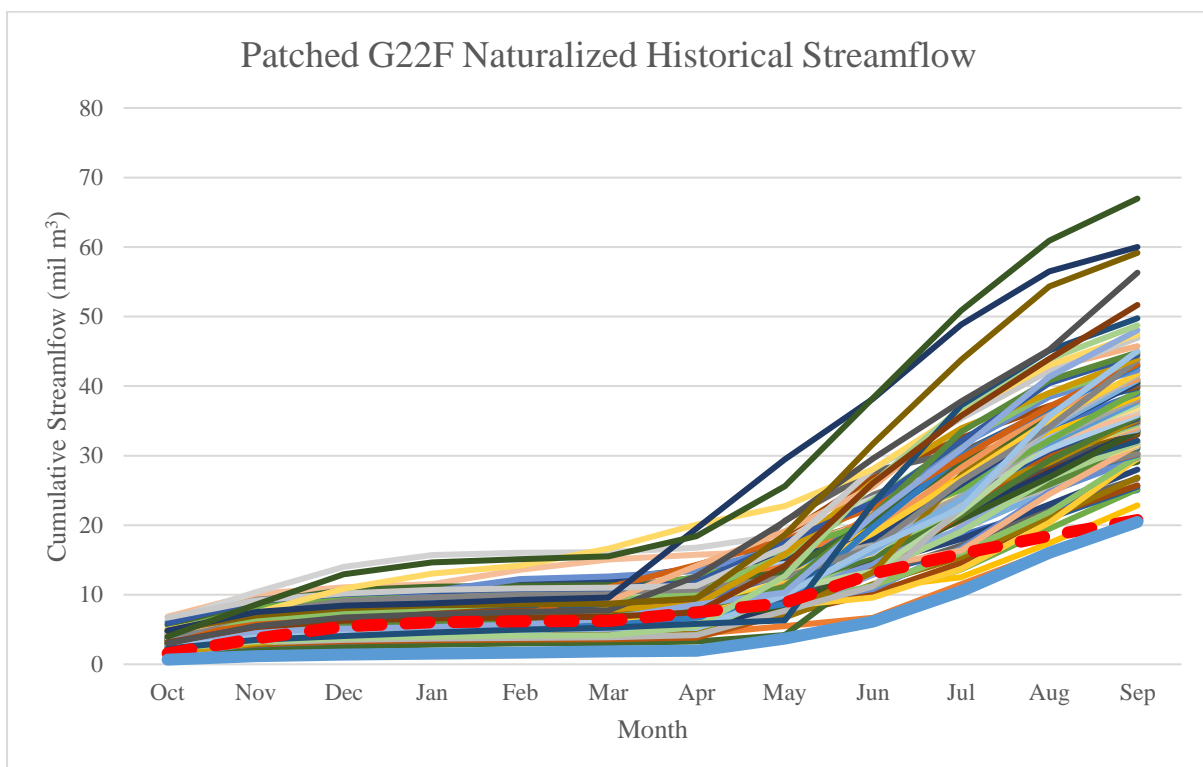
C.6.5 Long-term Reliability Curve for Scenario 2



C.6.6 Long-term Reliability Curve for Scenario 3



C.6.7 Patched Low Flow Sequence in the Naturalized Streamflow Sequence for catchment G22F



C.6.8 Unsorted Stochastic Yields for different Target Drafts

